HEAT TRANSFER ON A ROTATING SURFACE WITH AND WITHOUT PHASE CHANGE

by

J.R. KHAN

Thesis submitted for the degree of Doctor of Philosophy in the Faculty of Engineering of University of Newcastle upon Tyne.

Department of Chemical Engineering,
University of Newcastle upon Tyne,
England.

March, 1986

IN MEMORY OF MY FATHER

ACKNOWLEDGEMENTS

I would like to express my sincere gratitude to Mr. J.E. Porter for his help, discussions and inspiration throughout the work. His valuable guidance in data analysis and in compilation of this report is also appreciated.

I wish to extend my thanks to Mr. K.E. Peet, the head of department where this work was conducted.

Many thanks to my colleagues and technical staff of the department for their co-operation. In particular, Mr. E.T. Horsley, Mr. S. Latimer and Mr. B.E. Grover for their technical back-up, without which it would have been difficult to complete the experimental facility.

The provision of a financial grant by the Government of Pakistan is cheerfully acknowledged. Special thanks are also due to Engineering University,Lahore, for granting leave to pursue my studies in the United Kingdom.

Thanks are also due to Mrs. M.A. Grover for typing this report.

Finally, I would like to thank my family for their patience, understanding and encouragement.

ABSTRACT

This study is concerned with heat transfer to liquid films flowing across the surface of a rotating disc. Two cases of heat transfer have been considered, the first dealing with sensible heating of the liquid film, the second with heating and evaporation from the surface of the film. In both cases the heating medium was condensing steam.

A model for the thermal performance of such devices, has been constructed and compared with experimental data for water and methanol. Values of the temperature of the liquid leaving the disc periphery have been measured for a wide range of liquid flow rates and disc speeds. These results compare very favourably with the temperatures predicted by the proposed model. Similar comparisons have been made for the rates of evaporation measured when methanol is heated on such discs. Again predictions compare well with measured values, except in conditions of flow where film breakdown is known to occur.

If the flow on a disc surface, rotating at constant speed, is gradually reduced a flow will occur at which the surface is no longer completely wetted. Increasing the flow rate will produce rewetting of the surface at some slightly higher value of the flow rate. This mechanism of rewetting has been studied in some detail and a theoretical model has been developed.

The model has been tested under a wide range of operating conditions and comparison between measured and predicted minimum rewetting rates is quite good.

Power dissipation associated with the flow of liquid film across a disc has also been considered.

CONTENTS

CHAPTER ONE

INTRODUCTION

1.1. GENERAL

Following the energy crisis of the last decade considerable efforts have been made to improve the performance and efficiency of all processes which involve the use and transfer of energy. In overall process design the efficient utilisation of primary and secondary energy has become extremely important. High energy costs have forced engineers to pay detailed attention to actual energy requirements and their efficient use. Integration of individual and groups of process plant for improved overall energy efficiency has produced great benefits, mainly by removing the more easily identified source of waste and inefficiency. The improvement of operating conditions, better control and maintenance will contribute to this effort. In the future significant improvements in processes are only likely to come with major changes in the actual processes themselves. For example changes in manufacturing methods from catalytic to biochemical routes.

Whether current processes continue or are replaced by new technologies,efficient individual process operations such as chemical and biochemical reactions, together with heat and mass transfer will be extremely important. Therefore study of these processes and new techniques for their improvement remains an important area of process engineering.

In the case of heat transfer processes, attempts to increase film coefficients over those reported for conventional heat exchange geometries have been numerous as publications in the normal and patent literature demonstrates. Augmentation techniques of all types have been reported but they can be generally

classified into two types.

(i) Passive,

and (ii) Active.

Passive techniques require no major design modification, usually involving only use of the normal surfaces which have been treated in one of a variety of ways e.g., mechanically roughened or provided with surface extensions (fins). In some processes typically those involving condensation, heat transfer can be improved by modification of the way in which condensation occurs. Addition of certain chemicals at the condensation surfaces, or in the condensing vapour can be used to induce dropwise condensation rather than the less efficient process.

In active systems, mechanical means are utilised. This induces a variety of techniques such as;

1. Stirring.
2. Scraping.
3. Vibration of the heat transfer surface.
4. Rotation of the heat transfer surface.

Stirring and scraping have been widely used in the process industries and each technique has areas of application in which its use is necessary and economic. Vibration of the heat transfer surface is usually difficult in a practical exchanger, and involves complex drive arrangements. It is more likely that vibrations in the liquid streams, that is flow induced vibrations, are more likely to achieve practical success, but more study will be required before such techniques can be implemented.

Rotation of the heat transfer surface offer many advantages as an augmentation technique. In the first instance variation of the

speed of rotation of the surface offers a further degree of freedom in exchanger design and operation. The high gravitational field which rotation provides means that film processes are normally enhanced, and this would be improved much further by careful design of the surface structure (artificial roughness). The ability of a rotating surface to handle liquids containing a high concentration of solids may prove useful in many areas. In general the self cleaning action of the surface is an extremely attractive attribute.

General characteristics of rotating systems, such as high throughput, high heat and mass transfer performance, short contact time and low holdup seem to suggest a wide range of application is possible.

These applications will not be possible until the necessary design information becomes available. Information defining the range of operating conditions for particular forms of rotating structure is required. This will include the rotation speed, rheological properties of the liquids involved and the range of flow rate which can be handled.

This information together with design procedures for calculating thermal performance will enable an economic assessment of this type of device to be carried out successfully. In many cases attributes other than economic performance may prove to be the most important (e.g. compact design, controllability etc).

1.2. SCOPE OF THE PRESENT INVESTIGATION

The purpose of the present study is to measure (and predict) the rates of heat transfer to liquids flowing across the surface of a heated disc. Two cases will be considered. The first dealing with sensible heating only, the second with sensible

heating followed by liquid evaporation.

This investigation is also concerned with the use of the disc as the heat transfer surface for a compact heat exchanger. Therefore, in this work the heat transfer element will consist of two discs, separated by approximately 1mm. The test liquid will enter this narrow channel near the centre of the discs and will be collected as it leaves the periphery of the disc assembly. Vapour generated from the test liquid as it flows across the discs will be removed, either from the periphery of the disc (cocurrent flow) or from the centre of the assembly (counter current flow).

The heating medium from the rotating disc assembly, which will rotate in a sealed pressure chamber, will be condensing steam.

The condensation process will also benefit from rotation of the heat transfer surface. Even if film condensation occurs, film velocities will be very high due to the effect of the centrifugal force on the condensate films. This should enhance the film coefficient quite considerably.

In this series of experiments the steam space above the condensing surface will not be restricted, since this study is only concerned with the performance of a single, twin disc assembly.

In a practical machine many such assemblies may be required and therefore the steam space between the disc assemblies will become important. Since the steam flow into the narrow space between rotating disc assemblies will be counterflow to the condensate film leaving the same space, this flow will become quite complex as the spacing becomes small. This process will not

be part of the present study although the test section will be designed with multiple assembly use possible at a later date.

In any thin film processing unit, maintenance of a thin film over the whole of the transfer surface is crucial to efficient performance. Any breakdown of the film on the heating or evaporation side will cause loss of performance due to loss of contact area. If the coefficient on the heating side were the limiting one, then loss of performance would be even greater. In some cases heat transfer performance would be lost completely if the liquid flow following breakdown is in the form of a few high flow rivulets. It should be noted that film breakdown of the condensate film should be encouraged as this might produce higher performances.

As part of this study, minimum wetting rates will be considered. Heat transfer performance will be measured over a wide range of flowrate, which include the lower flowrates where heat transfer performance will be very high, but film breakdown is likely to occur.

Basic power dissipation in the generation of thin films will also be considered. This energy includes the kinetic energy contained in the liquid as it is discharged at the periphery of the disc, which might be recovered, together with that lost in viscous dissipation in flow across the disc surface.

CHAPTER TWO

LITERATURE SURVEY

2.1. INTRODUCTION

In general, when a liquid is introduced to the centre of a smooth disc, it will flow uniformally across the surface of the disc to be discharged at the periphery. The manner in which this flow process is achieved, depends on a number of factors of which the most important have been shown to be, the rheological properties of the liquid (in practice its viscosity and surface tension), the liquid flow rate and the rotary speed of the disc. Dependant on the conditions, the film can exhibit a completely smooth surface or a wide variety of wave and ripple characteristics as it flows across the surface. Under certain conditions the film may suffer break-down in the peripheral regions, exposing the surface of the disc. In extreme conditions, film flow can be disrupted completely to be replaced by liquid flow in the form of irregular rivulets.

A number of studies related to various aspects of film flow on rotating surfaces are reported in the literature. These range from the complex flow regimes which were noted above, to the techniques and difficulties associated with the measurement of film parameters such as film thickness and surface velocity. Whilst there is currently a general interest in flow, heat and mass transfer processes in and on discs having a wide variety of surface 'structure', most of the previous work has been concerned with flow on flat surfaces (discs).

Although not the immediate research area of this work, flow heat and mass transfer in the vicinity of a rotating surface

exposed to a continuous liquid or gaseous phase has been the subject of considerable research. This work can be classified into two convenient categories;

(a) The 'free' disc, a disc rotating in a medium of infinite extent, essentially quiescent at large distances from the surface and;

(b) The 'enclosed disc', a disc which rotates within a stationary chamber of finite dimensions, where disc/chamber interactions can be expected.

The free disc, which provides the first building block for the development of many useful models of heat transfer behaviour under these conditions, has been the subject of numerous theoretical and experimental studies. Kreith (37) has reviewed comprehensively the published literature dealing with 'free' surfaces.

The main area of interest of the present research concerns heat transfer with and without phase change in thin liquid films. The literature reviewed in this chapter is limited to those papers which make a significant contribution in this area. Additionally, a concise description of the hydrodynamics of thin film formed on rotating discs has been included not only because of the strong inter-relationship between heat transfer and fluid dynamics, but also because of the additional study of minimum wetting rates which forms part of this project. The highest rates of heat and mass transfer on the rotating surface might be expected to be associated with the thinnest film. However, maintenance of the 'thinnest' uniform film requires a knowledge of film breakdown mechanisms and minimum wetting rates.

2.2. HYDRODYNAMICS OF THIN FILMS ON A ROTATING DISC

2.2.1. Introduction

The general hydrodynamic behaviour of liquid films flowing across the surface of a rotating disc has been discussed in detail by Bell (6). In view of this the following review will be limited to those aspects of this type of flow behaviour relating to the process of heat transfer, and in the case of low velocity flows, the maintenance of a continuous film.

2.2.2. Theoretical Considerations

Whilst considerations such as flow rate, disc speed and the rheological properties of the flowing liquid can give rise to a large number of flow regimes, few of these will be applicable to industrial processes. In general high flow rates and high disc speeds will produce the increase in throughput and performance (heat or mass transfer), necessary to stimulate industrial interest. The hydrodynamics of these flows have been accurately described in terms of a simple balance between centrifugal force and the viscous forces in the film viz;

$$\upsilon \frac{d^2 u_r}{dy^2} = -r\omega^2 \qquad (2.2.1)$$

With the boundary conditions of zero velocity at the solid surface, and zero shear at the free liquid surface. For a wide range of operating conditions for industrial processes, film thickness will be such that the viscous forces in the film will be controlling, the effects of the Coriolis force and inertial forces being minimal. Furthermore the inlet conditions for flow onto the disc can be adjusted so that they do not influence conditions on the rotating surface.

2.2.3. Velocity Distribution In Thin Films

As a first approximation it can be assumed that the film formed on a rotating disc are sufficiently thin that laminar flow conditions will prevail. The flow is generally considered as quasi-parallel and the circumferential velocity component can be approximated by the product of angular velocity and radius (ωr).

The radial component can be estimated by integrating the equation (2.2.1) for the conditions of no slip at the disc surface ($y=0$) and for stress free conditions at ($y=\delta$). These situations provide the following boundary conditions.

$$u_r = 0 \quad \text{at } y=0$$

$$\frac{du_r}{dy} = 0 \quad \text{at } y=\delta$$

The radial velocity distribution across the film is found to be parabolic for these conditions;

$$u_r = \frac{r\omega^2\delta^2}{\nu}\left[(y/\delta) - \frac{1}{2}(y/\delta)^2\right] \qquad (2.2.2)$$

The average film velocity, $\bar{u}_r = \frac{1}{\delta}\int_0^{\delta} u_r\, dy$

$$\bar{u}_r = \frac{\omega^2 r\delta^2}{3\nu} \qquad (2.2.3)$$

Very little information, on velocity profile, is available, because the thickness of the liquid film is very small. In general the profile predicted by the Nusselt model has been validated for laminar flow regimes. However, for stationary systems semi-parabolic behaviour was reported by Wilkes et al (66) and Cook et al (23). This behaviour was predicted by the measurement of the velocity of the thin and the falling films.

2.2.4. The Film Thickness

The estimation of the film thickness as a function of radial position, rotational speed, flow rate, and rheological properties of the liquid has been based on the equation (2.2.3). The average velocity '$\bar{u}_r$' is redefined in terms of flow rate per unit area and equating with equation (2.2.3). i.e.

$$\bar{u}_r = \frac{Q}{2\pi r \delta} = \frac{\omega^2 r \delta^2}{3\nu}$$

$$\text{or } \delta = \left(\frac{3}{2\pi} \frac{Q\nu}{r^2\omega^2}\right)^{1/3} \qquad (2.2.4)$$

A non-dimensional form of equation (2.2.4) may be expressed as;

$$\frac{\delta}{r} = \left(\frac{3}{2\pi}\right)^{1/3} \left(\frac{Q\nu}{\omega^2 r^5}\right)^{1/3} \qquad (2.2.5)$$

Defining two dimensionless groups, (i.e. $Re = \frac{Q}{r\nu}$ and $Ta = \frac{\omega r^2}{\nu}$) the above equation can be written as;

$$\left(\frac{\delta}{r}\right) = \left(\frac{3}{2\pi}\right)^{1/3} (Re/Ta^2)^{1/3} \qquad (2.2.6)$$

Where Re = modified Reynolds number for disc flows

Ta = the Taylor number

This simple model neglects the effect of Coriolis force, which increases the variations in the tangential velocity of the film. Therefore, the film thickness could be greater than that predicted by equation (2.2.6).

Much experimental work has been devoted to the measurement of film thickness and other film parameters. Table 2.1 presents a selection of this work and figure 2.1 (a) shows the comparison of some of the more reliable data with the simple model. Bell (6) has shown that great care must be taken in the assessment of such data since many factors particularly the introduction

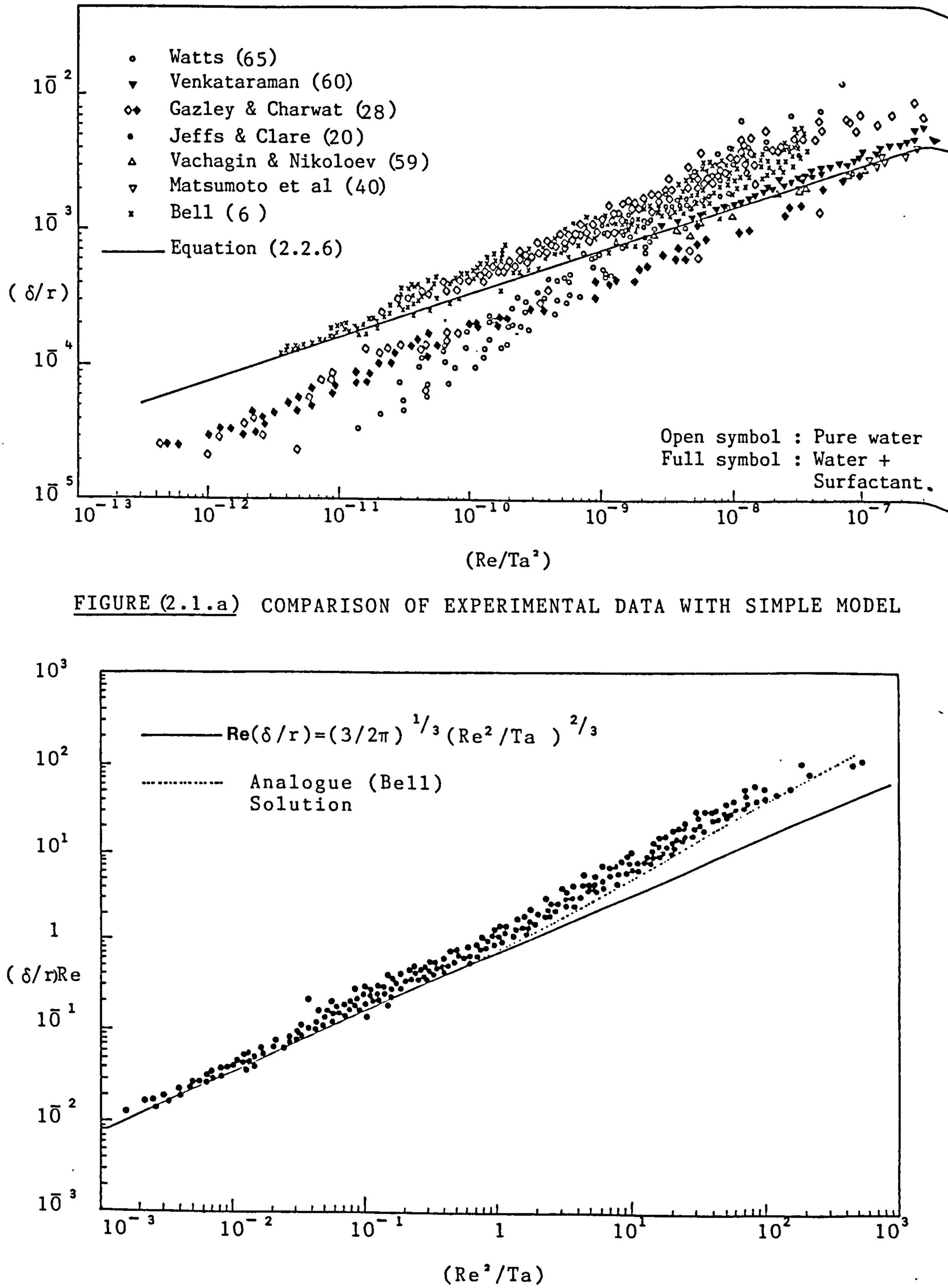

FIGURE (2.1.a) COMPARISON OF EXPERIMENTAL DATA WITH SIMPLE MODEL

FIGURE (2.1.b) FILM THICKNESS MEASUREMENT

TABLE 2.1. FILM THICKNESS MEASUREMENT TECHNIQUES

	TECHNIQUE	REFERENCE	REMARKS
(1)	Weighing of liquid drains	Warden (64) Fallah et al (26) Fulord (27)	Simple but special precautions have to be taken on the design of the distributor to avoid erroneous high drainage.
(2)	Shadow photographs	Brauer (8)	Very complicated, suitable for film thickness measurements only on stationary systems.
(3)	Weighing the hold-up	Kamei et al (33)	Simple but not accurate.
(4)	Infra-red light absorption	Stainthorp et al (55) Stainthorp and Allen (54) Charwat et al (17)	Accurate and suitable but dye may have to be added to enhance the sensitivity of the output.
(5)	Photographic method	Muenz et al (41) Clegg (22)	Complicated but accurate.
(6)	X-Ray	Solesiol (50)	Complicated and expensive.
(7)	Electrical conductivity method	Clare & Ashwood(19) Clare & Jeffs (20) Telles & Ducker (57)	Electrolyte is required.
(8)	Radioactive method	Jackson (31)	Complicated and expensive.
(9)	Capacitive technique	Venkataraman (60) Bell (6) Jazayer (32) Black (7)	Accurate and simple.
(10)	Micrometer probe with contact sensor	Espig & Hoyle(24)	The spray due to rotation or high voltages can increase the error.

of liquid to the disc surface can effect film conditions. In the presentation of film thickness data, the parameter Re/Ta^2 does not indicate the influence of the Coriolis force. Porter and Bell (45) noted that this effect should be negligible for Re^2/Ta less than 1. Bell's data are shown in figure 2.1.(b), which emphasise this point. The upper characteristic is an analogue solution for the flow equations including the Coriolis force.

2.2.5. Flow Regimes Associated With Flow On A Rotating Disc

The simple model described in the previous section does not explain the actual conditions which prevail on the rotating disc. Under certain conditions the 'smooth' film can exist,the film thickness and other parameters noted in the previous sections being presented with confidence. However, it should be recognised that a variety of flow regimes, related to flow rate, disc speed and the rheological properties of the liquid, are possible. These are shown, for water, in figure 2.2 (Bell) and can be summarised as follows.

(i) Broken film regime, at very low flow rates, a continuous film can not be established and the liquid flows in discreet rivulets across the disc.

(ii) Smooth film zone (without ripples), at low rotational speed and high flow rates, the entire surface of the disc is covered by a smooth film.

(iii) Fairly regular ripples, increasing the rotational speed a distinct change in the flow pattern is observed. The smooth film zone occupies the central part of the disc, while the outer surface of the disc is superimposed with regular ripples.

(iv) Extremely agitated ripples, further increase in the rotational speed causes reduction in smooth film zone. The regular

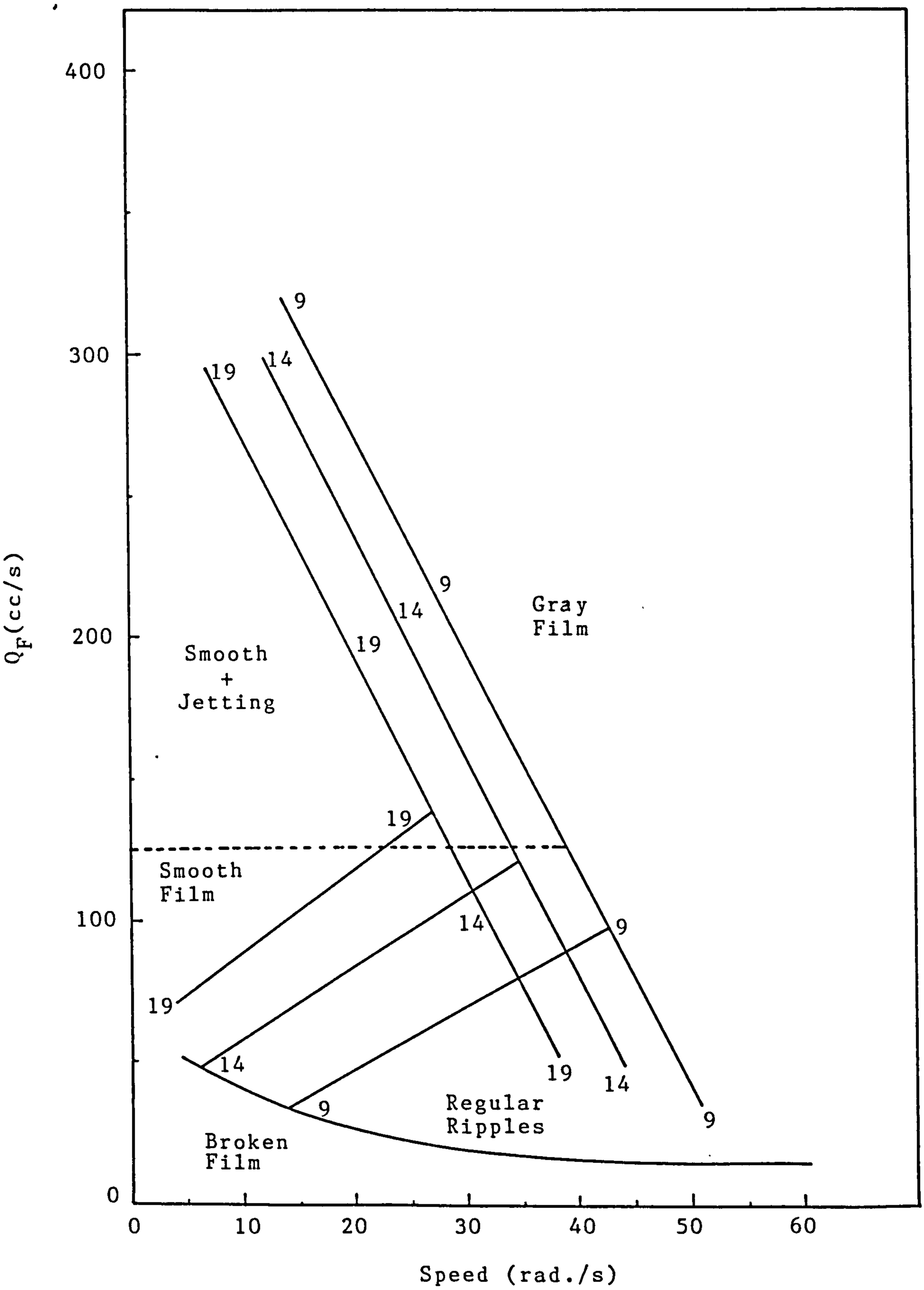

FIGURE 2.2. IDENTIFICATIONS OF VARIOUS FLOW REGIMES

ripples are also limited to a narrow region. The film appears to be extremely agitated in the rest of the disc. This zone of randomly distributed ripples is knownas the 'Gray Film' regime. It is a marked contrast to the smooth film in which the surface appears very agitated and the reflections from the polished disc surface are not visible.

(v) Jetting; high flow rates produce vigorous jetting at the inlet point. Jetting strongly depends on the geometry of the liquid distributor.

For practical applications the 'Gray film' is the most appropriate regime to support the higher heat/mass transfer rates.

Attempts to generalise these regimes are still incomplete, however some approximations are possible. Brauer (8) defined the following condition for various flow regimes, in the light of Nusselt (44) and Kapitsa (34) theories;

$Q'/\nu<4$;	the flow is strictly laminar and smooth (Nusselt theory)
$4\leq Q'/\nu<10$;	Undulations across the films (Kapitsa theory)
$10\leq Q'/\nu<20$;	Sinusoidal waves gradually replaced by regular waves.
$20\leq Q'/\nu$;	Random waves.
Where Q' =	Volumetric flow rate per unit length of the flow perimeter.

2.3. HEAT TRANSFER IN THIN FILMS FORMED BY ROTATING DISCS

Research activities, aimed at applying a new concept in heat transfer in which the overall resistance to heat flow is decreased by utilizing thin films, has been an area of interest for many years. Rotation of heat transfer surfaces is one technique in achieving such films. Discs have been employed by several investigators for heat transfer studies. A considerable amount of literature concerning heat transfer with phase change has been published, whilst little has been reported in connection with sensible heat transfer. The literature with respect to both has been reviewed in the following sections.

2.3.1. Sensible Heat Transfer

A preliminary study was made by Rees (46) and a model to calculate the overall heat transfer coefficient was developed, assuming that;

(a) the simple laminar flow model could accurately describe fluid dynamics of a rotating disc;

(b) the temperature profile within the liquid film was represented by the following cubic polynomial and was assumed to be applicable at all radii;

$$T = T_o + aZ + bZ^2 + cZ^3$$

The coefficients a,b,c were determined for the following boundary conditions;

(i) $T = T_o$ and $\frac{d^2T}{dZ^2} = 0$ at $Z = 0$

Since the fluid in contact with the surface was at rest and heat flow in the vicinity of the disc surface would be by thermal conduction. Thus, heat flux is given by;

$$q = -K(dT/dZ)\,|_{Z = 0} \qquad (2.3.1)$$

(ii) $T = T_\delta$ and $\frac{dT}{dZ} = 0$ at $Z = \delta$

Since the temperature for a differential element was assumed to be constant.

The temperature profile for these conditions was determined, i.e.

$$\left(\frac{T-T_o}{T_\delta-T_o}\right) = \left(\frac{3}{2}\frac{Z}{\delta} - \frac{1}{2}\frac{Z^3}{\delta^3}\right) \qquad (2.3.2)$$

The velocity profile, Nusselt model (44) for laminar flow conditions gives,

$$\frac{u}{u_\delta} = \left(\frac{2Z}{\delta} - Z^2/\delta^2\right) \qquad (2.3.3)$$

The physical properties were assumed to be independent of temperature and the values were read at the mean temperature, i.e.,

$$T_m = \left(\int_0^\delta uTdZ\right)/\int_0^\delta udZ$$

$$\text{Rate of heat transfer} = -KA\left(\frac{dT}{dZ}\right)\Big|_{Z=0} = h\,A(T_m-T_o) \qquad (2.3.4)$$

The film coefficient for the conditions described above, was found to be;

$$h = \frac{120}{61}(K/\delta) \qquad (2.3.5)$$

where $\delta = \left(\frac{3}{2\pi}\,\frac{Q\mu}{r^2\omega^2\rho}\right)^{1/3}$ (defined in Section 2.2.4.)

For a liquid-liquid heat exchanger the overall heat transfer coefficient can be defined as;

$$U = \frac{1}{r_o^2-r_i^2}\int_{r_i}^{r_o} r\left[\frac{1}{\frac{1}{h_H}+\frac{1}{h_c}+X_m/K_m}\right]dr \qquad (2.3.6)$$

The solution of the above integral equation for the conditions described above, provides the following correlation for the

estimation of overall heat transfer coefficient;

$$\frac{1}{U} = \frac{61}{90}\left[\frac{r_o^2-r_i^2}{r_o^{8/3}-r_i^{8/3}}\right]\left[\left(\frac{3\mu Q}{2\pi K^3\omega^2}\right)_H^{1/3} + \left(\frac{3\mu Q}{2\pi K^3\omega^2}\right)_C^{1/3}\right] + \frac{X_m}{K_m} \qquad (2.3.7)$$

Where H, & C stands for hot and cold liquids, respectively.

Rees verified experimentally the reliability of the model. The predicted values were very much higher when compared to the experimental data. However, the dependence on the rotational speed was found to be correct, whilst the inverse relation with flow rate could not be established experimentally.

Wood and Watts (67) developed an alternate model, in which entry effects were included and the temperature profile within the liquid film was estimated by the following simplified version of the energy equation;

$$\left(\frac{\delta T}{\delta r}\right) = \left(K/\rho C_p u\right)\frac{d^2T}{dZ^2} - \left(\frac{w}{u}\right)\frac{dT}{dZ} \qquad (2.3.8)$$

where w = normal velocity of the liquid film.

u = radial velocity of the liquid film.

This parabolic partial differential equation was solved numerically to determine the temperature profile in developing regions. Hence, rate of heat transfer and overall heat transfer coefficient can be determined. The experimental data, obtained by Watts (65) were also compared with the model developed by Rees (46). It was established that the higher discrepancies at lower rates, could be due to incomplete wetting of the heat transfer surface. At higher flow rates, a close agreement or even higher values were found. It was suggested that the experimental results are most probably influenced by the ripples on the liquid side which become more pronounced at higher flow rates. Such ripples would

enhance the rate of heat transfer and therefore this effect may provide an explanation for the increase in transfer coefficient with increase in flow rate.

Another heat transfer model, based on experimental data, was developed by Bell (6). The data were collected for steam-water system and the disc surface temperatures were measured at six radial positions. Since the direct measurement of the film temperature was likely to disturb the liquid film, the temperature was calculated by heat balance between the heat supplied and heat gained for the inlet and outlet conditions of the fluids. For this purpose, the disc was divided into six heat transfer areas and the condensate was collected for each area to determine the quantity of heat supplied. These, indirectly estimated film temperatures were used for heat transfer calculations and the following model, representative of the data to ± 50 per cent, was proposed;

$$Nu = 10^{-2} (Re^2/Ta)^{1/2} (r/R)^{3/2} (Pr)^2 \qquad (2.3.9)$$

The range of variables appropriate to this correlation are given below;

$$0.05 < Re^2/Ta < 3000$$

$$1.33 < r/R < 4.66$$

$$2.2 < Pr < 8.2$$

It should be noted that this correlation was presented for <u>all</u> heat transfer data recorded by Bell. It was suggested that these data included those experiments in which wetting of the heat transfer surface was not necessarily 'complete'. In this case evaluation of the heat transfer coefficient, based on the projected area of the rotating surface would produce low values. This may account for some scatter in the data.

Recently, Surzhik and Pukhovoi (56) studied the effect of operating parameters on the rate of heat transfer in a liquid film on a rotating surface. An aluminium disc of 0.5m diameter was used as a test surface. It was concluded that the rate of heat transfer increases with increasing rotational speed, probably due to the increase in liquid velocity and thinning of the liquid film. It was recommended that this information may be useful for the estimation of the optimum operating conditions of the thin film heat exchangers.

2.4. HEAT TRANSFER WITH PHASE CHANGE

A chronological survey of the studies concerning evaporation and condensation on a rotating disc is presented in the following sections.

2.4.1. Thin Film Evaporation

Various aspects of thin film evaporation have been investigated by several workers in connection with sea water desalination. The concept of thin film evaporation has developed progressively over a century. Some of the stages, in this context, have been listed below.

As early as 1863 common salt was produced by evaporating sea water in shallow brine pans under the sun. A large installation in the San-Francisco Bay is a witness to the fact that this type of evaporation still has some commercial importance. A technique to enhance the rate of evaporation by addition of heat absorbent dyes has been used in Isreal, Western India and Australia (30).

The earliest type of an evaporator reported in the literature involved steam heated double walled or coil type pans. Many subsequent improvements, in design as well as in operation have been introduced since then. In 1813, vacuum pan designed by

Haward was a major improvement in this context. The first, tubular evaporator was designed by Rillieux in 1851 (36). It was novel in design, and efficient in performance at that time. Since then a number of developments have been introduced to these basic types of evaporators.

More often, efforts have been focussed to improve heat transfer coefficients, to prevent scale formation, and to preserve product quality. Robert changed the geometry of the calanderia and forced circulation was employed to viscous solutions, which greatly improved the film coefficient. Another marked improvement was achieved by Kestner in 1899 who introduced climbing film evaporator (39). In this device the 'climbing' evaporating film, was induced by vapour drag. The saturated liquid feed is introduced to the bottom of the heated evaporator tube. Vapour generated over a relatively short length of the evaporator tube produces an annular flow regime over the remainder of the tube. Therefore, the major evaporation from the feedstock occurs in this region, i.e. the climbing film region, with liquid film flow induced by the high velocity vapour core. Due to the considerable improvement in film coefficients in such units, they became the workhorse of chemical industries. Kestner's thin film concept was further improved by Muller in 1940, who used falling film technique for evaporation. It was one of the most efficient methods for viscous solutions.

The first rotating thin film evaporator was developed by Hickman in 1957, a conical rotor was used for this purpose. A rotating disc multi-effect evaporator was designed and operated by Clark and Bromley (21), in 1961.

Subsequent developments in this area are discussed in the following section.

2.4.2. Rotating Disc As An Evaporating Surface

The basic study of Hickman (29) on condensation of steam, and the desalination of sea water in a rotating still was the first major contribution to the technology of rotating heat exchangers. This device consisted essentially of an inverted rotating cone with steam condensation on the outer surface, giving rise to evaporation of sea water flowing across the inner surface. A thin film in the range of 0.01 to 0.05 mm was maintained due to centrifugal action. The unit was operated successfully and the overall heat transfer coefficient was found to be 5 to 10 times higher than that obtained for a stationary unit.

Bromley (9) derived a correlation to predict overall heat transfer coefficient for the device used by Hickman.
To proceed with the derivation, Bromley used the following assumptions:

(i) The both films (i.e. evaporating and condensing) were exhibiting viscous flow behaviour.

(ii) There was no nucleation (bubble or drop formation) in the evaporating film.

(iii) No inert gas was present.

(iv) Conduction was the mode of heat transfer.

(v) Acceleration due to gravity 'g' was replaced by $4\pi^2 r N^2 \mathrm{Sin}\phi$.

(vi) The velocity profile was fully developed at any radius.

The following correlation for these conditions, was derived to determine $\overline{U}$;

$$\overline{U} = 1.37 \left(\frac{\rho^2 K^3 N^2 D_o^2 \ \mathrm{Sin}\ \phi}{W_F \mu}\right)^{1/3} \qquad (2.4.1)$$

where $\overline{U}$ is the overall heat transfer coefficient based on the liquid feed and condensate films only. If the metal wall has appreciable thermal resistance, the true value of the overall coefficient 'U' can be calculated from;

$$\frac{1}{U} = \frac{1}{\overline{U}} + \frac{X_m}{K_m} \qquad (2.4.2)$$

The values predicted by the equation (2.4.1) were compared with the Hickman's experimental data. The values ranged from +71 to -32%. The maximum deviation was observed either at low temperature difference or at very low product rates. Bromley explained that the deviation at low temperatures could be due to the omission of thermal resistance at the vapour-liquid phase boundary. However, it was suggested that generally the agreement was satisfactory, and the proposed mechanism of heat transfer calculation seemed to be reasonable.

Buckel et al (11) performed a series of experiments and they confirmed Bromley's model. Experimental results presented by Bromley, Humphery and Murray (10), were 6 to 12% below those values predicted by equation 2.4.1. They suggested the omission of the effect of liquid circumferential motion could be one reason for the discrepancy. Nevertheless, inspite of these small variations, the model provides a good basis to approximate the film coefficients for the design of such devices.

Clark and Bromley (21) developed a multiple effect rotating evaporator and employed a linearization technique for data analysis. A close agreement was found between the measured and theoretical results over a wide range of flow rates and rotational speeds, which confirmed the reliability of this technique.

Since 1970, Butuzov's group has published a series of articles in this area. A number of contributions have been listed in Table 2.2, a brief review of their work concerning thin film evaporation is presented here.

Butuzov et al (12 , 13) published a concise survey of the available literature together with a detailed description of their test facility. It was designed to desalinate sea water using dry saturated steam. This set-up was used by Butuzov and Rifert (14) and the results were correlated to an accuracy of ± 20% by the following equation:

$$\bar{h}_e(r_o/K) = 0.256 \left(\frac{\omega r_o^2}{\nu}\right)^{0.44} (Pr)^{0.35} \qquad (2.4.3)$$

Butuzov and Rifert (15) derived the following relationship assuming that radial velocity is very small compared to circumferential component;

$$\bar{h}_e = 1.54\ \phi_1\phi_2(h_{fg}{}^3\omega^2 r_o^2 \rho/W_F\nu)^{1/3} \qquad (2.4.4)$$

where $$\phi_1 = \frac{(W_D/W_F)}{1-(1-W_D/W_F)^{4/3}}$$

$$\phi_2 = [1-(r_i/r_o)^{8/3}] \Big/ [1-(r_i/r_o)^2]$$

The experimental data from previous study (14) was found to be scattered in the range of +30 to -25% of the curve obtained using this equation, and no explanation was given in this regard.

Rifert (47) developed another correlation, where the turbulent effects were considered, i.e.,

$$\frac{\bar{h}_e}{K}\left(\frac{\nu^2}{r\omega^2}\right) = 0.42 \left[\frac{1-(r_i/r_o)^{8/3}}{1-(r_i/r_o)^2}\right] \left[\frac{K_r}{1-(1-\frac{K_r}{2})^{4/3}}\right] (Re)^{-1/3} \qquad (2.4.5)$$

where $K_r = [2\pi q(r_o^2 - r_i^2)] / (h_{fg} W_x)$

q = heat flux W_x = Mass flow rate at any point x

Experimental data (14) was found to be very close (±8%) when compared with the values obtained by the above equation. It was probably due to inclusion of turbulent effects in the theoretical model. Barabash, Muzhilk and Rifert (4) also confirmed this model on the basis of their experimental data.

Wang, Greif and Laird (63) correlated the data obtained for a copper disc rotating in a steam chamber, to an accuracy of ±22% by the following equation;

$$\frac{h_e(\nu/\omega)^{1/2}}{K}\left[\frac{C_p(\Delta T)}{h_{fg}Pr}\right]^{-0.065} = 5.23 \qquad (2.4.6)$$

The main objective of this study was to investigate the influence of wipers on evaporating film formed by rotating discs. Details in this context are given in the following section.

2.4.3. Improvements In Rotating Film Evaporators

Two techniques, to improve the performance of such units, have been the subject of several investigations. These are, modification of heat transfer surface, and introduction of mechanical devices i.e., fixed wiping blades.

A series of experiments were performed by Bromley, Humphereys and Murray (10), using a number of rough surfaces of different configuration. The surface, which was gritted with a coarse sand paper, improved the overall heat transfer coefficient some 8 to 10%, compared to smooth rotating discs. Whilst mechanically grooved surfaces improved condensing film coefficient by 13%, but adverse effects were noted on evaporating film coefficients, probably due to liquid accumulation in the grooves.

The importance of the mechanical wipers has been recognised by many investigators because relatively high film coefficients can be achieved with the added bonus of self cleaning effects. Tleimat (58) and Wang (6) introduced this technique to rotating disc evaporation. A significant improvement in evaporating film coefficients was observed. Under certain conditions, over-all heat transfer coefficients were approximately double than those reported by Hickman (29) for similar conditions.

Wang (61) compared the performance of a rotating film evaporator, performing a series of experiments with and without wipers. Wang, Greif and Laird (63) published that the overall heat transfer coefficients for a wiping film improved 2 to 3 times, compared to the non-wiping conditions.

TABLE 2.2. SUMMARY OF HEAT TRANSFER STUDIES (WITH PHASE CHANGE) ON ROTATING SURFACES

INVESTIGATOR	NATURE OF INVESTIGATION		PROCESS		PROCESS CONDITIONS			MODEL/CORRELATION
	Theo.	Exp.	Cond.	Evap.	rpm range	Test Fluid	Test Surface	
Hickman (29)	-	*	*	*	400- 700	W & S	Inverted Cone	
Bromley (9)	*	-	*	*	-	W & S	Inverted Cone	$\bar{U} = 1.37 \left[\frac{K^3\rho^2N^2D_o \sin\phi}{W_F\mu}\right]^{1/3}$
Clark & Bromley (21)	-	*	*	*	700-1700	W & S	Multiple Disc	
Sparrow & Gregg (52)	*	-	*	-	-	V	Disc	$\frac{h_c(\nu/\omega)^{1/2}}{K} = 0.904 \left[\frac{Pr}{(C_p\Delta T/h_{fg})}\right]^{1/4}$
Nandapurkar & Beatty (42)	-	*	*	-	470-2400	OV	Disc	$h_c = 2.14N^{0.425}\left[\frac{K^3\rho^2h_{fg}}{\mu\Delta T}\right]^{1/4}$
Espig & Hoyle (25)	*	*	*	-	150-2200	S	Disc	$h_c = \frac{0.903}{\Delta T}\left[\frac{h_{fg}\rho^2K_c^3\omega^2\Delta T^3}{\mu}\right]^{1/4}$
Butuzov & Rifert (16)	*	-	-	*	-	W	Disc	$h_e = 2.18\left[\frac{K^3\rho^2N^2r_o^2}{W_F\mu}\right]^{1/3}$
Astaf'ev & Baklastov (3)	*	*	*	-	30- 750	S	Disc	$Nu = 1.38\,(Pr)^{0.25}(Ta)^{0.43}$
Chiranjivi & Apparo (18)	*	-	*	-	-	V	Disc	$\frac{h_c(\nu/\omega)^{1/2}}{K}\left[\frac{C_p\Delta T}{h_{fg}Pr}\right]^{1/4} = 1.15\left[\frac{\beta}{2.5+1.5\left(\frac{C_p\Delta T}{h_{fg}\beta Pr}\right)}\right]^{1/4}$

* Indicates; investigations have been carried out in that area.

W - Water V - Vapours

S - Steam OV - Organic Vapours

INVESTIGATOR	NATURE OF INVESTIGATION		PROCESS		PROCESS CONDITIONS			MODEL/CORRELATION
	Theo.	Exp.	Cond.	Evap.	rpm range	Test Fluid	Test Surface	
Butuzov et al (13)	*	*	-	*	200-2000	W	Disc	$h_e \left(\frac{r_o}{K}\right) = 0.256 \left(\frac{\omega r_o^2}{\nu}\right)^{0.44} (Pr)^{0.35}$
Butuzov & Rifert (14)	*	*	*	-	200-2000	S	Disc	$\frac{\bar{h}_c \Delta T r_o}{2\rho r_i \nu} = 0.452 \left[\frac{1}{Ta^{0.33}} \frac{K\Delta T}{h_{fg}\rho\nu}\right]^{3/4}$
Rifert (47)	*	-	-	*	-	-	Disc	$Nu = \frac{0.42\ K_r^{4/3} f\left(\frac{r_i}{r_o}\right) Re^{-1/3}}{1-\left(\frac{K_r}{2}\right)}$ where $K_r = \frac{2\pi q(r_o^2 - r_i^2)}{h_{fg} G_F}$
Butuzov & Rifert (15)	*	-	-	*	-	-	Disc	$\bar{h}_e W_F^{1/3} = 1.25 \left(\frac{K^3 r_o \rho}{\nu}\right)^{1/3} (\omega)^{2/3}$
Beckett et al (5)	-	*	*	-	400-1600	V	Disc	$Nu = \frac{2}{3} Re^{1/2} \left(\frac{C_p \Delta T}{Prh_{fg}}\right)^{1/4}$
Wang, Greif & Laird (63)	-	*	-	*	300- 500	W	Disc (With & Without Wiper)	$\frac{h_e(\nu/\omega)^{1/2}}{K} \left[\frac{C_p \Delta T}{h_{fg} Pr}\right]^{-0.065} = 5.23$
Rohsenow & Hartnett (49)	*	-	*	-	-	V	Disc	$h_c = \left(\frac{2K^3 h_{fg} \omega^2 \rho^2}{3\Delta T \mu}\right)^{1/4}$
Tleimat (58)	-	*	*	*	200- 800	W	Disc with Wipers	$U = \frac{K_m/\delta}{1+\frac{K_m C_2 \Delta T^{0.5}}{\omega^{0.5}\delta_m}\left[1+\frac{K_c}{K_d}(\delta_d - C_1 \Delta T_c^{0.5})\right]}$

2.5. CONDENSATION PROCESS

2.5.1. Introduction

Condensation occurs when the temperature of a vapour is reduced below its saturation temperature. In engineering practice this process occurs, generally when the vapours come in contact with a surface whose temperature is less than the saturation temperature. Condensation may occur in one of two possible ways, depending on the surface condition. The dominant form of condensation is one in which a continuous film covers the entire surface and under the action of gravity the film flows continuously from the surface. Film condensation is generally characteristic of the clean, uncontaminated surface. However, if the surface is coated with certain substances (e.g. Silicones, Teflons, Waxes and Fatty Acids), which inhibit surface wetting, or certain chemicals are included in the vapour phase, it is possible to maintain dropwise condensation. Although it is desirable to achieve dropwise condensation in industrial applications, it is often difficult to maintain such conditions. For this reason, and because the heat transfer coefficient for film condensation are usually much smaller than those for the dropwise mechanism, 'safe' design calculations are often based on the assumption of film condensation. In order to evaluate film coefficients, the first useful analysis was made by Nusselt (44). This analysis was based on laminar flow in the condensate film, zero shear at the condensate/vapour interface, with heat transfer controlled by conduction through the condensate film. The analysis produced the following expression to estimate local heat transfer coefficient for a vertical surface.

$$h_x = \left[\frac{g(\rho_c - \rho_v)K_c^3 h_{fg}}{4\nu_c (T_s - T_o)x}\right]^{1/4} \qquad (2.5.1.)$$

since, the local heat transfer coefficient, h_x, depends on $x^{-1/4}$; it follows that the average film coefficient for the entire surface can be defined,

$$h_m = \frac{1}{L}\int_0^L h_x \, dx = \frac{4}{3} h_L \qquad (2.5.2.)$$

For an inclined surface, at an angle 'ϕ' to the horizontal, equation (2.5.1) can be used with 'g' replaced by g sin ϕ.

Many experiments have been reported concerning condensation of pure saturated vapours on vertical, inclined and horizontal surfaces. Reasonable agreement between measured and predicted values has been found for $Re<40$.

where $Re = 4M/\mu$,

For $40<Re<2000$ the flow within the film is thought to remain laminar, however measured heat transfer coefficients are some 25-30% higher than those predicted by equation 2.5.1. Observations of the condensate films indicate that in this range of Reynolds number the surface of the film becomes wavy. This modified flow regime is thought to contribute to the increased heat transfer for $Re>2000$, the film is considered to be turbulent with heat transfer coefficients considerably higher than those for the laminar regimes.

Numerous investigators have modified the Nusselt analysis to account for such effects, as the sensible heat content of the condensate film, interface shear stress etc (38 , 48 , 51). All these extensions were for the condensation process driven by the gravitational field ($g = 9.81\ m/s^2$). In general these 'corrections' do not change the nominal values of coefficient

by a significant amount. Major changes in heat transfer can result only with change in the basic hydrodynamics of the film. In this context, film thinning and therefore higher heat transfer can be achieved by increasing 'g' i.e. inducing high values on rotating surfaces ($g \rightarrow r\omega^2$). Further improvement might be achieved by a combination of effects, say high 'g' environments with modified surface structures. These effects will be reviewed in the subsequent sections.

2.5.2. Condensation On A Rotating Disc (Theorectical Developments)

Sparrow and Gregg (52) were the first to make an analysis of the thin film condensation on a rotating disc. Despite the complexities associated with this type of condensation; a useful correlation was obtained by making the following assumptions;

(i) Laminar flow in the condensate film.

(ii) Constant physical properties.

(iii) The effects of bouyancy, viscous dissipation and shear at the condensate - vapour interface were neglected.

The Navier-Stokes equations together with the energy equation were solved for these conditions and the following correlation was developed;

$$Nu = \frac{h(\nu/\omega)^{1/2}}{K} = \frac{2^{1/4}}{3}\left[\frac{Pr}{(C_p \Delta T / h_{fg})}\right]^{1/4} \qquad (2.5.3)$$

The validity of this equation was recommended for a wide range of Prandtl number (i.e. $0.003 \leq Pr \leq 100$).

Experimental verification of this correlation was made by Nandapurkar and Beatty (42). A series of experiments were performed, where pure organic vapours were allowed to condense

on a water cooled disc, rotating about a vertical axis. The temperature of the condensate film and the surface temperature were measured at a number of locations to calculate film coefficients. The experimental data were found to be 25 to 30 per cent below the values predicted by equation (2.5.3). Nandapurkar and Beatty suggested that this discrepancy could be due to the assumption concerning the shear stress at liquid-vapour interface.

Sparrow and Gregg (53) reconsidered their previous model to investigate the influence of this force. A correction factor [i.e. $(\rho\mu)_\ell / (\rho\mu)_v$] was introduced to the equation 2.5.3, and predictions were made using both models. Comparison of the predicted values indicated that there is no significant influence of such forces. They gave a physical reason that when the vapour density and viscosity are very small, the vapour drag would play a minor role. Conversely the effects of vapour drag should increase as $(\rho\mu)_\ell / (\rho\mu)_v$ decreases.

In figure 2.3, the values predicted from these two models have been plotted together with the data obtained, using the following model result which was proposed by Chiranjivi et al (18) which also dealt with the effect of interfacial shear forces.

$$\frac{h(\nu/\omega)^{1/2}}{K}\left[\frac{(C_p\Delta T/h_{fg})^{1/4}}{Pr}\right] = 1.15\left[\frac{\beta}{2.5+1.51\left(\frac{C_p\Delta T}{h_{fg}}\right)\left(\frac{1}{\beta Pr}\right)}\right]^{1/4} \quad (2.5.4)$$

$$\text{where} \quad \beta = 1 + \frac{82}{210}\,(C_p\Delta T/h_{fg})$$

A trial and error technique was employed by Chiranjivi et al, where they used various velocity profiles in the film

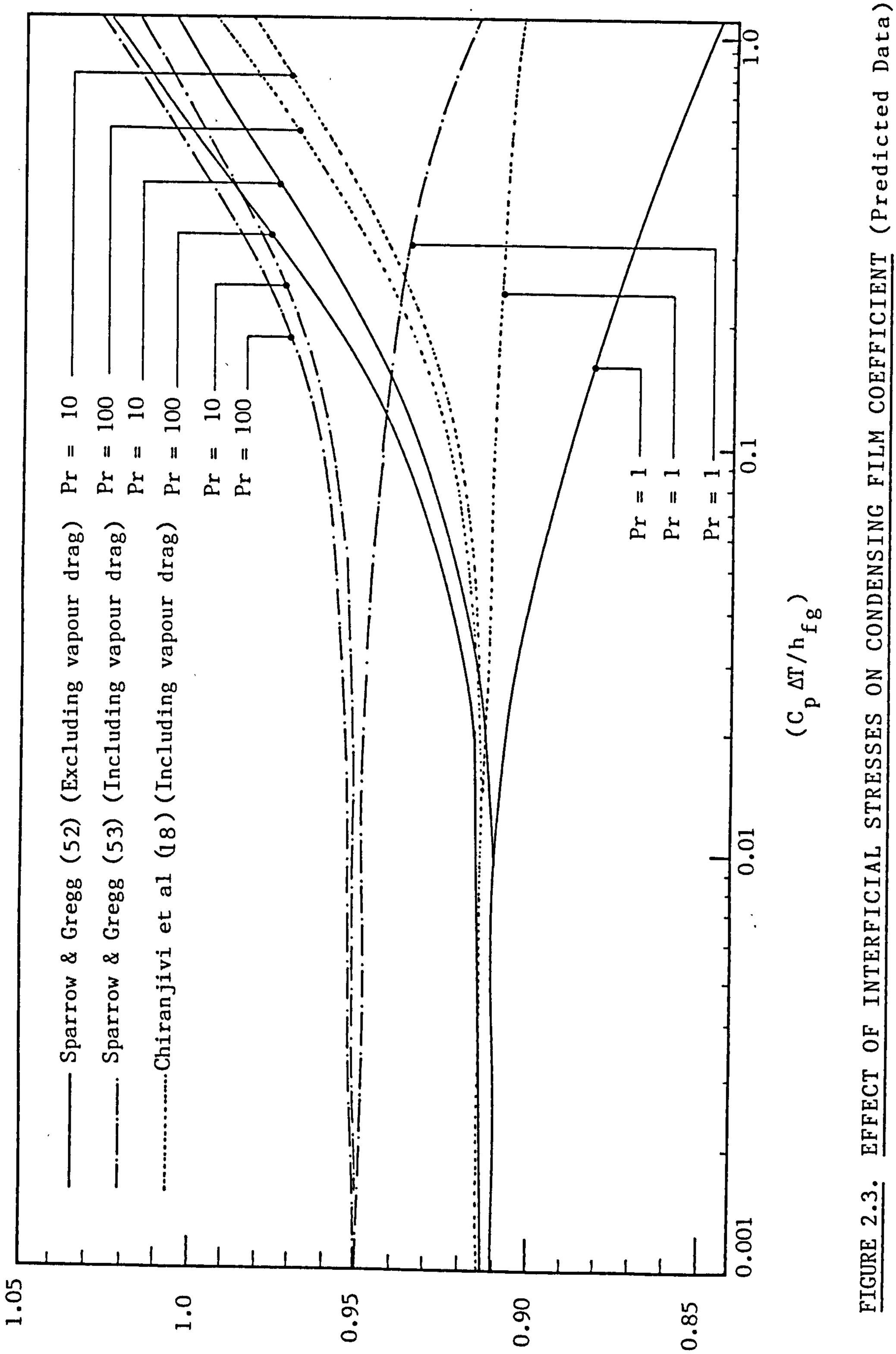
1.05
1.0
0.95
0.90
0.85
0.001
0.01
0.1
1.0
$[\left(\frac{h_c(\nu/\omega)^{\frac{1}{2}}}{K}\right)\left(\frac{C_p\Delta T/h_{fg}}{Pr}\right)^{\frac{1}{4}}]$
$(C_p\Delta T/h_{fg})$
Pr = 1
Pr = 1
Pr = 1
Pr = 10
Pr = 100
Pr = 10
Pr = 100
Pr = 10
Pr = 100
—— Sparrow & Gregg (52) (Excluding vapour drag)
—.— Sparrow & Gregg (53) (Including vapour drag)
—.·.— Chiranjivi et al (18) (Including vapour drag)
EFFECT OF INTERFICIAL STRESSES ON CONDENSING FILM COEFFICIENT (Predicted Data)

FIGURE 2.3.

to solve the simple energy balance equation, to develop the above expression. It was recommended to be applicable for a wide range of Prandtl number i.e. $1<Pr<100$.

It is apparent from figure 2.3, that maximum difference between the values predicted by Sparrow and Gregg's models (52 , 53) and those obtained by equation (2.5.4) occurs when $Pr = 1$ and $C_p \Delta T/h_{fg} = 1$. Therefore, the predictions from this equation would seem to be inaccurate for the liquids whose Prandtl number is less than 1. Another analysis valid for $Pr<1$, was made by Apparo et al (1), again interfacial stresses were considered in this analysis. The theoretical results were found to be 5 to 10 per cent lower than those predicted by Sparrow and Gregg's model. In general, the influence of such interfacial stresses seems to be very small.

Beckett et al (5) explained that the disagreement between Sparrow and Gregg's (52) theoretical values and the experimental data presented by Nandapurkar and Beatty, could be due to the presence of non-condensable gases on the condensing surface. Wang and Greif (62), on experimental evidence, validated the model proposed by Sparrow and Gregg, again suggesting that the data of Nandapurkar and Beatty might be subject to experimental errors.

Rohsenow and Hartnett (49) applied a force balance, considering shear and centrifugal forces on a differential element for a disc rotating about a vertical axis and the following expressions were developed;

$$\delta = (3K\Delta T \mu/2h_{fg}\omega^2\rho^2)^{1/4} \qquad (2.5.5)$$

$$h = \left(\frac{2K^3 h_{fg} \omega^2 \rho^2}{3 \Delta T \mu}\right)^{1/4} \qquad (2.5.6)$$

However, Rohsenow and Hartnett suggested that the analysis presented by Sparrow and Gregg is more comprehensive where momentum and convective terms have also been included.

2.5.3. Condensation Of Steam On A Rotating Disc (Experimental Investigations)

In conditions of steam condensation on a rotating surface, the heat flux is dependant on the following variables;

(i) Nature of steam i.e. dryness and saturation temperature.

(ii) The difference between the steam temperature and that of the condensing surface.

(iii) Rotational speed.

(iv) Nature and shape of the rotor.

(v) Radial position.

Hickman (29), in studying the evaporation of sea water, investigated the influence of these variables where dry and saturated steam was allowed to condense on a conical rotor. The results were presented in terms of an overall heat transfer coefficient. The theoretical assesment made by Bromley (9) is detailed in section 2.4.2. In this study overall performance of the unit was investigated, individual coefficients were not reported. Espig and Hoyle (25) performed a series of experiments on a water cooled disc, which was rotating in a chamber filled with dry, saturated steam. The experimental data were best correlated by;

$$(h/h_i) = 113/\omega^{0.415}(\Delta T)^{0.6} \qquad (2.5.7)$$

where h_i = coefficient of heat transfer to an isothermal surface.

A theoretical model, similar to equation (2.5.6), was developed, neglecting the shear forces at the vapour/condensate interface. Experimental and theoretical values from equation (2.5.6) were compared with Sparrow and Gregg's findings. Theoretical results obtained from both models were in good agreement, but the experimental data were found to be higher than predicted values. It was suggested that it could be due to instability of the condensate film, for example wave formation.

Astaf'ev and Baklastov (2) studied the condensation of steam on the underside of a horizontal disc. It was observed that the film coefficient had a varying dependency on rotational speed. When the disc speed was less than 300 rpm, condensate drops tended to fall from the disc surface rather than flow radially. For speeds greater than some 600 rpm, a continuous film was observed and the data were correlated with the following equation;

$$\delta \left(\frac{r\omega^2}{\mu^2}\right)^{1/3} = 1.55 \ (Re)^{1/3} \qquad (2.5.8)$$

where $Re = (4Q_c/\pi\nu D)$

Agreement within a satisfactory limit was found, the ±7% deviation was believed to be due to experimental error.

Butuzov et al (12,14) developed a rotary unit to study the condensation process on the underside of a disc. A series of experiments were performed using saturated steam. Condensate temperature, together with surface temperature was measured at a number of locations. It was observed that at low speed, where Astaf'ev and Baklastov (2) noticed the quick removal of the condensate droplets from the disc surface, data variation was

higher compared to the data obtained at higher speeds (N>500 rpm). Data at these speeds were 5 to 10% below the values predicted by equation (2.5.6) for unknown reasons.

Butuzov and Rifert (13) studied the condensation of superheated steam on a copper disc, rotating about a vertical axis. It was noticed that the average coefficients are 3 to 5 times higher compared to a stationary vertical surface. The results were correlated to an accuracy of ± 10% by the following equation :

$$Re_{bot} = 0.435\ Z_{bot}^{3/4} \qquad (2.5.9)$$

where $Z_{bot} = Ga^{1/3}(K\Delta T/h_{fg}\rho\nu)$

$$Ga = \frac{\omega^2 r^4}{\nu^2}$$

(Note: $Ga = Ta^2$, as $Ta = \frac{r^2\omega}{\nu}$ has been used in this report)

These experiments were performed, with rotational speed in the range of 10 to 224 rpm. A higher speed range (up to 2500 rpm) was investigated by Astaf'ev and Baklastov (3). Mean coefficients of the condensing film were correlated to an accuracy of ± 12% by the following expression;

$$h_c = 1.18\ \left(\frac{K^3\rho^2 h_{fg}}{\mu\Delta T}\right)^{0.25} (\omega)^{0.43} \qquad (2.5.10)$$

2.5.4. Advances In Rotating Disc Condensation

Generally, two techniques have been employed to improve further the performance of a rotating disc.

(i) Rough surfaces of many configurations, ranging from randomly sanded to mechanically grooved surfaces, have been employed by a number of investigators. These configurations were

generally chosen to promote turbulence rather than to increase surface area. Nicol and Medwell (43) established experimentally for a stationary system that the film coefficient improved significantly when the steam was allowed to condense on an artificially roughened pipe compared to a smooth surface. Bromley, Humphrey and Murray (10) tested a number of surfaces including radially grooved and sanded surfaces, for rotating disc condensation. The condensing coefficient was improved by 13 per cent in the case of a grooved surface, whilst 8 to 10 per cent improvement was achieved for a sanded disc. Performance of a number of surfaces is compared in figure 2.4.

(ii) The influence of steam impingement on rotating disc condensation process was investigated by Wang and Greif (62). Although the effect of impingement is to increase the heat transfer, the magnitude is insufficient to account for the high experimental results quoted in the literature, e.g. Espig and Hoyle (25).

2.5.5. Influence Of Non-Condensables On Condensation

Non-condensable gases, if allowed to accumulate, decrease the condensing temperature as well as hinder the condensing process by reducing the condensing film coefficients. Kern (35) has reported that when a small quantity (1 per cent by volume) of air is mixed with steam, the condensing coefficient falls from 11.56 to 6.36 KW/m^2-K with a temperature difference of 20°. When the air concentration is increased to 2 per cent, the coefficient further reduces to 4.33 KW/m^2-K, with the same temperature difference.

This effect could be responsible for the relatively low value of experimental results reported in many studies.

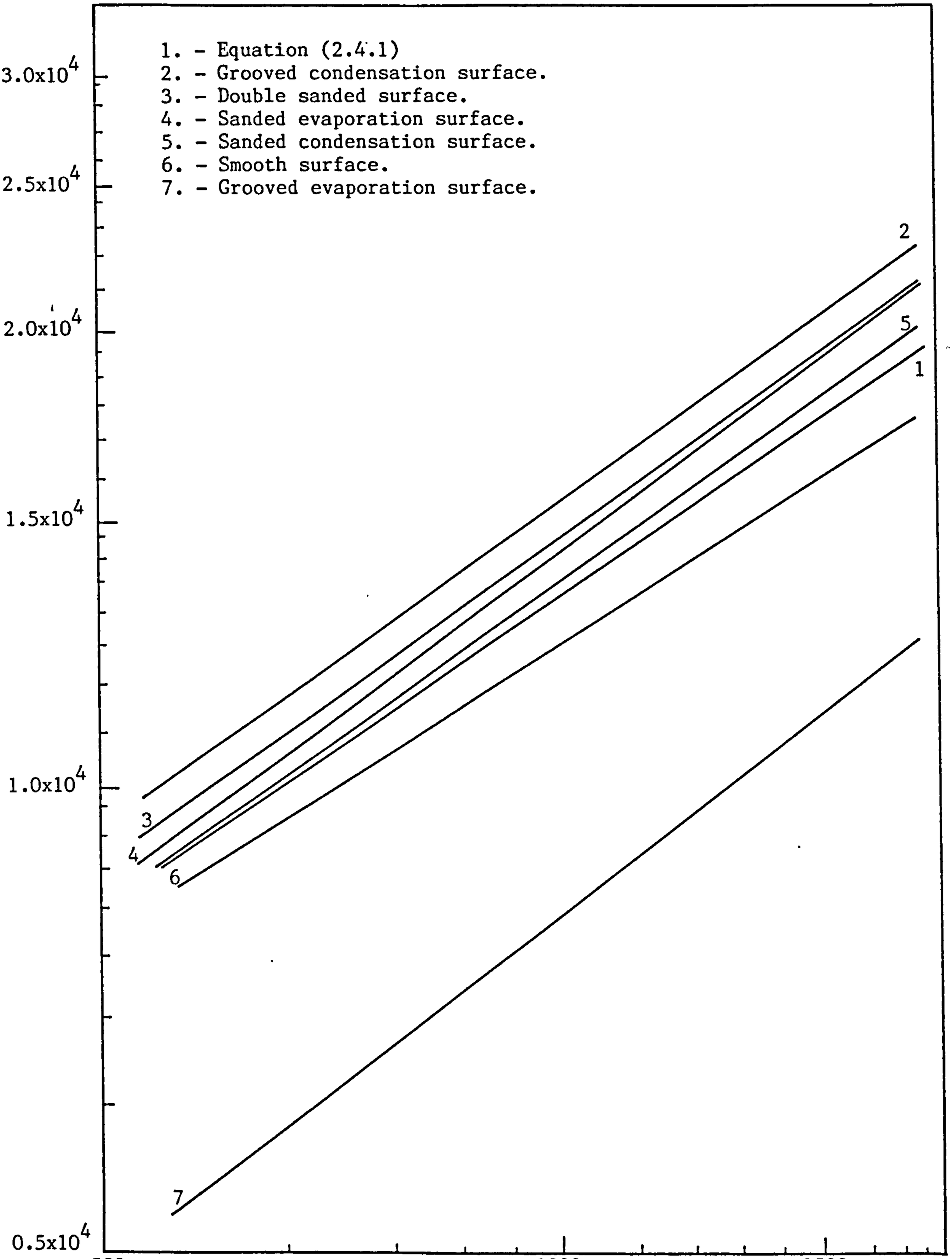

FIGURE 2.4. PERFORMANCE COMPARISON OF VARIOUS SURFACES

However, many investigators fail to indicate what precautions were taken to prevent the effect of non-condensables. Few investigators indicate what venting techniques they employed to reduce this effect.

CHAPTER THREE

EXPERIMENTAL SET-UP AND PROCEDURE

An experimental set-up was designed and constructed to perform a series of heat transfer experiments on a set of closely spaced rotating discs. Mechanical features and process details together with experimental procedure are discussed in this chapter.

The description of the above has been divided under the following subheadings:

1. Scheme of the experimental set-up;
2. Mechanical details of the test section;
3. Auxiliary equipment;
4. Experimental measurements;
5. Operating and experimental procedure.

3.1. SCHEME OF THE EXPERIMENTAL SET-UP

The experimental set-up, shown in photograph 'A' with a schematic layout in figure 3.1, is sub-divided into: (i) the test facility, and (ii) the flow circuit.

3.1.1. The Test Facility

The rotor and disc assemblies were the two major components of the test section, which in turn was the most important unit of the test facility. Constructional details of these components are given in subsequent sections. However, in summary, the test section comprised of two closely spaced discs, rotating about a vertical shaft in a stationary pressure vessel. The space between the discs was used as a sensible heating and evaporating region, whilst dry steam was allowed to condense on the outer surfaces of the discs. Test fluids (i.e. distilled water

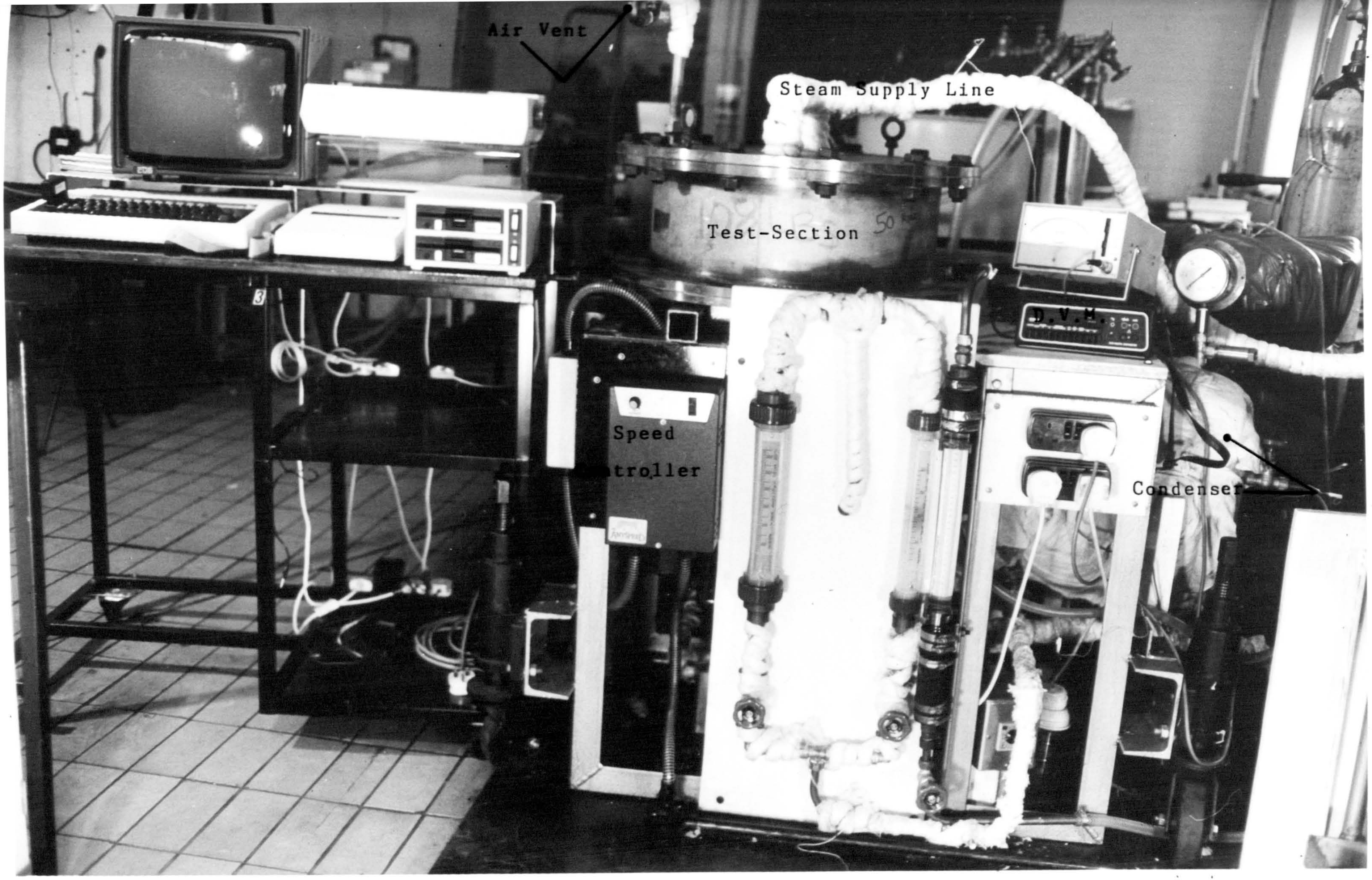

PHOTOGRAPH 'A' OVERALL VIEW OF EXPERIMENTAL SET-UP

DESCRIPTION OF THE EXPERIMENTAL SET-UP

1 - Test section

2 - Condenser

3 - Feed supply tank

4 - Immersion heaters

5 - Mixing tank

6 - Level sensor

7 - Centrifugal pump

8 - Rotameter

9 - Air vent

10 - Steam superheater

11 - Pressure reducing valve

12 - Tee-type strainer

13 - Pressure relief valve

14 - Vacuum breaker

15 - Nitrogen cylinder

(P) - Pressure gauge

- Steam trap

- Thermocouples

- To drain

- Gate valves

- 3 Way valve

- Power supply

Process streams

Steam supply line

Condensate

Cooling water

Nitrogen

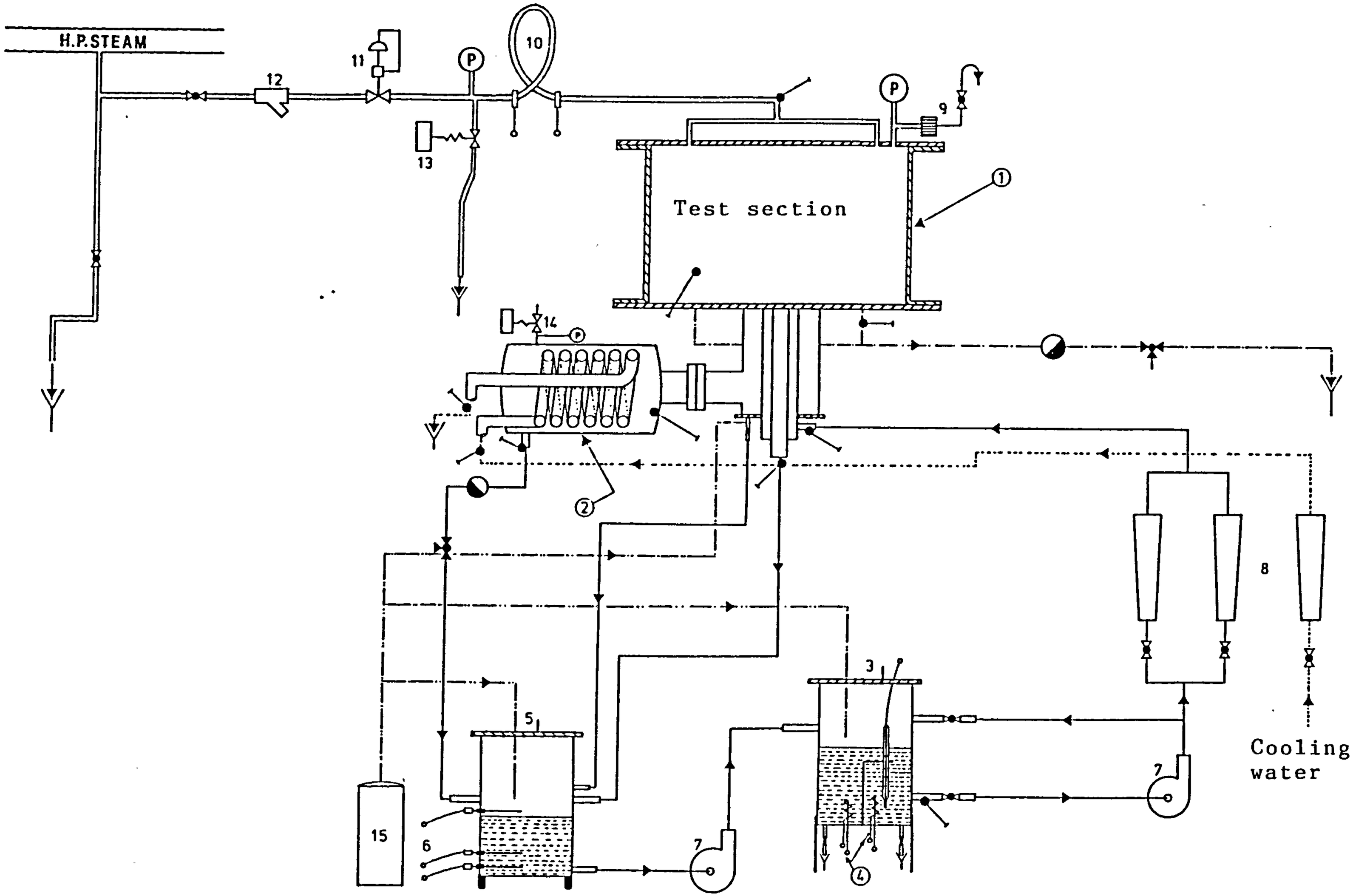

FIGURE 3.1 LAYOUT OF THE EXPERIMENTAL SET-UP

and methanol) were pumped to and distributed from the centre of the discs. This liquid, in the form of a thin film,flowed from the centre to the periphery of the disc under the action of centrifugal force. The feed was (in case of phase change) partially evaporated and the vapours were drawn back towards the discs, where they passed to a condenser. The vapours were recycled after condensation. A water cooled, coil type condenser was employed for this purpose. The heated feed was continuously transferred to a rotating trough via 8 ports provided at the outer periphery of the discs. The liquid was withdrawn by the pumping action of the rotating trough and two stationary pick-up nozzles which were partially immersed in the liquid. Finally, the liquid was collected along with the vapour condensate in a mixing tank, and the mixture was pumped back to the feed tank.

The discs were rotating in a sealed chamber, supplied with dry or slightly superheated steam, which condensed on the outer disc surfaces. The condensate formed on the rotating surfaces was thrown off due to centrifugal action. The condensate left the chamber via a steam trap after which condensate measurement was undertaken by timed, sample collection.

3.1.2. The Flow Circuit

The flow of various streams, shown in figures 3.1 and 3.7, can be classified as;

(i) Process streams: feed supply and re-cycling of heated liquid and condensate, in the case of phase change experiments; or a single heated feed stream.

(ii) Service streams: steam supply system and circulation of cooling water.

(i) Process Streams

Feed at a desired temperature was pumped to the rotary unit from a tank of 65 ℓ capacity. The tank was divided into two sections, using an 's' shaped longitudinal baffle for better mixing. Two immersion heaters, rated 2.75KW and 1.75KW, were provided in the tank. The lower rated heater in conjunction with a thermostat, regulated the feed temperature, while the other one served as a temperature booster. Power supply circuit is shown in figure 3.2. The feed, after passing through a set of pre-calibrated rotameters (calibration curves are given in Appendix H), entered the stationary annular feed channel of the machine and was delivered to the test section via a distributor. Design details of the distributor are given in section 3.2.3. The feed channel, made of 15mm and 22mm O.D. stainless steel tubes, was located concentrically with the central shaft of the rotor assembly. This arrangement provided three channels for the flow of feed, heated liquid and vapours. The flow of these streams within the test-section is shown in figure 3.7.

(ii-a) Steam Supply System (with superheater)

Steam was taken from the main laboratory steam network at approximately 6 bar. The pressure in the steam chamber was controlled by a pressure reducing valve (Spirax Sarco; type PN25 Rg5). Steam pressure was measured at two positions, following the pressure reducing valve and in the steam chamber.

A superheater was included in the steam line to produce slight superheating, so that the condition of the steam in the chamber was known. The superheater was an electrically heated coil. The coil of 0.2m diameter was directly connected to a

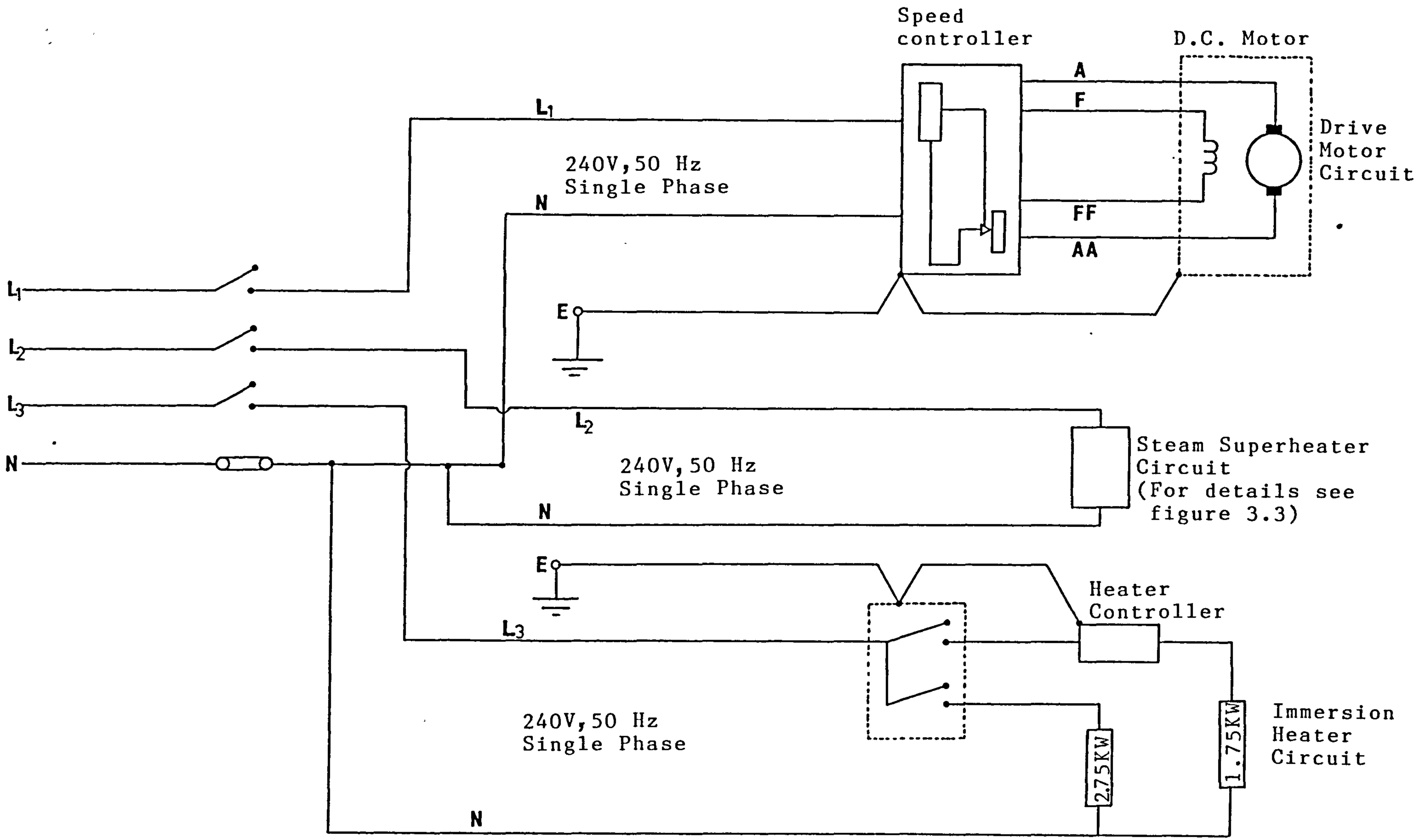

FIGURE 3.2 OVERALL POWER SUPPLY LOOP

step-down transformer (supplied from an auto-transformer) by means of stainless steel electrodes, copper clamping yokes and bus-bars. (The power supply loop is shown in figure 3.3, and design features are given in Appendix B.) The rest of the pipe-work was isolated from the superheater by two sets of Tufnol flanges and silicon rubber gaskets.

The required level of superheating could conveniently be achieved by regulating the power supply. The superheated steam was introduced to the pressure vessel, at two positions via an insulated flexible hose. Simultaneously, the condensate was withdrawn from the vessel at two points and drained through a steam trap.

(ii-b) Cooling Water

A known rate of cooling water was supplied, from the laboratory mains, to the condenser on a once through basis. Inlet and exit temperatures were measured by thermocouples. A rotameter was employed to determine the flow rate of cooling water (the calibration curve is given in Appendix H).

3.2. HEAT TRANSFER TEST SECTION-MECHANICAL DETAILS

Most of the mechanical details of the test section used in this study are shown in figures (3.4 to 3.7). The test section comprised of a number of rotating and non-rotating parts. The rotor and disc assemblies along with collecting trough were essential parts of the test section and they were rotating about a common axis. A pressure vessel, annular feed distributor and the scooping device for the removal of heated feed were the non-rotating parts of the assembly. During the design and construction of the machine the following features were considered:

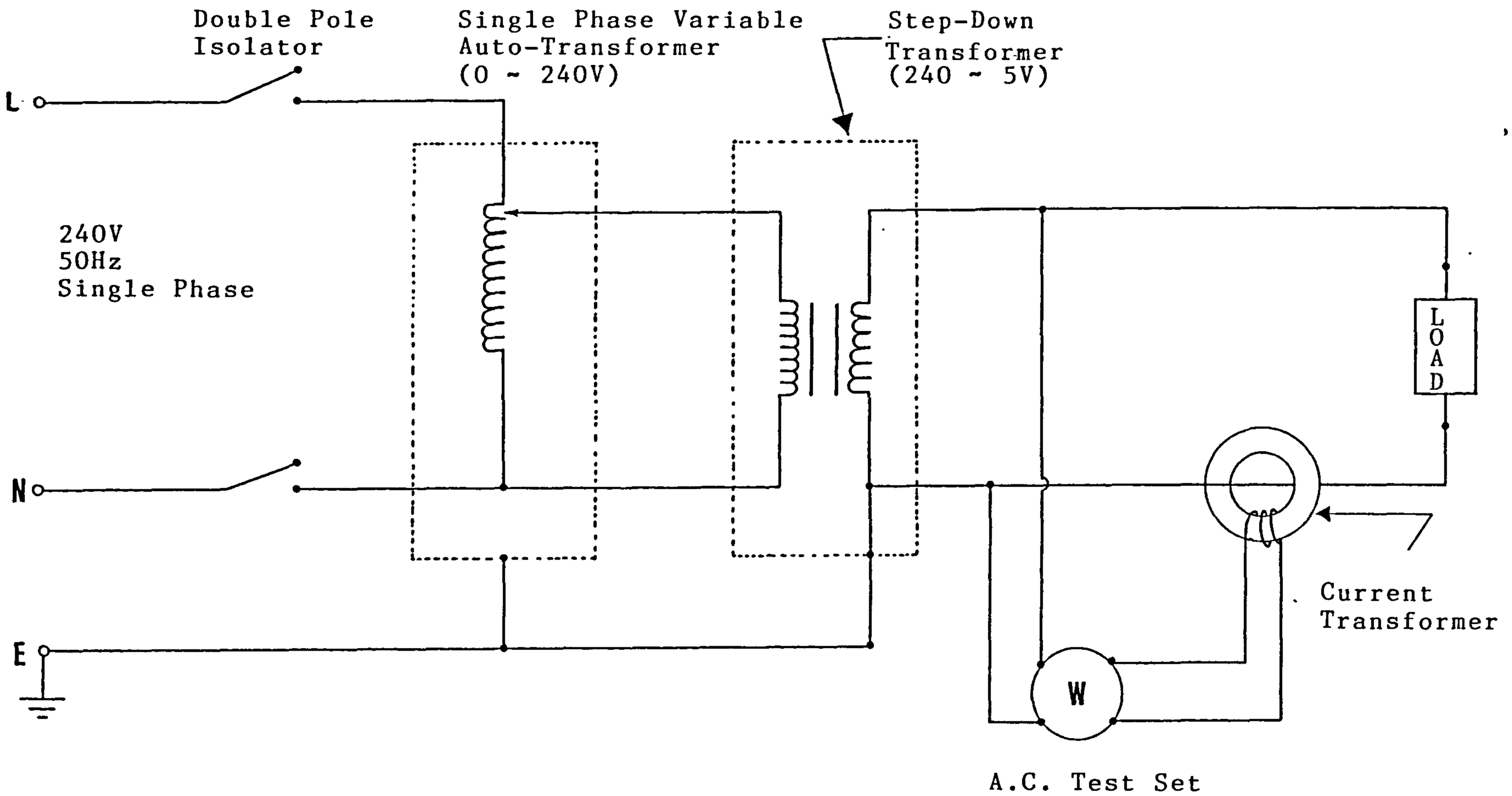

FIGURE 3.3 POWER SUPPLY LOOP FOR THE STEAM SUPERHEATER

(i) Stainless steel was chosen for construction of the test section, the feed tank and the vapour condenser. Although it is an expensive material and difficult to machine, it was selected for its anti-corrosive properties, and strength.

(ii) During the construction of the assembly screwed and flanged joints were preferred to welded and brazed joints, wherever possible. This permitted accurate fitting in the initial assembly, as well as facilitating any possible future modification.

(iii) Neoprene chord and 1mm thick glass fibre reinforced sheeting (manufactured by TBA Industrial Products Ltd., Reference Number - Permanite AF 2000) were used exclusively for sealing purposes. These materials can withstand temperatures up to 400°c.

In the following sections the mechanical details of the rotor and disc assemblies, along with main accessories, are given. (The complete assembly is shown in photograph 'B').

3.2.1. Constructional Details Of The Rotor Assembly

This assembly rotated about a hollow drive shaft set in bearings. The shaft was 300mm long and was bored out to 50.8mm, while the outer diameter was machined to suit bearing spacers, pulley and other accessories of the rotor as shown in figure 3.4. The bearings (manufactured by Timken Bearings Ltd., cup and cone numbers are 39250 and 39412 respectively) were mounted back to back in a housing (7)* at a distance of 38mm, using a pair of spacers. A mounting flange (8) was screwed onto the housing at 133.3mm diameter. The housing was sealed at each

---

* numbers within brackets indicate the part number of the assembly, as marked on the figures 3.4 and 3.5.

TEST FACILITY

Step Down Transformer

PHOTOGRAPH 'B' EXPERIMENTAL SET-UP & ANCILLARY EQUIPMENT

Steam Superheater

Tufnol Flanges

Feed Supply Tank

Test-Section

Mixing Tank

Condenser

end by mechanical seals (made by James Walker & Co. Ltd., Part Number 58E-2500). These seals were mainly associated with the lubrication of the bearings. Two seal housings (6, 12) were used to keep the seals in position and simultaneously, they also locked the bearings. The lower bearing was further protected by an adjustable sleeve (14) which was screwed onto the shaft. Finally, the bearings and seal housings along with their accessories were secured by two cover plates (5,13).

The drive pulley was mounted below this housing onto the shaft. The pulley was designed according to SPZ 710PB specifications. The both pulleys (drive and driven) were of the same diameter i.e., 105mm. A 1.5KW D.C. motor provided the main drive. The variable speed was achieved by a controller which provided a variable armature current. With this arrangement rotary speeds from 200 to 2000 rpm could be achieved (2000 rpm being the maximum speed of the motor). However, to prevent any mechanical/electrical failure the machine was limited to a speed 1500 rpm.

The space required for the drive belts was maintained by three 97mm long multi-purpose spacers (17). These spacers were screwed in the lower cover plate (13) to carry the load of the main structure. A tee-section (18) was mounted on the lower end of the shaft through the bottom seal housing (16). The tee-section was used for the removal of vapours, whilst leakage was prevented by a third mechanical seal.

The plate (2) serving as a base for the disc assembly, as shown in figure 3.5, was bolted to the boss (3). The boss, in turn, was screwed to the upper end of the central shaft and was secured with a locking device (4).

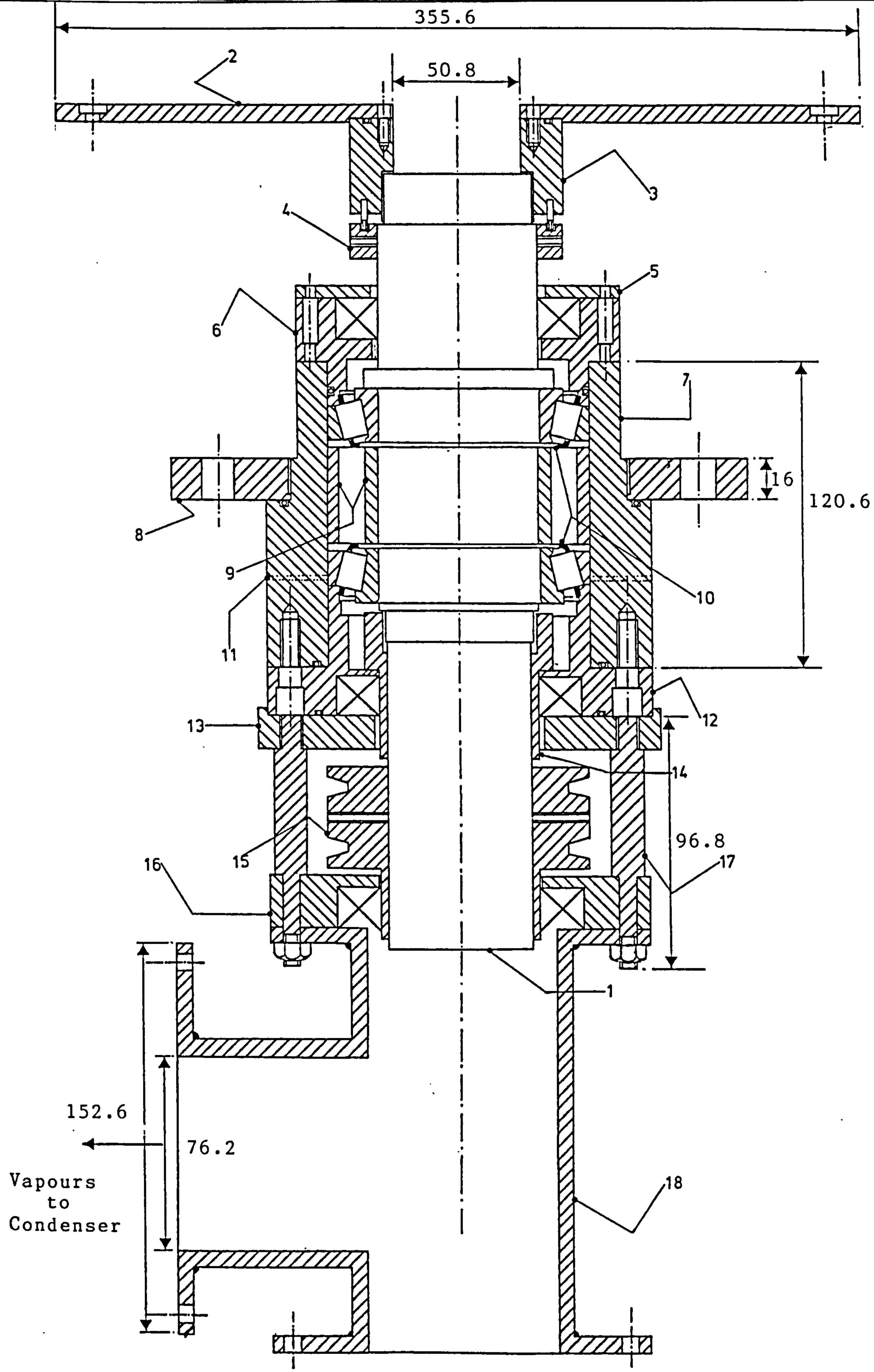

FIGURE 3.4 CROSS-SECTIONAL VIEW OF THE ROTOR ASSEMBLY

(Scale: half size; All dimensions are in mm)

LEGEND FOR THE FIGURES (3.4) AND (3.5)

PART NO.	DESCRIPTION	NO. OFF
1	Central shaft	1
2	Base plate	1
3	Boss to connect base plate with shaft	1
4	Boss and shaft lock	1
5	Cover plate for the top seal	1
6	Top seal housing	1
7	Bearing housing	1
8	Pressure vessel mounting flange	1
9	Bearing spacers	2
10	Single row straight bore type bearings	2
11	Grease nipples	2
12	Middle seal housing	1
13	Cover plate for middle seal	1
14	Adjustable sleeve/bearing lock	1
15	Pulley	1
16	Bottom seal housing	1
17	Support and spacer for bottom seal housing	3
18	Tee-section	1
19	Set of closely spaced discs	1
20	Feed distributor	1
21	Heated liquid collecting pins	8
22	Liquid collecting trough	1
23	Cover plate for collecting trough	1
24	Pick-up nozzle	2

PART NO.	DESCRIPTION	NO. OFF
25	Pick-up nozzle connecting arm	1
26	Boss to connect scooping unit with annular tube	1
27	Pressure vessel	1
28	Brass spacers	2
29	Annular feed channel	1
◎	'O' ring	7
▬▬	Gaskets	-
⊠	Mechanical seals	3

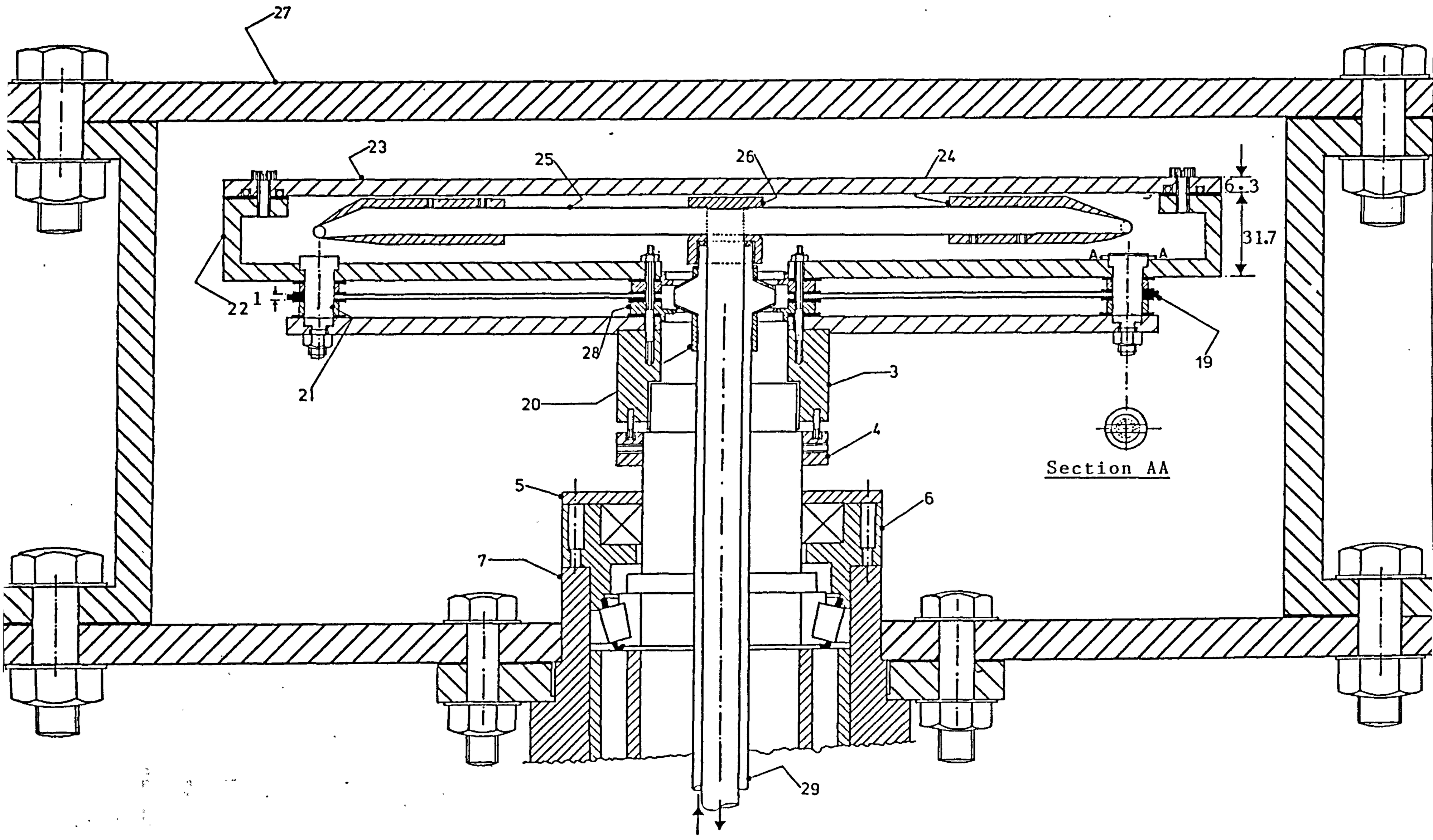

FIGURE 3.5 CROSS-SECTIONAL VIEW OF THE DISC ASSEMBLY
(Scale: half size; All dimensions are in mm)

3.2.2. Constructional Details Of The Disc Assembly

The mechanical details of the disc assembly (photograph 'C') are presented in figures 3.5 and 3.6.

The assembly comprised of two 0.5mm thick stainless steel discs of 355.6mm diameter, a base plate, a trough to collect heated feed, together with a number of spacers. The axial gap between the discs was 1mm. The narrow gap was achieved by the help of spacers made of gasket material. The uniformity of the gap was maintained by providing 1mm diameter dimples on one of the discs. 8,16,16 dimples were punched at 80, 210 and 340mm pitch circle diameter, respectively. The dimpled disc together with the design of the spacers for outer periphery is shown in figure 3.6(c). The pair of the discs was located concentric with the base plate and the trough by a number of specially designed pins. The design details are shown in figure 3.6(e). These pins facilitated the continuous removal of the heated liquid from the pair of the discs as explained in figure 3.6(d).

Unfortunately, with the said arrangement leakages from the outer periphery could not be prevented completely. However, 16 pairs of spacers were employed to enhance the compression (figure 3.6(b) explains this arrangement). Dowty Seals (ordinary metallic washers impregnated with neoprene) effectively prevented the leaks.

The central arrangement of the disc assembly, as shown in figure 3.7, was furnished with 12 spacers (I.D. = 3.2mm & O.D. = 5.2mm) made of gasket material and two brass spacers. This rotating heat transfer unit was mounted in the pressure vessel which was flanged at both ends. The vessel was also acting as

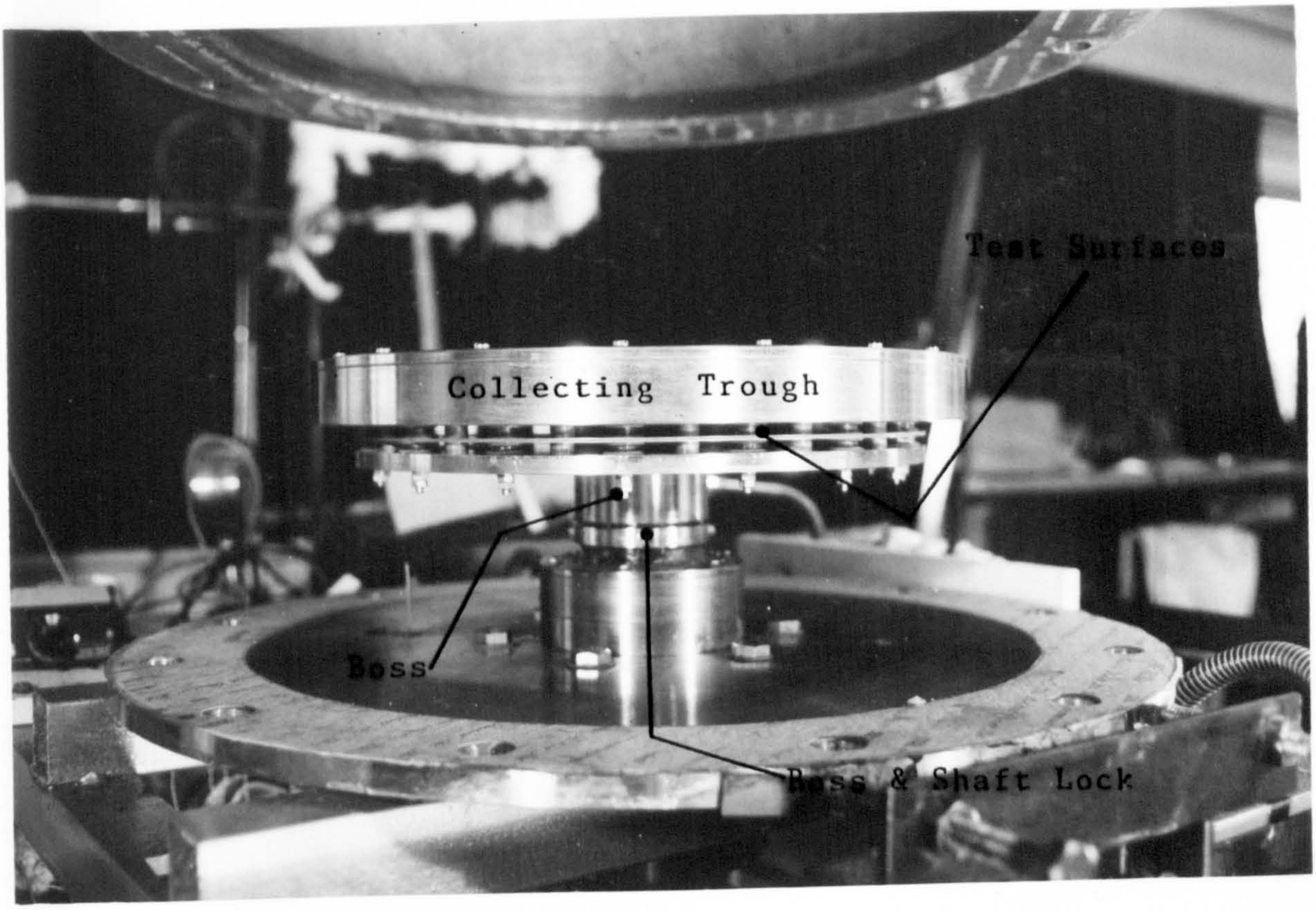

PHOTOGRAPH 'C' DISC ASSEMBLY

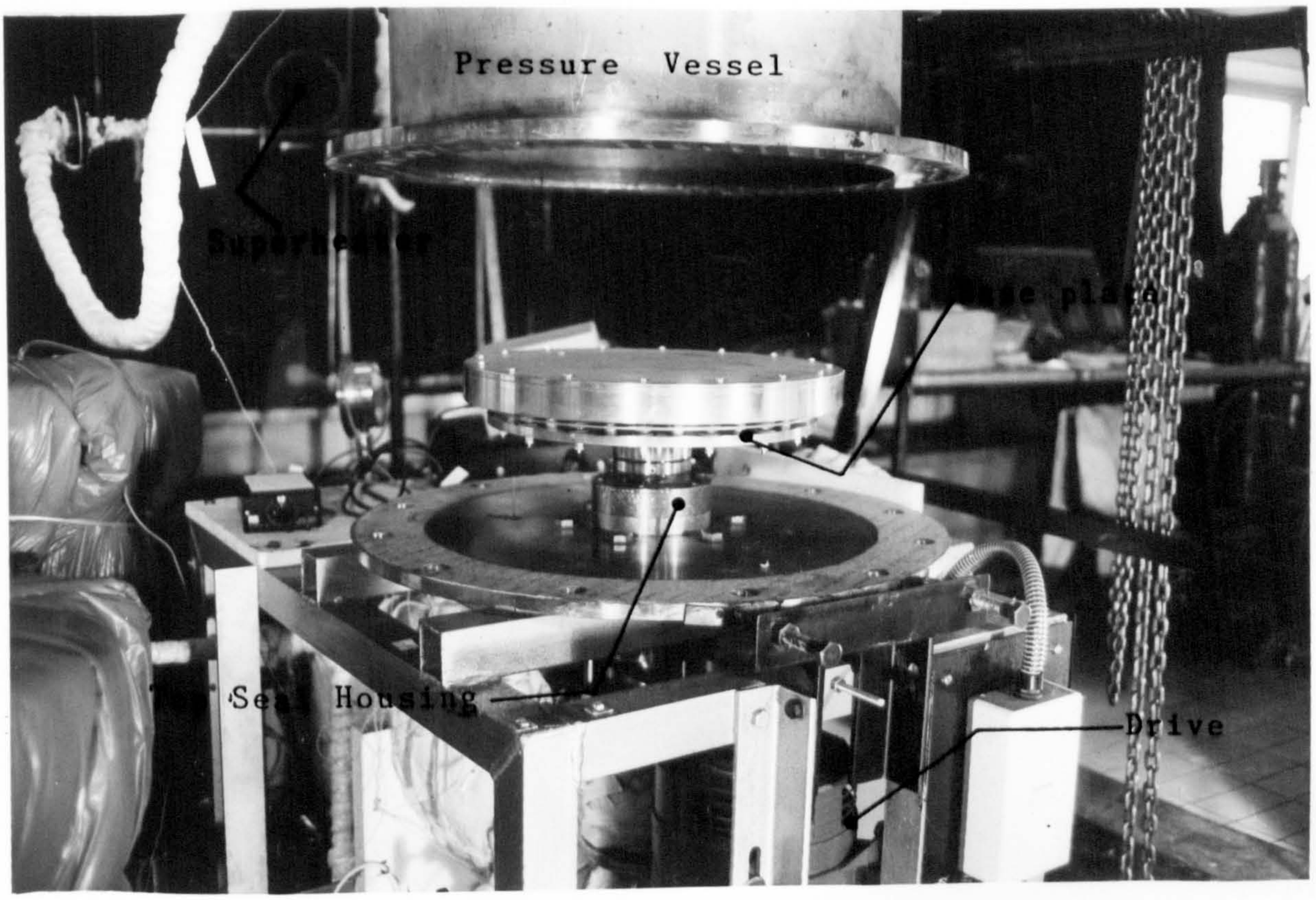

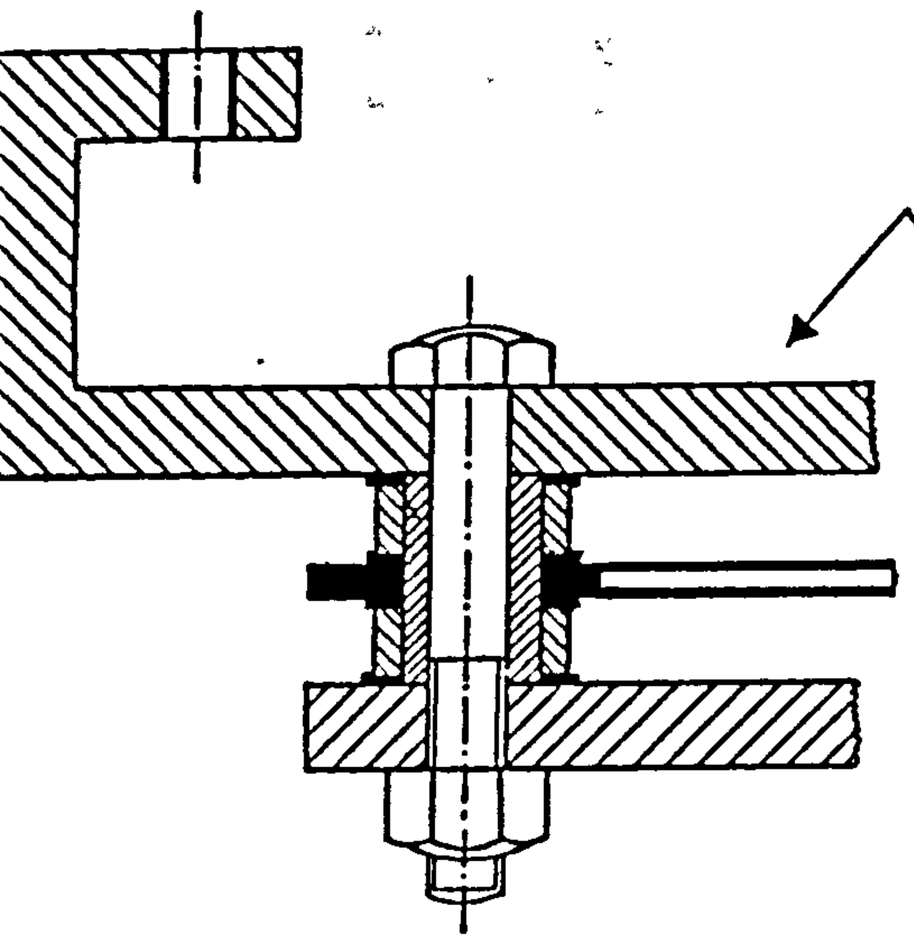

(a) Sealing and spacing arrangement (8 in number)

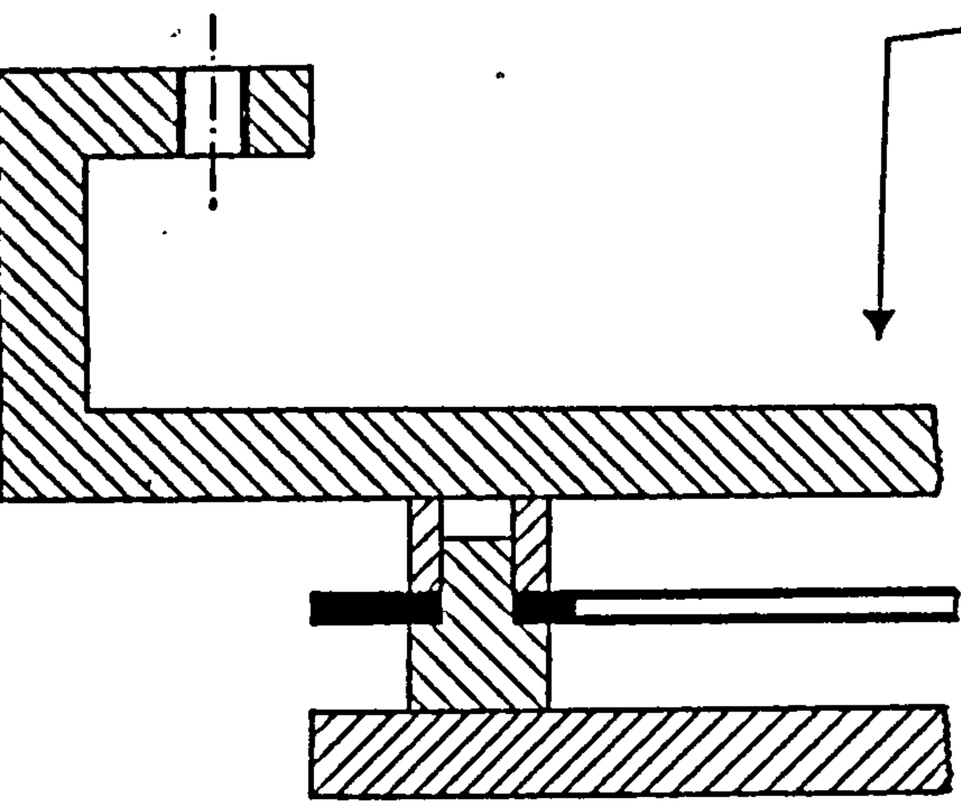

(b) Sealing arrangement (16 in number)

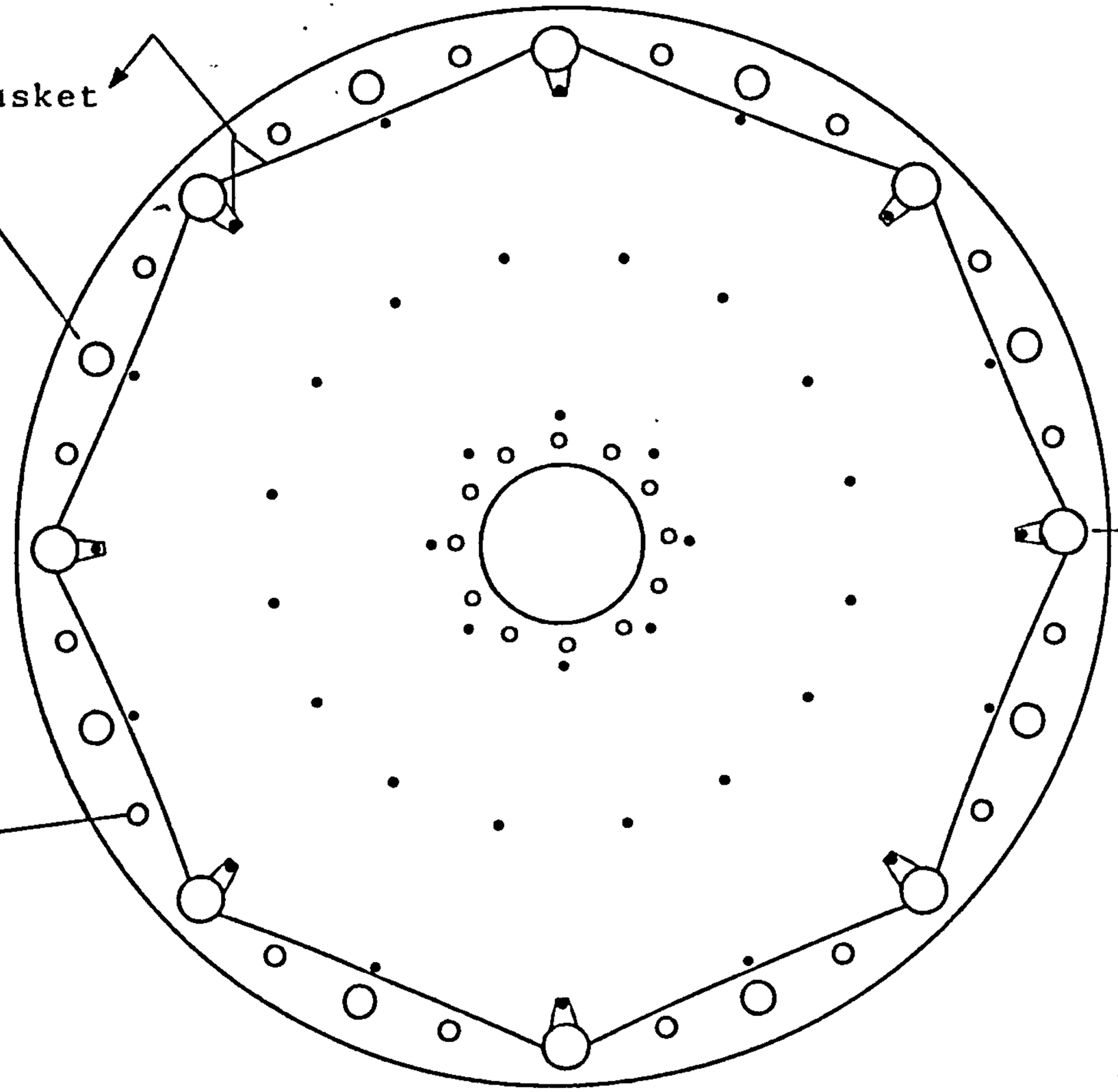

(c) Position of gaskets on dimpled disc (scale 3:1)

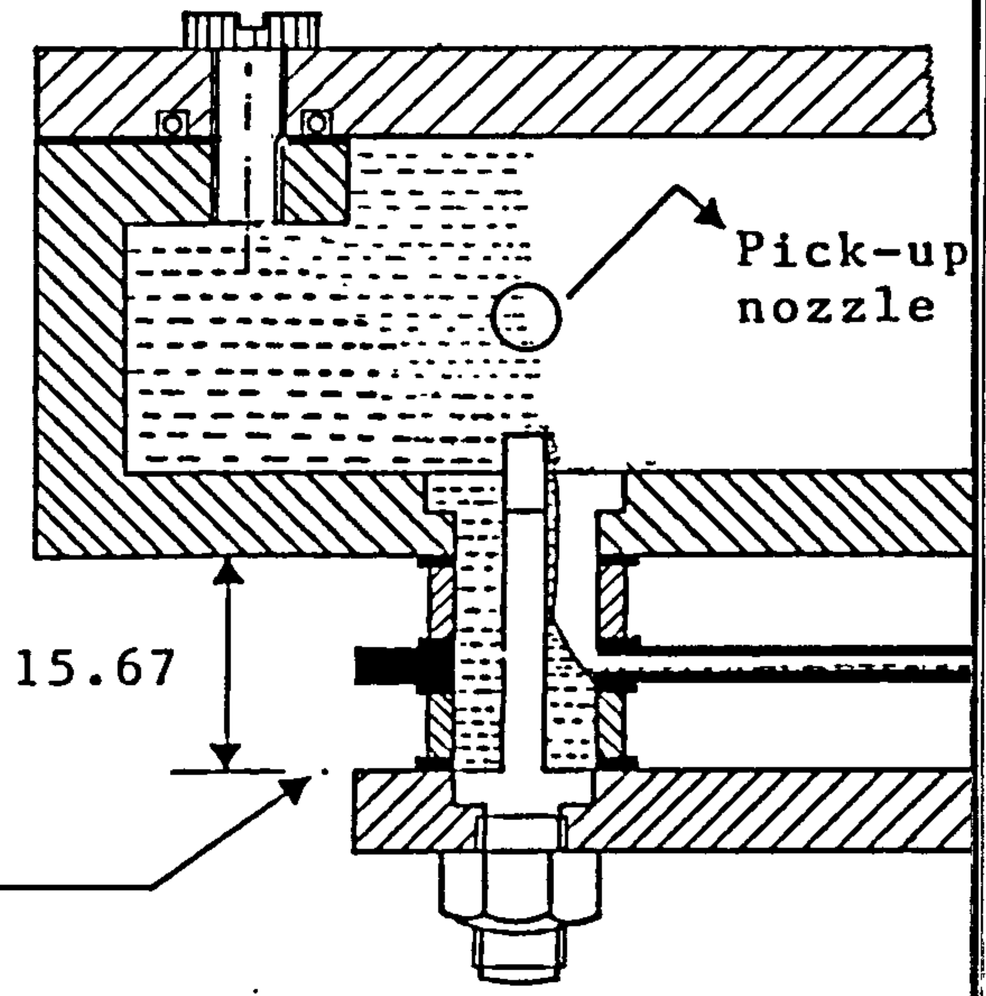

(d) Heated liquid collection arrangement (8 in number)

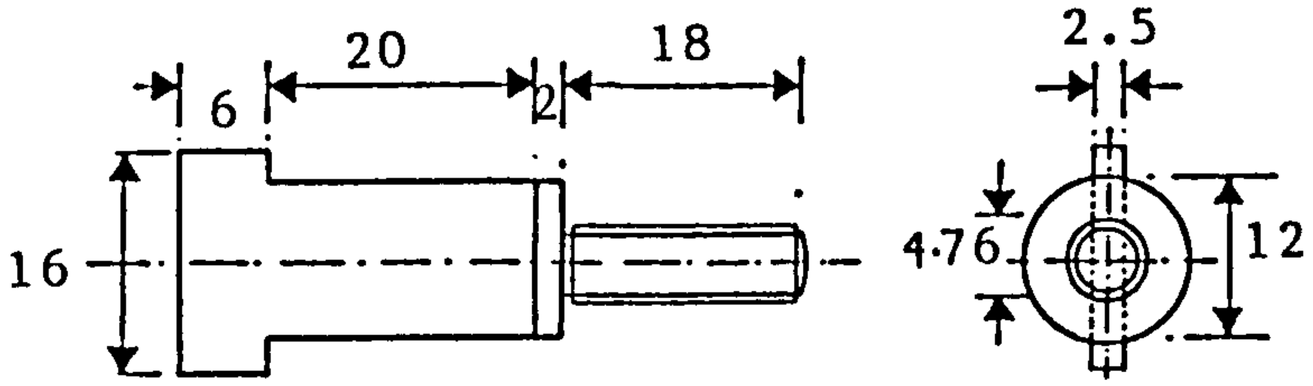

(e) Front and side views of heated liquid collection pin

FIGURE 3.6 VARIOUS SEGMENTS OF THE DISC ASSEMBLY (Full scale; All dimensions are in mm)

a steam chamber and steam was introduced at two positions for even distribution. A pressure gauge and an automatic air vent (manufactured by Spirax Sarco Limited, reference number AV10) were provided on the vessel and the vessel was heavily lagged with rock-wool.

The whole assembly, the condenser and the drive motor were placed on a metallic frame, the details are shown in figure 3.9.

3.2.3. The Test Section Accessories

The feed distributor and heated feed scooping device were two important accessories of the test section. Description of these devices are given in the following sections.

(i) The Feed Distributor

One of the major problems encountered in the development of the experimental set-up was, the even distribution of feed between the pair of spinning discs. A number of designs were tested, and the following arrangement was finally adopted as this effectively fulfilled the basic requirements, i.e.,

(a) an ability to introduce the feed uniformally, without splashing;

(b) the availability of sufficient free area to allow the counter-flow of the vapours.

The feed, flowing through the annulus of the feed tube, spreads via a distributor, as illustrated in figure 3.7. The distributor comprised of four nozzles and a sleeve. A full scale design of the nozzle and plan view of the distributor is also shown in figures 3.7(a) and 3.7(b). The dimensions were selected in such a way that the velocity of the emerging feed

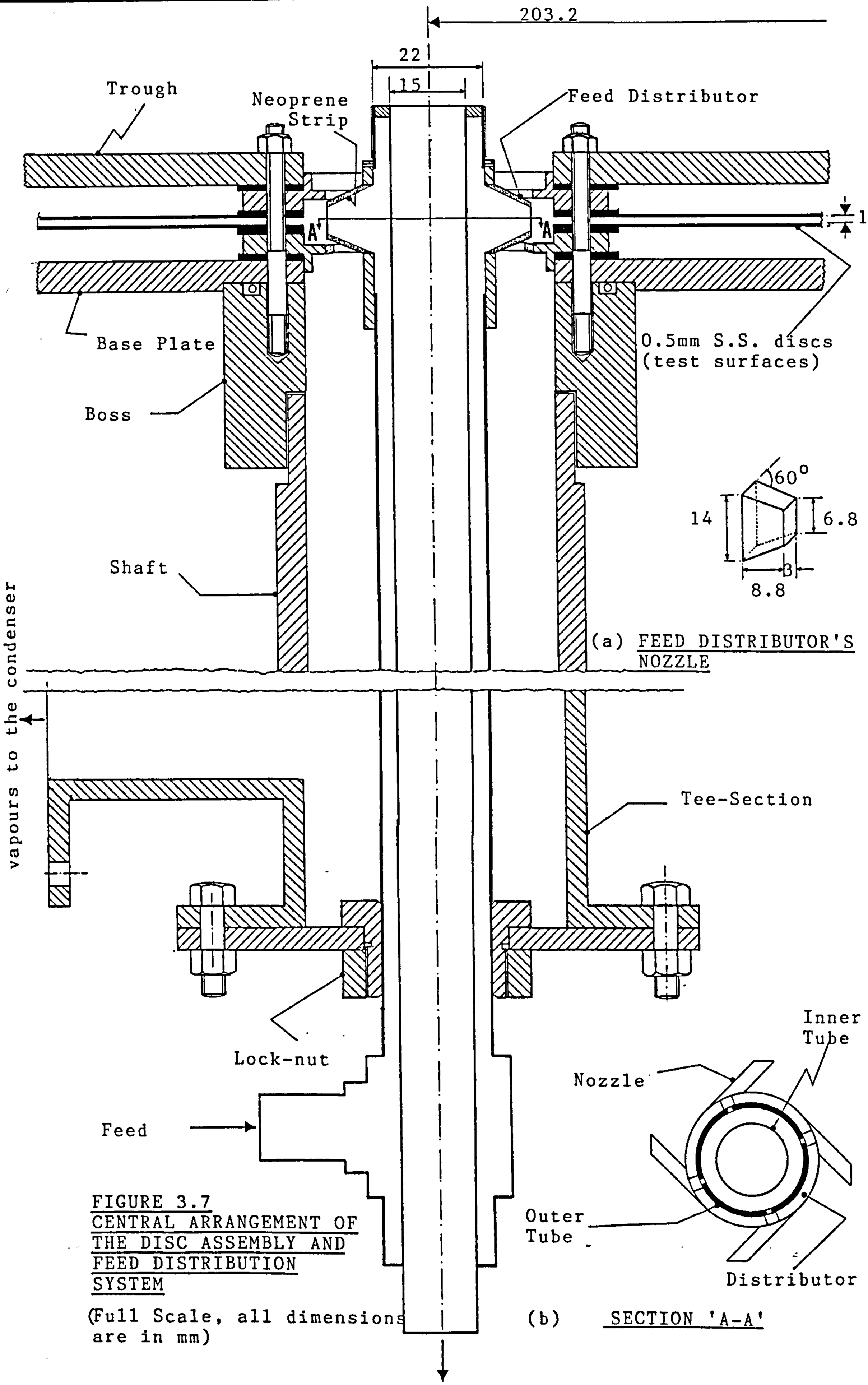

FIGURE 3.7
CENTRAL ARRANGEMENT OF THE DISC ASSEMBLY AND FEED DISTRIBUTION SYSTEM

(Full Scale, all dimensions are in mm)

would always be less than the angular velocity of the spinning discs at the distribution point. The liquid velocity was further reduced by attaching a 1mm thick neoprene strip on each horizontal side of the nozzles. Most of the splashing was prevented using this arrangement. A 2.5mm thick neoprene ring was provided at the lip of the lower spacer to prevent dripping of the liquid.

(ii) The Scooping Device

For efficient removal of the liquid from the rotating trough, a scooping device was designed. A pair of pick-up nozzles and a collector arm were the main parts of the scooping device (for mechanical details see figure 3.8). The leading edge of the nozzle was tapered at an angle of 30 degrees outwards to provide a sharp edge for picking-up the incoming liquid. To overcome machining difficulties due to the tapered structure of the nozzle, it was built in two pieces and brazed together. Two grub screws were used to locate the nozzles on the collector arm, which in turn was screwed on the central annular tube via a boss, as illustrated in figure 3.5.

This arrangement was capable of picking up 200 cc/s of liquid at an operating speed of 500 rpm. (Design calculations for the nozzle are given in Appendix C). Performance of the device was tested before the construction of the final assembly. It was established that such a construction offered the minimum drag and efficiently picked up the liquid.

3.2.4. Inspection And Maintenance Of The Rotary Unit

Regular maintenance of the machine at short intervals was not proposed at this stage. Most of the parts except self aligning bearings and mechanical seals, required very little

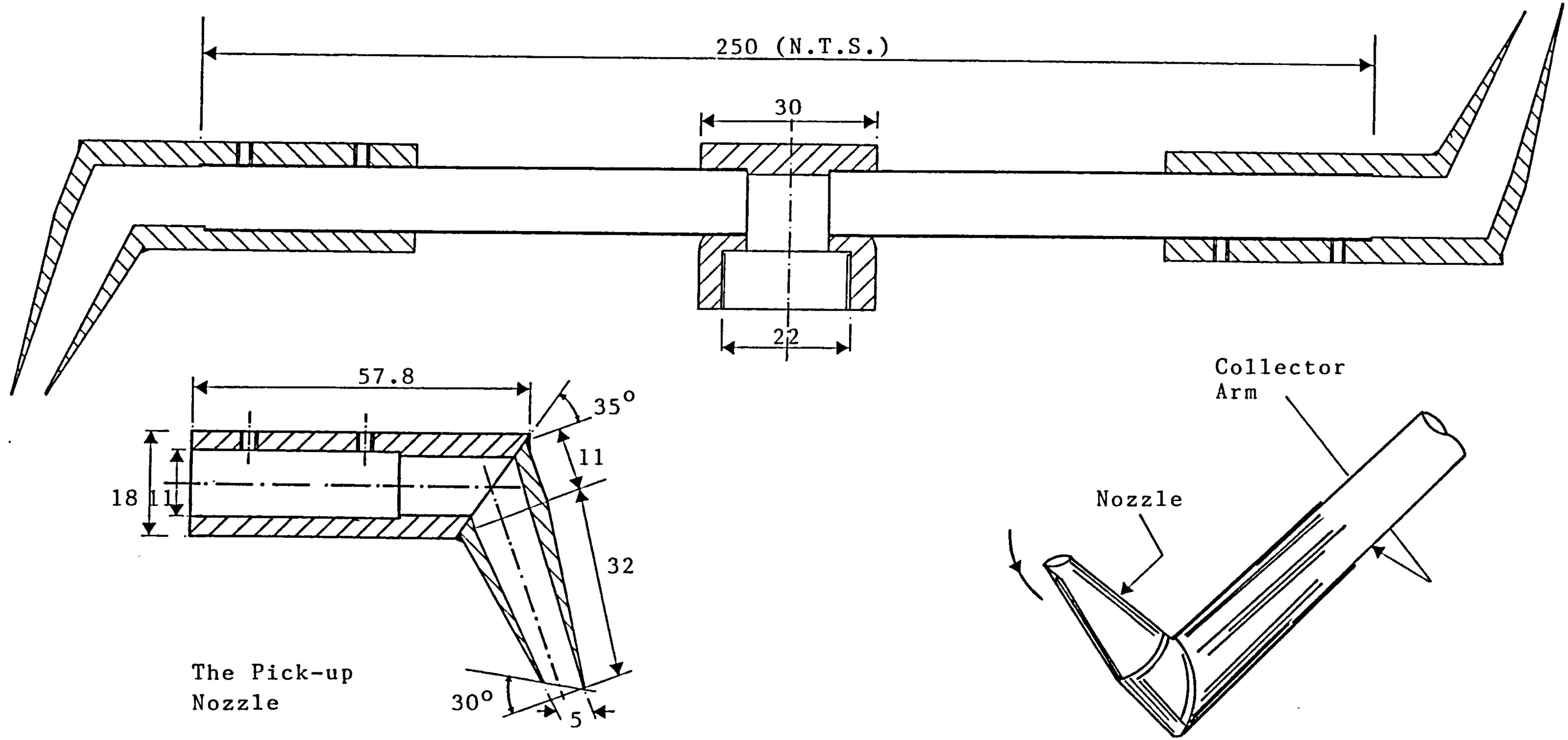

FIGURE 3.8 CROSS-SECTIONAL VIEW OF THE SCOOPING ARRANGEMENT
(Scale: Full size. All dimensions are in mm)

ISOMETRIC VIEW
OF THE SCOOPING
NOZZLE
(Not to Scale)

lubrication and no regular maintenance was required.

The fully enclosed bearings were lubricated via two grease nipples, provided in the bearing housing. To maintain an unbroken film of lubricants, checking and refilling is recommended after 500 hours of running.

3.3. AUXILIARY EQUIPMENT

The auxiliary equipment in the experimental set-up were a feed storage tank, a mixing tank, supporting frame, two centrifugal pumps, steam traps and an air vent. Each of these pieces of equipment was of standard design, and specific information had been given in the appropriate sections. Another piece of equipment which was important in the experimental work (i.e. the vapour condenser) warrants a detailed description.

A water cooled coil type condenser was designed and constructed and attached to the tee-section (as shown in figure 3.1) to condense the vapours coming from the test section. 12.5mm outer diameter tubes were used to construct a 200mm diameter spiral with 15 turns. This provided the required heat transfer area for condensation of 100 cc/s of steam. The shell, was made of 1.6mm thick stainless steel sheet, sealed at both ends and was externally strengthened by welding four longitudinal stiffening strips. An anti-vacuum valve was employed to inhibit the possibility of deformation under vacuum.

3.4. EXPERIMENTAL MEASUREMENTS

The following variables were measured and recorded:

(i) Flow Rate

Feed rate and flow rate of the cooling water was measured by a set of pre-calibrated rotameters; (calibration curves are given in Appendix H).

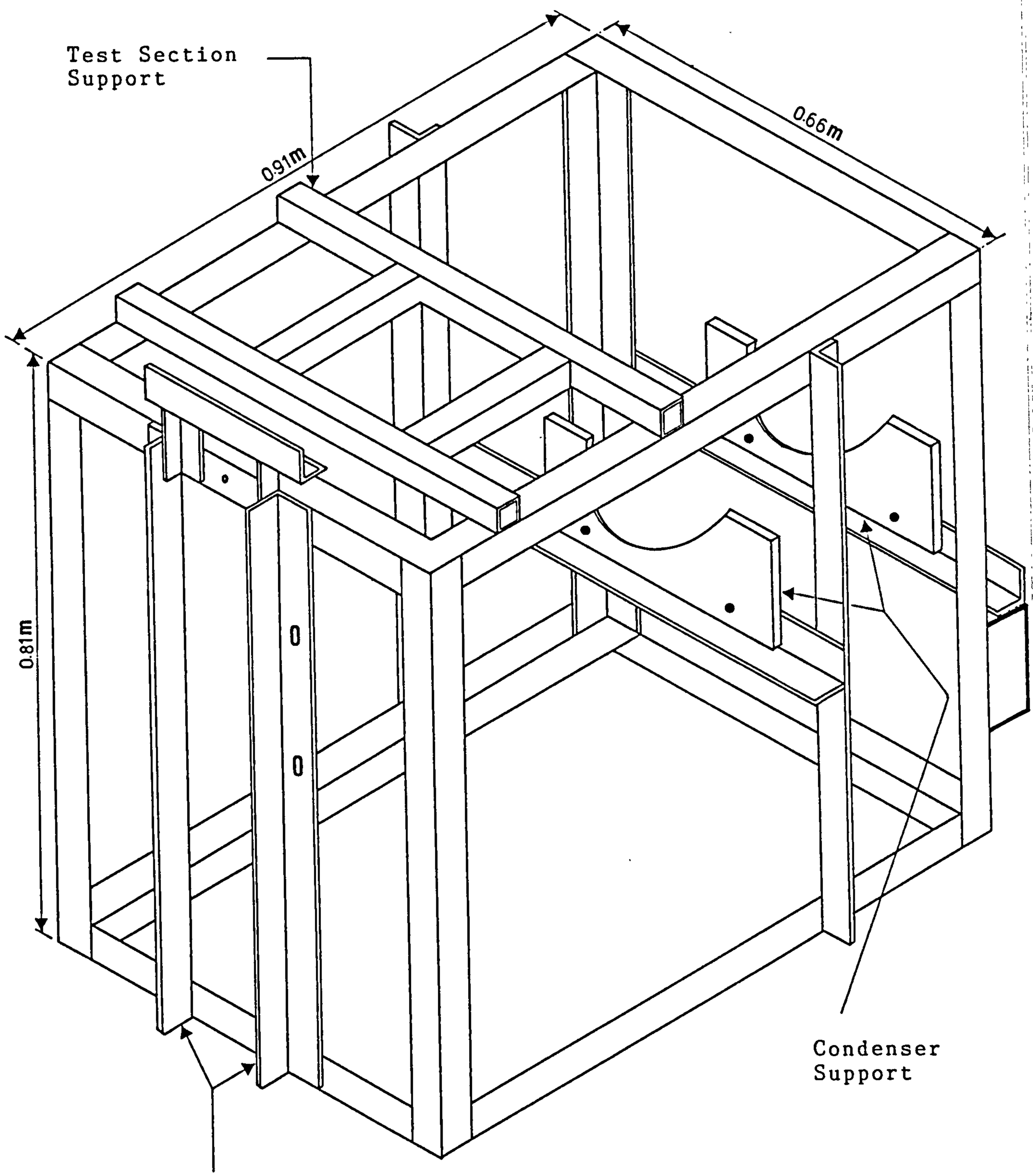

FIGURE 3.9 ISOMETRIC VIEW OF THE SUPPORTING FRAME

(SCALE 8:1)

(ii) Speed of Rotation

Rotational speed was measured with a tacho-generator, with output measured by digital voltmeter. It was calibrated using a stroboscope, calibration curve is given in Appendix H.

(iii) Temperature

For an accurate heat balance and in order to estimate the rate of evaporation in the case of phase change experiments, the temperatures of the hot and cold fluids were measured at a number of points, as shown in figure 3.1. Standard copper-constantan thermocouple wire (36swg) was used for this purpose. The junctions were secured with soft solder, and were mounted in stainless steel capillaries. A common cold junction was connected to all thermocouples using a 12 way selctor switch. The e.m.f. produced as a result of the temperature difference was measured on a digital voltmeter. The celsius temperatures were read, for the respective micro-voltages, from the international thermocouple reference table for copper-constantan. (See Appendix H). The accuracy of each junction was confirmed by direct calibration against a mercury thermometer which was accurate to $\pm$ 0.5°c.

(iv) Power Measurement

Two sets of electrical power measurements were made:

(a) power required for steam superheating.

(b) power dissipation in the drive motor.

In the case of the superheater, power measurement was made using an A.C. test set.

The power absorbed in the d.c. drive motor was determined by separate measurements of current and voltage in the field and armature circuit of the machine. Difference between power dissipation, with and without the flow of test liquid, were related to the kinetic energy given to the test liquid, together with frictional energy dissipation as the fluid flows across the test surface, and the energy losses in the pick-up elements.

(v) Pressure

The pressure in the condenser, steam chamber and in the steam supply line was measured by the use of Bourdon type pressure gauges.

(vi) Measurement Of Steam Condensate

The rate of steam condensation was determined by weighing samples of the condensate collected in a known time. The variations in such measurements for comparable conditions did not exceed $\pm$ 5 per cent.

3.5. OPERATING AND EXPERIMENTAL PROCEDURE

Details of the preliminary study, the shut-down procedure as well as the operating and experimental procedures are given in the following sections:

3.5.1. Preliminary Study

After installation of the rotor and disc assembly was completed, the rotating unit was balanced to minimise vibrations. A vibration analyser, sensitive to 0.01mm deflection, and a stroboscope were used to locate the relative unbalance point. Both static and dynamic balances were checked, deflection up to 0.05mm was assumed to be a safe limit.

A number of tests were performed with water and steam to ensure the sealing of the unit over the speed range of 500 to 1200 rpm.

Some preliminary decisions for the experimental programme were made at this time.

(i) Suitable operating conditions for feed rate were selected by calculating liquid film thickness and liquid head at delivery point (Appendix D).

(ii) The performance of the feed distributor was tested. Limits for useful working range were established as shown in Table 9.

(iii) The performance of the scooping device was checked and efficient behaviour was found over a wide range of operating conditions.

(iv) The power dissipated to drive the rotor and disc assemblies, with and without pick-up nozzle, under dry and wet conditions were determined.

(v) Minimum wetting rate for the disc under investigation was studied (Appendix A).

(vi) A careful study of the toxicity of methanol was made and a number of safety precautions, as mentioned in Appendix 'E',were undertaken.

3.5.2. Range Of Experimental Values

Following these preliminary tests it was decided to investigate heat transfer to thin liquid films (for sensible heating and sensible heating with subsequent evaporation) for the conditions listed below.

Feed flow rate:	10 cc/s to 130 cc/s.
Inlet temperature:	20°c to boiling point.
Speed of rotation:	500 to 1200 rpm.
Test fluid :	Water and Methanol.

The following start up, steady state operation and shut down procedures were adopted during experimentation.

3.5.3. Start-Up Procedure

(i) The electrical supply to the system, pressure in the steam line and availability of cooling water was checked.

(ii) The quantity of feed stock was checked and the thermostat was adjusted according to the required conditions and allowed to reach the desired temperature.

(iii) Before introducing feed to the test-section, the rotor was allowed to rotate at 300 to 500 rpm for 40 minutes, thereby warming up the bearings and mechanical seals. For thermal stabilisation of the test section steam was introduced to the pressure vessel and gradually increased to 0.1 bar (gauge) pressure, with the machine stationary.

3.5.4. Experimental Procedure

(i) The quantity of the steam condensate produced at the desired speed of rotation was measured before introducing the feed, in order to estimate the heat losses at ambient temperature. The feed pump was then switched on and the desired flow rate was attained.

(ii) Since the facility was heavily lagged and the residence time and hold up are very small, the conditions in the test section achieved a steady state very rapidly allowing collection of the following data to commence immediately.

(a) feed, condensate and cooling water flow rates,

(b) inlet and exit temperatures of feed, steam, cooling water, vapour and condensate,

(c) speed of rotation,

(d) power consumed by steam super-heater.

The accuracy of the experimental measurements was checked by an overall heat balance. It was verified by comparing the quantities of heat gained and heat supplied including the previously obtained data for heat losses. Generally, an agreement within 10 per cent was established, which was considered to be satisfactory, considering the nature of the measurements. The same procedure was repeated for various flow rates and for a range of rotational speeds.

3.5.5. Shut-Down Procedure

The steam superheater and feed stock heaters were switched off. The steam supply was stopped but the feed was continuously supplied to the rotating test section, until the temperature of the steam chamber became close to the feed stock temperature. Circulation of cooling water was continued for sufficient time so that all the vapours in the condenser were dispersed.

CHAPTER FOUR

THEORETICAL CONSIDERATIONS

The following discussion of heat transfer across a rotating disc is divided into three sub-sections which deal with the fundamentals of heat transfer, the sensible heat transfer calculations together with predictions concerning heat transfer with phase change. A brief note concerning power dissipation is also included.

4.1. FUNDAMENTALS OF HEAT TRANSFER ACROSS A ROTATING DISC

The operating configuration of heat transfer across the rotating(disc) surface is shown in figure 4.1. The thickness of the feed film on the upper surface of the disc decreases as the film passes across the disc, whilst the condensate film becomes thicker with increasing radius, due to progressive condensation. Since the experimental programme is concerned with smooth disc behaviour, the flow channel between adjacent discs has no provision for transfer of feed liquid between upper and lower surfaces. It is assumed on the basis of preliminary experiments, that under these conditions the film will reside on the lower surface of the channel. Figure 4.1 represents the assumed configuration.

The overall heat transfer process therefore consists of heat flow through a number of possible resistances for example;

(i) The non-condensable gas layer at steam-condensate interface.

(ii) The condensate film on the rotating disc surface.

(iii) The contaminants on condensing surface (i.e., oxides, dust and greasy material carried over in the steam).

(iv) The thermal resistance of the disc surface.

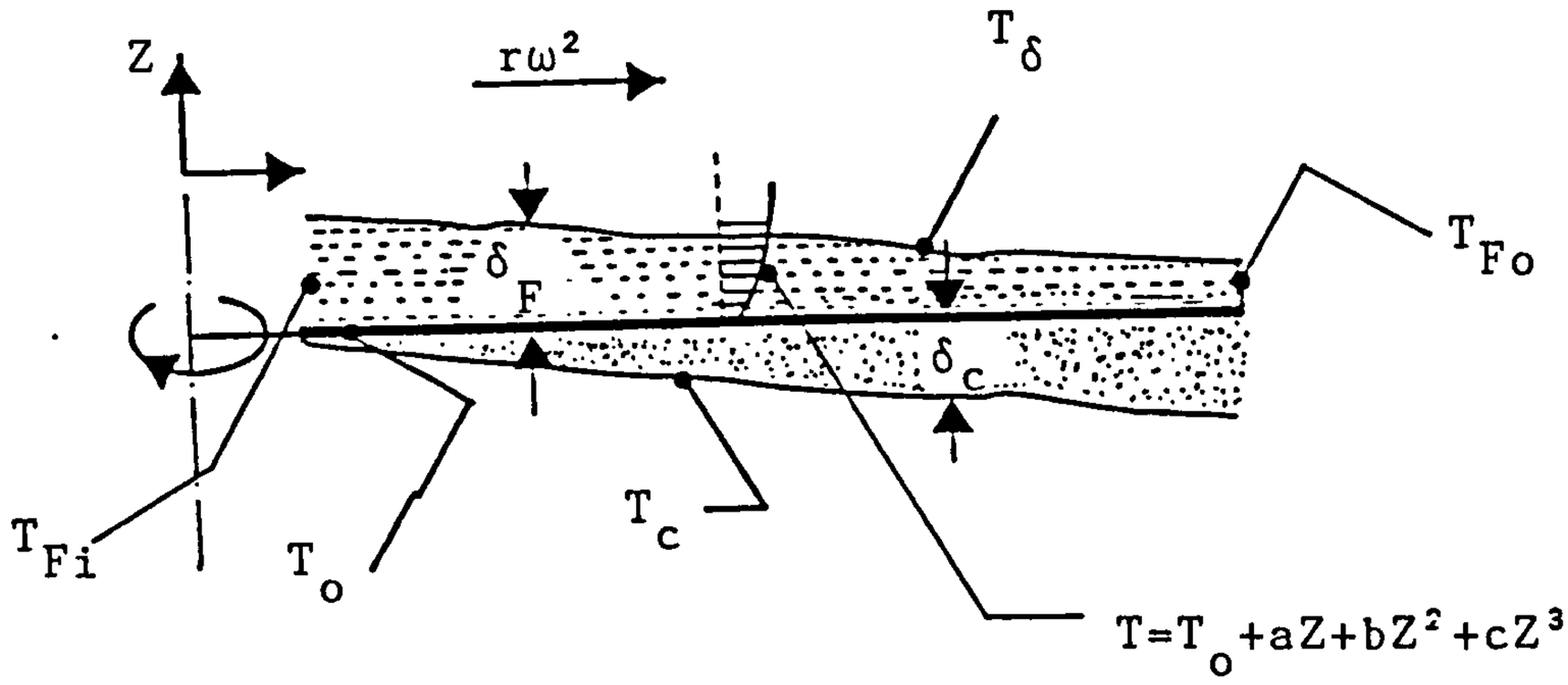

FIGURE 4.1. IDEALISED HEAT TRANSFER MECHANISM

(v) The contaminants on the feed surface, such as scale and corrosion products.

(vi) The liquid film on the feed side.

The effect of non-condensables on the condensation process will be tested during the experimental programme, and using the provision for gas venting, this effect will be reduced to negligible proportions. Since the equipment is newly constructed and will be used with clean liquids, there is little likelihood of reduced performance due to scale formation. Indeed, there is evidence from earlier work that the scouring effect of the films induces a self cleaning action.

The thermal resistance of the disc surface (3.5×10^{-5} m^2-K/W) is, in this case, negligible. This will be confirmed in a later section. Therefore, the thermal resistance due to the feed and condensate films constitute the major resistance to heat flow. Whilst estimates of the local film coefficients for both films can be made, the geometry and flow conditions for the rotating disc give rise to strong variation in these coefficients, indicating that the definition of an overall heat transfer coefficient

becomes very difficult. This definition would be further complicated by the assumption of constant physical properties which is rarely the case in heat transfer on rotating surfaces where large temperature changes are characteristics of the process. For these reasons the calculations of performance of the rotating disc is to be assessed on the basis of iteration calculations across the disc radius. In these calculations results of thermal analysis of thin film flows for the feed and condensate film are taken from previous studies (Watts (65) and Nusselt's analysis for the condensate film flowing on a vertical surface).

The structure of this analysis is given below.

4.2. THE STRATEGY OF SENSIBLE HEAT TRANSFER CALCULATIONS

In this analysis the disc has been divided into a number of concentric rings of equal width. A constant feed and rotary speed was set and a number of film parameters,(for both feed and condensate films) were calculated for each section of the disc surface. These include film thickness, average velocity and heat transfer coefficients. These parameters were estimated at the centre of each section and was assumed to prevail in that section. For the purpose of physical properties, the disc was divided into two constant property regions, (i.e., 40mm to 100mm in radial direction followed by the second region from 100mm to periphery of the disc).

The typical calculation strategy for each section is given below:

1. Liquid side film coefficient was estimated using the following correlation. (Derivation is given in Appendix F).

$$h_f = \frac{90}{61} \left(\frac{r_o^{8/3} - r_i^{8/3}}{r_o^2 - r_i^2}\right) \left[K_F \left(\frac{2\pi\omega^2\rho_F}{3Q_F\mu_F}\right)^{1/3}\right]$$

2. Heat flux; $q = h_f [(T_o)_{ass.} - T_{Fi}]$

where,

T_{Fi} = Feed inlet temperature,

$(T_o)_{ass.}$ = Assumed disc temperature = $\frac{T_s + T_{Fi}}{2} - 1$

$(To') = (To)ass. + q(x/k)$

T_s = Steam temperature, (To') = surface temperature on condensate side

3. Rate of condensate; $Q_c = (^{qA}/_{\rho_c h_{fg}})$

where, $A = \pi(r_o^2 - r_i^2)$

4. The thickness of the condensate film; δ_c

$$\delta_c = [3\mu_c(Q_c + Q_{c1})/2\pi(\frac{r_o + r_i}{2})\omega^2\rho_c]^{1/3}$$

Q_{c1} = Sum of the rate of condensate calculated for the previous segments.

5. Condensate mean velocity; u_m,

$$u_m = [\rho_c(\frac{r_o + r_i}{2})\omega^2\delta_c^2/3\mu_c]$$

6. Heat transfer coefficient of the condensing film was calculated, using the Nusselt model. Since it was developed for a stationary surface, therefore 'g' was replaced by '$r\omega^2$' which produced the following correlation,

$$h_c = 1.102K_c[\rho_c(\frac{r_o + r_i}{2})\omega^2/4\mu_c\delta_c u_m]^{1/3}$$

7. The disc temperature was calculated using h_c;

$$(T_o)_{cal.} = T_s - q/h_c$$

8. Calculated and assumed surface temperatures were compared for the following possibilities;

(a) If $(T_o)_{cal.} + 1 < (T_o')$, then another iteration was made starting from step 2, assuming that $(T_o)_{ass.} = (T_o)_{cal.} + 1$

(b) If $(T_o)_{cal.}-1 > (T_o')$, then the calculations were repeated from step 2, assuming that $(T_o)_{ass.} = (T_o)_{cal.}-1$

(c) If $(T_o)_{cal.} = (T_o)_{ass.} \pm 1$, then calculate liquid exit temperature, using the following equation;

$$T_{Fo} = (qA/Q_f \rho_F c_p) + T_{Fi}$$

9. The same procedure was followed for each consecutive section up to the periphery of the disc. The exit temperature of the previous segment was considered as the inlet temperature of the liquid for the next section.

A B.B.C. micro-computer was used for iterations and the program was written for the flow chart given in figure 4.2.

4.3. HEAT TRANSFER WITH PHASE CHANGE

The algorithm used for sensible heat transfer predictions was modified (as shown in figure 4.2) to account for the phase change with the following assumptions.

(i) When the liquid temperature approached within 5° of its boiling point, the bulk of heat supplied (more than 90 per cent) was assumed to be utilized as latent heat of evaporation.

(ii) Feed rate for each section was determined by subtracting the vapours calculated for the previous sections.

Estimated film flow rate at the edge of the disc was compared with minimum wetting rate from the work, reported in Appendix 'A'.

4.4. POWER CONSUMPTION

To compare measured power with predicted values of kinetic energy given to the test liquid together with frictional power dissipation, the following equations were used;

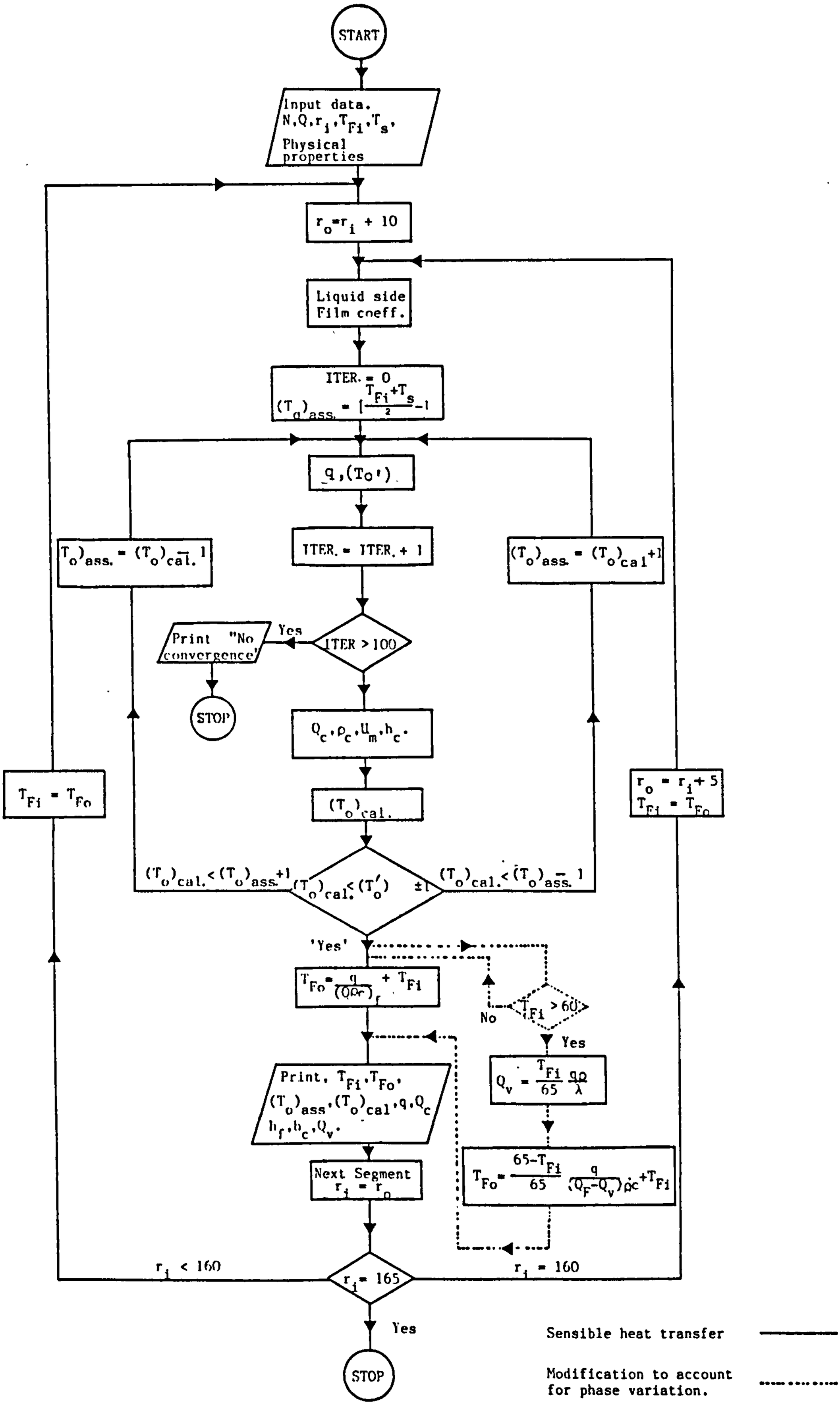

FIGURE 4.2. LOGIC DIAGRAM FOR HEAT TRANSFER PREDICTIONS

(i) $P_k = \frac{1}{2} Q\rho[(r^2\omega^2 + u_m^2)_o - (r^2\omega^2 + u_m^2)_i]$

where $u_m = (\rho Q^2\omega^2/12\pi^2\mu r)^{1/3}$

(ii) $P_f = \frac{Q\rho\omega^2}{2} (r_o^2 - r_i^2)$

The equation to estimate friction power dissipation has been derived in Appendix 'G', where the following model has also been developed;

$$P = \frac{1}{2} ReTa^2$$

Where P = Power number = $(\frac{P_f r\rho^2}{\mu^3})$

Re = Reynolds number = $(Q/r\nu)$

Ta = Taylor number = $(\omega r^2/\nu)$

CHAPTER FIVE

EXPERIMENTAL RESULTS AND DISCUSSION

5.1. SENSIBLE HEAT TRANSFER

Experiments were performed for the following conditions:

(i) Feed flow rate 10 cc/s to 130 cc/s (i.e. $60<Re<800$)

(ii) Disc speed 600 to 1200rpm (i.e. $1.7\times10^6<Ta(3.42\times10^6)$

(iii) Steam pressure 0.1 bar (gauge)

(iv) Steam condensation temperature ≃ 100°c.

(v) Feed inlet temperature range 20°c to 45°c.

(vi) Rate of heat transfer 1.5 to 34.4 kW (equivalent to 20 kW/m² to 430 kW/m²)

(vii) Surface tension range (adjusted by addition of surfactant) 70×10^{-3}(N/m) to 39×10^{-3}(N/m)

In addition to these operating variables the effect of non-condensables on rate of heat transfer was investigated. Data obtained for these conditions are presented in Tables 1 to 6.

5.1.1. Accuracy Of The Experimental Measurements

A general estimate of the overall accuracy of the experimental measurements needs to be considered, although the following measures were undertaken during experimentation:

(i) Each instrument, employed for measurements, was calibrated and checked periodically.

(ii) A new set of thermocouples was used and the accuracy of each junction was confirmed by direct calibration against a mercury in glass thermometer, accurate to ± 0.5°c.

(iii) The test section was calibrated for heat losses before performing any set of experiments.

The accuracy of the experimental measurements was checked by an overall heat balance. This was determined by comparing the heat transferred to feed with the heat supplied by the condensing steam, including the allowances for calibrated heat losses. Generally, an agreement within ten per cent was found (as shown in figure 5.1) which was assumed to be satisfactory.

A typical set of model calculations are presented in a subsequent section. This model is based on a heat transfer process involving three possible thermal resistances, those due to the liquid feed and condensate films, together with an allowance for the thermal resistance of the intervening disc wall. Relative values of these film coefficients with a constant disc speed of 1200 rpm for a range of liquid feed flowrates are shown in Table 5.1. This shows the influence of the wall resistance on the overall coefficients for a range of operation conditions. In practice the effect of the wall resistance is much less than would be suggested by Table 5.1 due to influence of temperatures approach on overall performance.

TABLE 5.1. OVERALL HEAT TRANSFER COEFFICIENT

(N = 1200 rpm X_m = 0.5mm K_m = 15.1 W/m-K)

Q_f (cc/s)	h_f	h_c	U	U^*
		(kW/m^{2}K)		
10	17.10	46.44	12.49	8.82
50	10.01	45.41	8.20	6.51
90	8.23	46.91	7.00	5.62
130	7.28	48.36	6.32	5.20

Where $\frac{1}{U} = \frac{1}{h_f} + \frac{1}{h_c}$

$$\frac{1}{U^*} = \frac{1}{h_f} + \frac{1}{h_c} + \frac{X_m}{K_m}$$

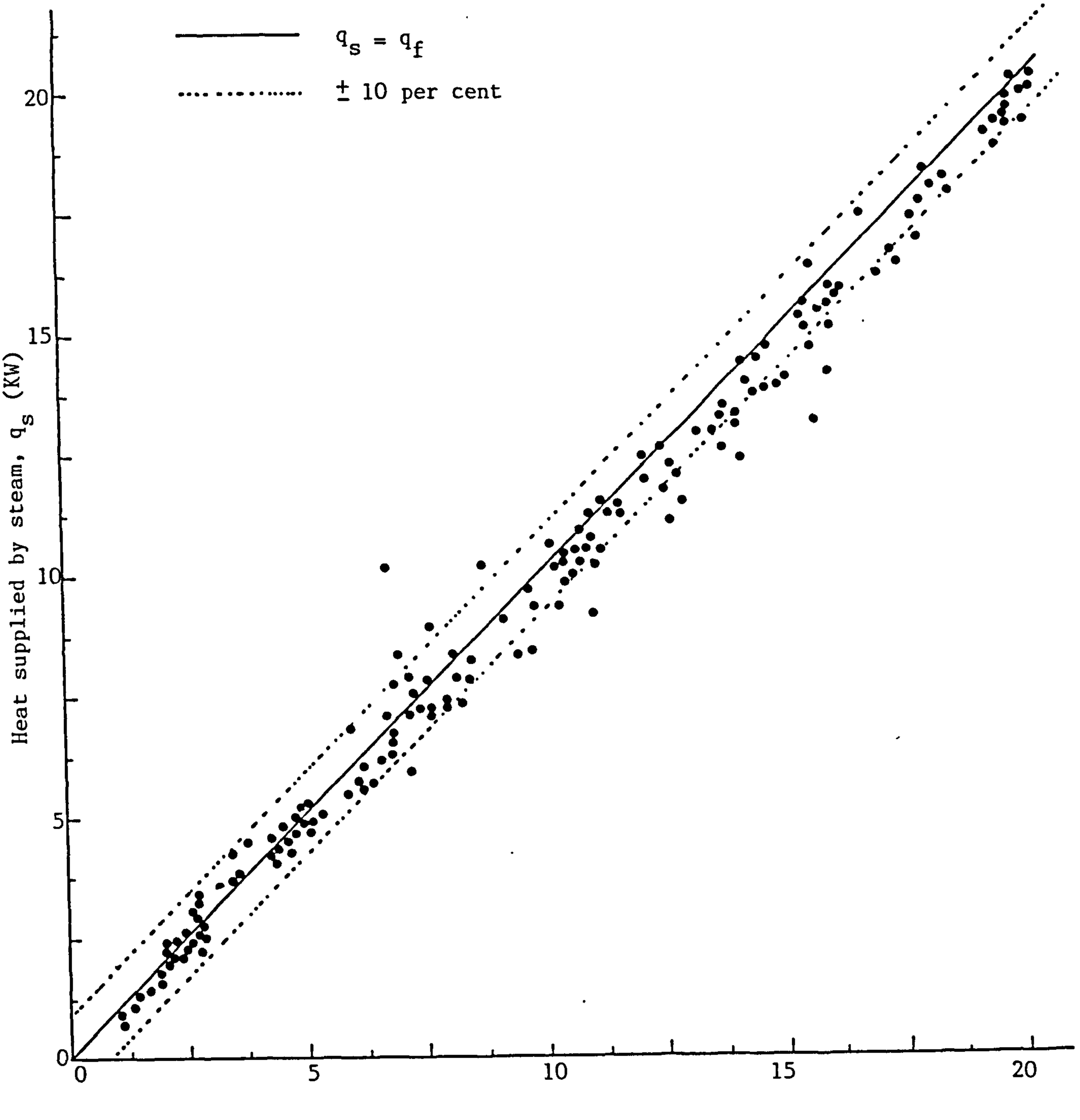

FIGURE 5.1 OVERALL BALANCE FOR SENSIBLE HEAT TRANSFER

5.1.2. Effect Of Feed Rate

Typical characteristics showing the temperature of the feed liquid as it leaves the disc surface are shown in figures 5.2, 5.3, 5.4 and 5.5 for the disc speeds of 1200, 1000, 800, and 600 rpm respectively. Since each of these graphs shows similar behaviour, common characteristics will be discussed with reference to figure 5.3 (1000 rpm). Six characteristics are displayed on the figure. The upper one is the result of calculations based on the model developed in section 4.2. This indicates that at feed rates up to about 40 cc/s the feed attains a temperature equal to that of the disc. For high flow rates there is a gradual decrease in exit temperature. This is explained by noting that for a constant disc speed, increasing flow rate will produce increasing film thickness at all disc radii, and this will result in lower heat transfer rates. This assumes that laminar conditions are maintained in the film despite the increased film thickness.

Two solid curves represent the experimental data for the same range of feed rates. The lower characteristic gives exit temperatures measured when the condensing steam was known to contain air. These data were taken before the condensing space had been equipped with automatic air venting. Improvement in heat transfer following the installation of air venting is shown by the upper solid curve. This demonstrates the importance of air or non-condensables venting on the efficient operation of condensing equipment.

Similar behaviour is apparent in the performance at disc speeds 1200, 800 and 600 rpm. However the experimental data, with purging of air via the vent valve, is still lower than predicted values, particularly at flow rates in excess of 40cc/s. Further

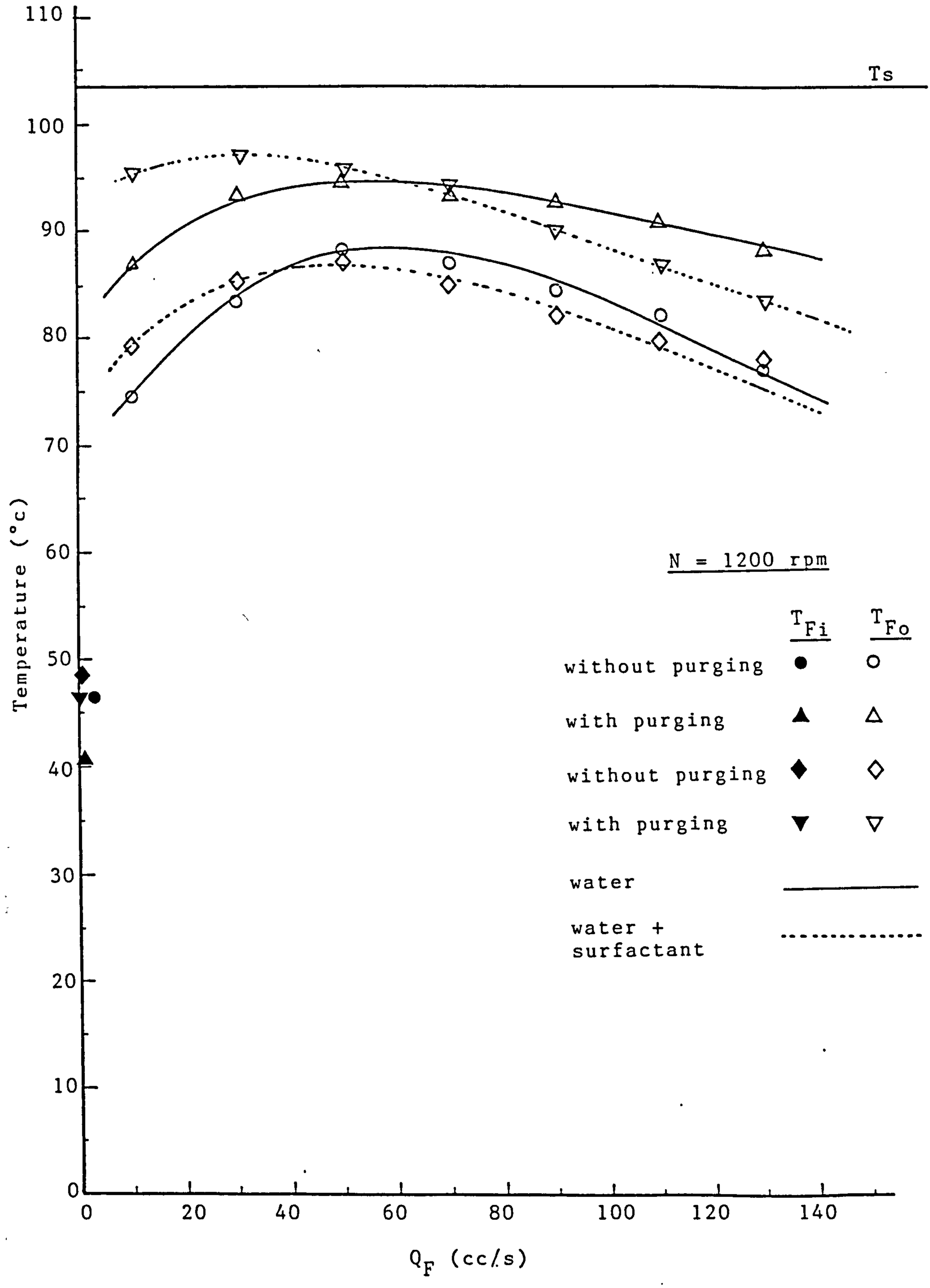

FIGURE 5.2. EFFECT OF FEED RATE

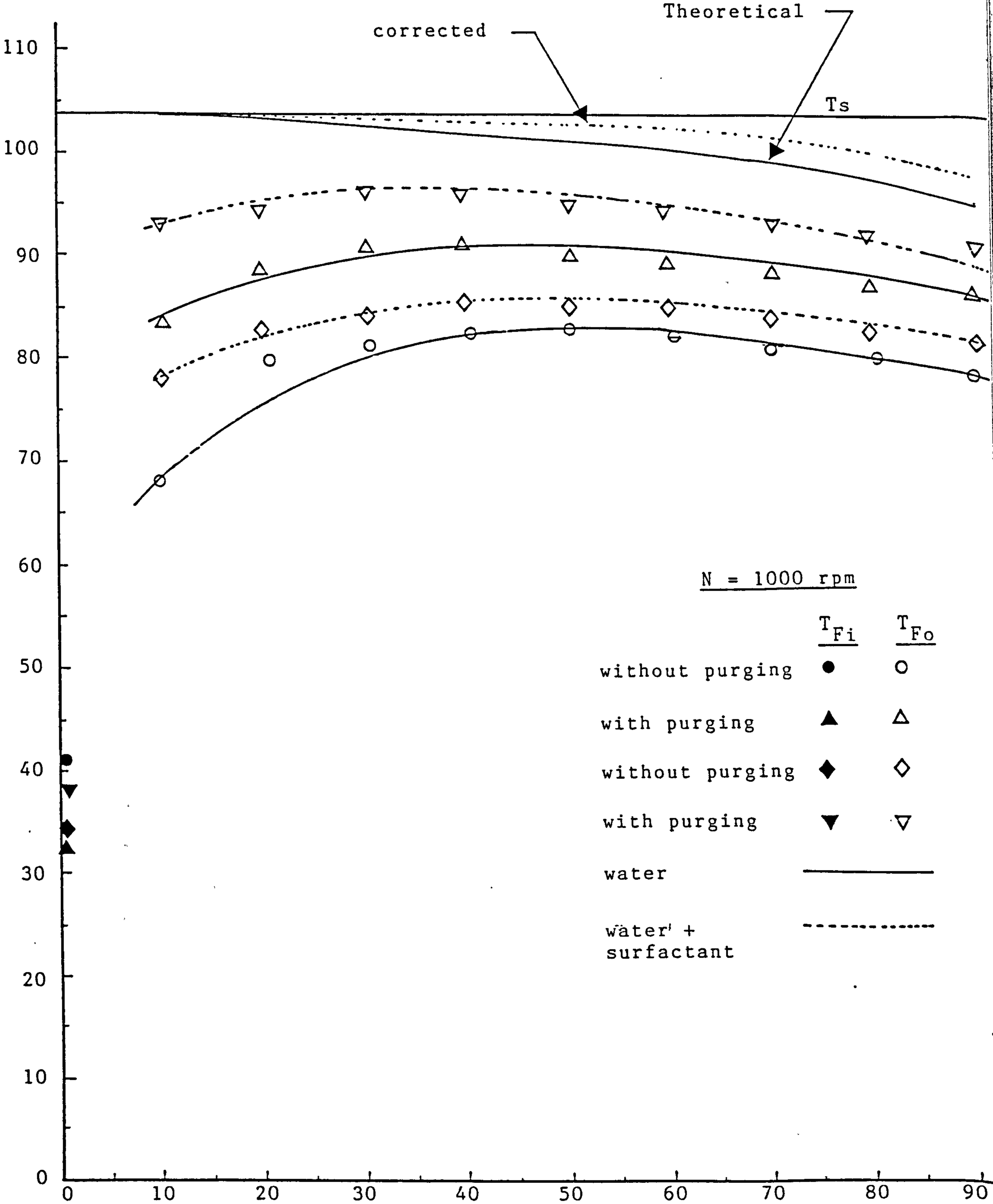

FIGURE 5.3. EFFECT OF FEED RATE

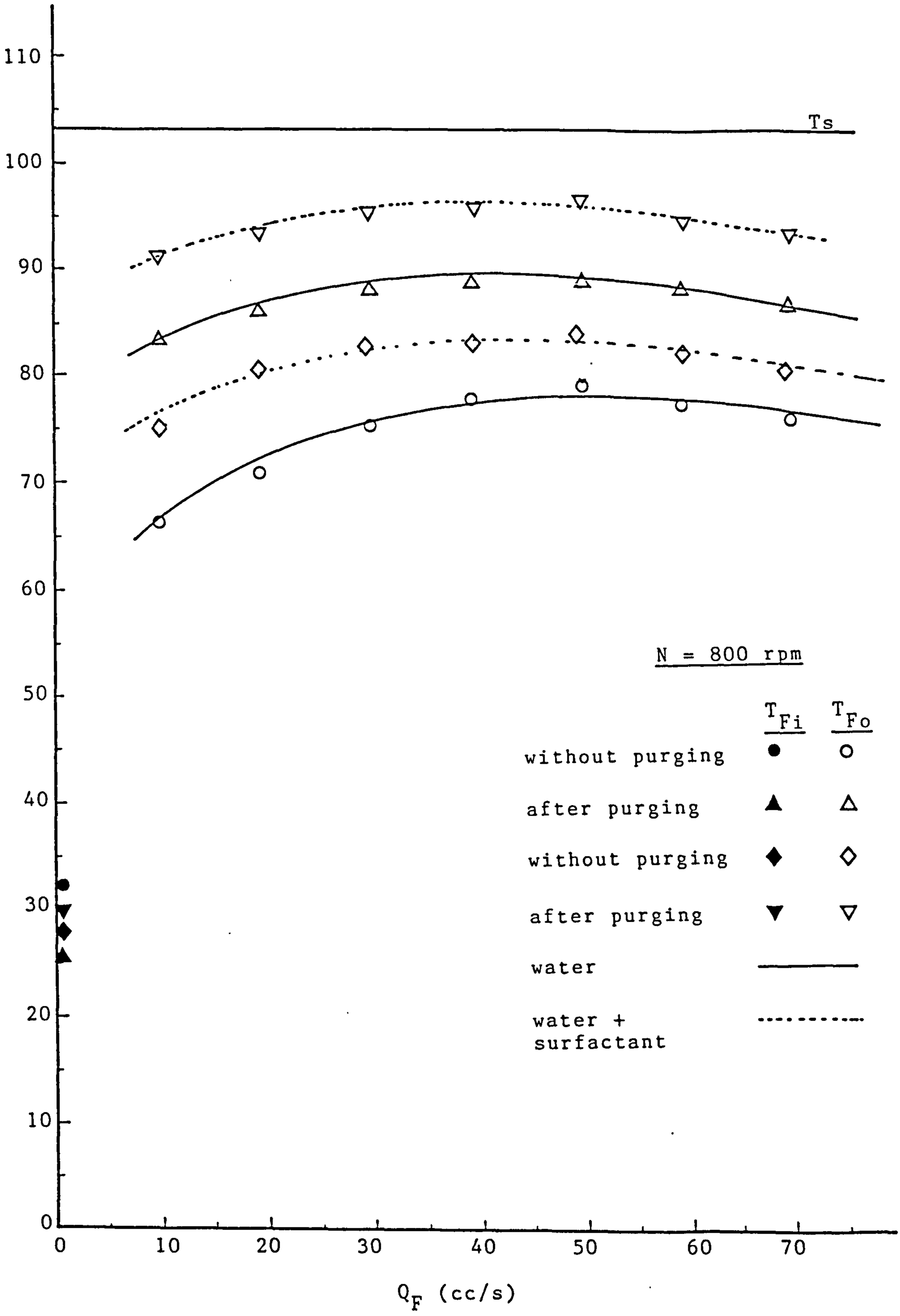

FIGURE 5.4. EFFECT OF FEED RATE

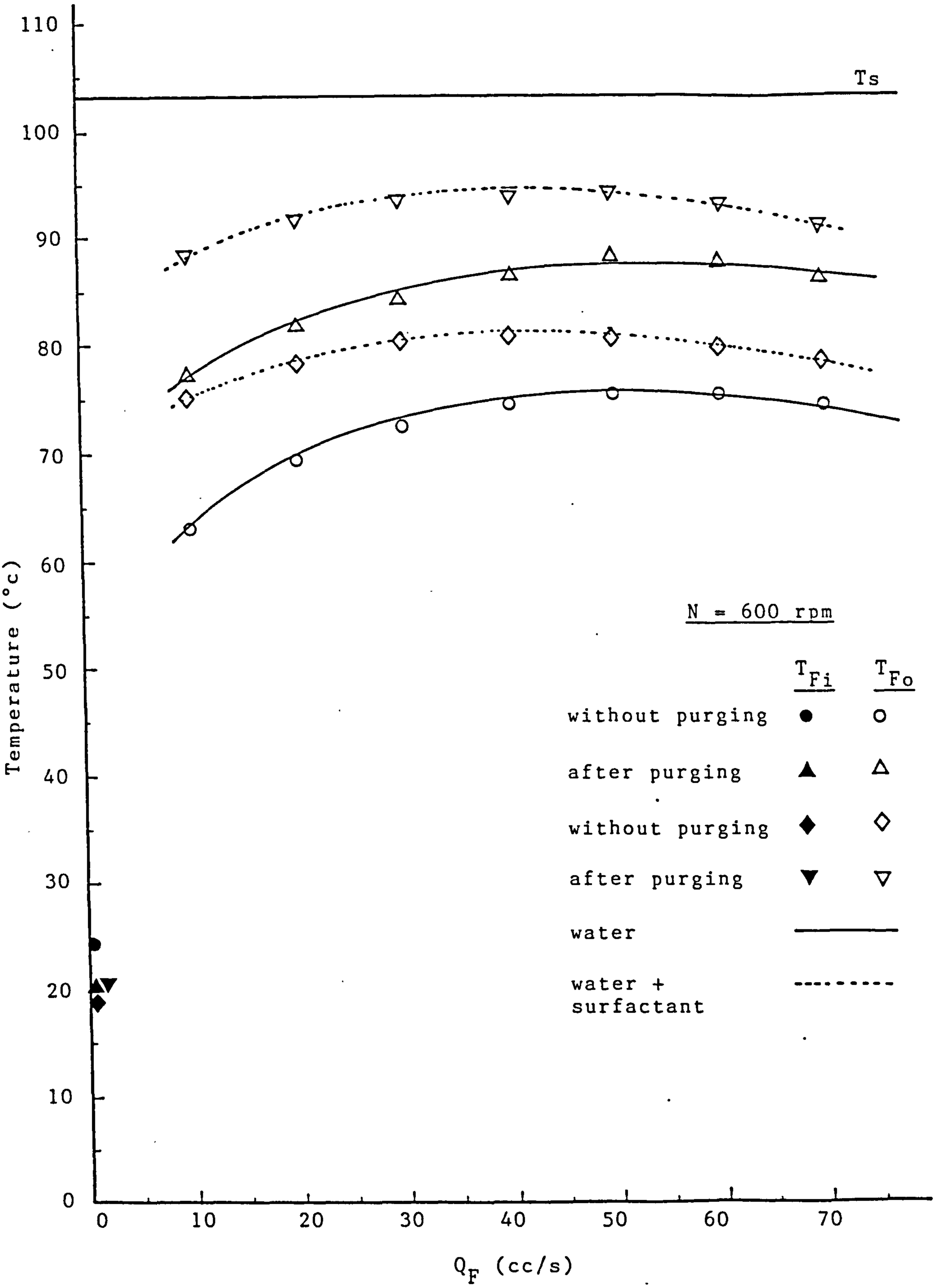

FIGURE 5.5. EFFECT OF FEED RATE

attempts to achieve complete air removal and maintain continuous purging did not increase exit temperatures. The effect of surfactant in the feed produced a small improvement in exit temperature over this range of flow rate. The reason for this effect cannot be explained at this time.

Comparison of the upper experimental characteristic with the model results indicates that there is still a discrepancy in exit temperature of some 5 to 8°. It was noted earlier that this outlet temperature was measured at a point beyond the drive unit. The liquid from the machine passes through a central tube, coaxial with the annular flow channel taking feed (at a much lower temperature) to the disc. Therefore heat exchange between the feed liquid coming from and going to the disc would give rise to a drop in temperature between exit from the disc and the point of measurement.

Similar arguments apply throughout the range of feed rate investigated with higher corrections necessary at the lower feed rates. This error was not appreciated until the experimental programme was completed and therefore confirmation of the magnitude of the error was not possible. However the geometry of the feed channel was such that an estimation is possible. The channel was treated as a counterflow concentric tube heat exchanger with constant mass flow rate in both streams. In this exchanger inlet feed temperature was known, as was the final exit temperature of this liquid. Estimates of the feed temperature at the inlet and exit of the disc surface could be made. A typical result of this calculation, for the case of disc exit temperatures is shown in figure 5.3. In general this correction was in the range 7 to 10°c and therefore the true exit temperatures were slightly higher

than predicted values. Observations of film behaviour made during the minimum wetting rates indicated that this might be the case, since under the range of conditions of these experiements the film surface was always covered with ripples/waves etc. This would obviously enhance the heat transfer processes within the film.

However, the discrepancies at lower feed rates might also be due to the effects of incomplete surface wetting. For the conditions of figure 5.3 measurements and theoretical predictions for minimum wetting can be found in Appendix 'A' (Table A.1). Measured values of minimum wetting rate range from 19.2 cc/s for distilled water to 7.95 cc/s for water with high concentration of surfactant. The effect of surfactant in the lower feed rate is clearly shown.

5.1.3. Effect Of Disc Speed

Whilst this effect is shown clearly on the model predictions, figures 5.6 and 5.7 have been included to demonstrate one aspect of the process. In both figures it can be seen that in the range of flow rates investigated, the feed exit temperature show only small increases for substantial increase in disc speed. This is to be expected since in all cases the feed temperature at exit is approaching the disc surface temperature. Therefore the effect shown is essentially due to the reduced driving force. Any increases in heat transfer performance resulting from increased disc speed are not demonstrated by these graphs.

5.1.4. Model Data

A complete range of model predictions are shown on figures 5.8 to 5.26. These show the variation of mean temperature of the feed as it crosses the disc surface. At the lower flow

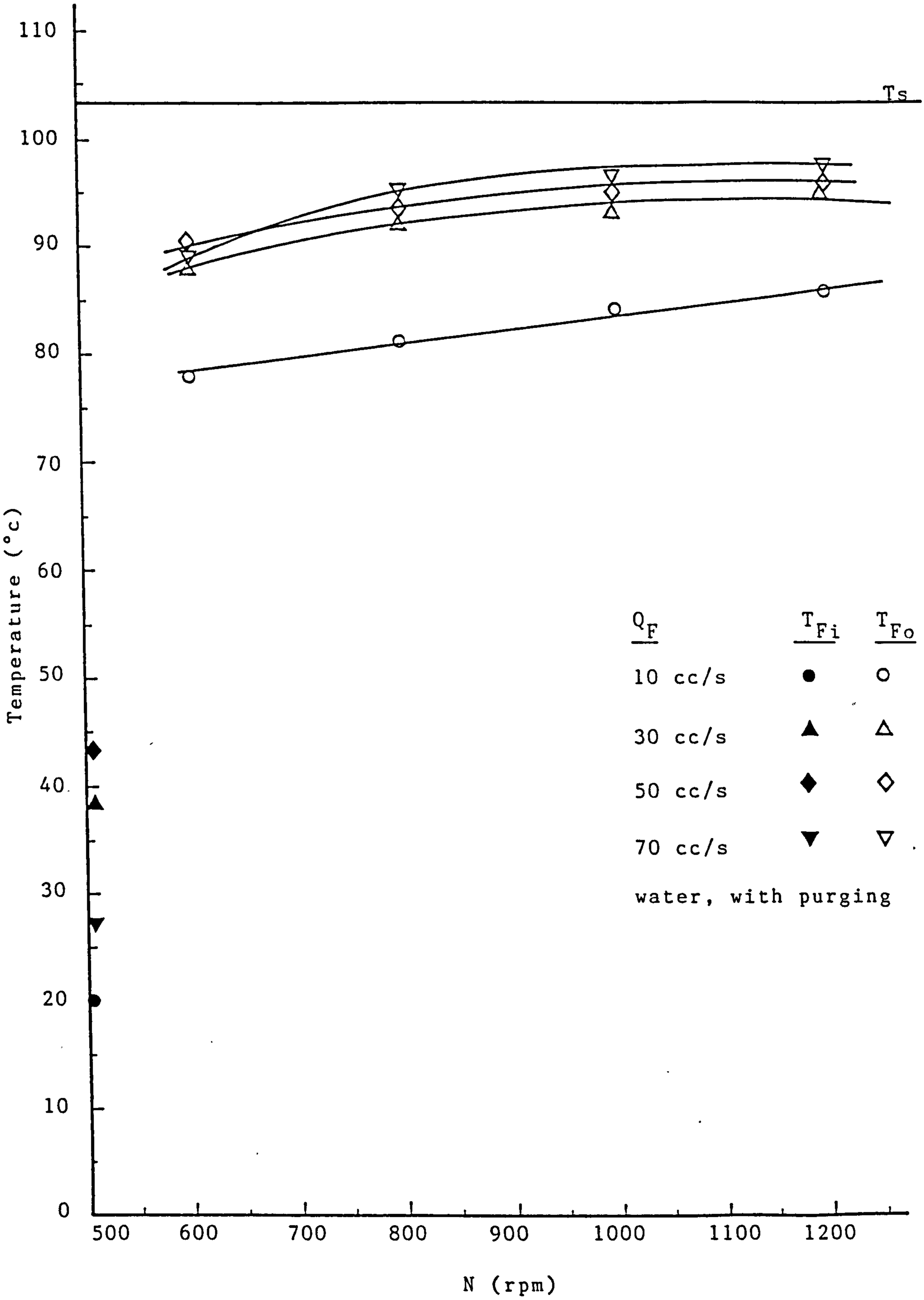

FIGURE 5.6. EFFECT OF DISC SPEED

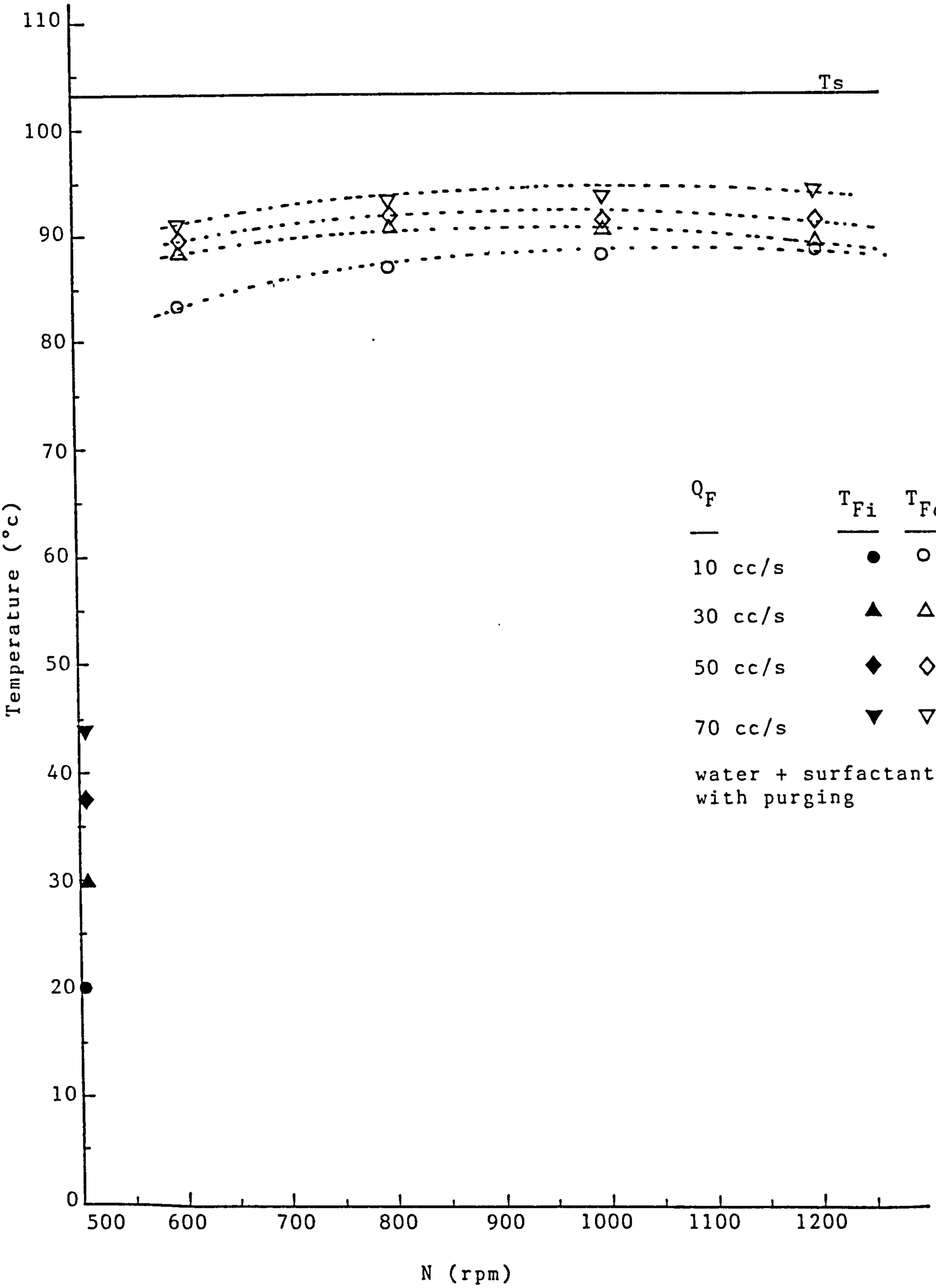

FIGURE 5.7. EFFECT OF DISC SPEED

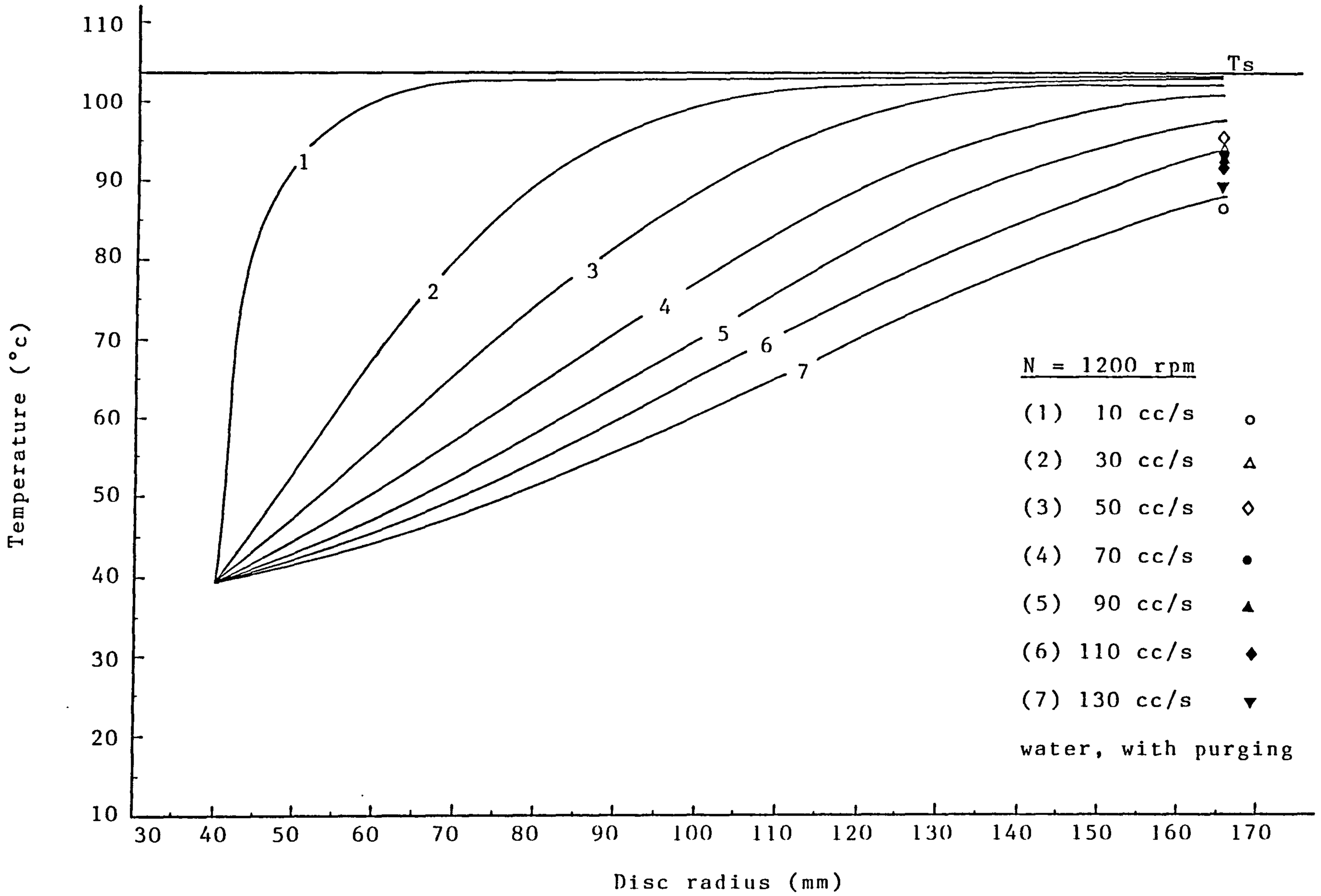

FIGURE 5.8. COMPARISON OF MEASURED & PREDICTED TEMPERATURES

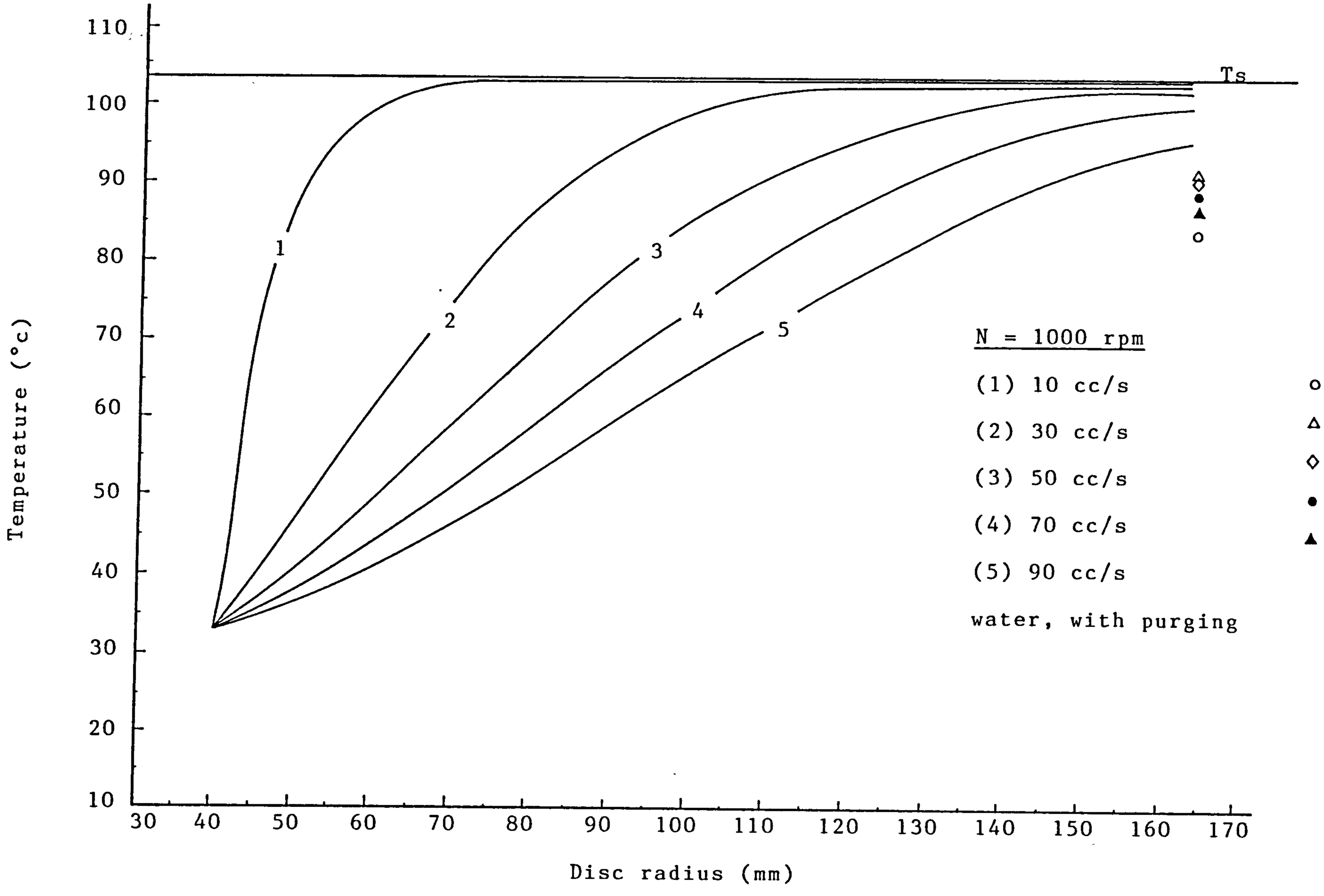

FIGURE 5.9. COMPARISON OF MEASURED & PREDICTED TEMPERATURES

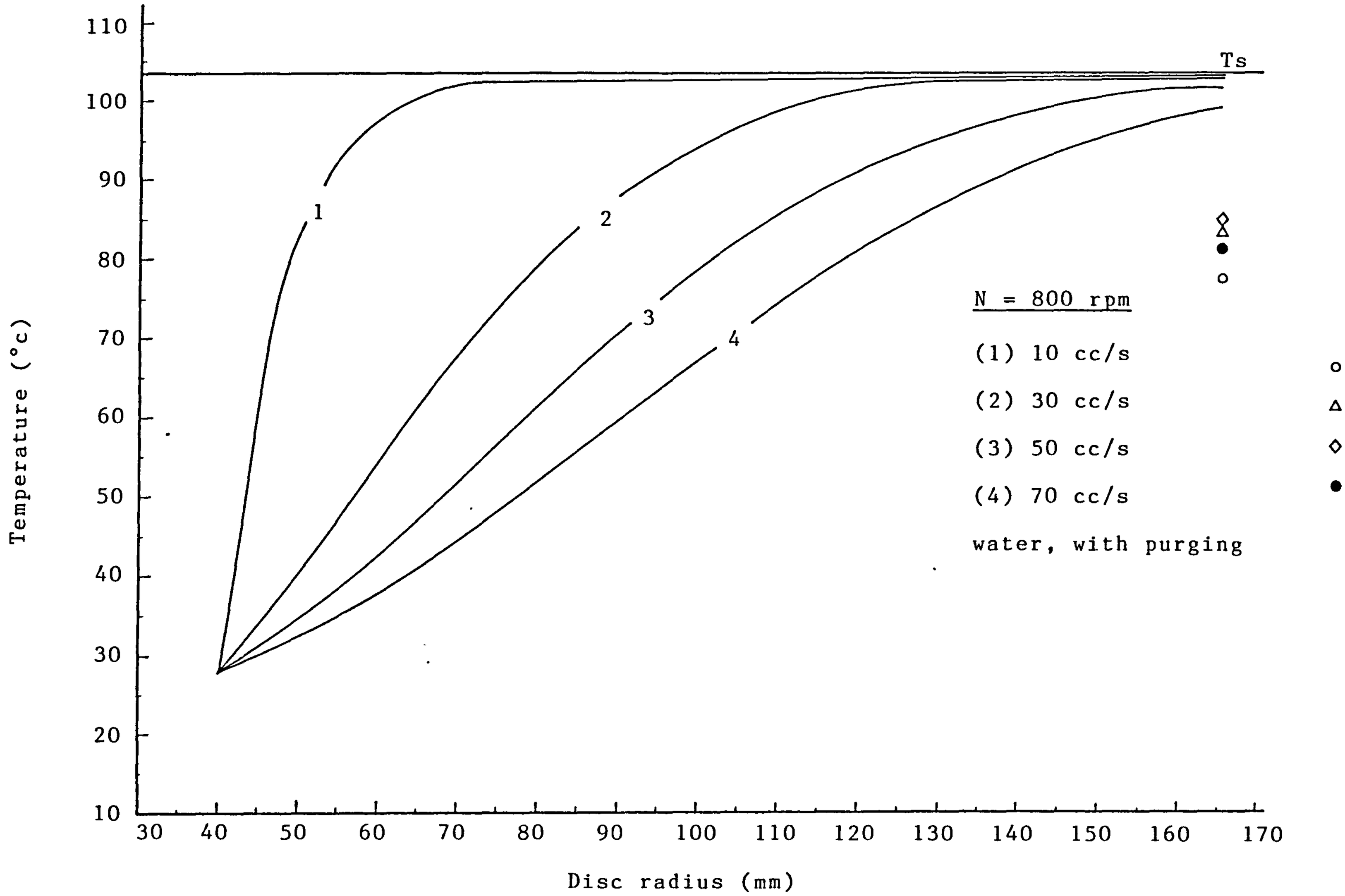

FIGURE 5.10 COMPARISON OF MEASURED & PREDICTED TEMPERATURES

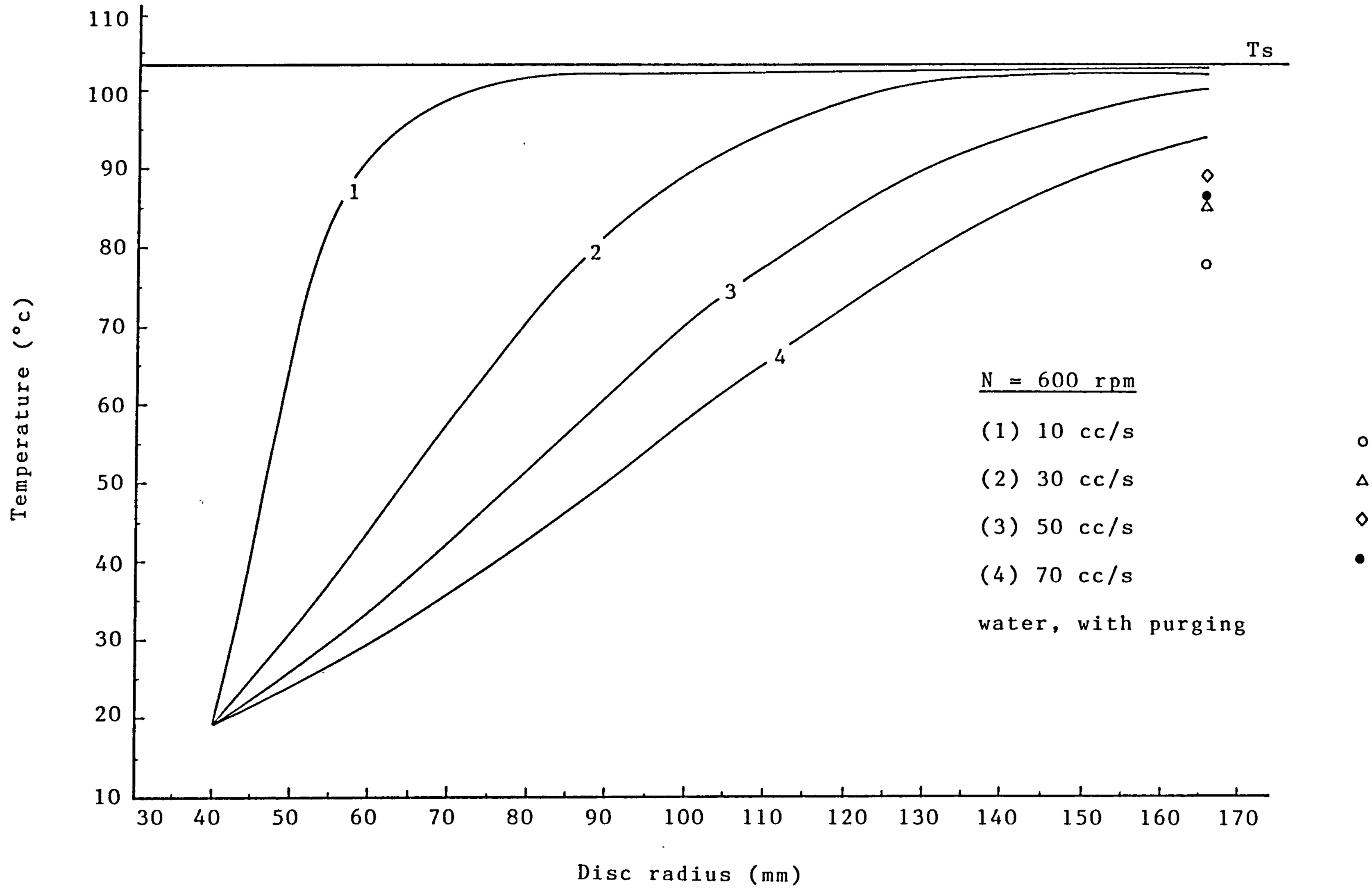

FIGURE 5.11 COMPARISON OF MEASURED & PREDICTED TEMPERATURES

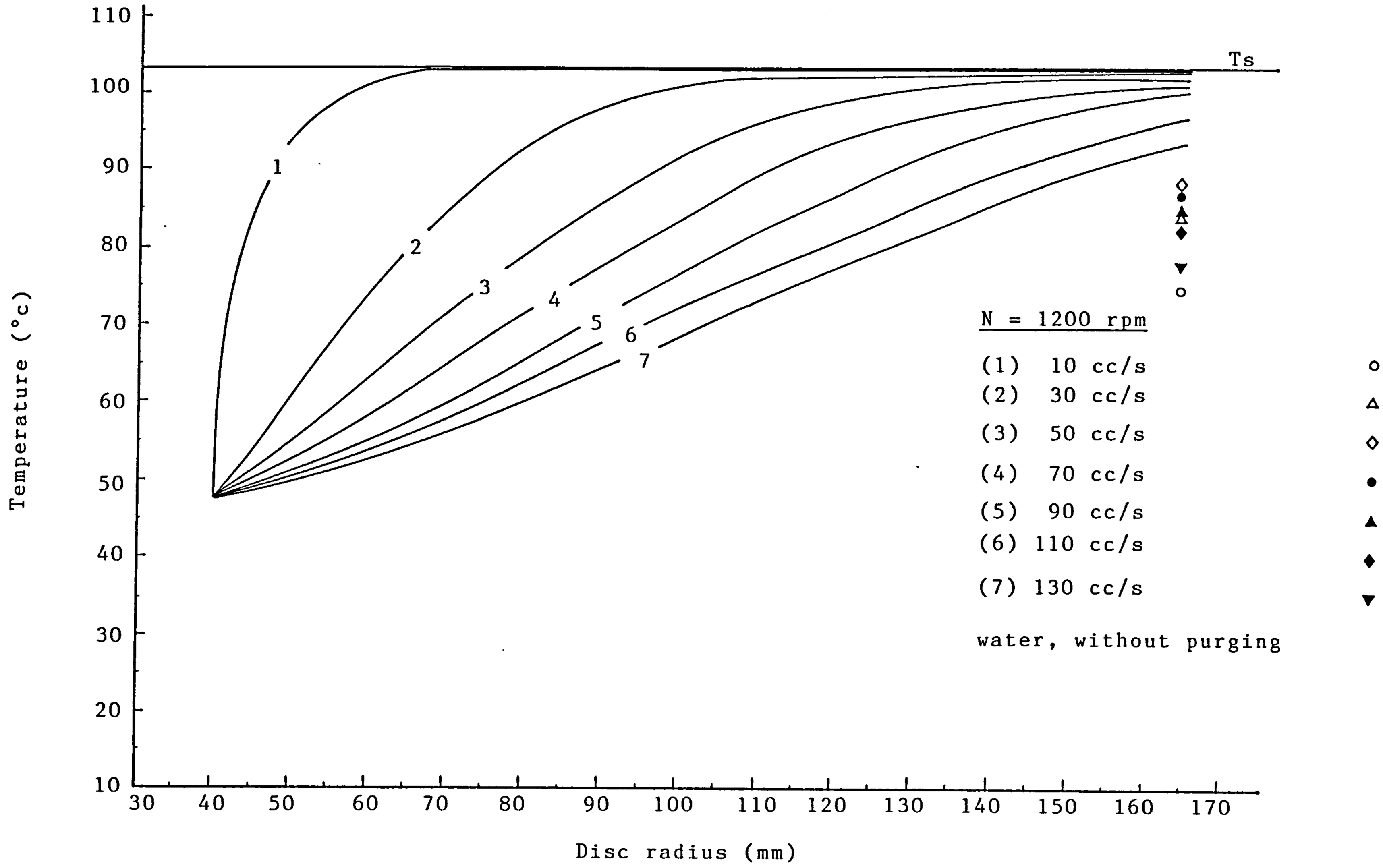

FIGURE 5.12 COMPARISON OF MEASURED & PREDICTED TEMPERATURES

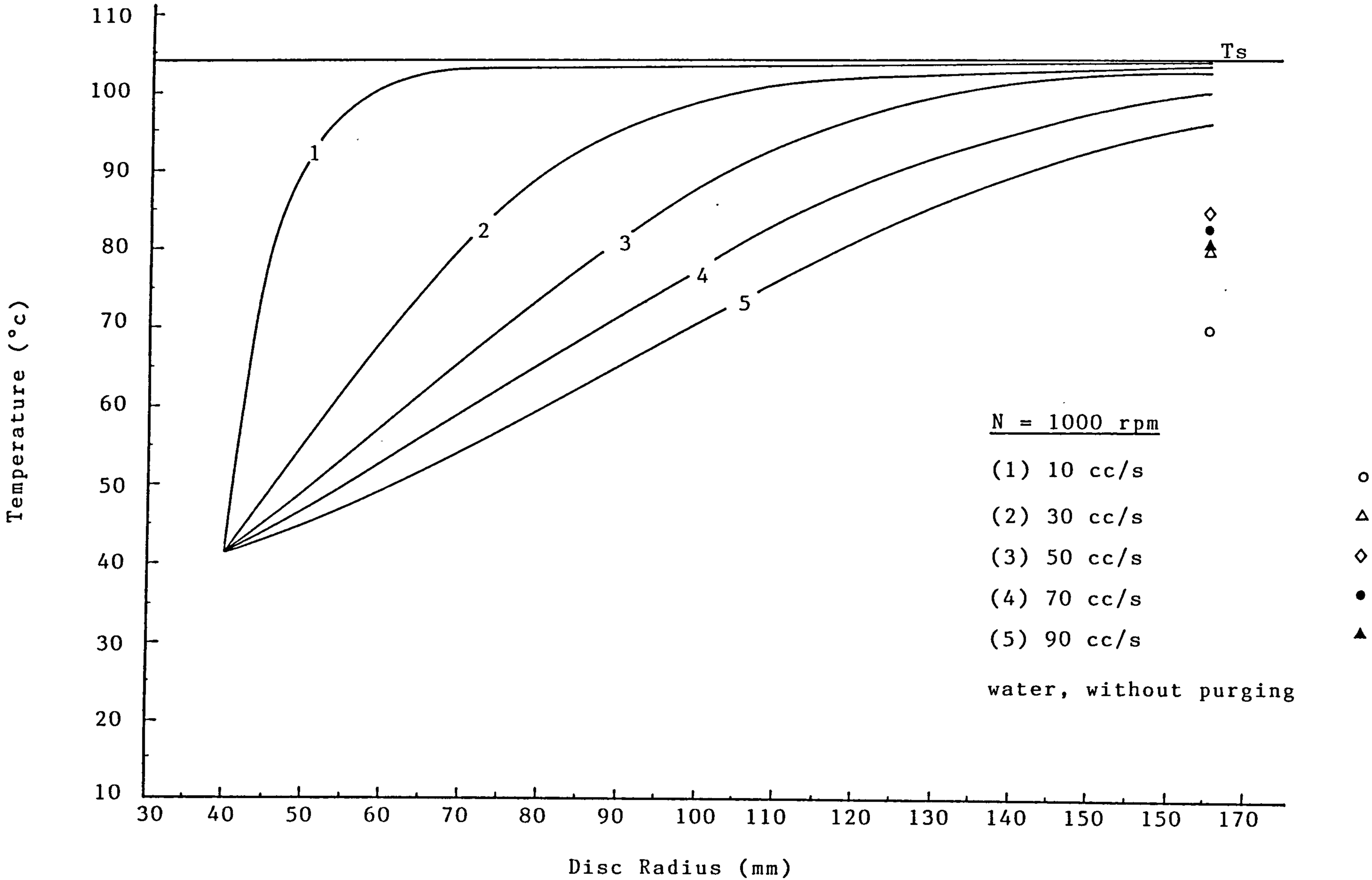

FIGURE 5.13 COMPARISON OF MEASURED & PREDICTED TEMPERATURES

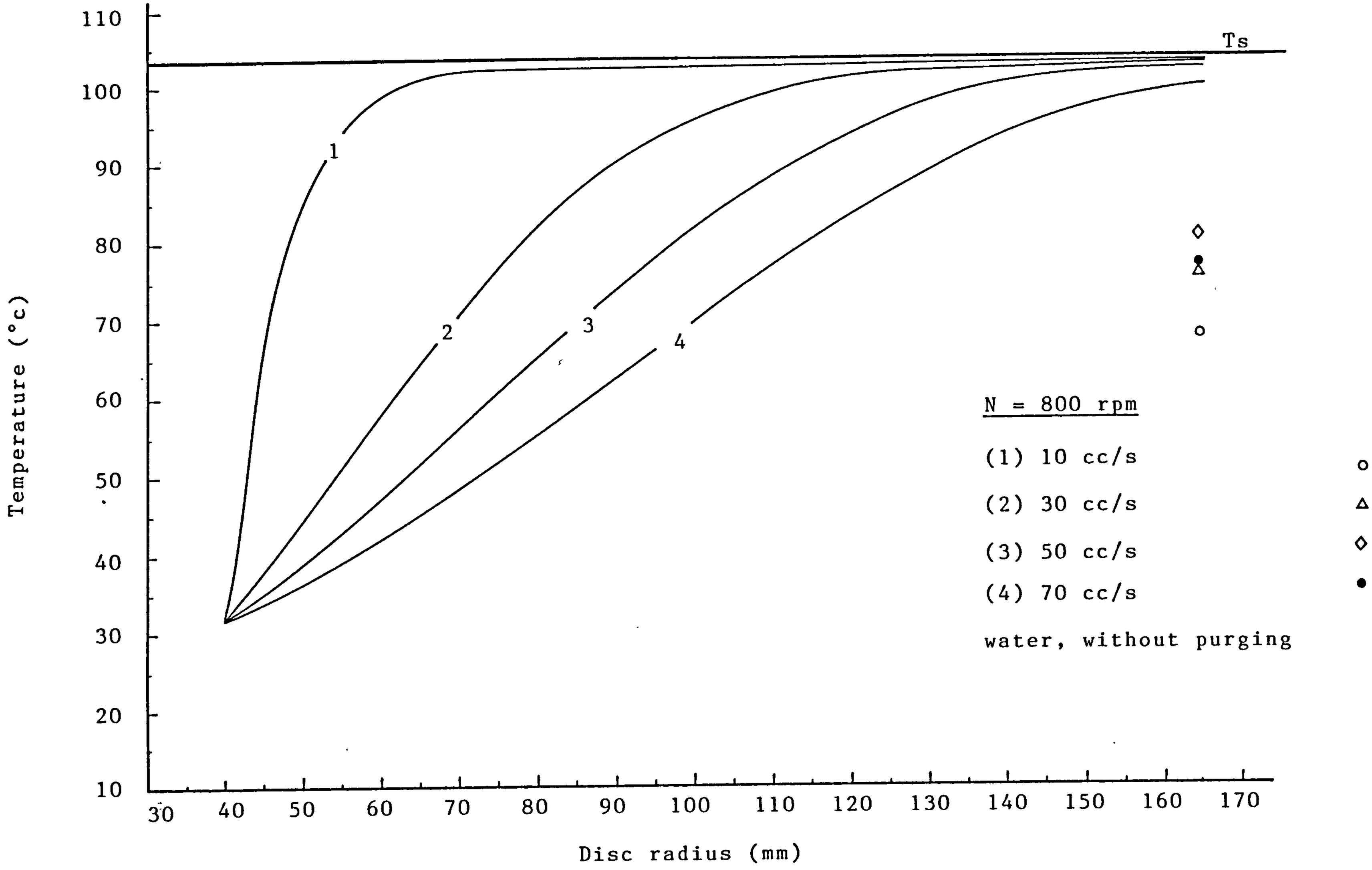

FIGURE 5.14 COMPARISON OF MEASURED & PREDICTED TEMPERATURES

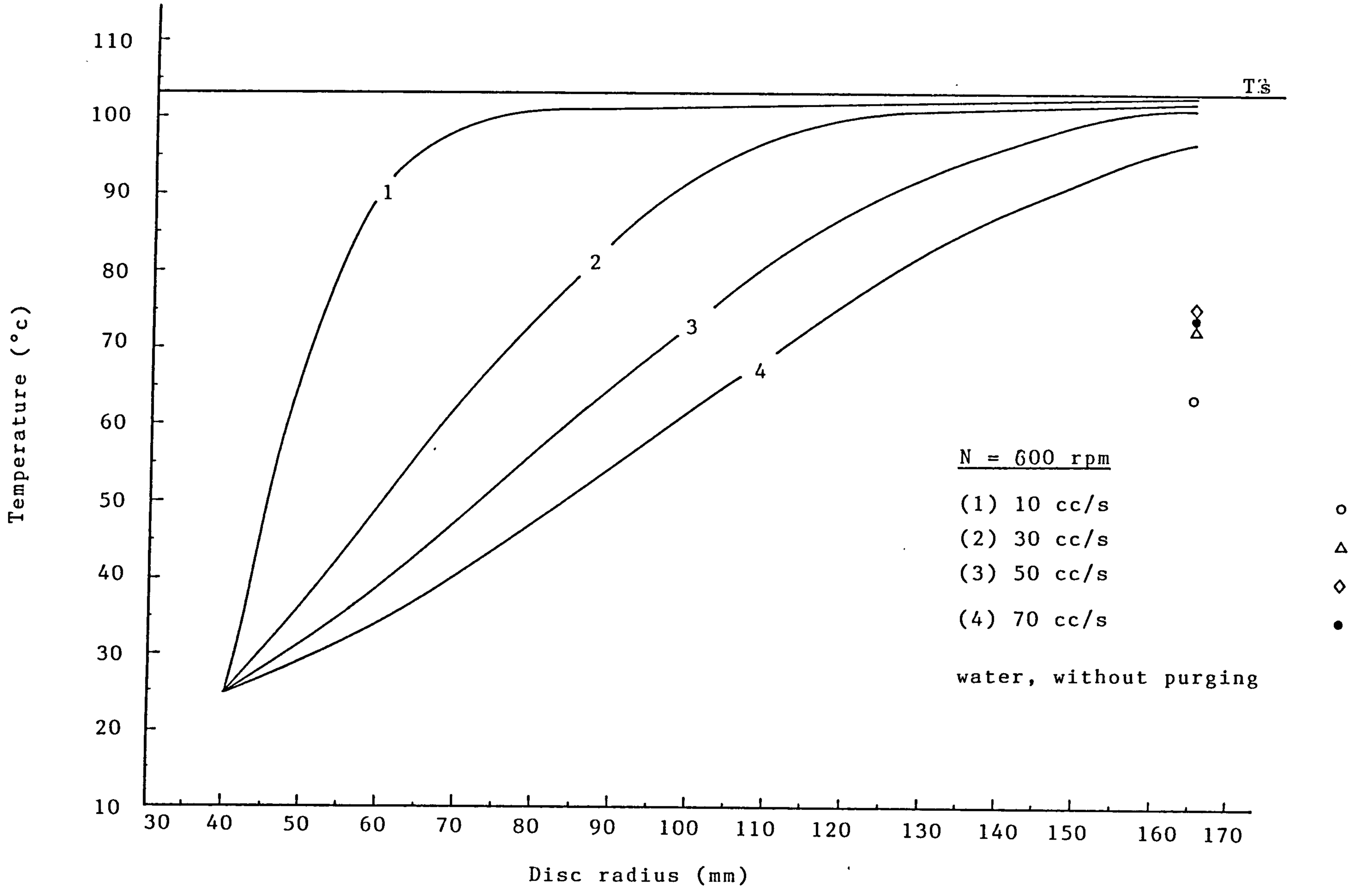

FIGURE 5.15 COMPARISON OF MEASURED & PREDICTED TEMPERATURES

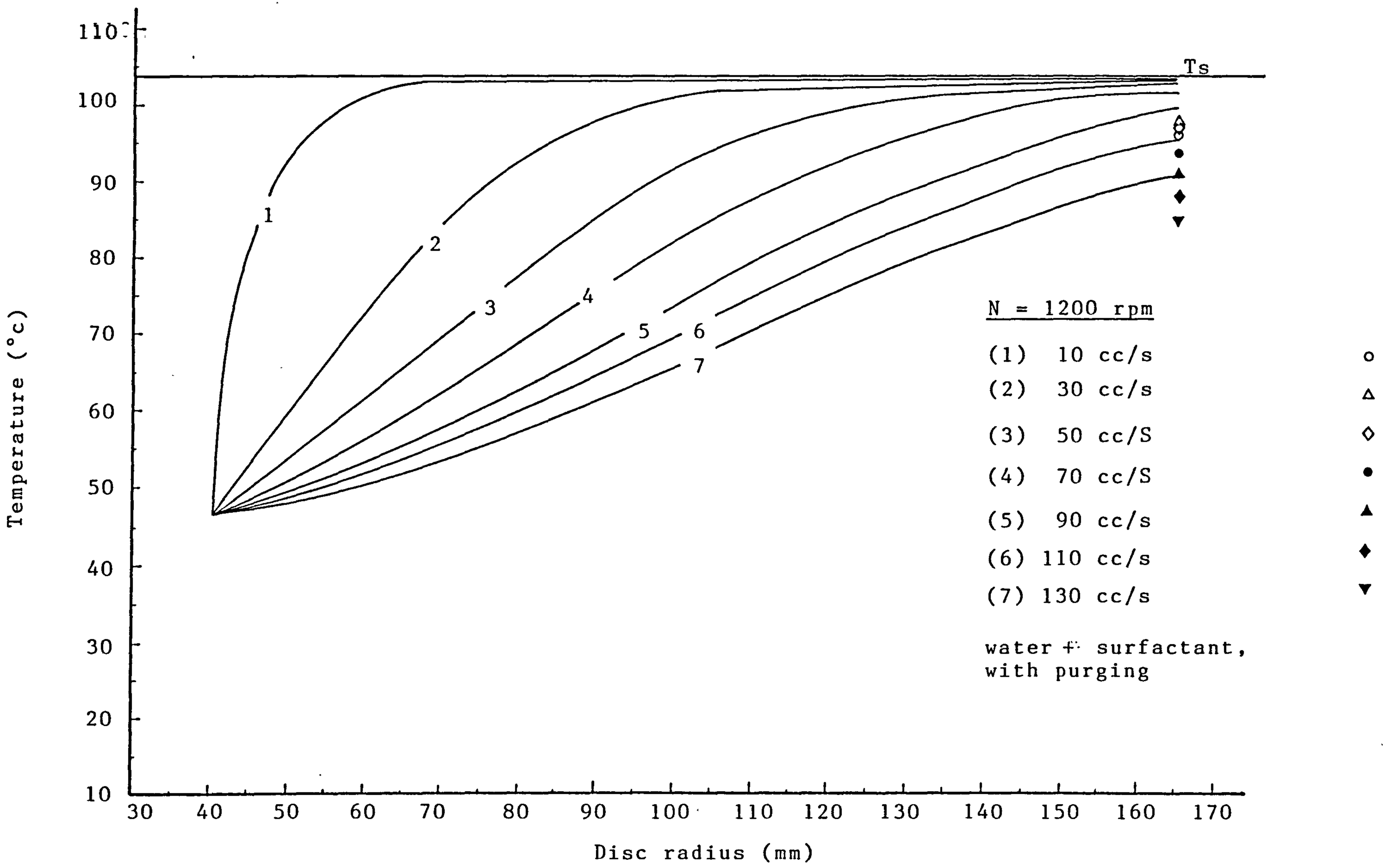

FIGURE 5.16 COMPARISON OF MEASURED & PREDICTED TEMPERATURES

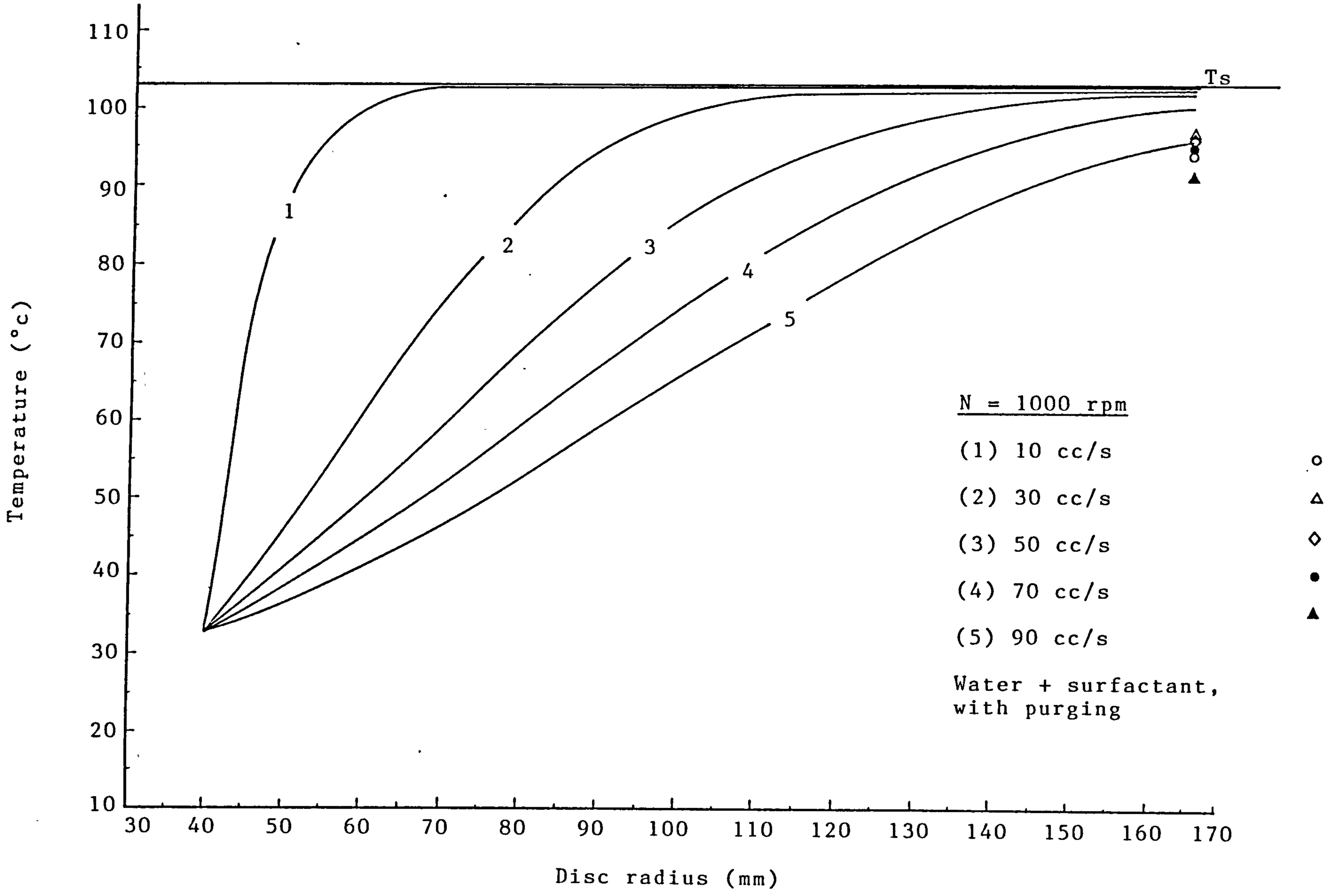

FIGURE 5.18 COMPARISON OF MEASURED & PREDICTED TEMPERATURES

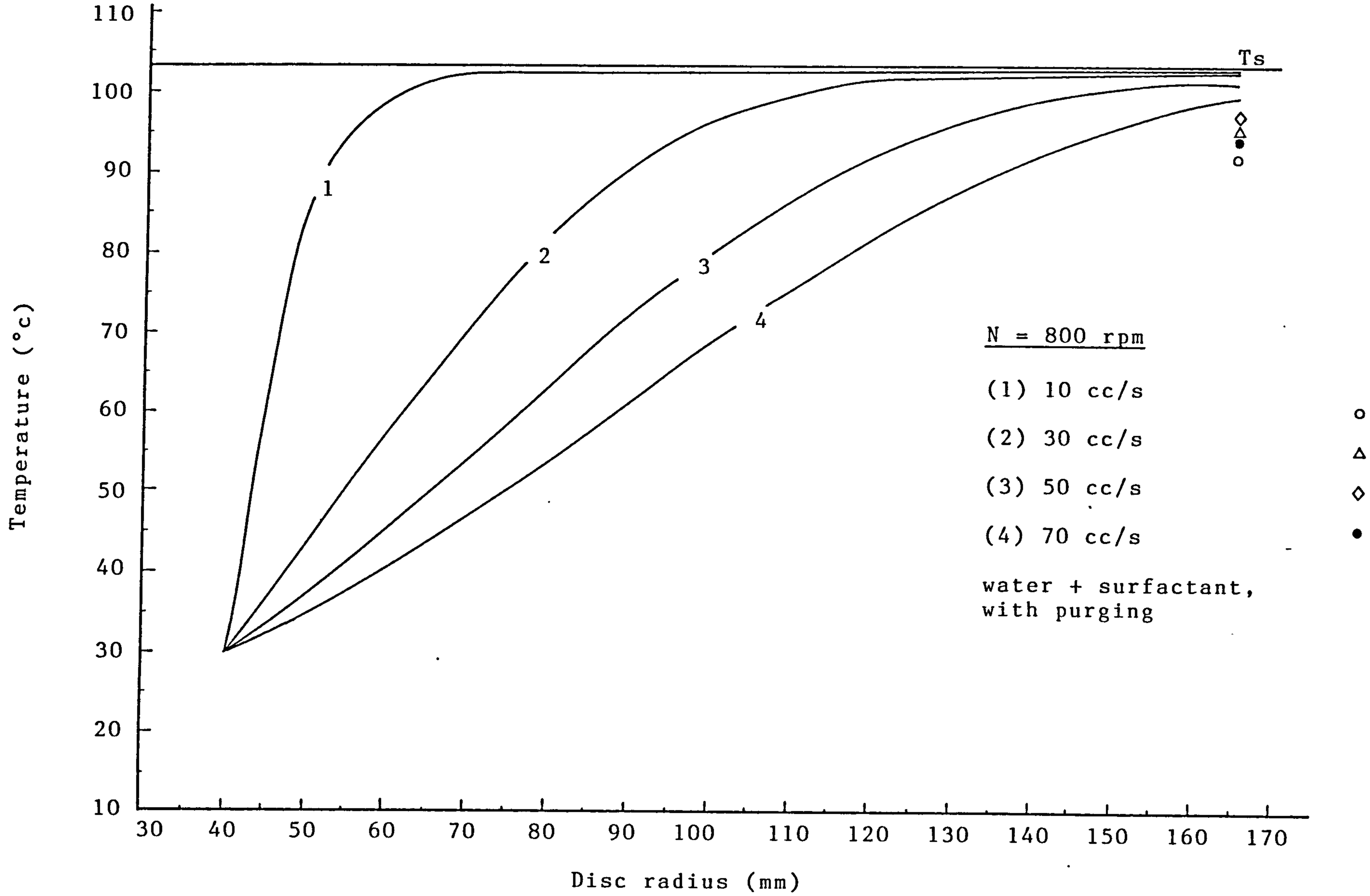

FIGURE 5.19 COMPARISON OF MEASURED & PREDICTED TEMPERATURES

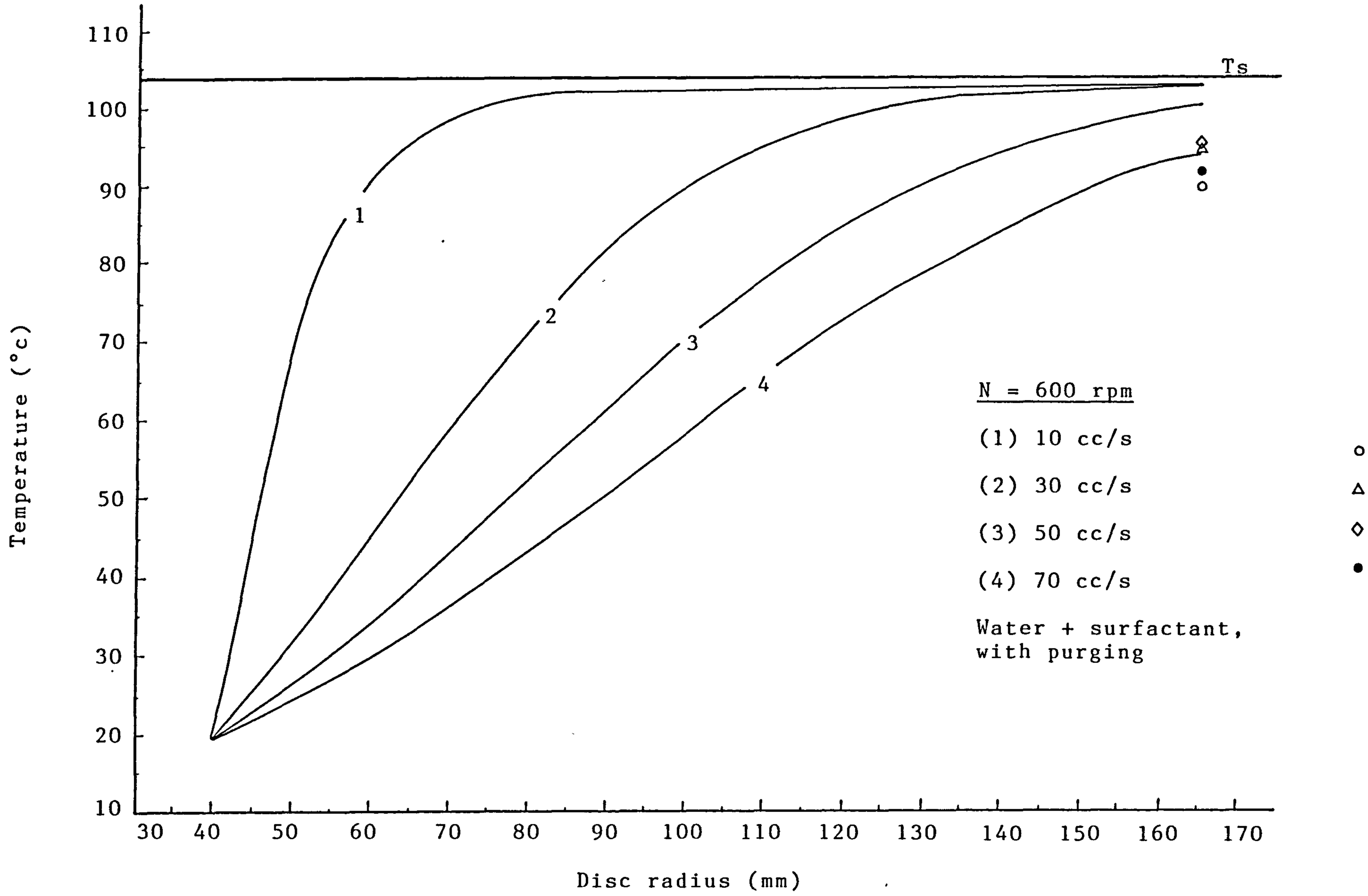

FIGURE 5.20 COMPARISON OF MEASURED & PREDICTED TEMPERATURES

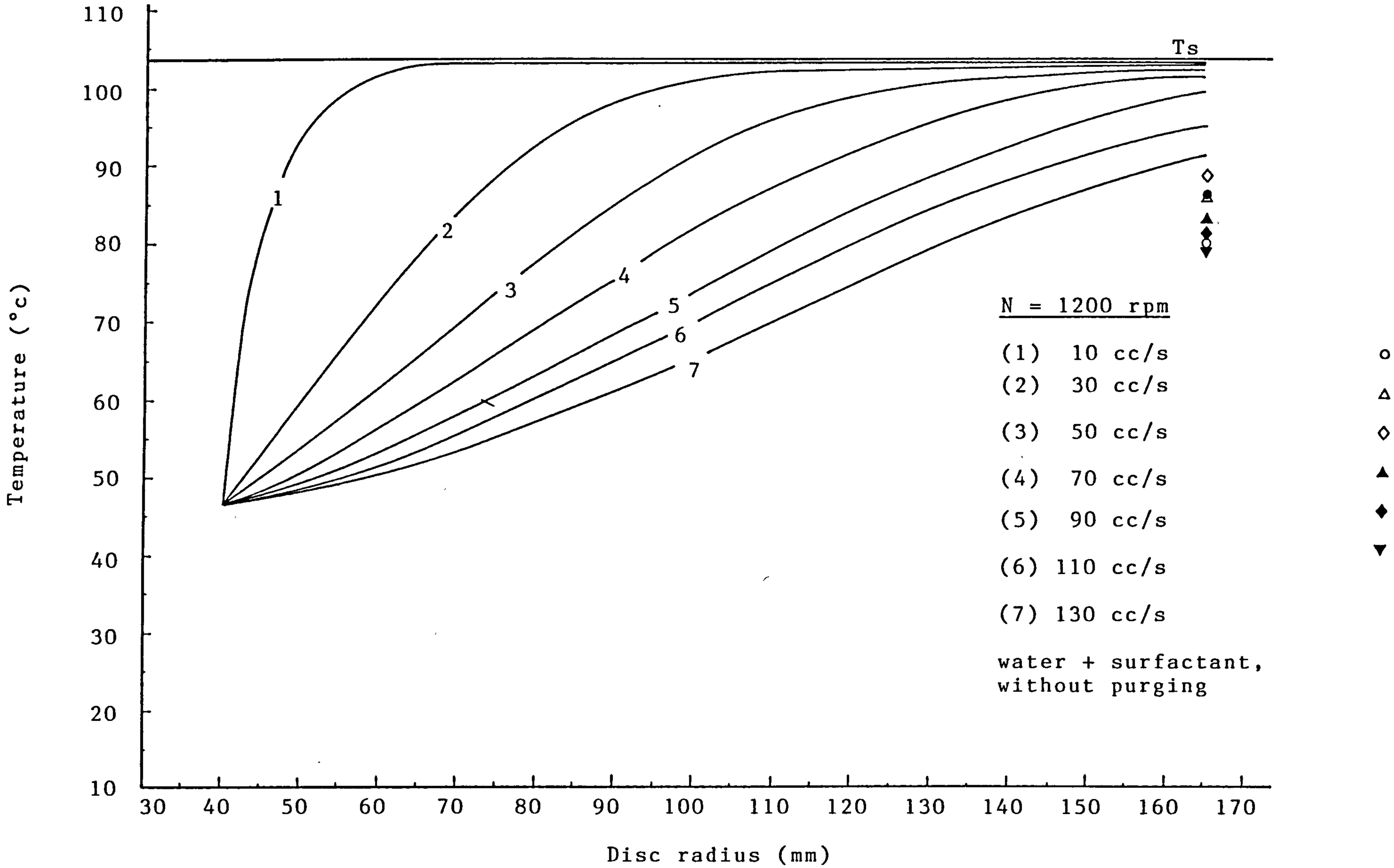

FIGURE 5.21 COMPARISON OF MEASURED & PREDICTED TEMPERATURES

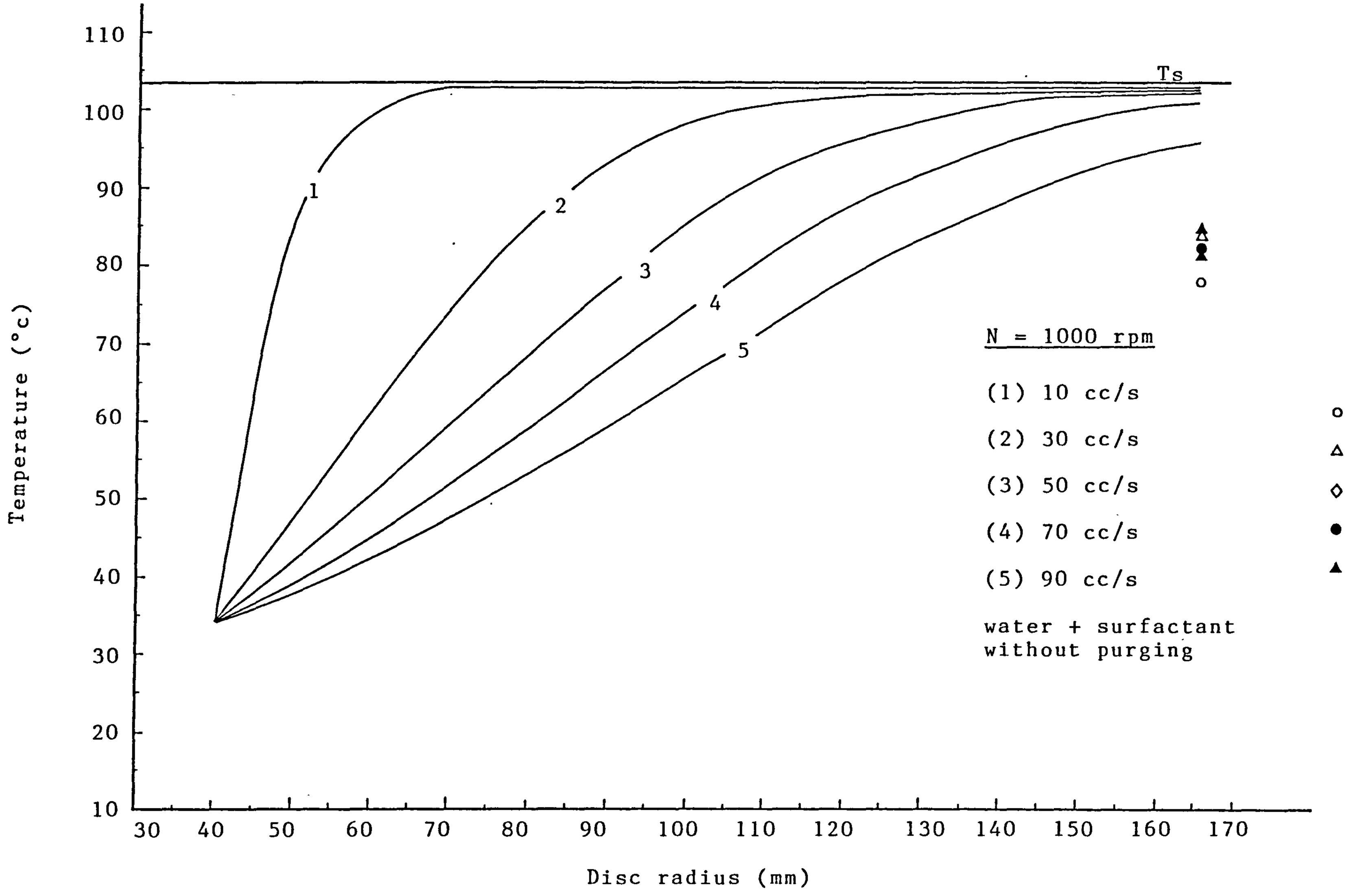

FIGURE 5.22 COMPARISON OF MEASURED & PREDICTED TEMPERATURES

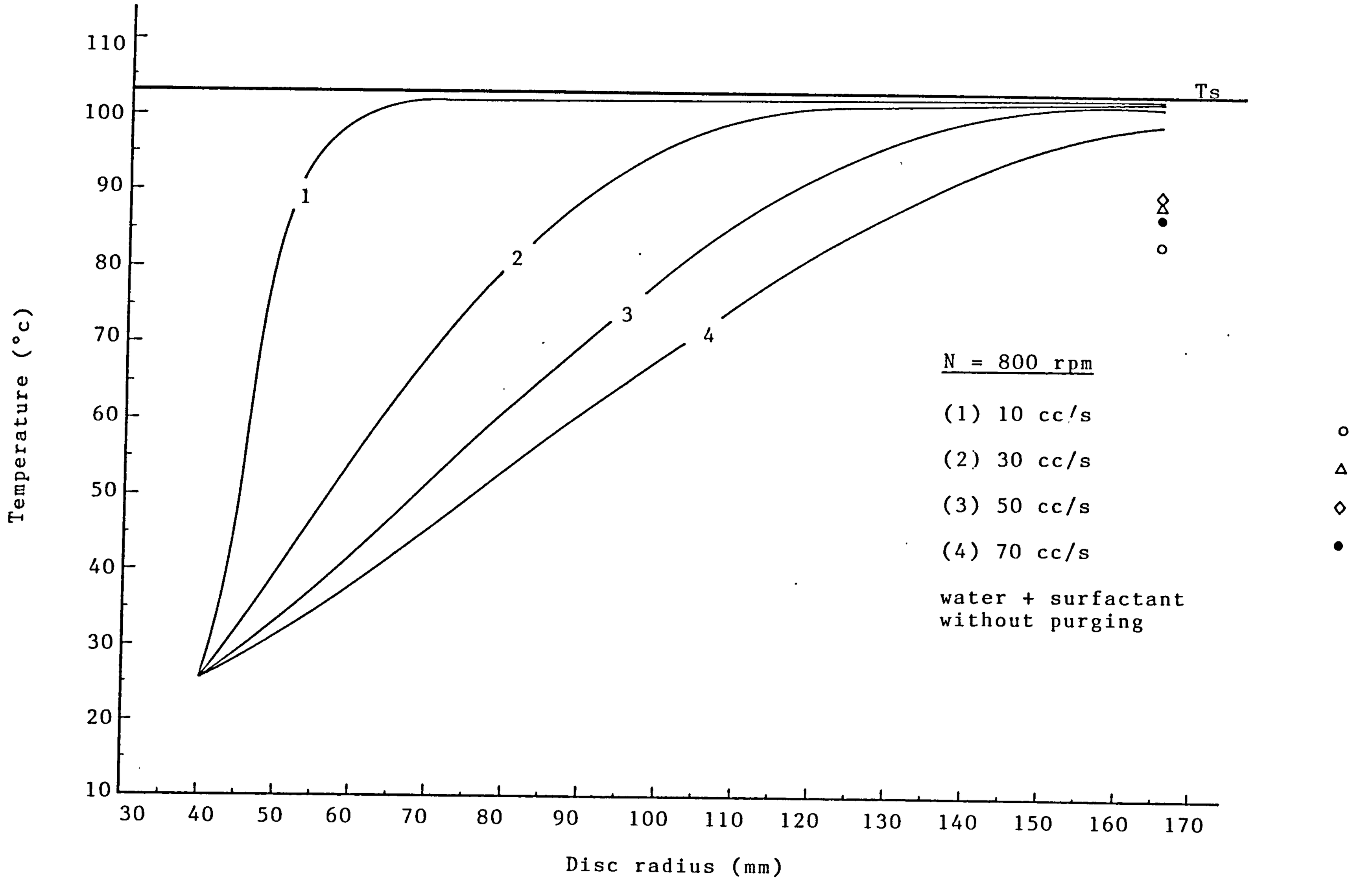

FIGURE 5.23 COMPARISON OF MEASURED & PREDICTED TEMPERATURES

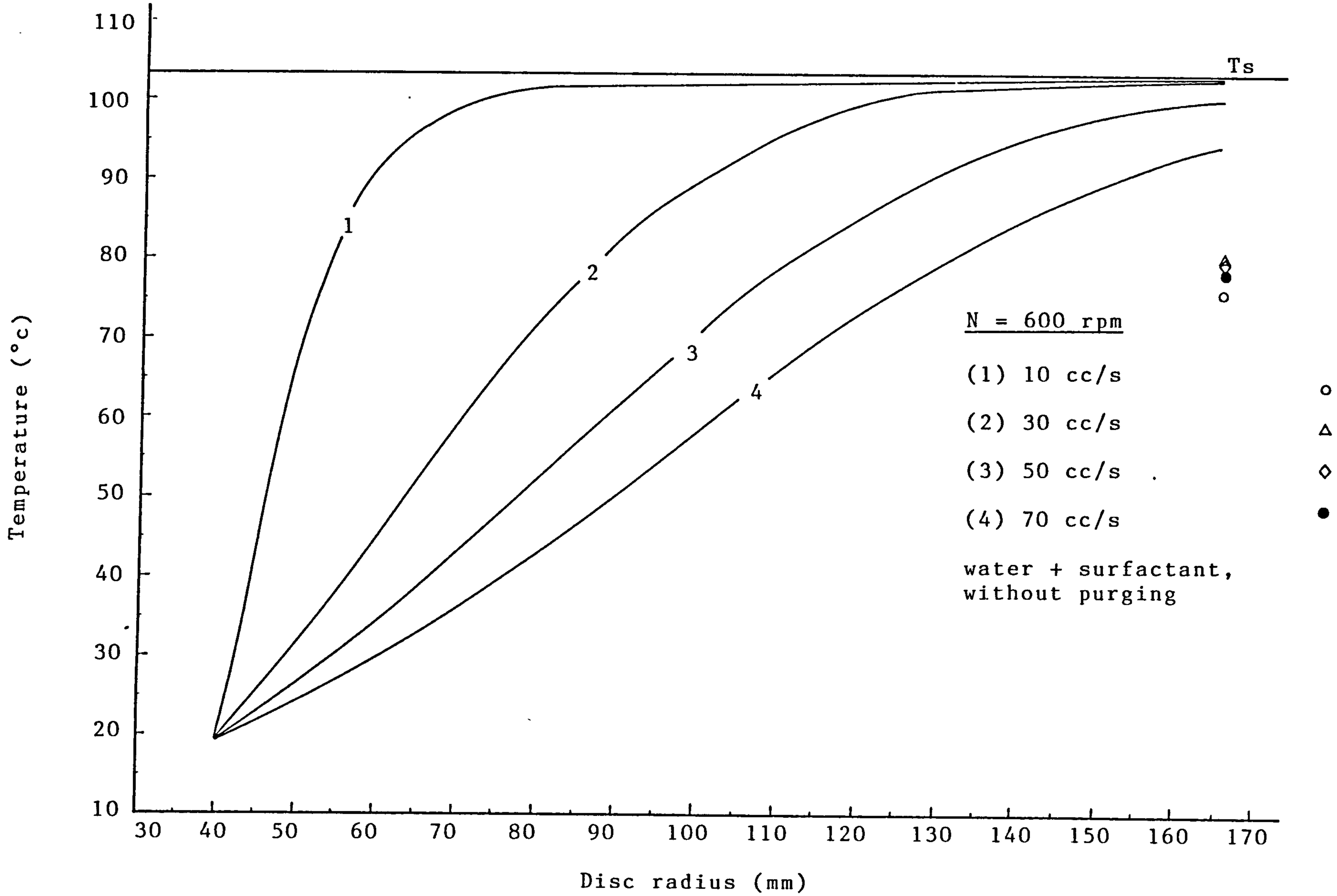

FIGURE 5.24 COMPARISON OF MEASURED & PREDICTED TEMPERATURES

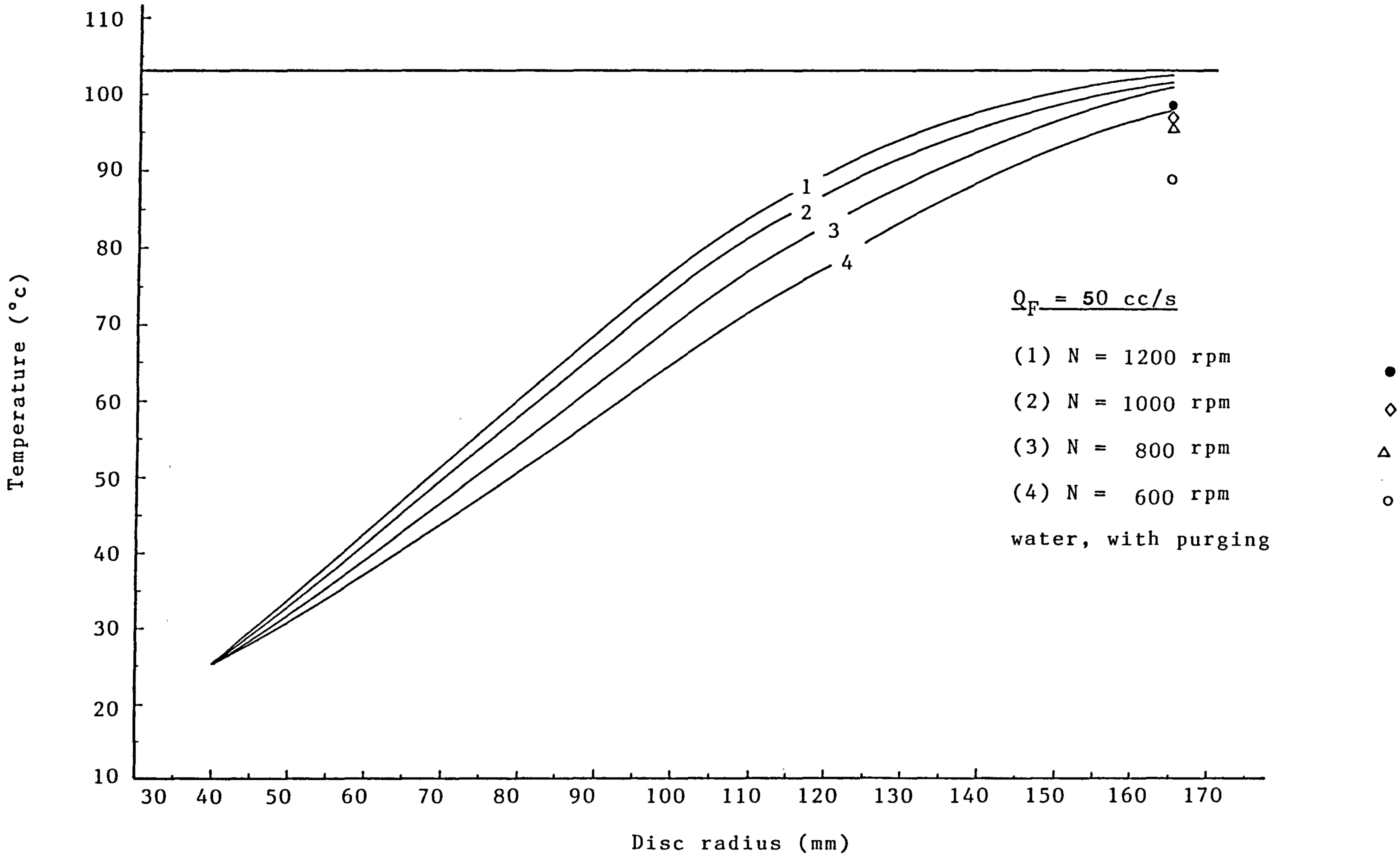

FIGURE 5.25 COMPARISON OF MEASURED & PREDICTED TEMPERATURES

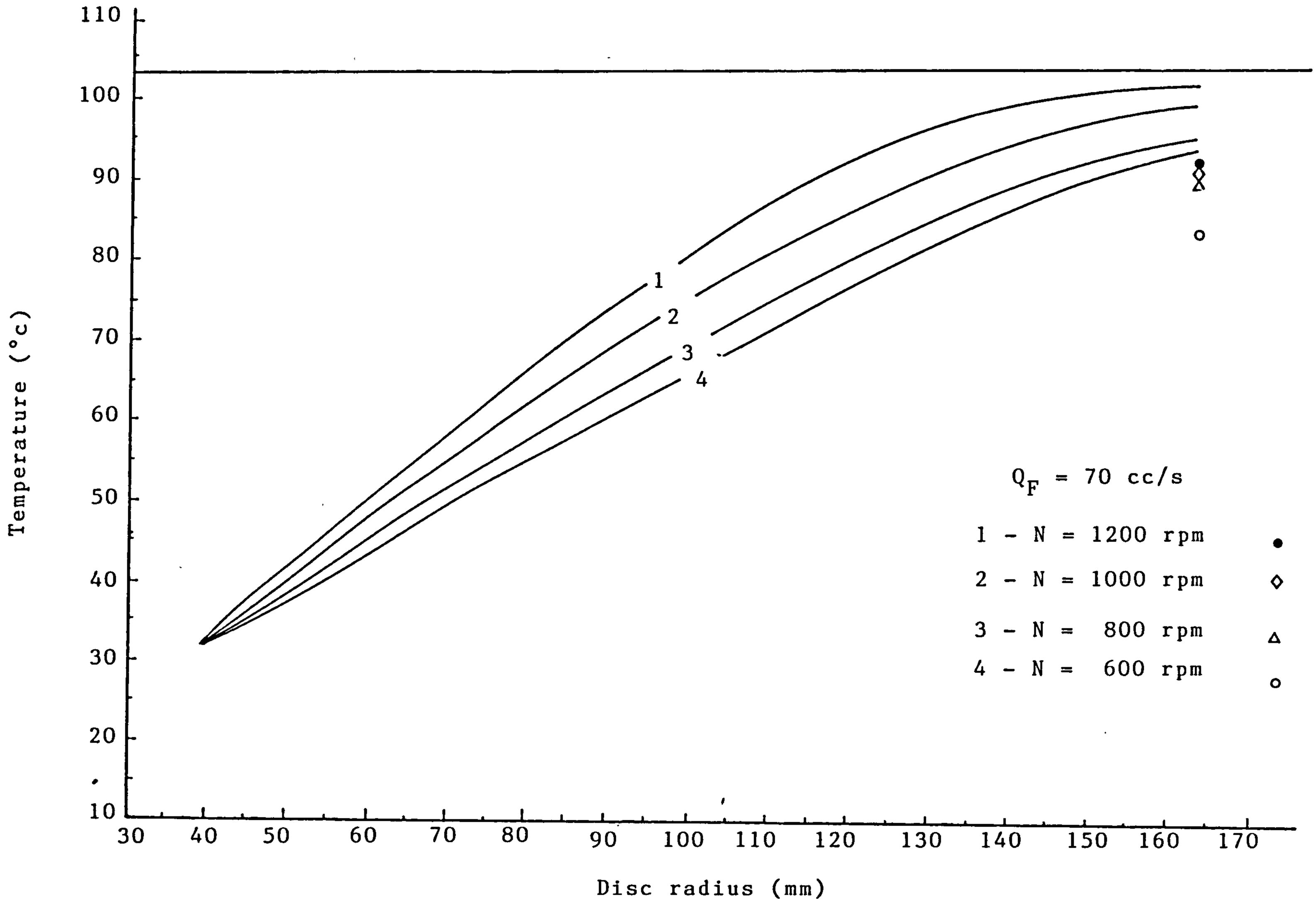

FIGURE 5.26 COMPARISON OF MEASURED & PREDICTED TEMPERATURES

rates the feed attains disc temperature before reaching the disc periphery and therefore the definition of heat transfer coefficients is not possible for these situations. Since this work is concerned with step wise calculations based on a model for film flow heat transfer, the need to define heat transfer coefficients for the disc geometry is unnecessary.

5.2. HEAT TRANSFER WITH CHANGE OF PHASE

A series of experiments were carried out in which methanol was heated to saturation temperature and evaporated at the disc surface. The range of experimental parameters was essentially the same as for water. The heating medium was steam at approximately 0.1 bar gauge pressure. Safety requirements demanded that the methanol supply tanks, heat exchange spaces, condenser etc, had to be blanketed with nitrogen.

Since the influence of air in the steam condensing chamber had been studied in the earlier experiments all work with methanol was conducted with this chamber continuously purged.

Heat balance results for this configuration are shown in figure (5.27). Hence heat transferred to the feed included sensible heat to raise the methanol from inlet temperature to saturation temperature plus the latent heat absorbed in the generation of vapour. This was determined from the sensible heat gain in the cooling water supplied to the methanol condenser. A separate heat balance on this unit was not possible since measurement of condensed methanol by weighing could not be undertaken due to safety requirements. Unfortunately the heat balance achieved in this series of experiments was less accurate than that reported for sensible transfer with water.

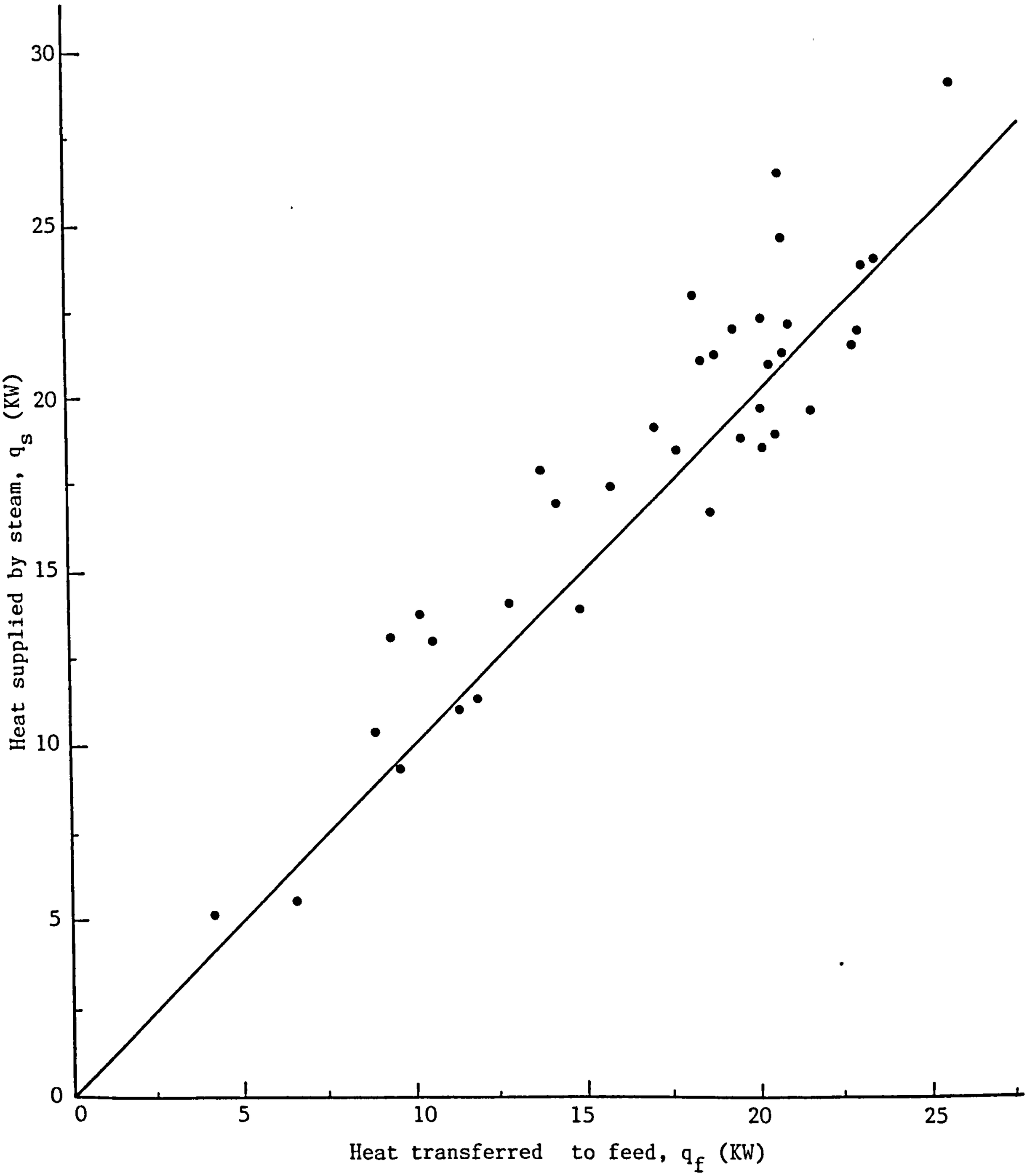

FIGURE 5.27 OVERALL BALANCE FOR HEAT TRANSFER WITH PHASE CHANGE

Model temperature distributions across the disc are shown in figures (5.28) to (5.32). Initial results were determined assuming that the methanol reached saturation temperature below any substantial evaporation started. Once the saturation temperature had been reached it was assumed that heat transfer to the film resulted in equivalent evaporation from the free surface without major resistance at the interface. Film thinning resulting from this evaporation was accounted for in these calculations. Figures (5.33) and (5.34) show the extent of film thinning resulting from evaporation. As is expected, at constant disc speed the radius at which evaporation commences increases with increasing flow.

At the lower flow rates, evaporation may result in film flow rates at the disc periphery which approach minimum wetting rates. If film breakdown occurs, the area exposed will not contribute to further heat transfer.

Since contact angles for methanol on stainless steel, at temperatures approaching saturation value, are extremely difficult to measure by the Sessile drop technique, estimates of minimum wetting rates have been calculated as follows, using the model developed in Appendix 'A'. [i.e. We $(1-\cos\theta_d) = 1.2$]

$$\text{where} \qquad We = 9\left(\frac{2\pi}{3}\right)^{5/3}\left[\frac{\sigma^3 \nu\, r^4}{\rho^3 Q^5 \omega^2}\right]^{1/3}$$

$\sigma = 18.4 \times 10^{-3}$ N/m $\qquad\qquad$ $\rho = 745.8$ kg/m^3

$\mu = 3.1 \times 10^{-4}$ (NS/m^2) $\qquad\qquad$ N = 1200 rpm

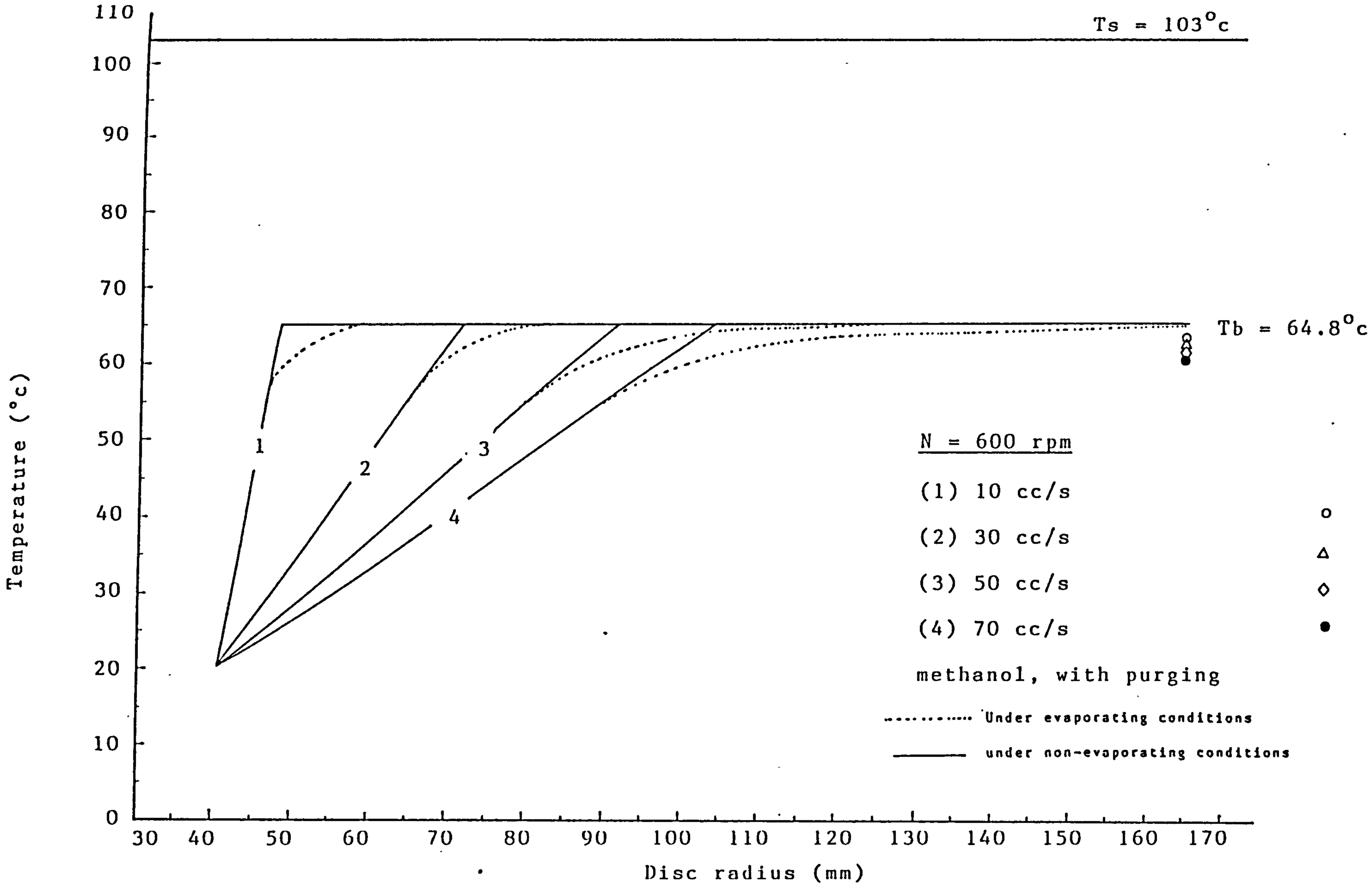

FIGURE 5.28 COMPARISON OF MEASURED & PREDICTED TEMPERATURES (With Phase Change)

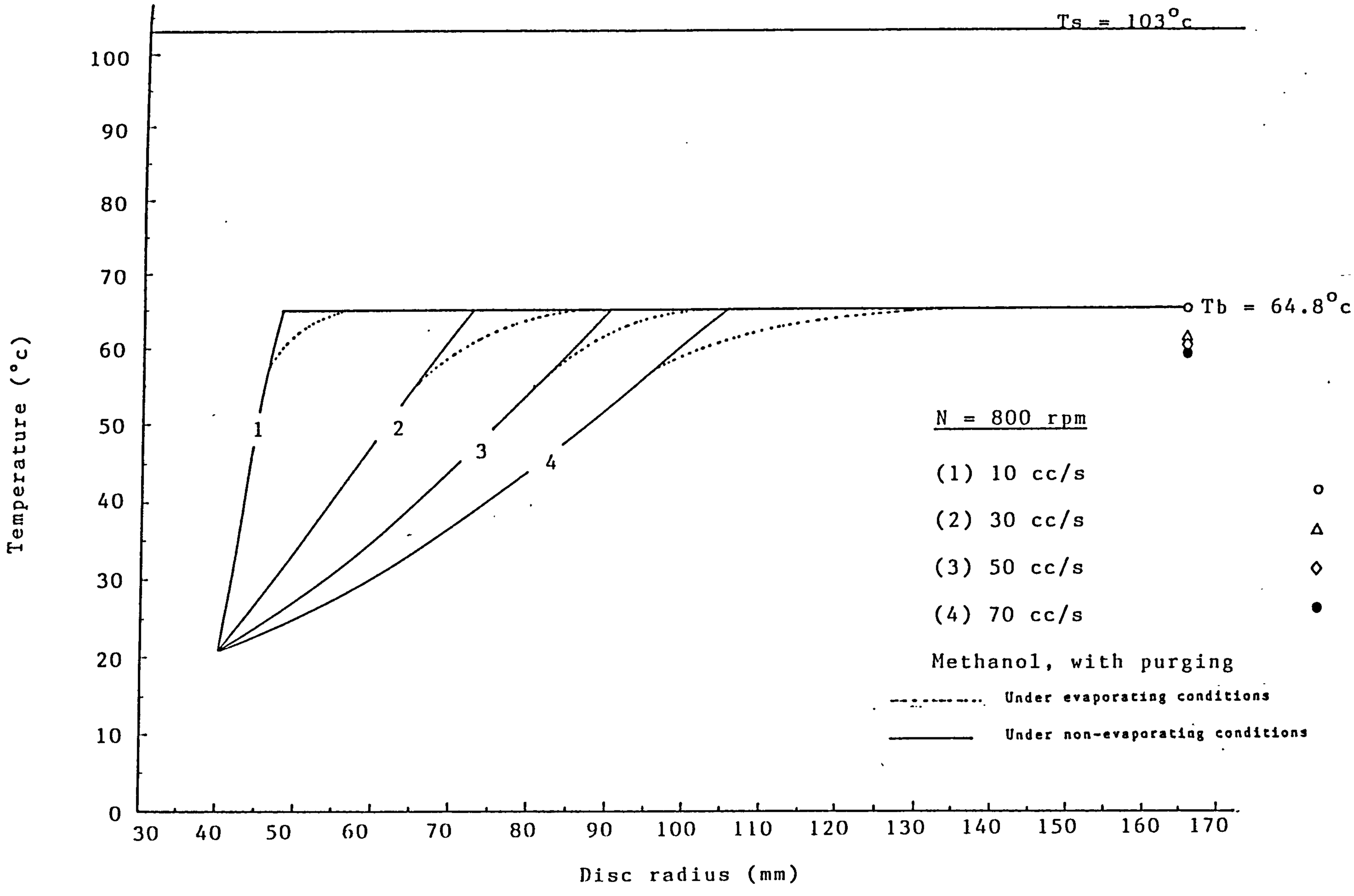

FIGURE 5.29 COMPARISON OF MEASURED & PREDICTED TEMPERATURES (With Phase Change)

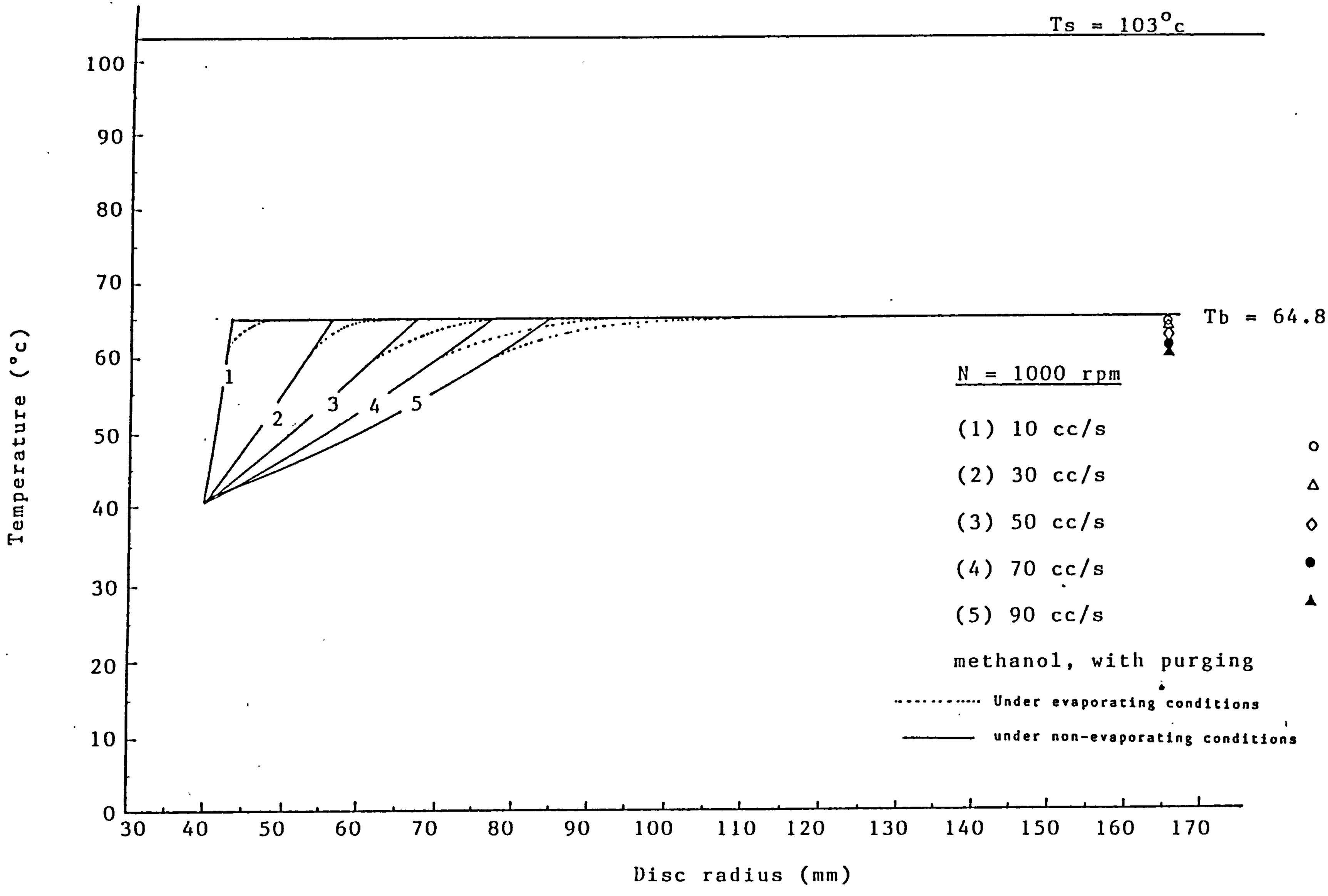

FIGURE 5.30 COMPARISON OF MEASURED & PREDICTED TEMPERATURES (With Phase Change)

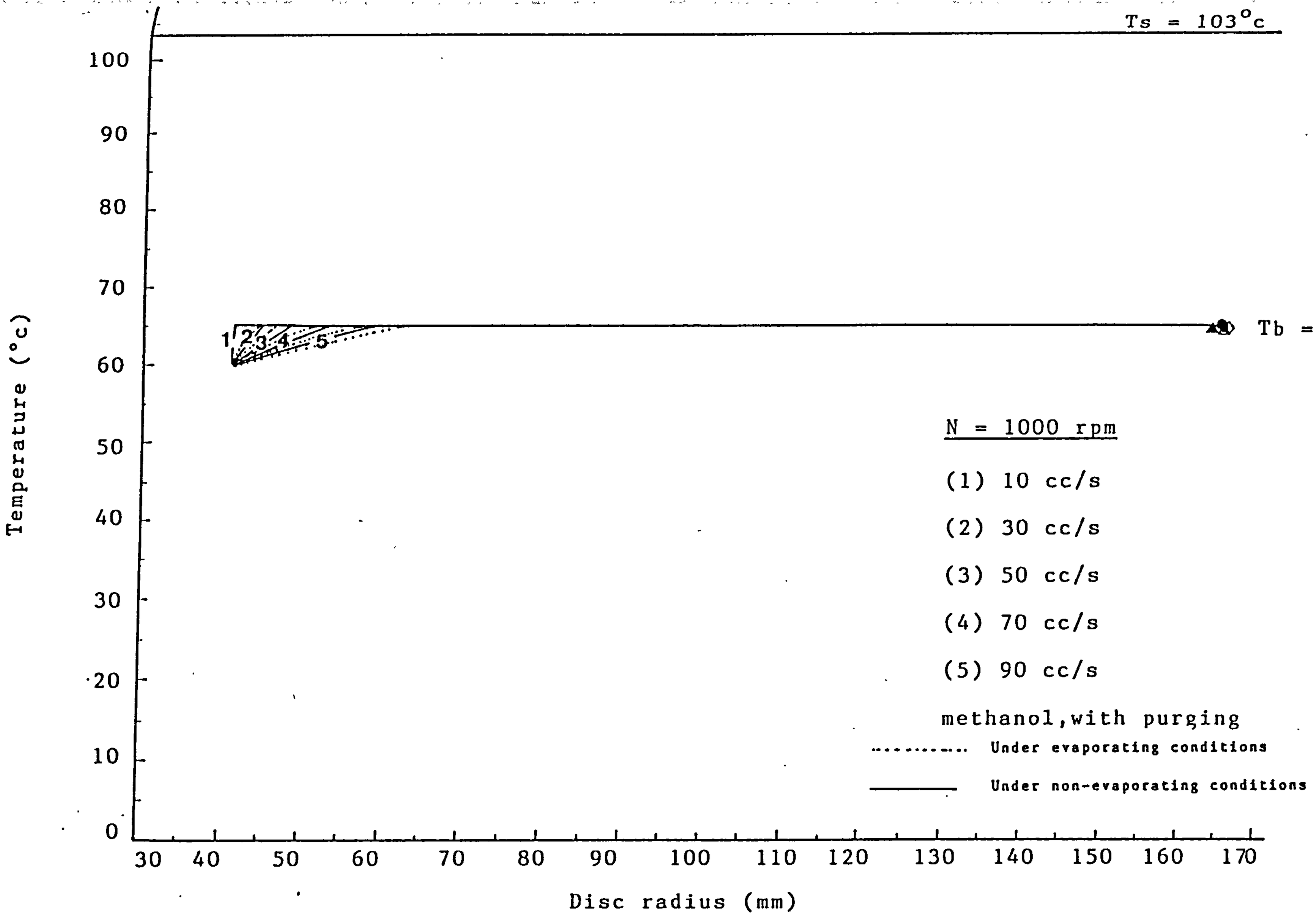

FIGURE 5.31 COMPARISON OF MEASURED & PREDICTED TEMPERATURES (With Phase Change)

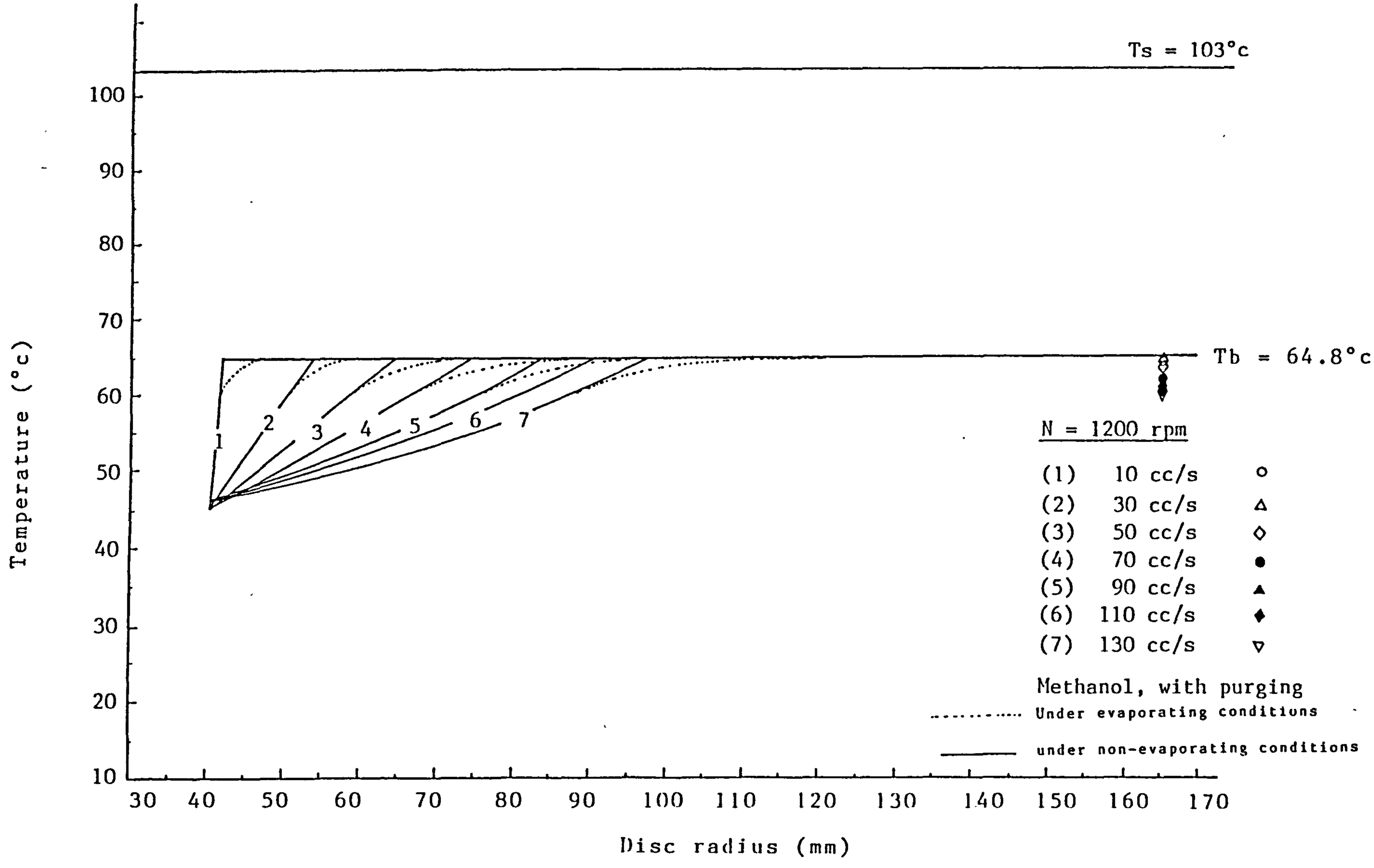

FIGURE 5.32 COMPARISON OF MEASURED & PREDICTED TEMPERATURES (With Phase Change)

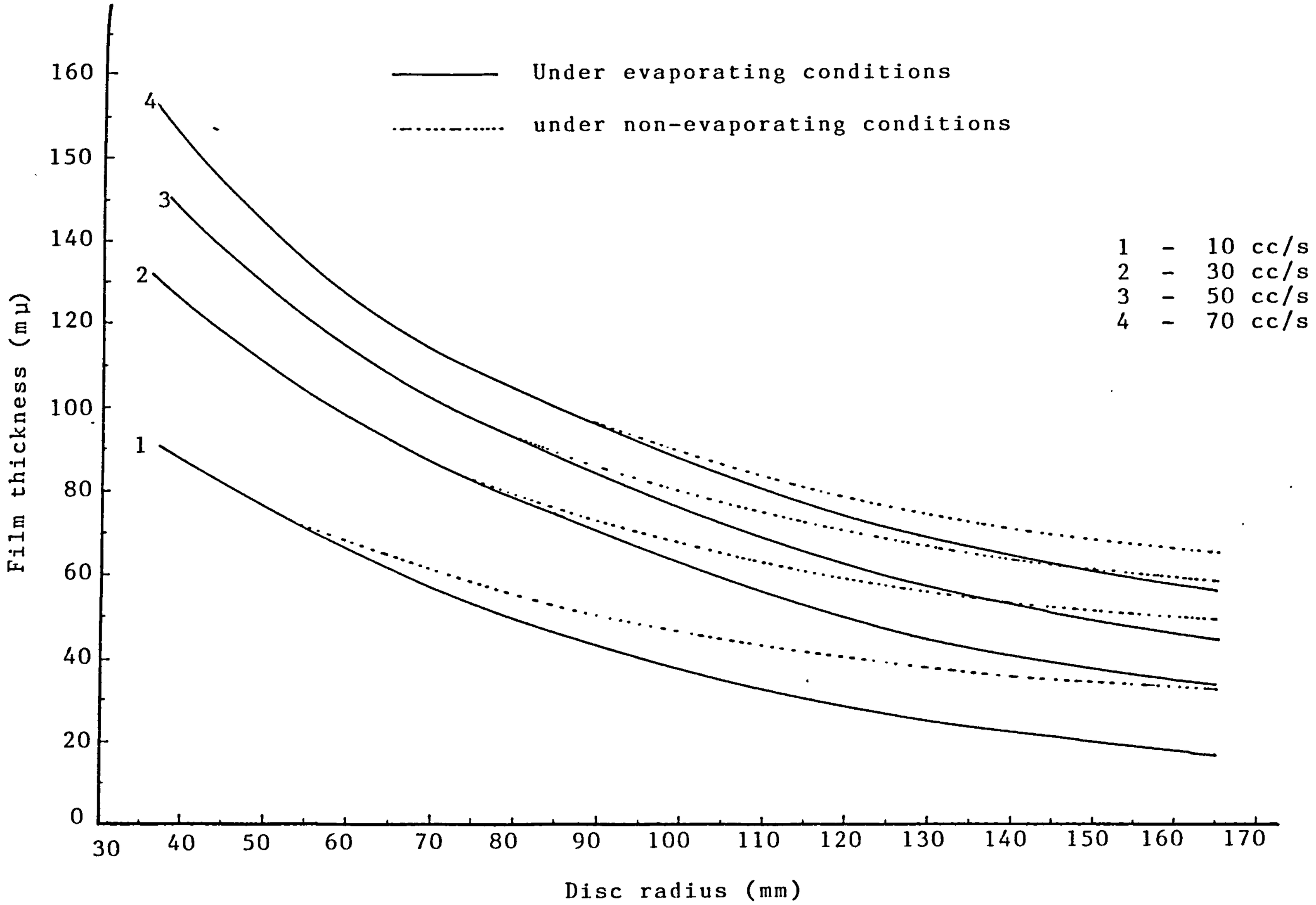

FIGURE 5.33 PREDICTED VALUES OF FILM THICKNESS (METHANOL)

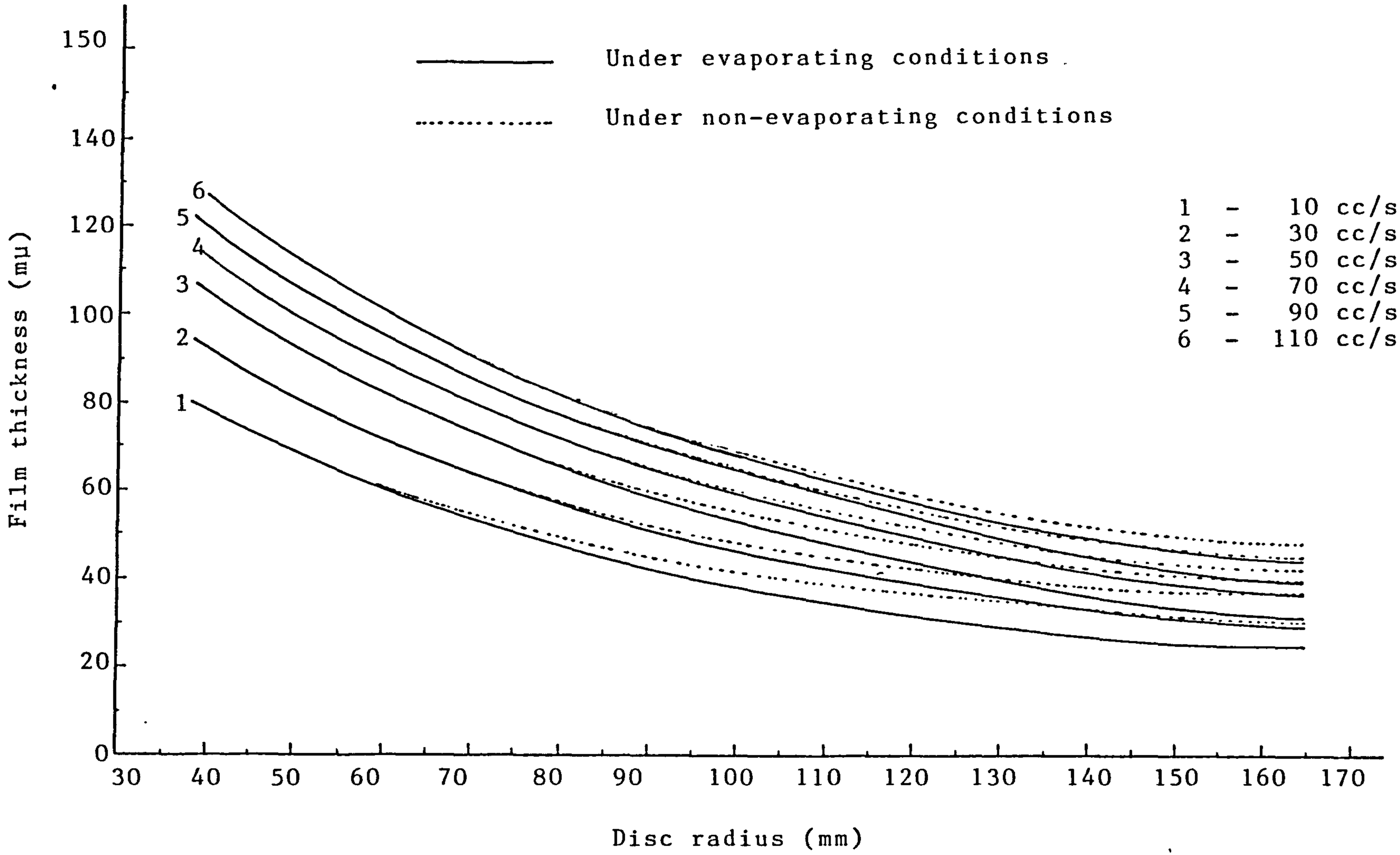

FIGURE 5.34 PREDICTED VALUES OF FILM THICKNESS (METHANOL)

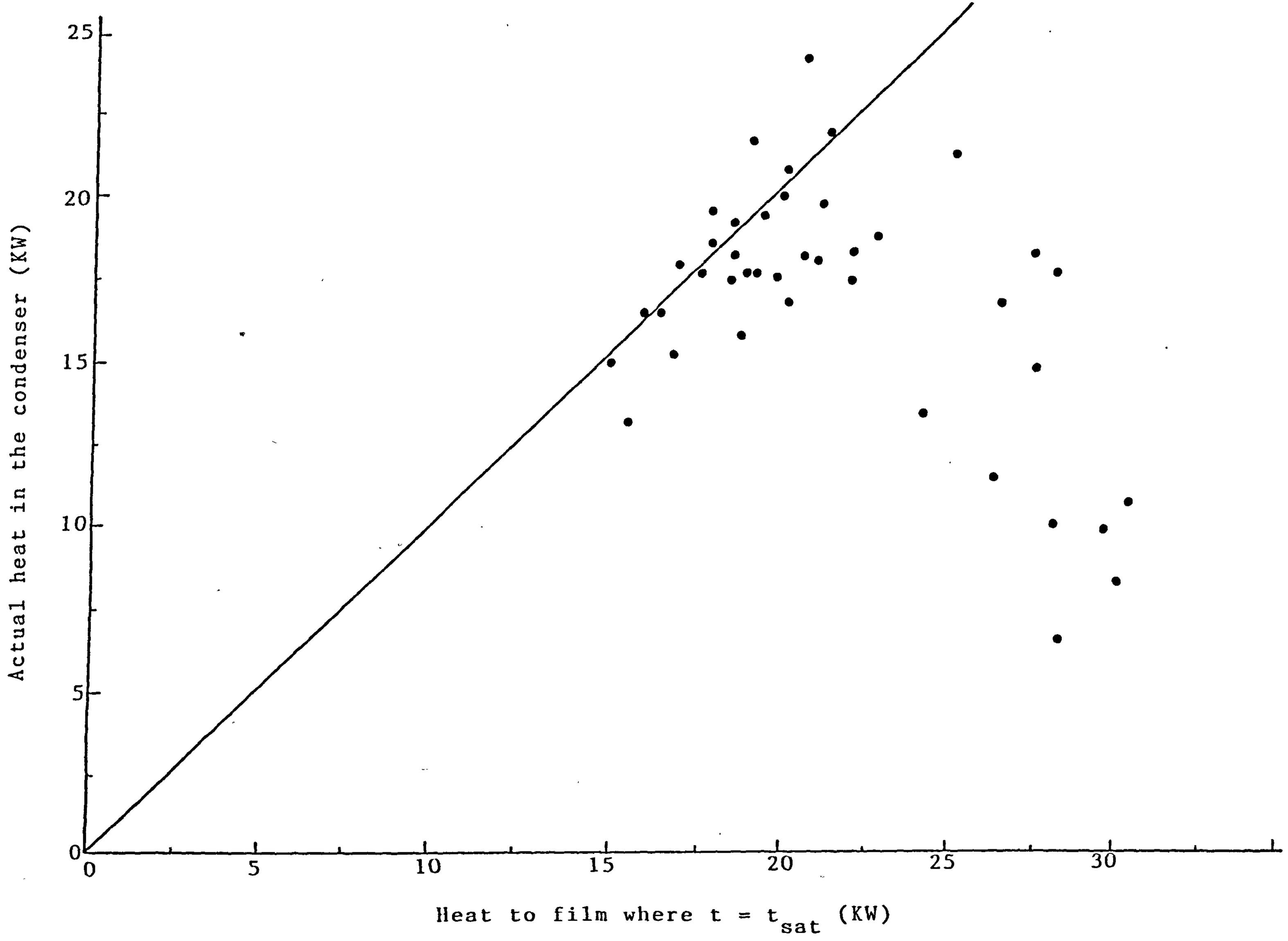

FIGURE 5.35 OVERALL BALANCE FOR HEAT TRANSFER IN METHANOL CONDENSER

TABLE 5.2.

CONTACT ANGLE FOR METHANOL (B.P. = 64.8°c)

ON

STAINLESS STEEL TO ACHIEVE COMPLETE WETTING

Q(cc/s)	We	$(1-\cos\theta_d)$	θ_d°
2.5	269.9	4.4×10^{-3}	5.4
5	85.03	1.41×10^{-2}	9.6
10	26.78	4.48×10^{-2}	17.2
15	13.62	8.81×10^{-2}	24.3
20	8.44	0.142	30.9

For assumed values of an actual minimum wetting rate 'Q' the appropriate contact angle 'θ_d' would have been as shown. Since the contact angle between water and stainless steel decreases strongly with decrease in surface tension, the low value of 'σ' for methanol indicates that minimum wetting rates at 1200 rpm might be expected in the range of 10-15 cc/s. At low disc speeds the minimum wetting rates will be higher than this range.

The effect of dry surface conditions is demonstrated in figure 5.35. In this characteristic the calculated heat transfer to the film, from the point at which the film temperature reaches saturation value, (i.e. the heat which produces vapour) is compared to the quantity of vapour determined from the vapour condenser measurements. It is noted that this balance is extremely poor for flow rates less than 30 cc/s, the region in which dry surface conditions might have been present.

Dry surface conditions might also be induced by the formation of vapour bubbles within the liquid film. Again disruption of the film by this mechanism would be more significant at the lower flow rates.

Few data for boiling within very thin, high velocity, films are available in the literature, however the mechanism by which dry patches, formed by bubble growth, are re-wetted should be the same as that proposed for the higher minimum wetting rate. Further studies will be required to determine this limit to heat transfer performance.

5.3. POWER CONSUMPTION

The power required to drive the rotor assembly, with and without the flow of test liquids was measured. These power measurements were determined from difference between the sum of armature and field power absorbed by the d.c. drive motor, with wet and dry conditions. This technique does not account for the small increases in frictional power dissipation in the mechanical drive system which are expected from the increased load resulting from the change from dry to wet disc conditions.

These data are presented in Table 11 and shown in figures (36) and (37). In this case the differences in wet and dry power dissipation represent, essentially, the kinetic energy given to the liquid between entry to, and discharge from the disc, together with the frictional (viscous) dissipation in the film as it crosses the disc surface.

It has been shown in Appendix G that the kinetic energy given to the liquid and the frictional power dissipation are equal and are given by

$$P_f = \frac{1}{2} Q_f \rho \omega^2 (r_o^2 - r_i^2)$$

$$\text{or} \simeq \frac{1}{2} Q_f \rho \omega^2 r_o^2$$

Therefore, the total power dissipation is proportional to

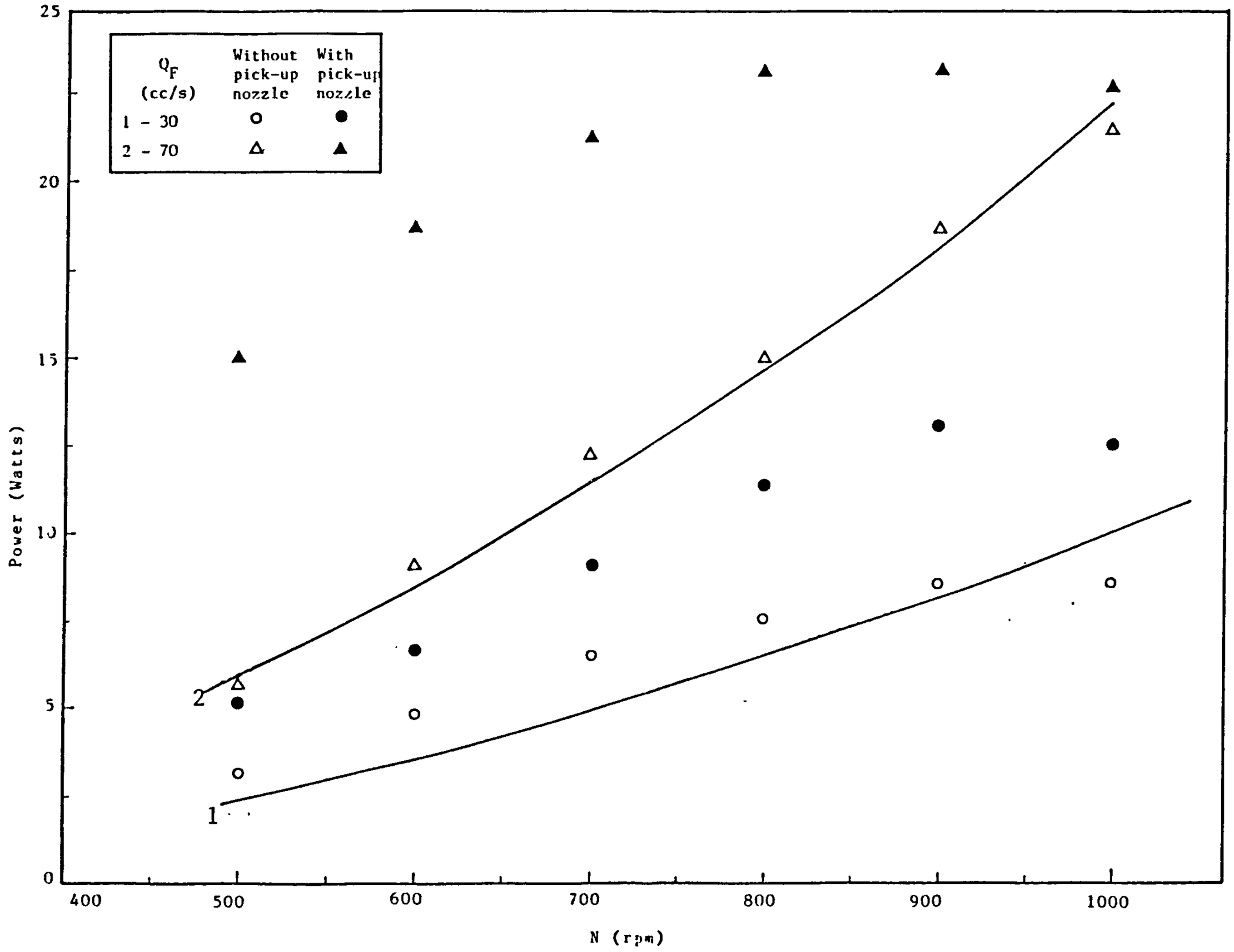

FIGURE 5.36 COMPARISON OF MEAUSRED & PREDICTED DATA ON POWER DISSIPATION

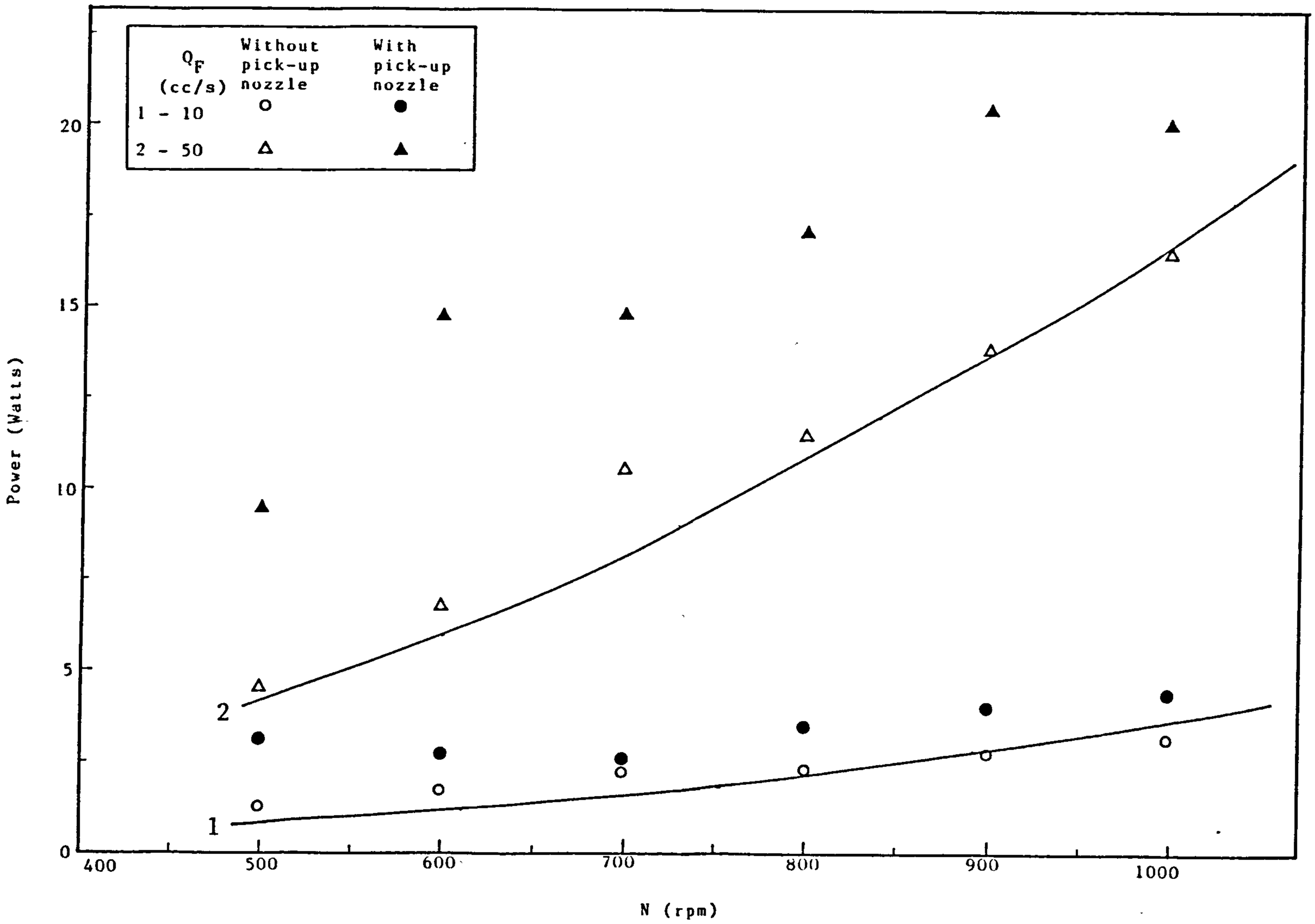

FIGURE 5.37 COMPARISON OF MEASURED & PREDICTED DATA ON POWER DISSIPATION

flow rate and the square of the disc speed. The experimental data from this study confirm these results.

The frictional losses associated with the film flow have been estimated from the total power by subtraction of the kinetic energy component and this has been correlated as suggested in Appendix G. The resultant equation determined by regression analysis is (regression coefficient, 0.95)

$$P = 0.708\ (Re)^{0.88}\ (Ta)^{2.08}$$

The equation compares favourably with the predicted correlation. The high value of the constant coefficient might be due to dissipation resulting from wave formation at free surface of the film which would be expected with the range of flow rates, disc speeds etc.

During operation of the exchanger the liquid is removed from the disc assembly by stationary scoops. The power dissipation resulting from the system is also shown in figures (36 & 37) and the data are summarised in Table 12. Since the design of such discharge system was not part of the present study, no further comment will be made. However, it should be noted that discharge facilities could consume large amounts of power and need careful design.

CHAPTER SIX

CONCLUSIONS

Heat transfer to a liquid film flowing across a steam heated disc has been measured for a wide range of liquid flow rates and disc speeds. A model of this process has been proposed based on heat transfer between two liquid films; the condensate and feed liquid films, for both feed heating, and feed heating with evaporation.

Predictions from this model have been compared with the measured values of feed temperature at the disc periphery for water. With methanol as the test liquid, liquid temperature always reached the saturation value before the edge of the disc, giving rise to considerable evaporation. The model was modified to account for evaporation.

When experimental conditions were correctly adjusted, comparisons with the model were quite good, except at low flow rates with low disc speeds. Under such conditions complete wetting of the disc surface is difficult to maintain.

A study on minimum wetting rate behaviour on the disc has been undertaken and a model presented for this process. Comparison between experimental data and model predictions are good, although the model requires a knowledge of contact angle between the disc surface and the test liquid. This is a difficult parameter to measure with accuracy and requires further study.

Power dissipation in generation of the film flows has been measured and again compares favourably with predicted values.

Since the heat transfer measurements cover a range of values of Reynolds number ($Re = Q/r\nu$) and Taylor number ($Ta = r^2\omega/\nu$), a maximum value to (Re^2/Ta) of approximately 100, the results of this study should come in the range of operating conditions relevant to industrial applications.

CHAPTER SEVEN

SUGGESTIONS FOR FUTURE WORK

Further research in the following areas is likely to be useful in the near future.

(1) The heat transfer predictions have been shown to be accurate on the assumption that the liquid feed actually resides on the lower disc surface only. Simple experiments with an isolated disc indicate that this condition is likely to be satisfied in the present apparatus. This could be confirmed experimentally, by repeating the heat transfer measurements for the lower disc assembly with the upper disc suitably insulated, to prevent condensation.

Since two surfaces are available for heat transfer, it would be more desirable to measure heat transfer in this system with an attempt made to ensure that the liquid feed is split between both surfaces, completely wetting both.

(2) Further work is required to establish minimum wetting rates for films undergoing evaporation. For compact heat transfer channels of this type, these conditions can only be determined from a drop in heat transfer performance due to the onset of dry surface conditions.

(3) For multiple channel exchangers condensation between closely spaced surfaces will require considerable study. Radial flow of vapour into the narrow channel between two plates, counterflow to condensate films on the plates, is a complex process, which has not been discussed in the literature.

REFERENCES

1. Apparo, K.V., Chiranjivi, C., and Chary, S.P., "An Approximate Analysis of Condensation on a Rotating Disc" Indian Jou. Tech. 6 (1968) pp 286-296.
2. Astaf'ev, V.B., and Baklastov, A.M., "Condensation of Steam on a Horizontal Rotating Disc" Thermal Eng. U.S.S.R. 17 (1970) pp 82-85.
3. Astaf'ev, V.B., and Baklastov, A.M., "Flow of the Film and Heat Transfer with Steam Condensation on a Rotating Disc" Thermal Eng. U.S.S.R. 17 (1970) pp 111-113.
4. Barabash, P.A., Muzhilk, A.A., and Rifert, V.G., "Some Experimental Results on Hydrodynamics and Heat Transfer in Evaporation of a Liquid Film on a Rotating Surface" Prom. Teplote - Kh. 2 (2) (1980) pp 43-48.
5. Beckett, P.M., Hudson, P.C., and Poots, G., "Laminar Film Condensation Due to a Rotating Disc" Jou. Eng. Maths. 7(1) (1973) pp 63-73.
6. Bell, C., "The Hydrodynamics and Heat Transfer Characteristics of Liquid Films on a Rotating Disc" Ph.D. Thesis, University of Newcastle Upon Tyne, (1975)
7. Black, R.H., "Capacitance Method of Measuring Water Film Thickness" Trans. Am. Soc. Civ. Eng. 126(1) (1961) pp 88-91
8. Brauer, H., "Stromung Und Warmeit Bergang Bes Rieselfilmen" Vereines Deat. Ingr. Forschungsheft, (1956) pp 457-462
9. Bromley, L.A., "Prediction of Performance Characteristics of Hickman-Badger Centrifugal Boiler Compression Still" Ind. Eng. Chem. 50 (1958) pp 233-237
10. Bromley, L.A., Humphrey, R.F., and Murray, G.W., "Condensation on and Evaporation from Radially Grooved Rotating

Discs" Jou. Heat Transfer (ASME series 'C') (1966) pp 80-86

11. Buckel, W.L., Beck, W.D., Irwin, J.R., Putman, A.A., and Eibling, J.A., "A Study and Development of the Hickman Sea-Water Still" Research and Development Progress Report No. 43, Saline Water U.S. Department of The Interior Washington D.C., (1960)

12. Butuzov, A.I., Pukhovoy I.I., and Rifert, V.G., "Heat Transfer During Distillation of Sea Water on a Rotating Disc" Teplofiz Teplotekk 6 (1970) pp 54-57

13. Butuzov, A.I., Pukhovoy, I.I., and Rifert, V.G., "Heat Transfer Attendent to Sea Water Desalination on a Rotating Disc" Heat Transfer - Soviet Research 2 (6) (1970) pp 33-36

14. Butuzov, A.I., and Rifert, V.G., "An Experimental Study of Heat Transfer during Condensation of Steam at a Rotating Disc" Heat Transfer - Soviet Research, 4 (6) (1972) pp 150-154

15. Butuzov, A.I., and Rifert, V.G., "Heat Transfer During Steam Generation in a Film on a Rotating Disc" IZV. Vyssh. Ucheb. Zared Mashinostr 1 (1972) pp 81-85

16. Butuzov, A.I., and Rifert, V.G., "Heat Transfer in Evaporation of Liquid from a Film on a Rotating Disc" Heat Transfer - Soviet Research, 50 (1) (1973) pp 88-94

17. Charwat, A.F., Kelly, R.E., and Gazley, C., "The Flow and Stability of Thin Films on a Rotating Disc" Jou. Fluid Mech. 53 (1972) pp 227-255

18. Chiranjivi, C., Apparo, K.V., and Chary, S.P., "Effect of Vapour Drag on Condensation on a Rotating Disc" Indian Jou. Technology, 8 (1970) pp 205-209

19. Clare, H., and Ashwood, P.F., "Measurement of the Thickness

of a liquid Film on the Surface of a Rapidly Rotating Disc" Inst. Practice, 16 (1962) pp 70-79

20. Clare, H., and Jeffs, R.A., "Some Measurements of the Thickness of Fluid Film on a Spinning Disc" National Gas Turbine Establishment, Draft Report 12.12.1960.

21. Clark, R.L., and Bromley, L.A., "Saline Water Conversion by Multiple Effect Rotating Evaporator" Chem. Eng. Prog. 57 (1) (1961) pp 64-70

22. Clegg, A.J., "Studies of Film Flow on Wetted Wall Columns" Ph.D. Thesis,Surrey University, (1969)

23. Cook, R.A., and Clark, R.H., "The Experimental Determination of Velocity Profiles in Smooth Falling Liquid Films" Canadian Jou. Chem. Eng. 49 (1971) pp 412-416

24. Espig, H., Hoyle, R., "Waves in Thin Liquid Layer on a Rotating Disc" Jou. Fluid Mechanics, 92 (1965) pp 671-677

25. Espig, H., and Hoyle, R., "The Transfer of Heat from Condensing Steam to a Cooled Rotating Disc" Proc. Inst. Mech. Engrs. 182 (3H) (1967-68) pp 406-412

26. Fallah, A., Hunter, T.G., and Nash, A.W., "Measurement of Liquid Film Thickness by Weighing Method" Jou. Soc. Chem. Ind. 53 (1934) pp 3697-3704

27. Fulord, G.D., "The Effect of Thickness of Flowing Films on Heat and Mass Transfer" Thesis Digest, Brim. University. Chem. Eng. 1951

28. Gazley, C., and Charwat, A.F., "The Characteristics of a Thin Liquid Film On a Spinning Disc" Third All Union Conf. on Heat & Mass Transfer Minsk, 14th-18th May, 1968.

29. Hickman, K.C.D., "Centrifugal Boiler Compression Still" Ind. Eng. Chem. 49 (1957) pp 786-798

30. I.C.I. Magazine, 40 No. 301 (1962)

31. Jackson, M.L., "Liquid Films in Viscous Flow" Jou. 1 (231) (1955) pp 231-240

32. Jazayeri, A., "Hydrodynamic of Newtonian and Non-Newtonian Liquids Across a Rotating Disc" Ph.D. Thesis, Univ. of Newcastle Upon Tyne (1980)

33. Kamei, S., and Oishi, J., "Mass and Heat Transfer in a Falling Liquid Film Un-Wetted Wall Tower" Mem. Fac. Eng. Kyoto Univ.18 (1) (1956) pp 128-129

34. Kapitsa, P.L., "Wave Motion of a Thin Layer of a Viscous Liquid" Jou. Exp. & Theo. Phys. U.S.S.R., 4 (1948) pp 112-116

35. Kern, D.Q., "Process of Heat Tansfer" McGraw. Hill Book Company, (1950)

36. Knapp, F., and Et al "Chemical Technology" Vol. (iii), Bailliere London (1851) pp 406-416

37. Kreith, F., "Convective Heat Transfer in Rotating Systems" Advances in Heat Transfer, 5 (1968) pp 129-246

38. Koh, J.C.Y., and Sparrow, E.M., "The Two Phase Boundary Layer in Laminar Film Condensation" Int. Jou. Heat Mass Transfer, 2 (1961) pp 69-82

39. Lindsey, E., "Evaporation" Chemical Engineering, Apirl (1953)

40. Matsumoto, S., et al., "The Thickness of a Viscous Liquid Film on a Rotating Disc" Jou. Chem. Eng. Japan, 6 (1973) 503-506

41. Muenz, K., and Marchello, J.M., "Technique for Measuring Amplitudes of Small Surface Waves" The Review of Sci. Instruments. 35 No. 8 (1964) pp 953-959

42. Nandapurkar, S.S., and Beatty, K.O.Jr., "Condensation on a Horizontal Rotating Disc" Chem. Eng. Prog., (Sym) 56 (30) (1960) pp 129-137

43. Nicol, A.A., and Medwell, L.O., "Surface Roughness Effects on Condensing Films" ASME Pub. No. 65-HT-43, 8th National Heat Transfer Conference, Los Angeles, Aug. (1965)

44. Nusselt, W., "Die Oberflachen Kondensation des Wasserdamfes" Z. Ver. Deut. Ing. 60 (1916) pp 541-569

45. Porter, J.E., and Bell, C., "Liquid Flow Across a Horizontal Rotating Disc" Conf. Mixing and Polymer Processing at Delft University of Technology, The Netherlands, (1976)

46. Rees, E.L., "Flow and Heat Transfer on a Rotating Disc" M.Sc. Thesis Swansea University, U.K. (1962)

47. Rifert, V.G., "Heat Transfer Analysis with Liquid Film Vaporisation on a Rotating Disc" Inz. Fizi. Khim., 25 (1973) pp 232-236

48. Rohsenow, W.M., "Heat Transfer and Temperature Distribution in Laminar Film Condensation" Trans. ASME 78 (1956) pp 1645-1648

49. Rohsenow, W.H., and Hartnett, J.P., "Condensation on a Rotating Disc" Hand Book of Heat Transfer, (1973) pp 12.7-12.8

50. Solesio, J.H., "Hydrodynamics of Liquid Films" Physico-Chemical Hydrodynamics (Vol. 2), Levich Pub. Comp. (1971) pp 711-715

51. Sparrow, E.M., and Gregg, J.L., "A Boundary Layer Treatment of Laminar Condensation" Jou. Heat Transfer, 81 (1959) pp 13-18

52. Sparrow, E.M., and Gregg, J.L., "A Theory of Rotating Condensation" Jou. Heat Transfer, 81 (1959) pp 113-120

53. Sparrow, E.M., and Gregg, J.L., "Effect of the Vapour Drag on a Rotating Condensation" Jou. Heat Transfer, 82 (1960) pp 71-72

54. Stainthorp, F.P., and Allen, J.M., "The Development of Ripples on the Surface of a Liquid Film inside a Vertical Tube" Trans. Inst. Chem. Engrs., 43 (1965) pp 785-791

55. Stainthorp, F.P., and Batt, R.S.W., "The Effect of Co-Current and Counter-Current Air Flow on the Wave Properties of Falling Liquid Films" Trans. Inst. Chem. Engrs., 45 (1967) pp 7372-7377

56. Surzhik, T.V., and Pukhovoi, I.I., "Experimental Study of Heat Transfer on a Rotating Disc Surface" Khim Technol (Kiev), 6 (1984) pp 43-44

57. Telles, A.S., and Duckler, A.F., "Statistical Characteristics of Thin Vertical Wavy Liquid Films" Ind. Eng. Chem. (Fund.), 9 (3) (1970) pp 412-416

58. Tleimat, B.W., "Performance of Rotating Flat Disc Wiped Film Evaporator" ASME publication, 71-HT-37, (1971)

59. Vachagin, F.D., and Nikolaev, V.S., "Flow of a Viscous Liquid over the Surface of a Rapidly Rotating Flat Disc" IZV. Khim. Ikhim. Tekh. 3 (1960) pp 1097-1102

60. Venkataraman, R.S., "Mass Transfer to an Expending Interface" Ph.D. Thesis, Leeds University, England (1966)

61. Wang, C.S., "Heat and Mass Transfer from a Rotating Disc with Phase Change" Ph.D. Thesis, University of California Berkeley, C.A., U.S.A. (1979)

62. Wang, C.S., and Greif, R., "The Effect of Impingement on Heat Transfer in Rotating Condensation" Int. Jou. Heat Mass Transfer, 24 (7) (1981) pp 1097-1104

63. Wang, C.S., Greig, R., and Laird, A.D.K., "Study of Heat Transfer in a Rotating Disc Evaporation" Desalination 33 (3) (1980) pp 259-276

64. Warden, C.P., "Film Thickness Measurements" M.Sc. Thesis, Mass. Inst. Tech. Cambridge, Massachusetts (1930)

65. Watts, B.E., "The Flow, Heat and Mass Transfer Characteristics of Rotating Disc" Ph.D. Thesis, Swansea University (1971)

66. Wilkes, J.O., Nedderman, R.M., "The Measurements of Velocities in Thin Films of Liquids" Chem. Eng. Sci. 17 (1962) pp 177-187

67. Wood, R.M., and Watts, B.E., "The Flow Heat and Mass Transfer Characteristics of Liquid Film on Rotating Discs" Trans. Inst. Chem. Engrs. 51 (1973) pp 315-322.

LIST OF SYMBOLS

SYMBOL	DESCRIPTION	(UNITS)
A	Area	(m^2)
a,b,c.	Constants in the expression for sensible heat content as function of temperature.	(-)
C_p	Specific heat	(J/kgK)
D,d	Diameter	(m)
g	Gravitation acceleration	(m/s^2)
h	Heat transfer coefficient	(W/m^2K)
h_{fg}	Latent heat of vaporization	(J/kg)
K	Thermal conductivity	(W/mK)
L	Linear dimension	(m)
M	Mass flow rate per unit length	(kg/ms)
N	Rotational speed	(rpm)
P_f	Frictional power	(W)
P_k	Kinetic power	(W)
Q	Volumetric flow rate	(m^3/s)
q	Heat flux	(W/m^2)
R,r	Radius	(m)
T	Temperature	(C,K)
T_F	Feed temperature	(C,K)
T_m	Mean temperature	(C,K)
T_o	Surface temperature	(C,K)
T_{sat}	Vapours saturation temperature	(C,K)
U	Overall heat transfer coefficient	(W/m^2K)
u	Velocity	(m/s)
u_m	Mean velocity	(m/s)
u_r	Radial component of velocity	(m/s)
W	Mass flow rate	(kg/s)
X_m	Metal wall thickness	(m)
x,y,z.	Rectangular co-ordinates	(m)

GREEK SYMBOL		
δ	Film thickness	(m,μm)
θ	Angle	(degrees)
λ	Latent heat	(J/kg)
μ	Viscosity	(Ns/m^2)
ν	Kinematic viscosity	(m^2/s)
ρ	Density	(kg/m^3)

τ	Shear stress	(N/m^2)
ϕ	Angle	(-)
ω	Angular velocity	(1/s)

DIMENSIONLESS NUMBERS

PARAMETER	SIGNIFICANCE	FORMULA
Nu: Nusselt Number	$\frac{\text{convective heat transfer}}{\text{conductive heat transfer}}$	(hL/K)
Pr: Prandtl Number	$\frac{\text{kinematic viscosity}}{\text{thermal diffusivity}}$	$(C_p\mu/K)$
P: Power Number	$\frac{\text{frictional force}}{\text{viscous force}}$	$(P_f r\rho^2/\mu^3)$
Re: Reynolds Number	$\frac{\text{inertial force}}{\text{viscous force}}$	$(Q/r\nu)$
Ta: Taylor Number	$\frac{\text{Coriolis force}}{\text{viscous force}}$	$(r^2\omega/\nu)$

SUBSCRIPTS

C - cold liquid
c - condensate
e - evaporation
D - distillate
F,f - feed
H - hot liquid
i - inside
L - liquid
m - mean
o - outside
r - radial
s - steam
v - vapour

APPENDIX A

MINIMUM WETTING RATE OF A ROTATING DISC

If the flow, initially sufficient to completely wet the surface of a disc rotating at constant speed, is gradually reduced, a point will be reached at which the flow cannot maintain complete wetting. If this experiment is conducted under normal or process conditions, as opposed to clinically clean conditions, two minimum wetting rates can be defined. The first, and lower rate, is encountered as the flow rate is reduced from a value which completely wets the surface. As might be anticipated, initial film breakdown occurs at the periphery of the disc where film thickness is a minimum. The mechanism of this process is quite complex and undoubtedly involves the interaction of film dynamics, liquid properties, the surface/liquid combination, surface and edge geometry in the vicinity of the disc periphery, and also the presence of contaminating materials in the liquid (particulate material). The initial pattern of breakdown involves the appearance of stable dry spots near the disc edge. Further reduction in flow rate will produce additional dry spots, which eventually coalesce and produce a catastrophic collapse of the film. In this condition the liquid crosses the disc surface, not as a film, but as a series of rivulets with large areas of the disc surface exposed. Obviously any breakdown of the film which leads to the exposure of disc surface will be detrimental to any thin film process involving mass or heat transfer. Since the achievement of high transfer rates will involve producing the thinnest film, which fully wets the surface, a knowledge of film breakdown, and the associated minimum wetting rates is crucial.

It was noted above that initial film breakdown can be achieved by gradually reducing the flow to the disc. If this initial breakdown has occured i.e., a limited number of dry spots have appeared, we can define a second minimum wetting rate as that which is now required to drive the final dry spot from the surface by a gradual 'increase' in flow rate. This second wetting rate is higher than that which precipitated the first dry spot when the flow was reduced.

A model can be established for the second process. Since it also gives a flow rate higher than that which might induce film breakdown from the fully wetted conditions, it is regarded as a suitable design criterion for this limiting condition.

Although some work has been carried out on the onset of dry spot formation in two phase flows (Hartley and Murgatroyd (6)), no simple standard criterion is available for a rotating surface. Thus, for water, Butuzov and Pukhovoi (1) observed an incomplete film at a flow rate less than 4 cc/s for a disc rotating in the range of 95 to 290 rpm. Whereas, Clare and Jeffs (4) noted a broken film for feed rates less than 10 cc/s at 3000 rpm. The film breakdown phenomenon was experimentally investigated by Charwat etal (3) and 'incipient' dry spots were observed during the formation of the thin films at lower rates. Butuzov etal (2) tested a number of surfaces to determine the minimum irrigation rates but none of these studies produced a quantitative correlation.

A.1. THEORETICAL DEVELOPMENT

Consider a force balance in the vicinity of the nose of the dry spot 'A' of figure A.1 (d), cross section through this area is shown in figure A.1 (c). A force balance is

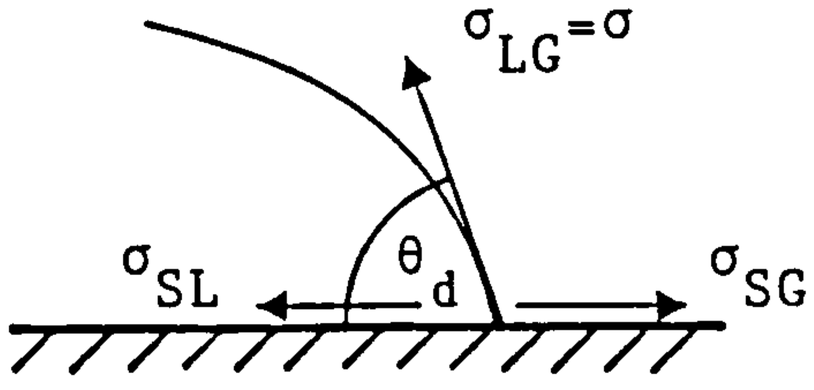

a) Stationary Condition

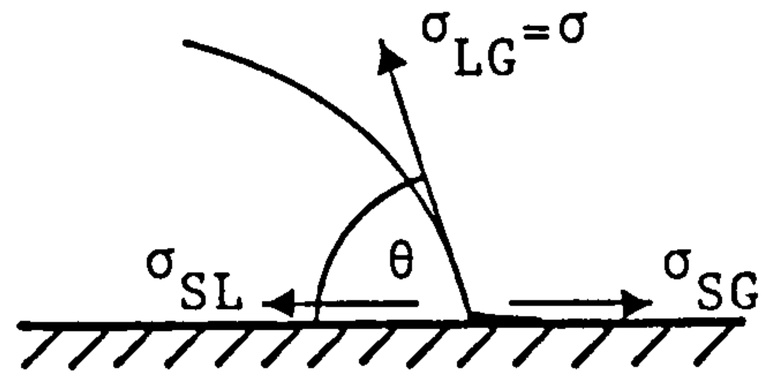

b) Dynamic Condition

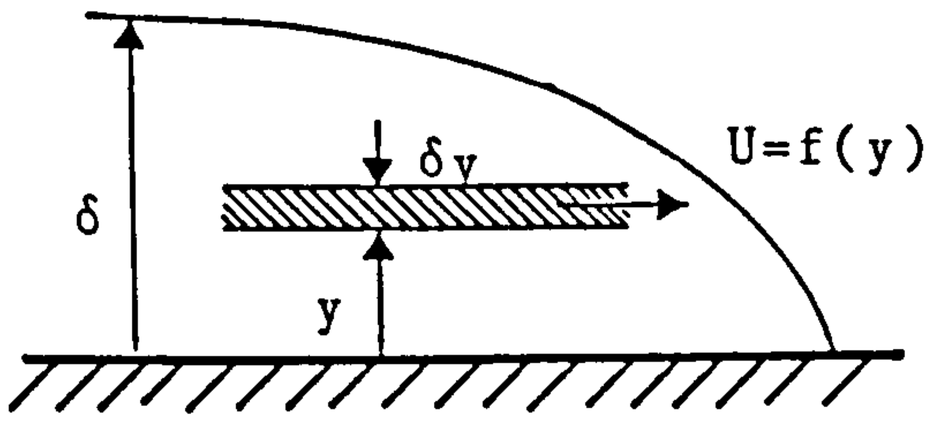

c) Cross Section "A'-A"

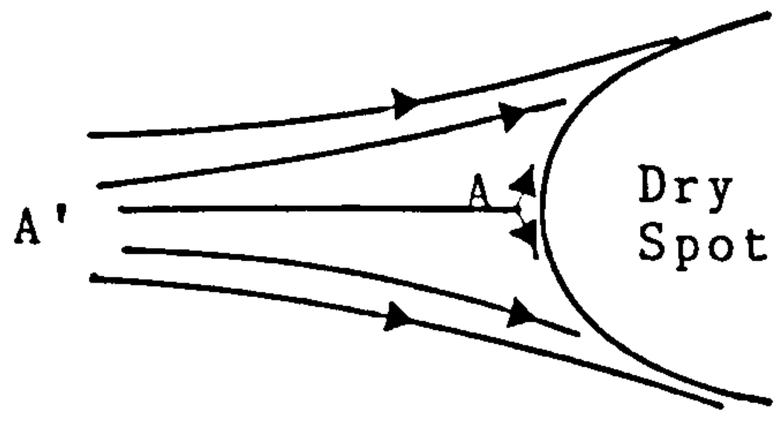

d) Plan View of a Dry Spot

FIGURE A.1. DRY SPOT ON A SOLID SURFACE

Force balance for the conditions shown in above figures,can produce the following equations;

(i) $\sigma_{SL}+\sigma\cos\theta_d=\sigma_{SG}$ (Stationary Condition)

(ii) $\sigma_{SL}+\sigma\cos\theta=\sigma_{SG}+\int_0^{\delta}\rho u^2dy$ (Dynamic Condition)

where $\int_0^{\delta}\rho u^2dy$: rate of change of momentum per unit width.

θ_d : Contact angle with a dry surface.

θ : Contact angle with a wet surface.

Comparing equation (i), and (ii), we have;

$$\sigma(\cos\theta-\cos\theta_d)=\int_0^{\delta}\rho u^2dy$$

For (removal of a dry spot) $\theta=0,\cos\theta=1$ hence $\delta=\delta_c$

$$\therefore\ \sigma(1-\cos\theta_d)=\int_0^{\delta_c}\rho u^2dy.$$

conducted (as shown in figures A.1 (a) and A.1 (b)) in this region; we have

Surface force = $\sigma(1-\cos\theta_d)$ /unit width

Where θ_d = contact angle at solid — liquid interface.

Rate of change of momentum of the film in this region

$$= \int_0^{\delta_c} \rho u^2 dy$$

Where u = f(y), the velocity distribution in the film.

For a stable dry patch, the surface tension forces must be balanced by the momentum force, therefore the minimum wetting rate may be defined as the condition under which

$$\sigma(1-\cos\theta_d) = \int_0^{\delta_c} \rho u^2 dy \qquad (A.1)$$

Substitution of 'u', which has already been defined in section 2.2.3, leads to

$$\sigma(1-\cos\theta_d) = \frac{\rho^3 r^2 \omega^4}{\mu^2} \int_0^{\delta_c} \left(\delta y - \frac{y^2}{2}\right)^2 dy$$

If this equation is integrated we findthat critical film thickness is δ_c where,

$$\delta_c = 1.5 \left[\delta/\rho(1-\cos\theta_d)^{1/5} (\mu/\rho r\omega^2)^{2/5}\right] \qquad (A.2)$$

The film thickness can also be expressed in terms of volumetric flow rate (see section 2.2.4), hence:

$$1.5 \left[\frac{\sigma}{\rho}(1-\cos\theta_d)^{1/5} (\mu/\rho r\omega^2)^{2/5}\right] = \left(\frac{3}{2\pi}\right)^{1/3} \left(\frac{Q_c\mu}{r^2\omega^2\rho}\right)^{1/3} \qquad (A.3)$$

This equation can be simplified to give

$$7.5\ (1-\cos\theta_d) = \frac{1}{\left(\frac{3}{2\pi}\right)^{5/3} \left(\frac{\sigma^3 \upsilon r^4}{\rho^3 Q_c^5 \omega^2}\right)^{1/3}} \qquad (A.4)$$

The denominator on the r.h.s. of equation (A.4), which is dimensionless, has the form of the Weber number, and Charwat et al (3) suggested that it should have this title,

$$\therefore We = 9 \left(\frac{2\pi}{3} \right)^{5/3} \left(\frac{\sigma^3 \nu r^4}{\rho^3 Q^5 \omega^2} \right)^{1/3}$$

$$\therefore 7.5 \ (1-\cos\theta_d) = 9/We$$

$$\text{or } We \ (1-\cos\theta_d) = 1.2 \qquad (A.5)$$

This equation provided a standard criterion to predict minimum wetting rate, therefore, the condition to achieve complete wetting can be established or maintained i.e., the product of Weber number and $(1-\cos\theta_d)$ should be 1.2.

A similar model can also be obtained, adopting the Hartley and Murgatroyd (6) technique in which the Bernoulli equation is applied to the same region of the dry patch this leads to the result.

$$We \ (1-\cos\theta_d) = 0.6 \qquad (A.6)$$

The equation (A.3) is rearranged to estimate minimum wetting rate;

$$Q_c = (7.5)^{3/5} \left(\frac{2\pi}{3}\right)(1-\cos\theta_d)^{3/5}\left(\frac{r^4 \mu \sigma^3}{\rho^4 \omega^2}\right)^{1/5} \qquad (A.7)$$

A.2. TEST FACILITY AND MEASUREMENTS

A series of experiments were conducted to measure minimum wetting rates on discs having a variety of surface conditions. Minimum wetting rates for discs of 25cm and 31cm diameter were measured for a range of liquids, flow rates and disc speeds. These were conducted using an existing rotating disc facility. The layout of the set-up and the mechanical details of the rotating section are given in figures A.2 and A.3, respectively. However additional data, for example surface tension and contact angles required to test the model, necessitated further

LEGEND

1. Rotating disc
2. Stationary Vessel
3. Stroboscope Illuminator
4. Stroboscope Power Unit
5. Feed Reservoir
6. Speed of rotation Photo-Sensor
7. Volt-meter
8. Electric Motor
9. Speed Regulator
10. Triggering Unit (to synchronize stroboscope illuminations)
11. Feed Supply Pump
12. Needle Valve
13. Flow Sensor
14. Flow Meter
15. Power Supply
16. Digital volt-meter
17. Rotary Union Feed Distributor

—— Feed supply and re-cycle line

═══ Power supply

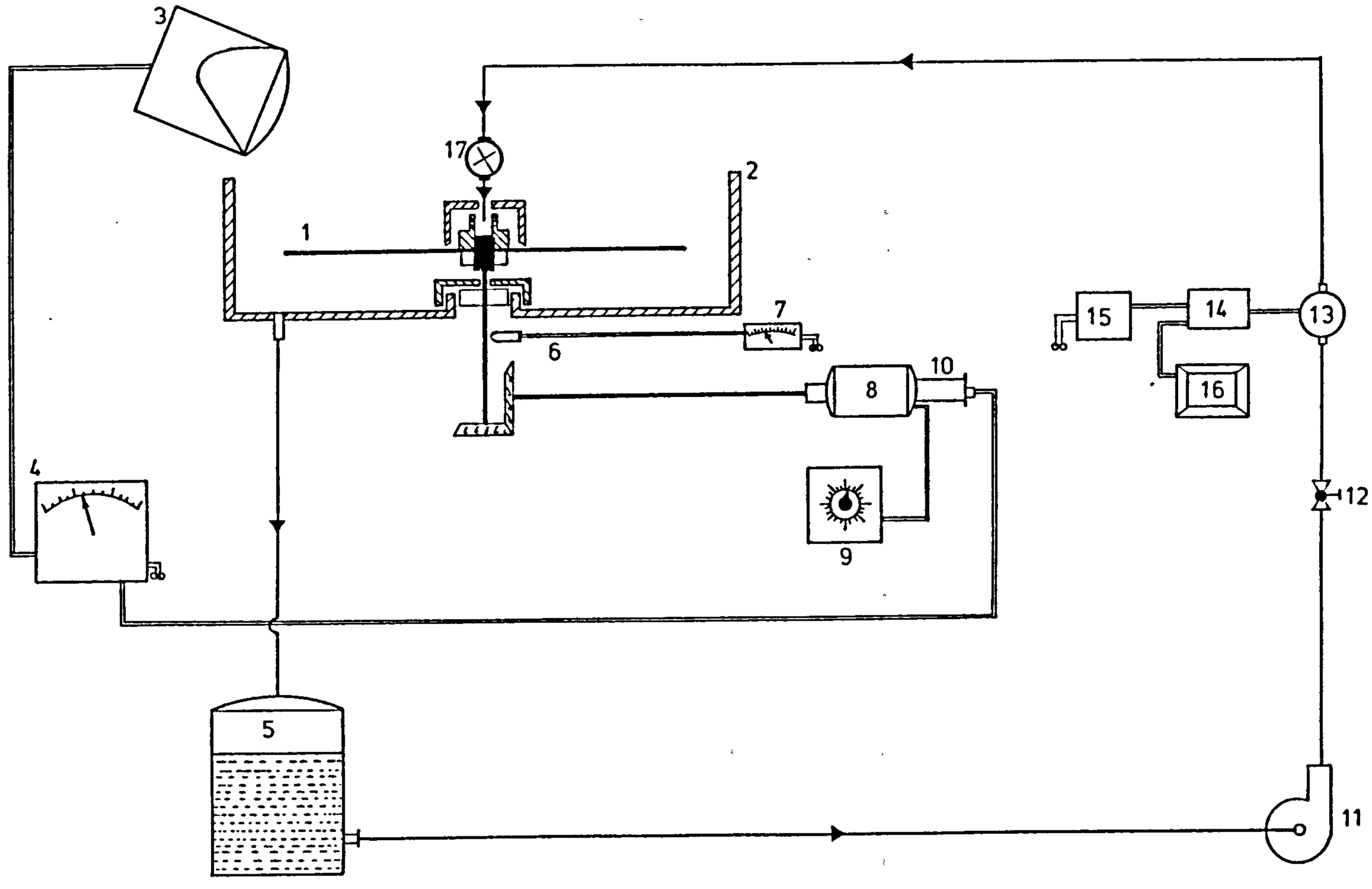

FIGURE A.2. A SCHEMATIC DIAGRAM OF EXPERIMENTAL SET-UP

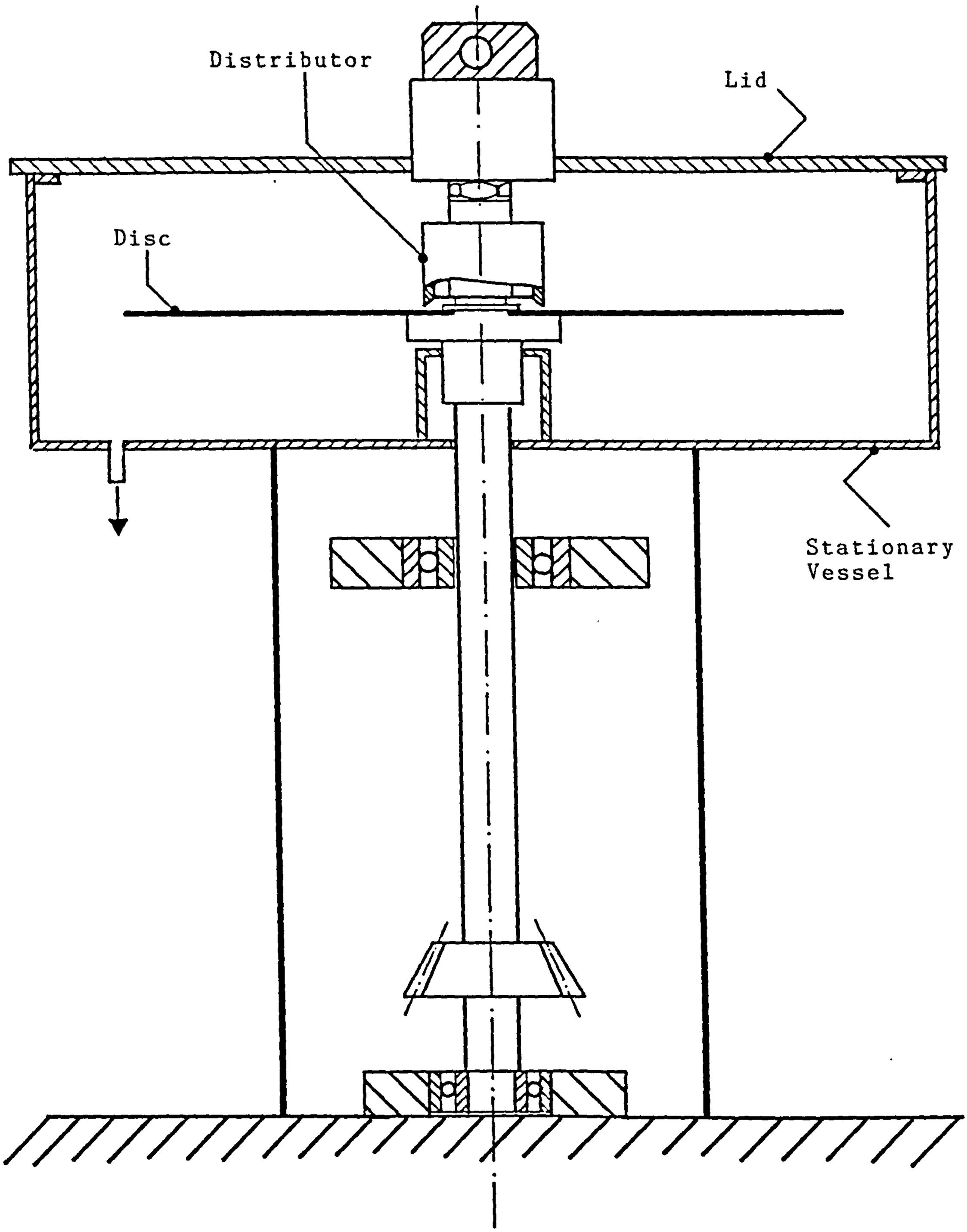

FIGURE A.3. MECHANICAL DETAILS OF THE ROTATING DISC ASSEMBLY

detailed measurement.

Surface tension was determined using the simple Dunouy tensiometer. The determination of accurate contact angle proved a more difficult task. The use of the Sessile drop (5) technique seemed most appropriate for this measurement. Since the location of dry spots could be identified accurately this technique meant that contact angle in the immediate vicinity of the dry spot under investigation could be determined.

The surface under test was thoroughly degreased with acetone, washed, dried and dimensions of the Sessile drop were measured. The disc was mounted onto the rotor assembly and the desired speed was attained. Liquid was introduced to the disc surface and flow rate was gradually increased, until the last dry spot was removed from the surface. To determine the minimum rate for complete wetting, the liquid rate was reduced very slowly and the flow rate just before the appearance of any dry spot was recorded. The position of the last dry spot was located for re-estimation of the contact angle at this particular location and it was used for calculations. The same procedure was employed for each surface under investigation using a number of test fluids.

A.3. RESULT AND DISCUSSION

Stainless steel, brass, chrome and nickel plated discs were used to carry out minimum wetting rate experiments for the conditions listed below;

Speed of rotation	500rpm to 1500rpm
Surface tension of the test liquids	38.0 dynes/cm to 69.0 dynes/cm
Contact angles	9° to 36°

In general, it was found that the minimum wetting rate is directly proportional to the contact angle and have an inverse relation with the rotary speed, as shown in tables A.1 to A.4.

The experimental data were expressed in terms of a dimensionless parameter i.e., "$We(1-\cos\theta_d)$" and it was compared with the models (discussed in section A.1), where as they differ by a factor of 2, whilst the regression analysis of the experimental data produced the following correlation;

$$We\ (1-\cos\theta_d)^{1.109} = 0.834$$

The measured and the predicted values have been plotted in figure A.4. It is apparent from the plot that the measured values and the regression line are very close to the model based on the assumption that the surface tension forces are balanced by the momentum forces. A similar behaviour can be observed for the critical flow rates as well as for the film thicknesses (as shown in figures A.5 to A.9). In contrast to this model, a high discrepancy was found towards Hartley and Murgatroyd's model which was modified for a rotating system where it was assumed that a force at the upstream stagnation point of a dry spot can be related to change in Kinetic energy. This considerable deviation could be due to the presence of certain unaccounted forces, e.g. frictional or form forces. Murgatroyd, after comparing the available data, in a subsequent publication (7) pointed out the existance of additional forces of unknown magnitude such as shear and form forces. Due to such forces, the predicted values could be expected to be less than the actual values. This behaviour is generally observed in this work. However, the experimental data fit more closely to the first model perhaps due to higher value of the parameter, which may compensate the

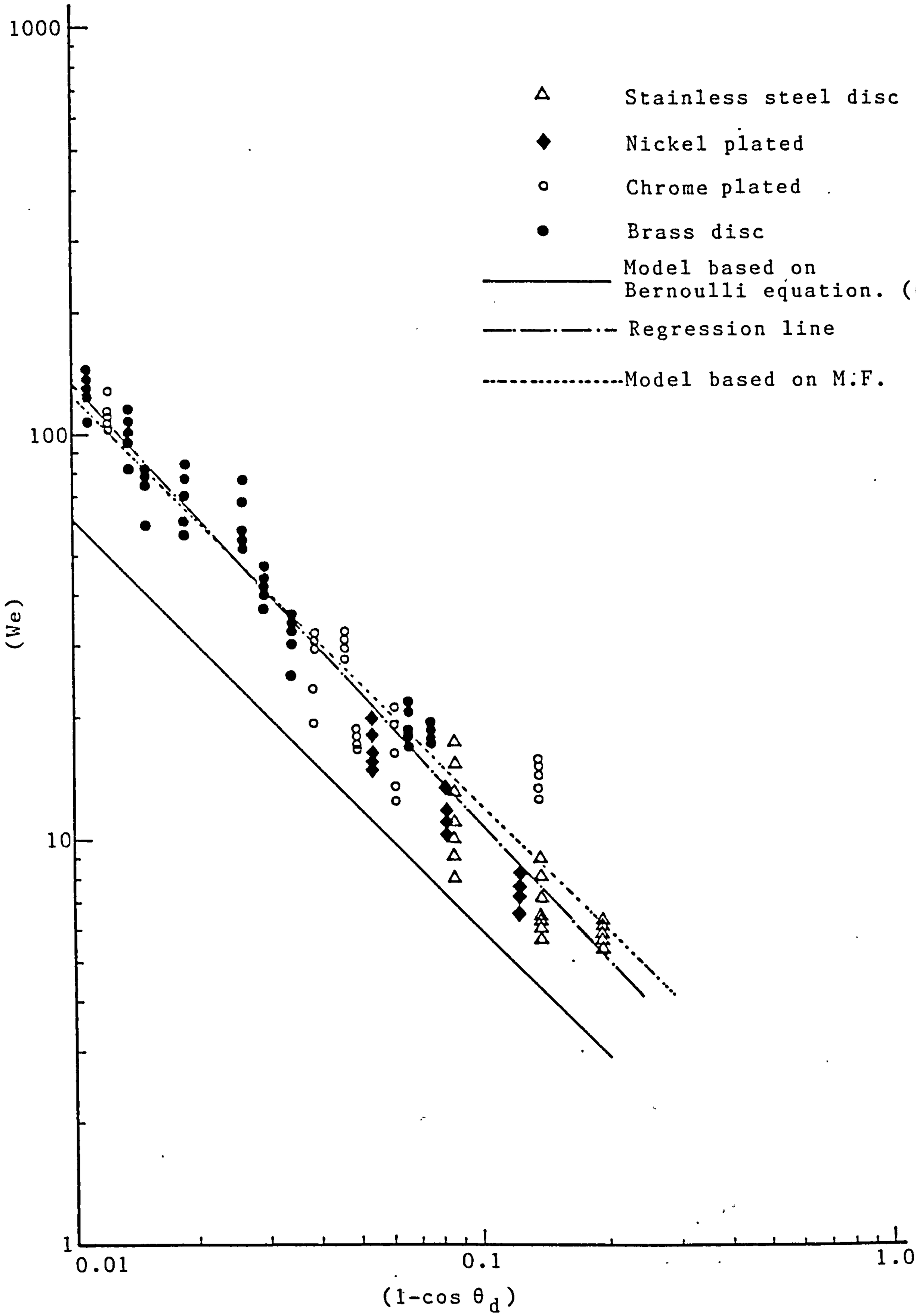

FIGURE A.4 OVERALL COMPARISON OF EXPERIMENTAL & THEORETICAL DATA

STAINLESS STEEL DISC (radius = 168mm)

	σ	θ_d °	
(1)	68.5	36.4	●
(2)	52.0	30.5	▲
(3)	45.8	23.8	◆

Model based on B.E. ——————

Model developed by R.A. —·—·—·—

Model based on M.F. ·····

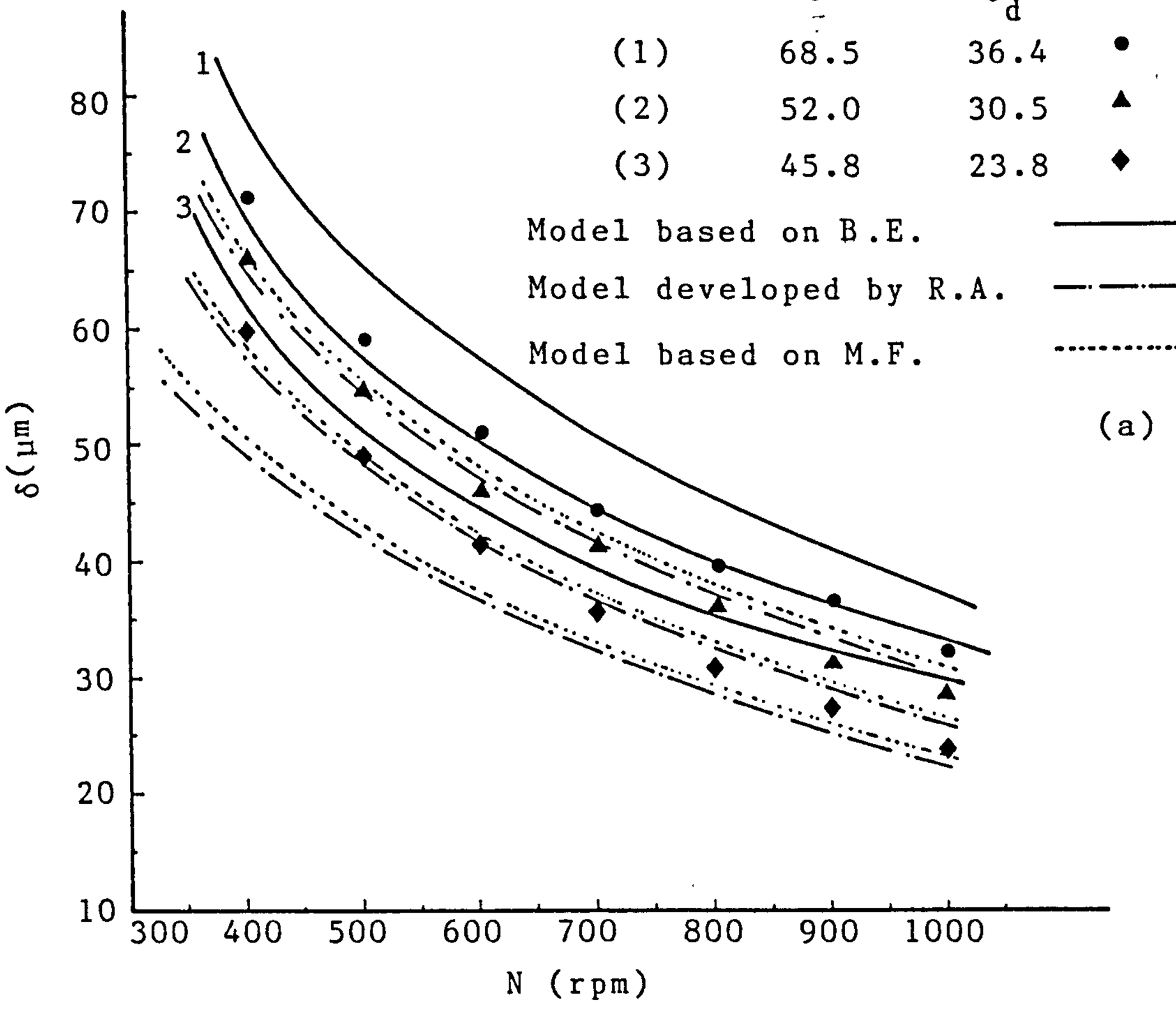

(a)

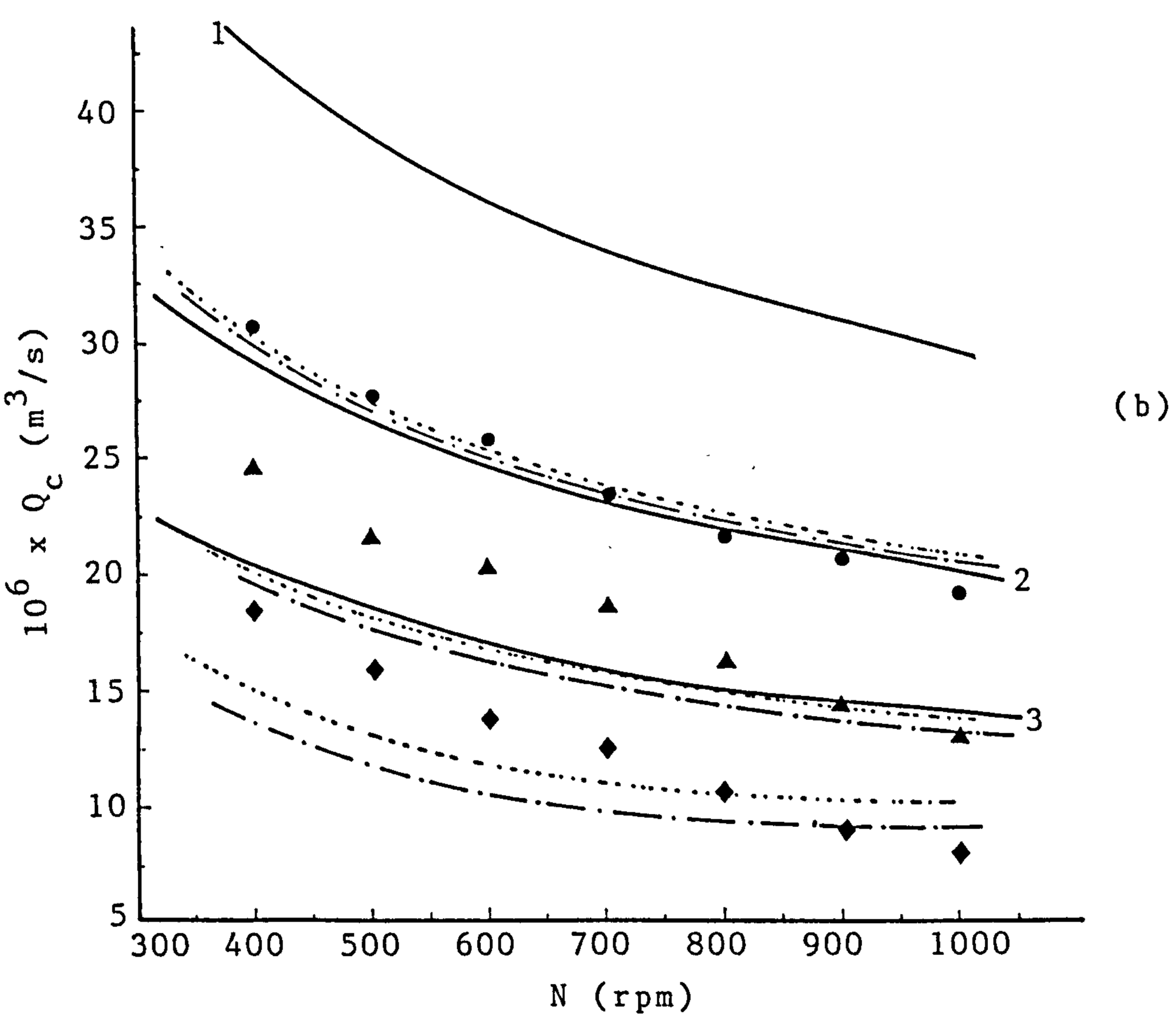

(b)

FIGURE A.5. COMPARISON OF MEASURED & PREDICTED DATA

(a) Film thickness (b) Minimum wetting rate

NICKEL PLATED (radius = 155mm)

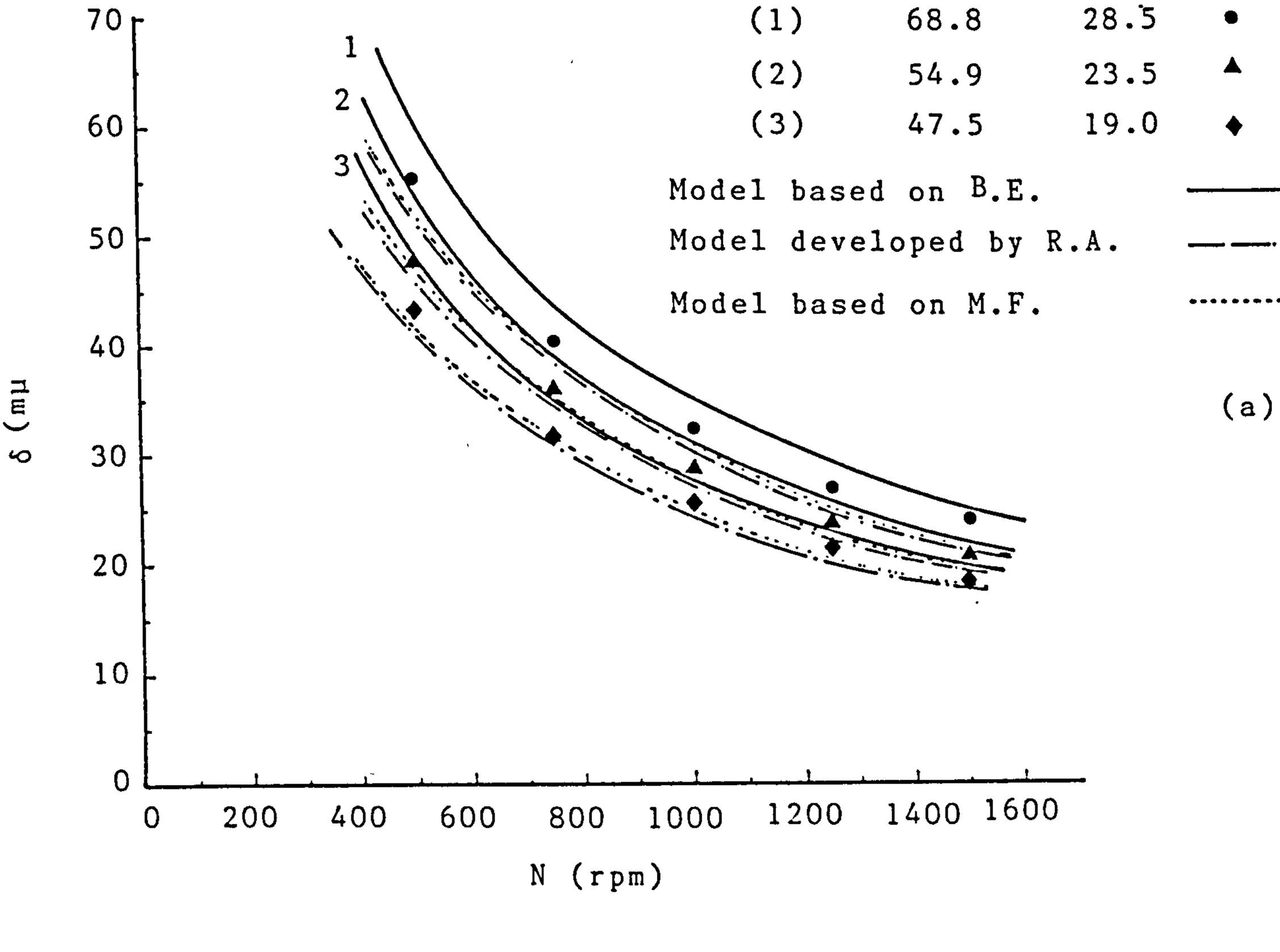

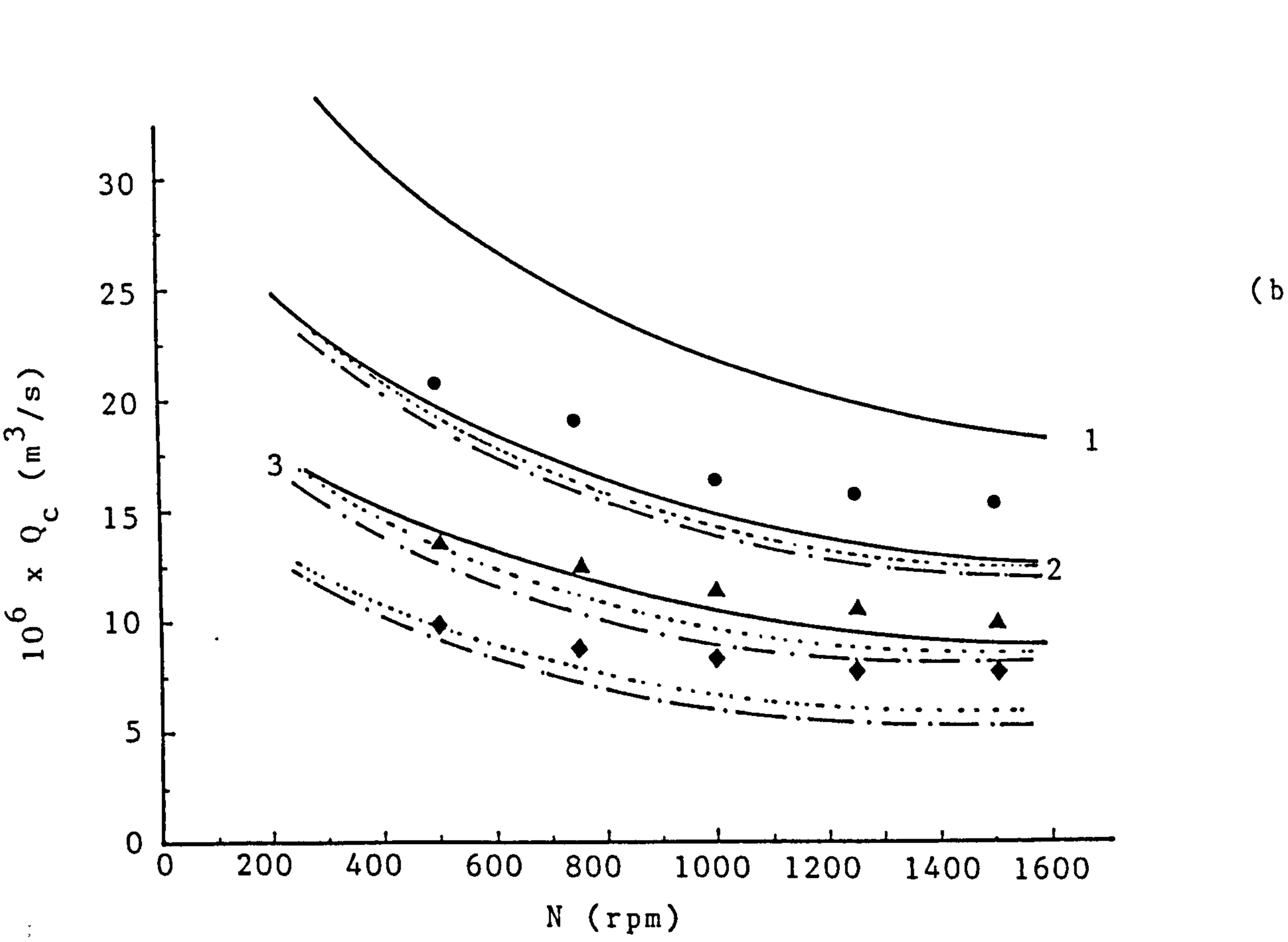

FIGURE A.6. COMPARISON OF MEASURED & PREDICTED DATA

(a) Film thickness (b) Minimum wetting rate.

BRASS DISC (radius = 125mm)

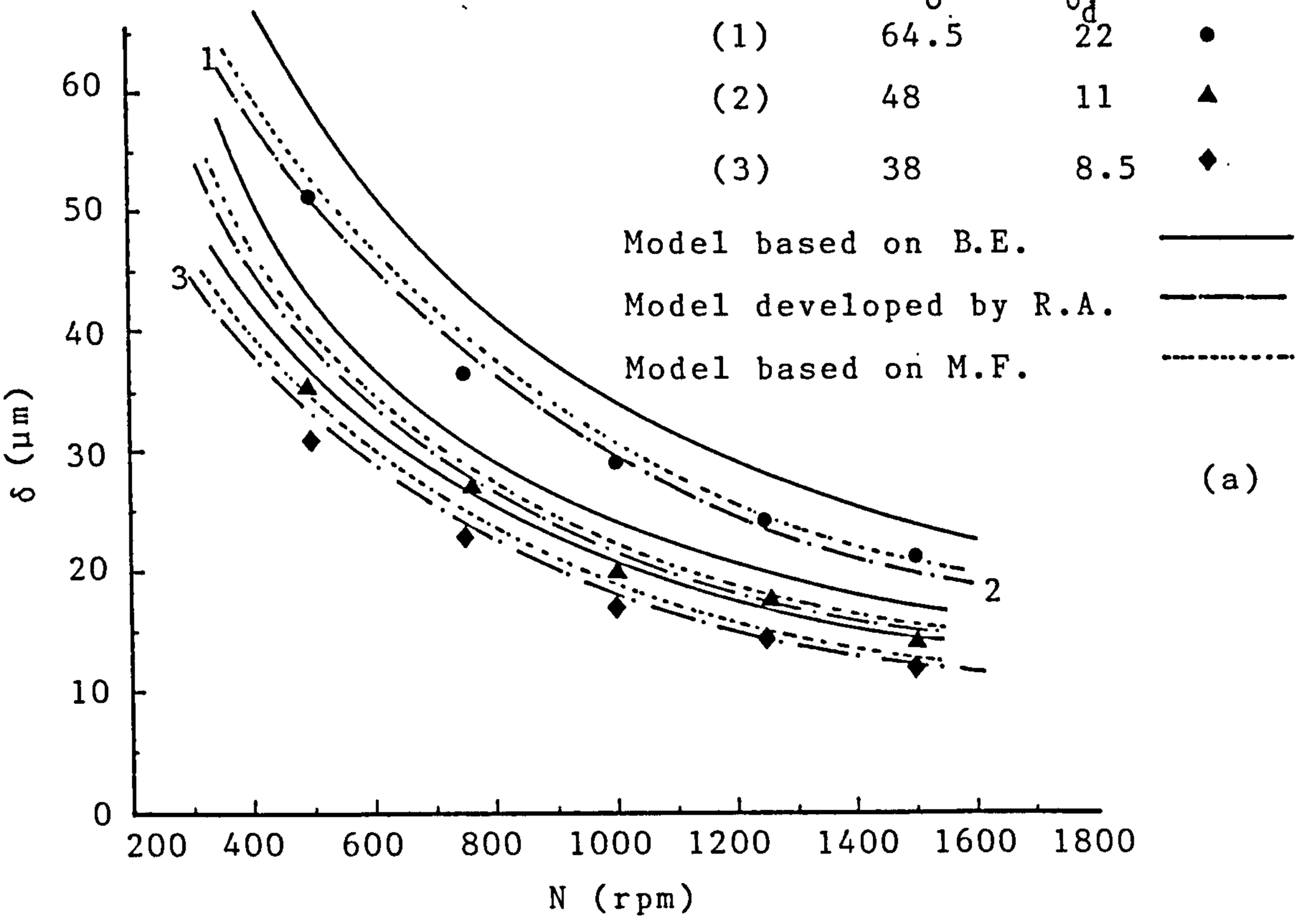

(a)

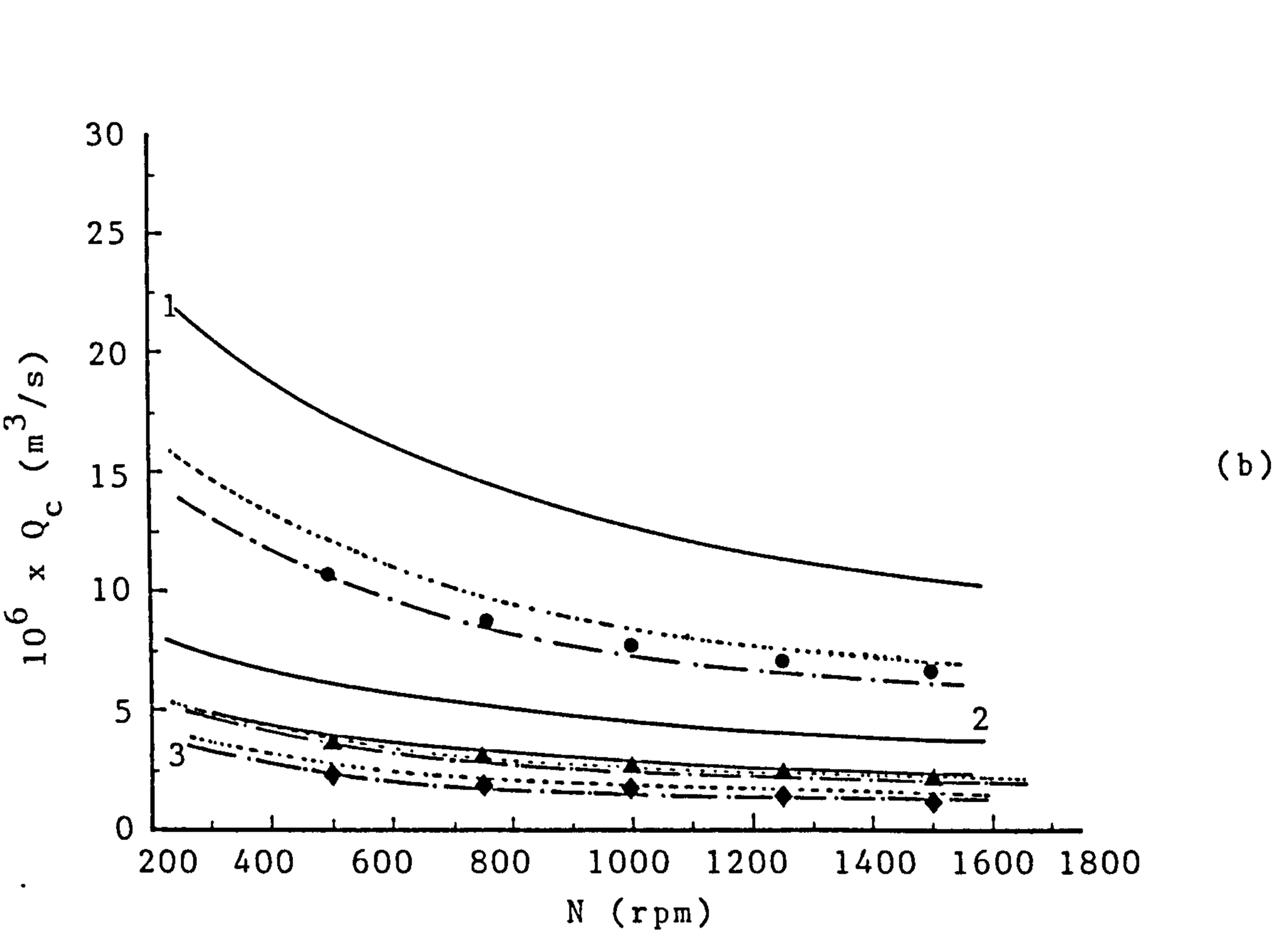

(b)

FIGURE A.7. COMPARISON OF MEASURED & PREDICTED DATA

(a) Film thickness (b) Minimum wetting rate.

BRASS DISC (radius = 155mm)

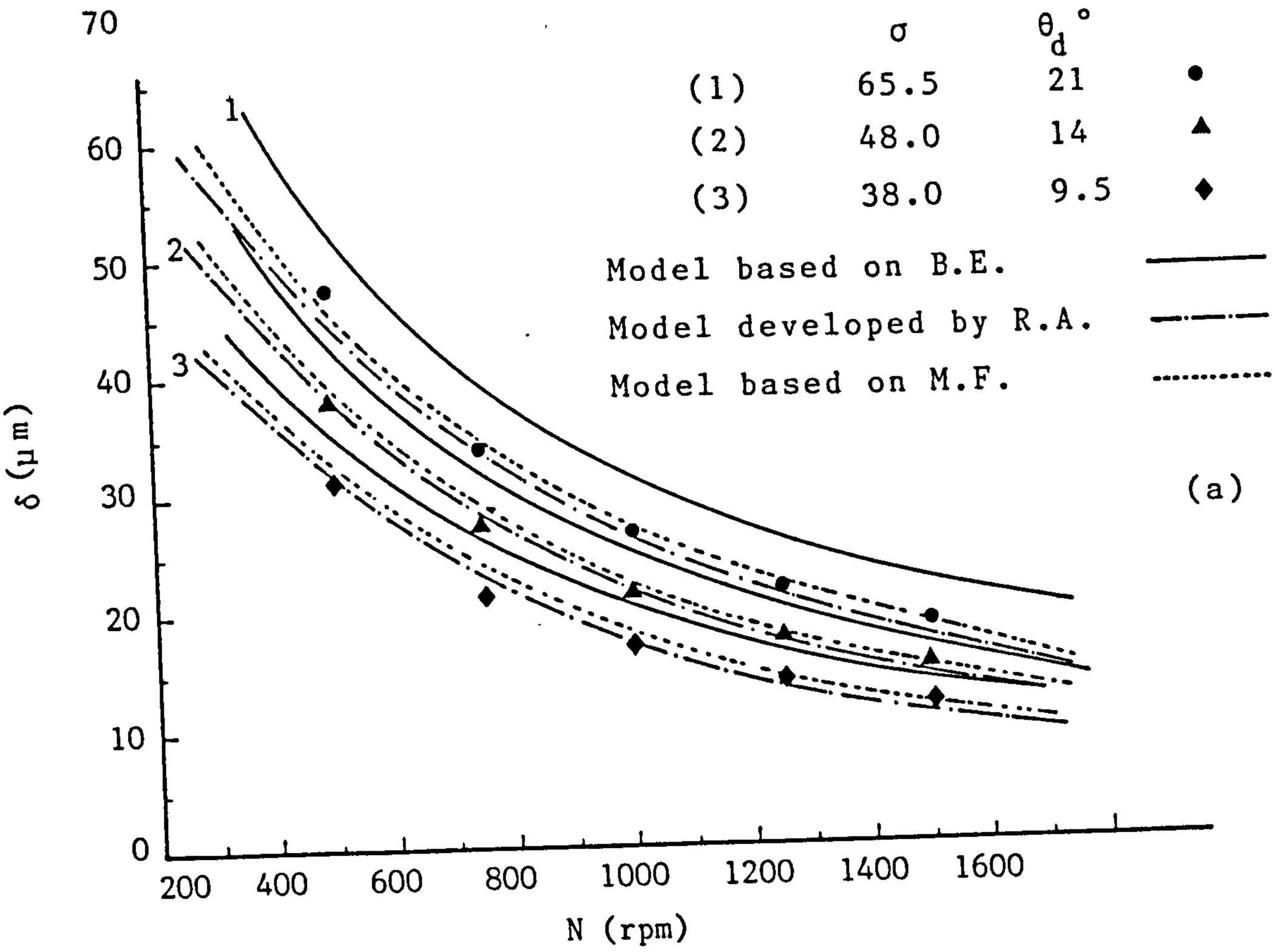

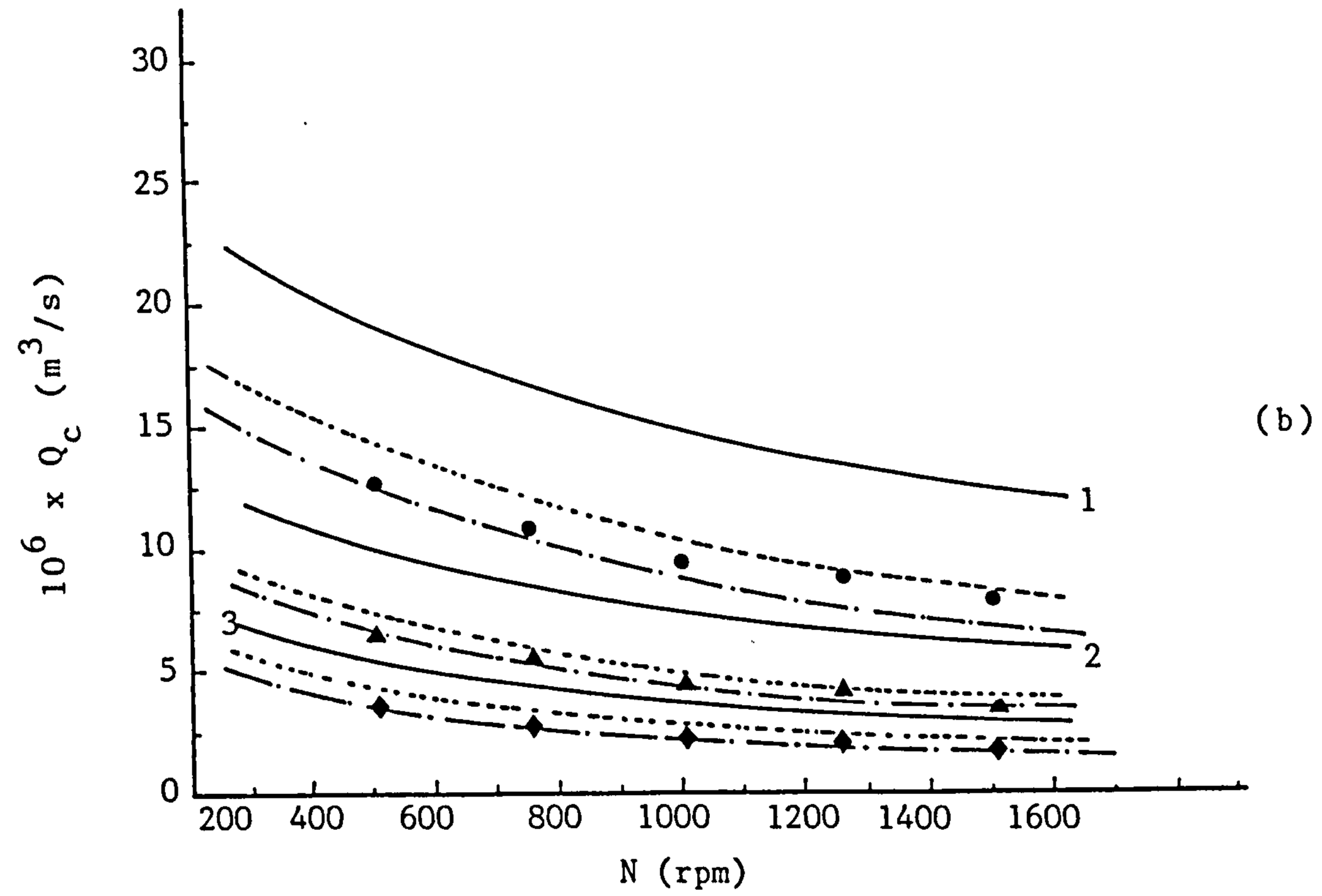

FIGURE A.8. COMPARISON OF MEASURED & PREDICTED DATA

(a) Film thickness (b) Minimum wetting rate.

CHROME PLATED (radius = 155mm)

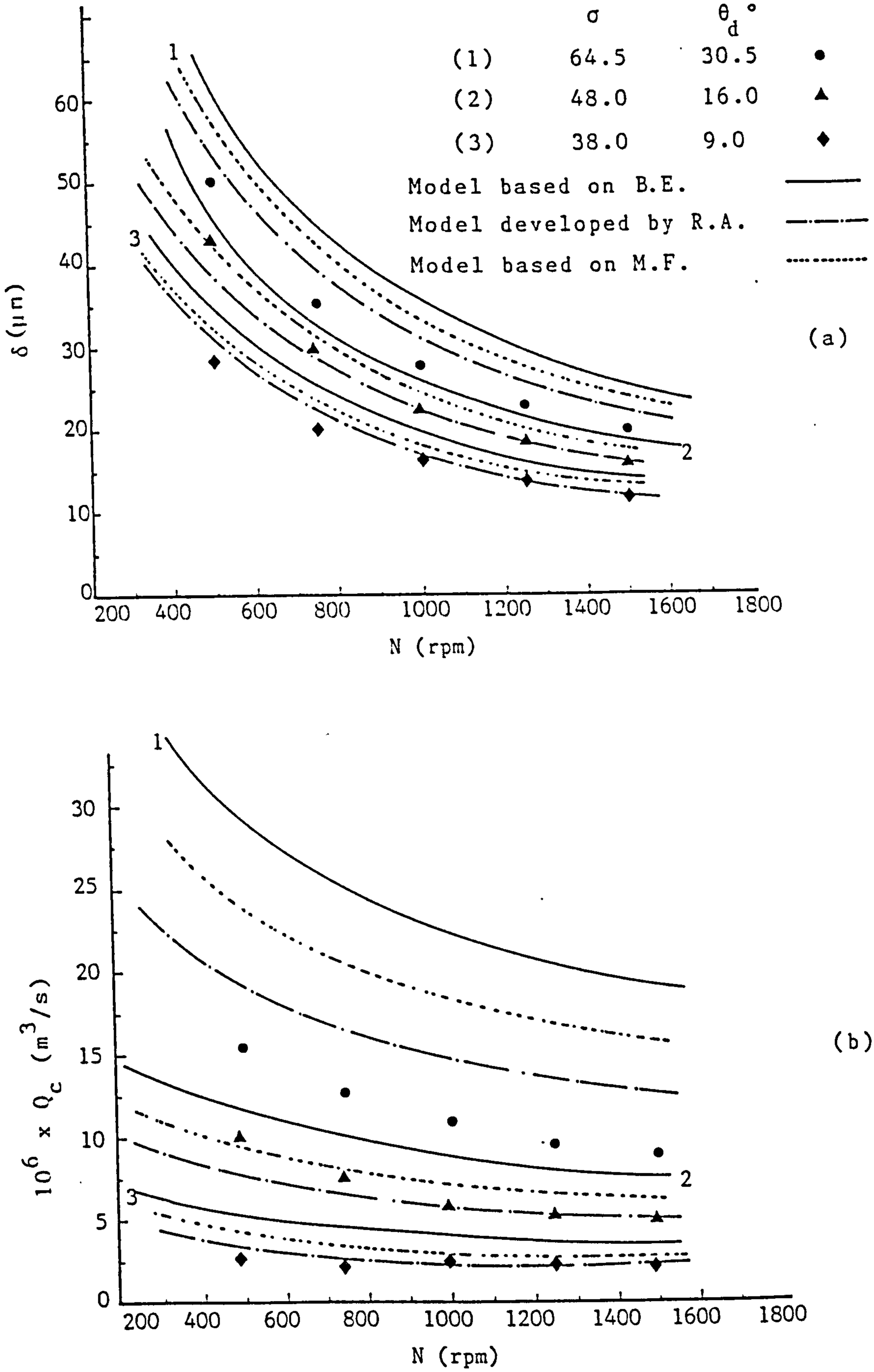

FIGURE A.9. COMPARISON OF MEASURED & PREDICTED DATA

(a) Film thickness (b) Minimum wetting rate.

unaccounted forces.

A.4. CONCLUSIONS AND RECOMMENDATIONS

In view of the above discussion, it may be concluded that the model developed in this study is more reliable for predicting the minimum wetting rate. However, it is suggested that the role of additional forces involved be identified and their effect should be included in the Hartley and Murgatroyd's model for true representation of the forces involved. It may introduce an additional term in this model.

REFERENCES

1) Butuzov, A.I., and Pukhovoi, I.I., "Flow regime of liquid film on a rotating surface." Inzh. Fiz. Zh. 31(2) (1976) pp 217-224.

2) Butuzov, A.I., etal, "Experimental determination of the minimum irrigation density in a thin-film rotating disc apparatus" Fluid Mechanics - Soviet Research 5(1) (1976) pp 28-33.

3) Charwat, A.F., Kelly, R.E., and Gazley, C., "The flow and stability of thin liquid films on a rotating disc" Jou. Fluid Mech., 53(2) (1972) pp 227-255.

4) Clare, H., and Jeffs, R.A., "Some measurements of the thickness of fluid films on a spinning disc" National Gas Turbine Establishment, Draft Report 12.12.1960.

5) Hartland, S., and Hartley, R.W., "Axisymmetric fluid and liquid interfaces." Elsevier Scientific Publishing Company (1976) pp 552-574.

6) Hartley, D.E., and Murgatroyd, W., "Criteria for the break-up of thin liquid layers flowing isothermally over solid surfaces" Int. Jou. Heat Mass Transfer, 7 (1964) pp 1103-1015.

7) Murgatroyd, W., "The role of shear and form forces in the stability of a dry patch in two-phase film flow" Int. Jou. Heat Mass Transfer, 8 (1965) pp 297-301.

NOMENCLATURE

SYMBOL	SIGNIFICANCE	UNITS
B.E.	Bernoulli equation	
M.F.	Momentum force	
N	Speed of rotation	(rpm)
Q	Volumetric flow rate	(m^3/s)
Q_c	Critical flow rate	(m^3/s)
r	Disc radius	(m)
u	Velocity distribution in the film	(m/s)
y	Vertical distance from the disc	(m)
GREEK SYMBOL		
δ	Liquid film thickness	(μm)
δ_c	Liquid film thickness at critical flow rate	(μm)
θ	Contact angle at solid-liquid interface (wet condition)	(degree)
θ_d	Contact angle at solid-liquid interface (dry condition)	(degree)
μ	Viscosity of liquid	(kg/m-s)
ρ	Liquid density	(kg/m^3)
σ	Surface tension of test liquid	(dy./cm)
σ_{LG}	Interfacial tension between liquid and gas	(dy./cm)
σ_{SG}	Interfacial tension between solid and gas	(dy./cm)
σ_{SL}	Interfacial tension between solid and liquid	(dy./cm)

GREEK SYMBOL	SIGNIFICANCE	UNITS
ν	Kinamatic viscosity of the liquid	(m^2/s)
ω	Angular velocity	(rad/s)

DIMENSIONLESS NUMBER		
We: Weber number	(Surface tension/Inertia)	$9(\frac{2\pi}{3})^{5/3}(\frac{\sigma^3 \nu r^4}{\rho^3 Q^5 \omega^2})^{1/3}$

TABLE A.1 MINIMUM WETTING RATE DATA

DISC MATERIAL : STAINLESS STEEL
DISC RADIUS : 168.00mm
SURFACE TENSION = 69.50*1E-03 N/m
CONTACT ANGLE = 36.40 DEGREES

N	(OC)exp.	(OC)K.E.	(OC)M.F.	(δ)	(δ)K.E.	(δ)M.F.	WE	PAR
400.00	30.58	44.23	29.19	69.24	77.76	67.59	5.67	1.11
500.00	27.56	40.46	26.70	57.65	65.05	56.54	5.81	1.13
600.00	25.60	37.61	24.82	49.82	56.22	48.87	5.82	1.14
700.00	23.20	35.36	23.34	43.51	49.69	43.20	6.19	1.21
800.00	21.50	33.52	22.13	38.81	44.66	38.82	6.43	1.25
900.00	20.60	31.98	21.11	35.37	40.64	35.33	6.38	1.24
1000.00	19.20	30.66	20.24	32.21	37.36	32.48	6.69	1.30

DISC MATERIAL : STAINLESS STEEL
DISC RADIUS : 168.00mm
SURFACE TENSION = 52.00*1E-03 N/m
CONTACT ANGLE = 30.50 DEGREES

N	(OC)exp.	(OC)K.E.	(OC)M.F.	(δ)	(δ)K.E.	(δ)M.F.	WE	PAR
400.00	24.59	30.24	19.96	64.40	68.50	59.55	6.10	0.84
500.00	21.64	27.66	18.26	53.19	57.30	49.81	6.51	0.90
600.00	20.10	25.72	16.97	45.96	49.53	43.05	6.52	0.90
700.00	18.40	24.18	15.96	40.28	43.78	38.06	6.81	0.94
800.00	16.20	22.92	15.13	35.32	39.34	34.20	7.70	1.07
900.00	14.30	21.87	14.43	31.33	35.81	31.13	8.77	1.21
1000.00	12.90	20.96	13.84	28.22	32.91	28.61	9.70	1.34

DISC MATERIAL : STAINLESS STEEL
DISC RADIUS : 168.00mm
SURFACE TENSION = 45.80*1E-03 N/m
CONTACT ANGLE = 23.80 DEGREES

N	(OC)exp.	(OC)K.E.	(OC)M.F.	(δ)	(δ)K.E.	(δ)M.F.	WE	PAR
400.00	18.42	20.93	13.81	58.49	60.59	52.67	8.70	0.74
500.00	15.80	19.14	12.63	47.90	50.68	44.06	9.68	0.82
600.00	13.75	17.79	11.74	40.50	43.80	38.08	10.80	0.92
700.00	12.30	16.73	11.04	35.22	38.72	33.66	11.73	1.00
800.00	10.50	15.86	10.47	30.57	34.80	30.25	13.97	1.19
900.00	8.96	15.13	9.99	26.81	31.67	27.53	16.82	1.43
1000.00	7.95	14.51	9.57	24.02	29.11	25.31	19.14	1.63

TABLE A.2 MINIMUM WETTING RATE DATA

DISC MATERIAL : NICKEL PLATED
DISC RADIUS : 155.00mm
SURFACE TENSION = 68.80*1E-03 N/m
CONTACT ANGLE = 28.80 DEGREES

N	(QC)exp.	(QC)K.E.	(QC)M.F.	(δ)	(δ)K.E.	(δ)M.F.	WE	PAR
500.00	20.65	28.68	18.93	55.25	61.20	53.20	8.36	1.03
750.00	18.90	24.39	16.10	40.95	44.25	38.46	7.39	0.91
1000.00	16.35	21.74	14.35	32.22	35.15	30.56	7.77	0.96
1250.00	15.68	19.88	13.12	27.38	29.40	25.56	7.18	0.89
1500.00	15.45	18.48	12.20	24.13	25.41	22.09	6.52	0.81

DISC MATERIAL : NICKEL PLATED
DISC RADIUS : 155.00mm
SURFACE TENSION = 54.90*1E-03 N/m
CONTACT ANGLE = 23.50 DEGREES

N	(QC)exp.	(QC)K.E.	(QC)M.F.	(δ)	(δ)K.E.	(δ)M.F.	WE	PAR
500.00	13.50	19.71	13.01	47.96	54.00	46.95	13.54	1.12
750.00	12.45	16.76	11.06	35.63	39.04	33.94	11.82	0.98
1000.00	11.32	14.94	9.86	28.50	31.02	26.96	11.44	0.95
1250.00	10.45	13.66	9.02	23.92	25.95	22.55	11.26	0.93
1500.00	9.70	12.70	8.38	20.67	22.42	19.49	11.29	0.94

DISC MATERIAL : NICKEL PLATED
DISC RADIUS : 155.00mm
SURFACE TENSION = 47.50*1E-03 N/m
CONTACT ANGLE = 19.00 DEGREES

N	(QC)exp.	(QC)K.E.	(QC)M.F.	(δ)	(δ)K.E.	(δ)M.F.	WE	PAR
500.00	9.80	14.04	9.27	43.10	48.23	41.93	19.97	1.09
750.00	8.85	11.94	7.88	31.81	34.87	30.31	18.06	0.98
1000.00	8.30	10.64	7.02	25.70	27.70	24.08	16.59	0.90
1250.00	7.95	9.73	6.42	21.84	23.17	20.14	15.36	0.84
1500.00	7.55	9.05	5.97	19.01	20.03	17.41	14.83	0.81

TABLE A.3 MINIMUM WETTING RATE DATA

DISC MATERIAL : BRASS(ROUGH)
DISC RADIUS : 125.00mm
SURFACE TENSION = 64.50*1E-03 N/m
CONTACT ANGLE = 15.00 DEGREES

N	(QC)exp.	(QC)K.E.	(QC)M.F.	(δ)	(δ)K.E.	(δ)M.F.	WE	PAR
500.00	8.64	10.72	7.07	47.69	50.88	44.23	25.10	0.86
750.00	6.50	9.11	6.01	33.11	36.78	31.98	30.77	1.05
1000.00	5.46	8.12	5.36	25.80	29.22	25.40	33.97	1.16
1250.00	4.91	7.43	4.90	21.46	24.44	21.25	34.94	1.19
1500.00	4.50	6.91	4.56	18.46	21.13	18.37	35.78	1.22

DISC MATERIAL : BRASS(ROUGH)
DISC RADIUS : 125.00mm
SURFACE TENSION = 38.00*1E-03 N/m
CONTACT ANGLE = 8.50 DEGREES

N	(QC)exp.	(QC)K.E.	(QC)M.F.	(δ)	(δ)K.E.	(δ)M.F.	WE	PAR
500.00	2.40	3.96	2.61	31.13	36.49	31.73	124.84	1.37
750.00	2.21	3.36	2.22	23.12	26.39	22.94	109.33	1.20
1000.00	1.75	3.00	1.98	17.66	20.96	18.22	133.13	1.46
1250.00	1.54	2.74	1.81	14.59	17.53	15.24	141.96	1.56
1500.00	1.48	2.55	1.68	12.75	15.15	13.17	134.33	1.48

DISC MATERIAL : BRASS(POLISHED)
DISC RADIUS : 125.00mm
SURFACE TENSION = 48.00*1E-03 N/m
CONTACT ANGLE = 11.00 DEGREES

N	(QC)exp.	(QC)K.E.	(QC)M.F.	(δ)	(δ)K.E.	(δ)M.F.	WE	PAR
500.00	3.70	6.20	4.09	35.96	42.38	36.84	76.69	1.41
750.00	3.30	5.27	3.48	26.42	30.64	26.64	70.82	1.30
1000.00	2.80	4.70	3.10	20.65	24.34	21.16	76.87	1.41
1250.00	2.70	4.30	2.83	17.59	20.36	17.70	70.39	1.29
1500.00	2.25	3.99	2.64	14.66	17.60	15.30	84.46	1.55

Cont'd...

TABLE A.3 MINIMUM WETTING RATE DATA

DISC MATERIAL : BRASS(ROUGH)
DISC RADIUS : 155.00mm
SURFACE TENSION = 64.50*1E-03 N/m
CONTACT ANGLE = 13.00 DEGREES

N	(QC)exp.	(QC)K.E.	(QC)M.F.	(δ)	(δ)K.E.	(δ)M.F.	WE	PAR
500.00	6.50	10.53	6.95	36.42	42.45	36.90	52.01	1.33
750.00	5.40	8.95	5.91	26.14	30.69	26.68	54.06	1.39
1000.00	4.66	7.98	5.27	20.55	24.38	21.19	57.05	1.46
1250.00	3.88	7.30	4.82	16.66	20.39	17.73	66.71	1.71
1500.00	3.37	6.78	4.48	14.08	17.63	15.32	74.71	1.91

DISC MATERIAL : BRASS(ROUGH)
DISC RADIUS : 155.00mm
SURFACE TENSION = 48.00*1E-03 N/m
CONTACT ANGLE = 10.00 DEGREES

N	(QC)exp.	(QC)K.E.	(QC)M.F.	(δ)	(δ)K.E.	(δ)M.F.	WE	PAR
500.00	5.10	6.44	4.25	33.60	36.04	31.33	57.99	0.88
750.00	3.55	5.48	3.62	22.73	26.06	22.65	80.91	1.23
1000.00	3.29	4.88	3.22	18.30	20.70	17.99	75.82	1.15
1250.00	3.01	4.47	2.95	15.31	17.31	15.05	75.79	1.15
1500.00	2.78	4.15	2.74	13.21	14.96	13.01	76.62	1.16

DISC MATERIAL : BRASS(ROUGH)
DISC RADIUS : 155.00mm
SURFACE TENSION = 38.00*1E-03 N/m
CONTACT ANGLE = 9.50 DEGREES

N	(QC)exp.	(QC)K.E.	(QC)M.F.	(δ)	(δ)K.E.	(δ)M.F.	WE	PAR
500.00	3.70	5.27	3.48	30.19	33.70	29.29	78.35	1.07
750.00	2.80	4.48	2.96	21.00	24.36	21.18	95.12	1.30
1000.00	2.46	3.99	2.63	16.61	19.35	16.82	97.43	1.34
1250.00	2.09	3.65	2.41	13.56	16.19	14.07	110.15	1.51
1500.00	1.99	3.39	2.24	11.81	13.99	12.16	105.86	1.45

DISC MATERIAL : BRASS(POLISHED)
DISC RADIUS : 125.00mm
SURFACE TENSION = 64.50*1E-03 N/m
CONTACT ANGLE = 22.00 DEGREES

N	(QC)exp.	(QC)K.E.	(QC)M.F.	(δ)	(δ)K.E.	(δ)M.F.	WE	PAR
500.00	10.70	16.90	11.16	51.21	59.22	51.48	17.58	1.28
750.00	8.86	14.37	9.49	36.71	42.82	37.22	18.37	1.34
1000.00	7.85	12.81	8.46	29.11	34.01	29.57	18.56	1.35
1250.00	7.20	11.72	7.73	24.38	28.45	24.73	18.47	1.34
1500.00	6.76	10.89	7.19	21.14	24.59	21.38	18.17	1.32

Cont'd...

TABLE A.3 MINIMUM WETTING RATE DATA

DISC MATERIAL : BRASS(POLISHED)
DISC RADIUS : 155.00mm
SURFACE TENSION = 64.50*1E-03 N/m
CONTACT ANGLE = 21.00 DEGREES

N	(DC)exp.	(DC)K.E.	(DC)M.F.	(δ)	(δ)K.E.	(δ)M.F.	WE	PAR
500.00	12.78	19.00	12.54	47.09	53.35	46.38	17.42	1.16
750.00	10.80	16.16	10.66	33.99	38.57	33.53	17.60	1.17
1000.00	9.30	14.40	9.50	26.70	30.64	26.64	18.64	1.24
1250.00	7.80	13.17	8.69	21.70	25.63	22.28	21.53	1.43
1500.00	7.20	12.24	8.08	18.71	22.15	19.26	21.79	1.45

DISC MATERIAL : BRASS(POLISHED)
DISC RADIUS : 155.00mm
SURFACE TENSION = 48.00*1E-03 N/m
CONTACT ANGLE = 14.00 DEGREES

N	(DC)exp.	(DC)K.E.	(DC)M.F.	(δ)	(δ)K.E.	(δ)M.F.	WE	PAR
500.00	6.72	9.82	6.48	38.02	42.81	37.22	37.81	1.12
750.00	5.49	8.35	5.51	27.13	30.95	26.91	40.42	1.20
1000.00	4.48	7.44	4.91	20.93	24.59	21.38	46.81	1.39
1250.00	4.28	6.81	4.49	17.77	20.57	17.88	43.53	1.29
1500.00	3.90	6.33	4.18	15.26	17.78	15.45	45.01	1.34

DISC MATERIAL : BRASS(POLISHED)
DISC RADIUS : 155.00mm
SURFACE TENSION = 38.00*1E-03 N/m
CONTACT ANGLE = 11.00 DEGREES

N	(DC)exp.	(DC)K.E.	(DC)M.F.	(δ)	(δ)K.E.	(δ)M.F.	WE	PAR
500.00	4.60	6.40	4.22	33.51	37.11	32.26	56.28	1.03
750.00	3.70	5.44	3.59	23.79	26.83	23.33	61.73	1.13
1000.00	3.00	4.85	3.20	18.32	21.32	18.53	72.27	1.33
1250.00	2.42	4.43	2.93	14.70	17.83	15.50	89.08	1.64
1500.00	2.39	4.12	2.72	12.96	15.41	13.40	80.55	1.48

TABLE A.4 MINIMUM WETTING RATE DATA

DISC MATERIAL : CHROME PLATED(POLISHED)
DISC RADIUS : 155.00mm
SURFACE TENSION = 64.50*1E-03 N/m
CONTACT ANGLE = 30.50 DEGREES

N	(QC)exp.	(QC)K.E.	(QC)M.F.	(δ)	(δ)K.E.	(δ)M.F.	WE	PAR
500.00	15.50	29.51	19.48	50.21	61.78	53.71	12.63	1.75
750.00	12.69	25.09	16.56	35.86	44.67	38.83	13.45	1.86
1000.00	10.81	22.37	14.76	28.07	35.49	30.85	14.51	2.01
1250.00	9.44	20.46	13.50	23.13	29.68	25.80	15.67	2.17
1500.00	8.82	19.02	12.55	20.02	25.66	22.30	15.54	2.15

DISC MATERIAL : CHROME PLATED(POLISHED)
DISC RADIUS : 155.00mm
SURFACE TENSION = 48.00*1E-03 N/m
CONTACT ANGLE = 20.00 DEGREES

N	(QC)exp.	(QC)K.E.	(QC)M.F.	(δ)	(δ)K.E.	(δ)M.F.	WE	PAR
500.00	12.90	15.02	9.91	47.24	49.33	42.88	12.77	0.77
750.00	10.49	12.77	8.43	33.66	35.66	31.00	13.75	0.83
1000.00	8.48	11.38	7.51	25.89	28.33	24.63	16.18	0.98
1250.00	6.95	10.41	6.87	20.88	23.70	20.60	19.42	1.17
1500.00	6.15	9.68	6.39	17.76	20.48	17.81	21.08	1.27

DISC MATERIAL : CHROME PLATED(POLISHED)
DISC RADIUS : 155.00mm
SURFACE TENSION = 38.00*1E-03 N/m
CONTACT ANGLE = 17.50 DEGREES

N	(QC)exp.	(QC)K.E.	(QC)M.F.	(δ)	(δ)K.E.	(δ)M.F.	WE	PAR
500.00	6.70	11.14	7.35	37.98	44.65	38.81	30.09	1.39
750.00	5.47	9.47	6.25	27.10	32.28	28.06	32.20	1.49
1000.00	5.04	8.44	5.57	21.77	25.64	22.29	30.47	1.41
1250.00	4.64	7.72	5.10	18.25	21.45	18.65	30.14	1.39
1500.00	4.25	7.18	4.74	15.70	18.54	16.12	30.89	1.43

DISC MATERIAL : CHROME PLATED(ROUGH)
DISC RADIUS : 155.00mm
SURFACE TENSION = 38.00*1E-03 N/m
CONTACT ANGLE = 9.00 DEGREES

N	(QC)exp.	(QC)K.E.	(QC)M.F.	(δ)	(δ)K.E.	(δ)M.F.	WE	PAR
500.00	3.01	5.03	3.32	29.09	34.26	29.78	114.04	1.40
750.00	2.37	4.28	2.82	20.51	24.77	21.53	129.61	1.60
1000.00	2.29	3.81	2.52	16.74	19.68	17.10	113.30	1.39
1250.00	2.14	3.49	2.30	14.11	16.46	14.31	109.32	1.35
1500.00	2.06	3.24	2.14	12.34	14.23	12.37	103.16	1.27

Cont'd...

TABLE A.4 MINIMUM WETTING RATE DATA

DISC MATERIAL : CHROME PLATED(ROUGH)
DISC RADIUS : 155.00mm
SURFACE TENSION = 64.50*1E-03 N/m
CONTACT ANGLE = 18.00 DEGREES

N	(QC)exp.	(QC)K.E.	(QC)M.F.	(δ)	(δ)K.E.	(δ)M.F.	WE	PAR
500.00	12.77	15.82	10.44	47.08	50.19	43.63	17.44	0.85
750.00	10.45	13.45	8.88	33.62	36.29	31.54	18.59	0.91
1000.00	9.35	11.99	7.91	26.74	28.83	25.06	18.47	0.90
1250.00	8.74	10.97	7.24	22.54	24.11	20.96	17.81	0.87
1500.00	7.91	10.19	6.73	19.31	20.84	18.12	18.63	0.91

DISC MATERIAL : CHROME PLATED(ROUGH)
DISC RADIUS : 155.00mm
SURFACE TENSION = 48.00*1E-03 N/m
CONTACT ANGLE = 16.00 DEGREES

N	(QC)exp.	(QC)K.E.	(QC)M.F.	(δ)	(δ)K.E.	(δ)M.F.	WE	PAR
500.00	10.10	11.52	7.60	43.54	45.15	39.25	19.19	0.74
750.00	7.60	9.79	6.46	30.23	32.64	28.37	23.52	0.91
1000.00	5.80	8.73	5.76	22.81	25.93	22.54	30.45	1.18
1250.00	5.20	7.98	5.27	18.96	21.69	18.86	31.48	1.22
1500.00	4.80	7.42	4.90	16.35	18.75	16.30	31.86	1.23

APPENDIX 'B'

DESIGN OF THE STEAM SUPERHEATER

The superheater was designed to satisfy the following conditions:

(i) Steam required to evaporate 100cc of water per second at 100 KN/m^2 and feed was supplied at its boiling point.

(ii) Dryness of the steam was assumed to be, Φ = 97%

(iii) Degree of superheat = 2°c.

Calculations

Heat required to evaporate 100cc/s of water;

$$q = Q_f \rho (h_{fg} - h_f)$$
$$= 184KW$$

Steam required for the above duty;

$$m_s = q/h_{fg} = 0.07 \text{ Kg/s}$$
$$= 0.12 \text{ m}^3/\text{s}$$

Heat duty of the superheater

Heat required to dry the steam;

$$q_d = m_s (1 - \Phi) (h_{fg} - h_f)$$
$$= 4.67KW$$

Heat required to superheat the steam;

$$q_s = m_s C(\Delta T)$$
$$= 0.263KW$$

Total heat load of the superheater;

$$= q_d + q_s$$
$$= 4.93 \simeq 5.0KW$$

Length of the heating coil

A stainless steel tube (O.D = 21.33mm and I.D = 15.8mm) was bent into a coil and the length of the coil was determined as follows:

A step down transformer of 5KW power (5 volts and 1000 amps) was used for the power supply and the equivalent resistance for the system was 0.005 ohms.

Resistance can also be expressed as: $R = \frac{\rho L}{A}$ (1)

Where ρ is resistivity and its value for stainless steel is

1×10^{-6} ohm - m, $A = \frac{\pi}{4} (D_o^2 - D_i^2)$ and L is length, o.81m of the tube was calculated using the equation (1) for the required conditions and the length was bent into a coil of 0.2m diameter.

APPENDIX 'C'

DESIGN OF THE PICK-UP NOZZLE

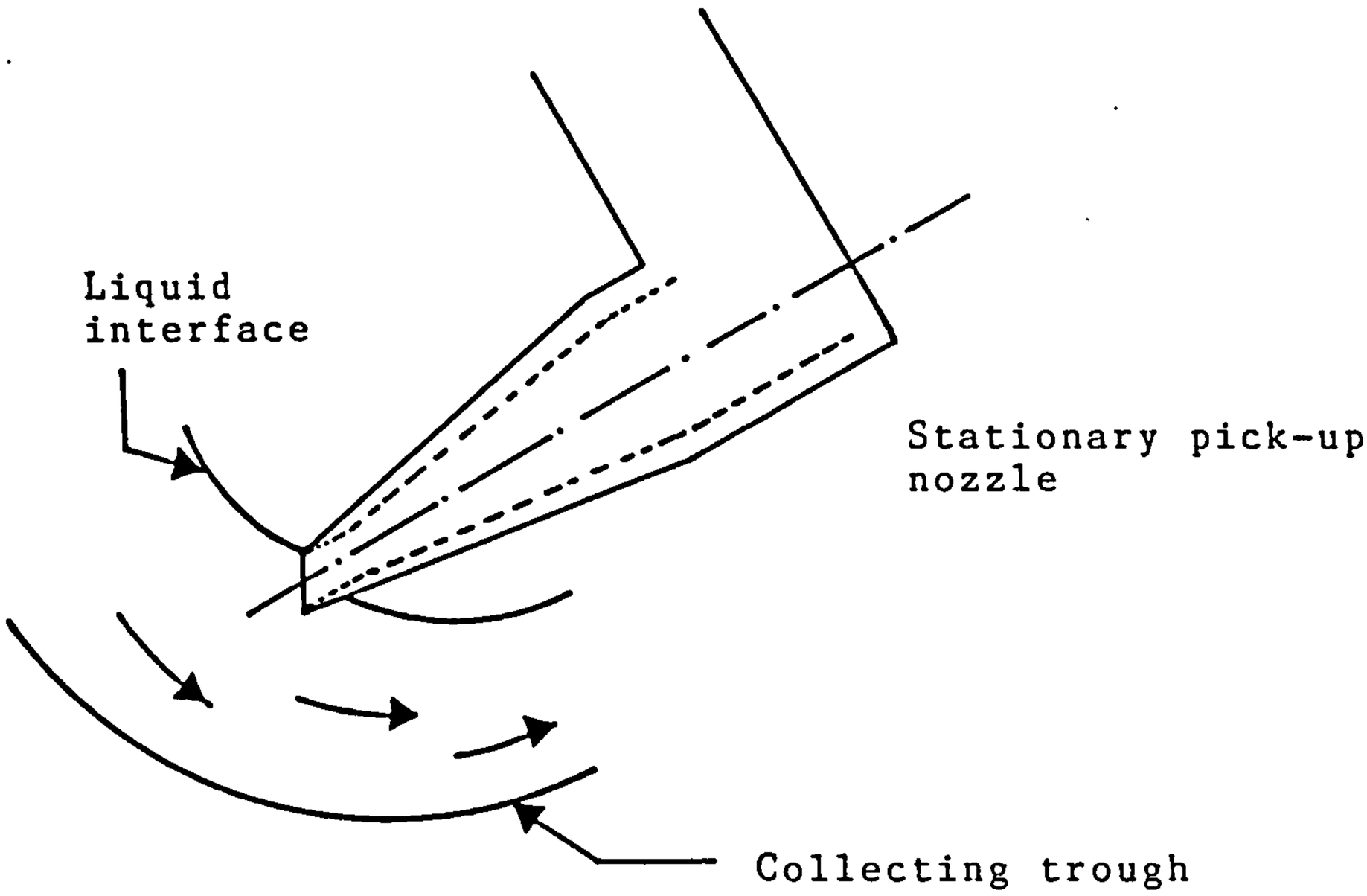

PLAN VIEW OF THE SCOOPING ARRANGEMENT

DESIGN CALCULATIONS

The pick-up nozzle, as described in the above diagram, was designed to pick 200cc of liquid per second from the trough rotating at 500 rpm

Radial position for the pick-up nozzle = 165.1mm

Angular velocity of the liquid at pick-up point due to rotation, $= r\omega = 8.64$ m/s

Liquid velocity at the inlet of the nozzle, $= \frac{\text{Liquid rate}}{\text{Flow area}}$

For an efficient performance of the nozzle, it was assumed that the liquid inlet velocity should be less than the angular velocity of the liquid in the rotating trough.

Hence, $$\frac{(200 \times 10^{-6})}{\frac{\pi}{4} D^2} < 8.64$$

$$D \geq 9.65 \simeq 10\text{mm}$$

Two pick-up nozzles, each of 5mm diameter, were decided for the efficient removal of the liquid.

APPENDIX 'D'

ESTIMATION OF LIQUID HEAD

The following correlation was derived (for the conditions shown in figure 1) to estimate the liquid head;

velocity at depth 'h' = $\sqrt{2gh}$

For a rotating system 'g' was replaced by $r\omega^2$,

hence; the velocity = $\sqrt{2hr\omega^2}$

volumetric flow rate = $2\pi r(dh)\sqrt{2hr\omega^2}$

Total flow rate = $Q = \int_0^H (2\pi r\sqrt{2hr\omega^2})dh$

Integration of the above equation and rearrangement produced the following correlation;

$$H = (3Q/2^{5/2}\pi r^{3/2}\omega)^{2/3}$$

where, 'H' - liquid head

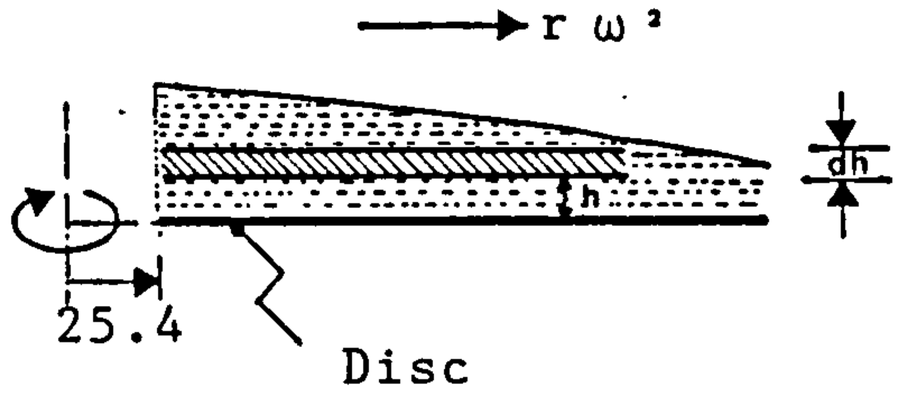

Figure 1 : Liquid film on a rotating disc

Liquid head was determined for a number of combinations of flow rates and rotary speeds at disc radius (i.e. 25.4mm), where the liquid was distributed.

The results are plotted in figure given below.

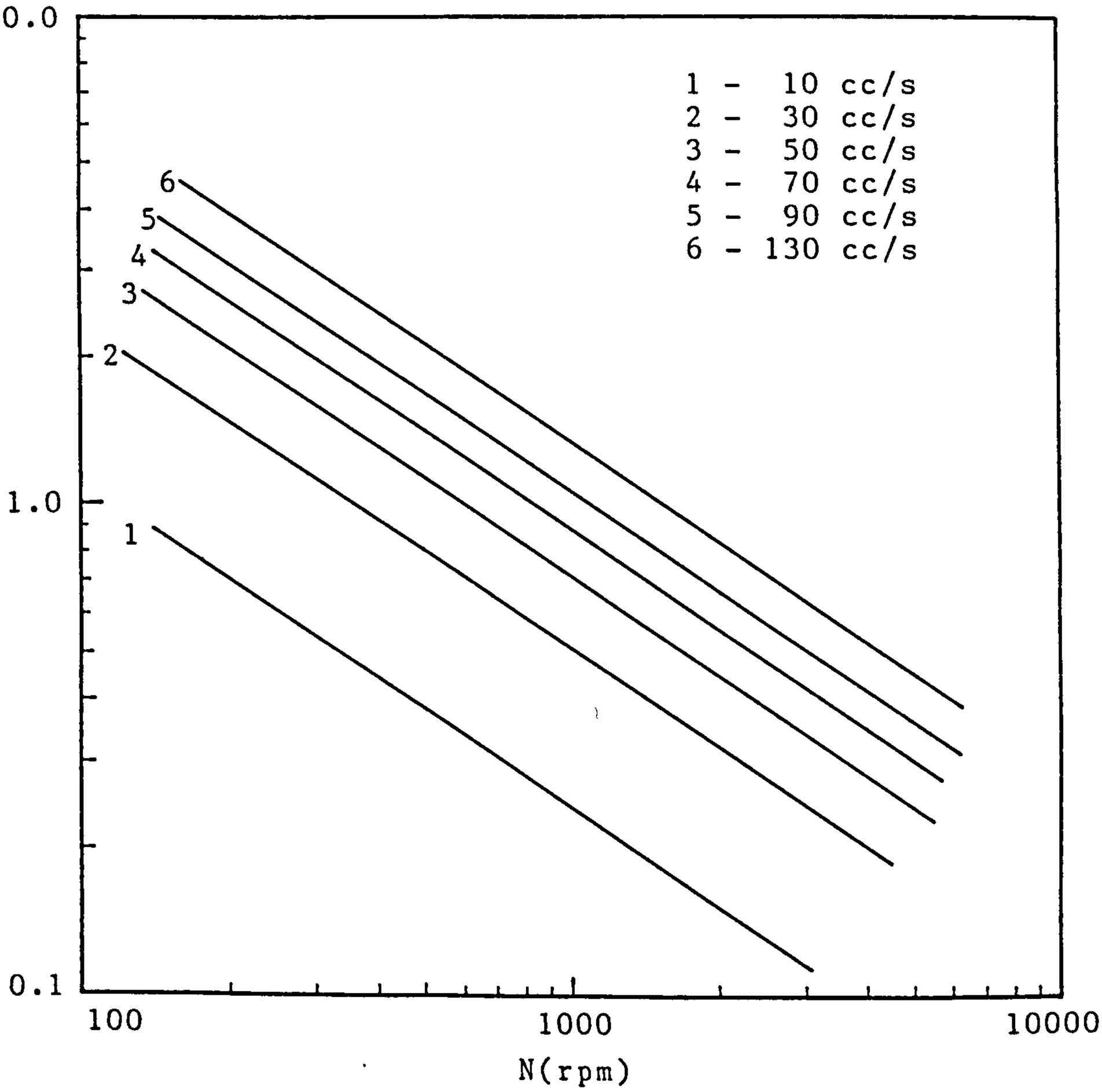

FIGURE D.1 PREDICTED VALUES OF THE LIQUID HEAD

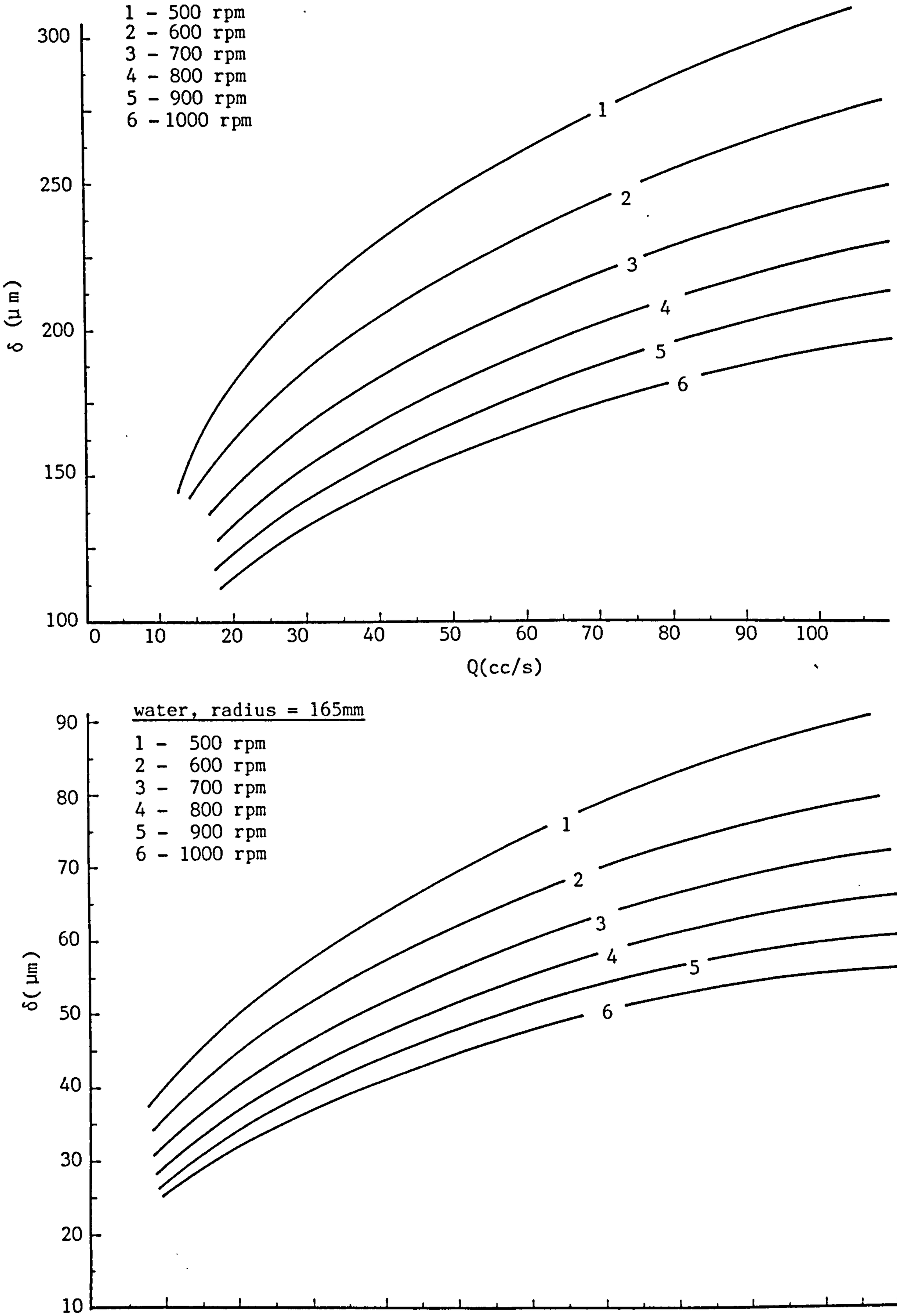

FIGURE D.2 PREDICTED VALUES OF FILM THICKNESS

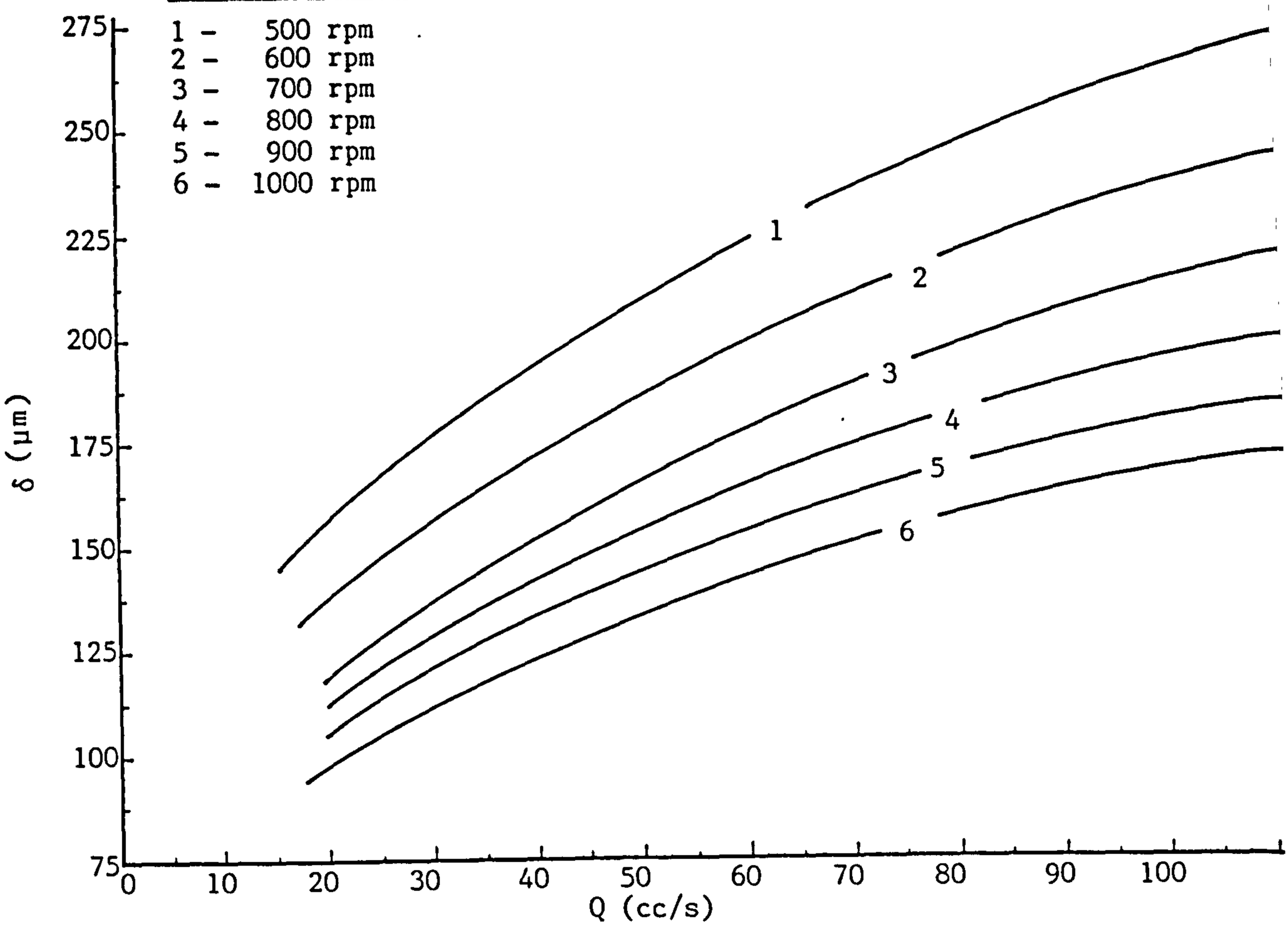

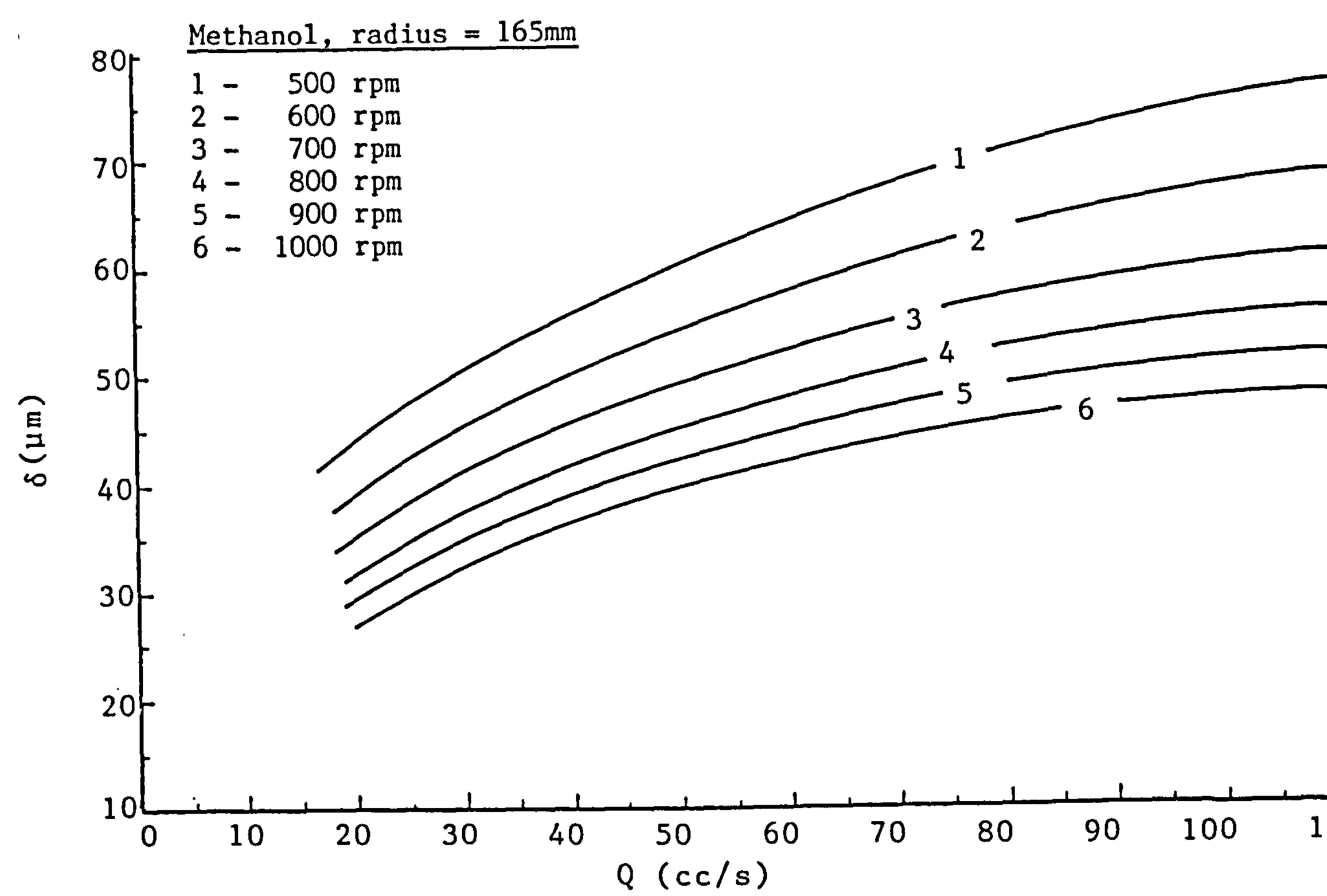

FIGURE D.3 PREDICTED VALUES OF FILM THICKNESS

APPENDIX 'E'

METHANOL

PHYSICAL PROPERTIES

The appropriate thermo-physical properties of methanol (B.P. = 64.8°c) are given below;

PROPERTY	20°c	50°c	64.8°c
Density (kg/m^3)	791.5	765.0	745.8
Viscosity (kg-m/s)	5.78×10^{-4}	3.93×10^{-3}	3.10×10^{-4}
Thermal conductivity (W/m-K)	0.204	0.193	0.185
Heat capacity (kJ/kg-k)	2.46	2.52	2.57
Surface tension (N/m)	22.6×10^{-3}	20.1×10^{-3}	18.4×10^{-3}
Heat of vaporization (kJ/kg)	1191.1	1147.2	1130.4

HAZARDOUS PROPERTIES

Methanol has no immediate warning or irritating properties for human identification except at high concentrations.

The literature on toxicology of methanol, indicates a wide variation in tolerance to methanol among human beings. It has been concluded that the exposures to 200 ppm are not considered hazardous even if the variation in individual response is kept in mind. Severe exposures may cause dizziness, unconsciousness, cardiac depression and eventually death. The first symptoms may be blurring of vision, headache and a feeling of intoxication.

The flammable limits in air are 6.72 to 36.5 per cent and an auto-ignition temperature of 385°c has been reported. Methanol could be very dangerous when exposed to heat or flames.

PREVENTIVE MEASURES

The following preventive measures were observed while methanol was used as a test fluid:

1: Reactivity towards the materials of construction, in particular for the gasket and 'O' ring material together with neoprene, were verified.

2: The feed was gradually heated by steam passing through the test section instead of electrical heating.

3: An inert media, nitrogen, was provided for blanketing in the feed tank, mixing tank, test section as well as in the condenser.

4: A bellows pump, in conjunction with a Drager tube (sensitive to methanol vapours), was used for determination of methanol concentration in the surroundings of the experimental set-up.

APPENDIX 'F'

LIQUID SIDE HEAT TRANSFER COEFFICIENT

A model, based on the laminar flow theory, was used for the estimation of heat transfer coefficient of the liquid flowing across a rotating disc.

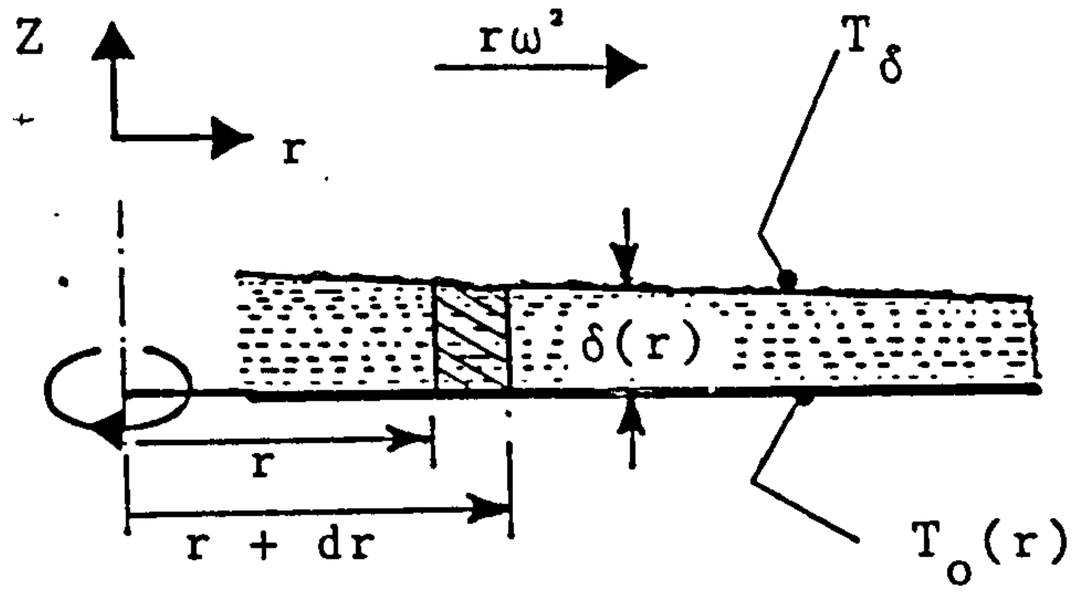

Figure 1. Heat transfer to a thin liquid film

A differential heat balance for the conditions shown in figure 1, led to the following equation;

$$\frac{\delta}{\delta r}\left[Q \quad \rho C_p(\Delta T)\right] = -2\pi\, r\, K \left(\frac{\delta T}{\delta Z}\right)\Big|_{Z=o} \qquad (1)$$

The derivation was subjected to the following conditions;

(i) Laminar flow and constant properties were assumed for the liquid. The properties were read at mean temperature which can be defined as;

$$Tm = \int_0^{\delta} uTdZ \Big/ \int_0^{\delta} udZ \qquad (2)$$

(ii) The temperature and velocity profiles were assumed to be fully developed, at all radii.

(iii) Conduction was assumed to be predominant mode of heat flow for the liquid in the vicinity of the disc.

(iv) The temperature profile within the liquid film was represented by the following cubic polynomial,

$$T = T_o + aZ + bZ^2 + cZ^3 \qquad (3)$$

Where a, b, c are the coefficients of the equation and were determined, using the following boundary conditions.

(a) $T = T_o$ and $\frac{\delta^2 T}{\delta Z^2} = 0$ at $Z = 0$

(b) $T = T_\delta$ and $\frac{\delta T}{\delta Z} = 0$ at $Z = \delta$, because the temperature in the differential element was assumed to be constant.

Differentiating equation (3) twice and applying the boundary conditions, the temperature profile in the film became,

$$[(T - To) / (T_\delta - To)] = \left(\frac{3Z}{2\delta} - \frac{1}{2}\frac{Z^3}{\delta^3}\right) \quad (4)$$

While, the velocity profile was used from the Nusselt model. It was derived for the similar conditions of flow i.e. laminar

$$\frac{u}{u_\delta} = \frac{2Z}{\delta} - Z^2/\delta^2 \quad (5)$$

Substitution of the values of T and u into equation (2) from equation (4) and (5); and then integrating, led to;

$$\left(\frac{T - To}{Tm - To}\right) = \frac{40}{61}\left(\frac{3Z}{\delta} - \frac{Z^3}{\delta^3}\right) \quad (6)$$

or $$\left(\frac{dT}{dZ}\right)\Big|_{Z=o} = \left(\frac{120}{61\delta}\right)(Tm - To) \quad (7)$$

Rate of heat transfer per unit area can be written as;

$$'q' = -K \left(\frac{dT}{dZ}\right)\Big|_{Z=o} = hr\ (Tm - To) \quad (8)$$

Where "hr" is the local value of the heat transfer coefficient at the distance 'r' from the origin.

Comparison of equation (7) and (8), led to the following simplified expression, to define local heat transfer coefficient;

$$hr = \frac{120}{61} \left(K/\delta \right) \tag{9}$$

Where, 'δ' is the thickness of the liquid film and it can be determined by the equation given in chapter 2, i.e.,

$$\delta = (3Q\ \mu/2\pi\omega^2\rho\ r^2)^{\frac{1}{3}} \tag{10}$$

Substituting the value of 'δ' into equation (9) and the average value of heat transfer coefficient for the effective heat transfer area was obtained by integrating equation (9)

$$\overline{h}_L = \frac{1}{A} \int_{Ri}^{Ro} hr\ dA$$

$$\overline{h}_L = \frac{90}{61} \left(\frac{Ro^{8/3} - Ri^{8/3}}{Ro^2 - Ri^2} \right) \left[K_L \left(\frac{2\pi\omega^2\rho}{3Q\mu} \right)^{\frac{1}{3}}_L \right] \tag{11}$$

APPENDIX 'G'

POWER CONSUMPTION

Frictional Power

The pressure drop 'Δp' over a differential element of width 'dr' and thickness 'δ' (as shown in fig. 1) was considered for the development of an expression to determine the frictional power.

Simple force balance around the annular element can be written as:

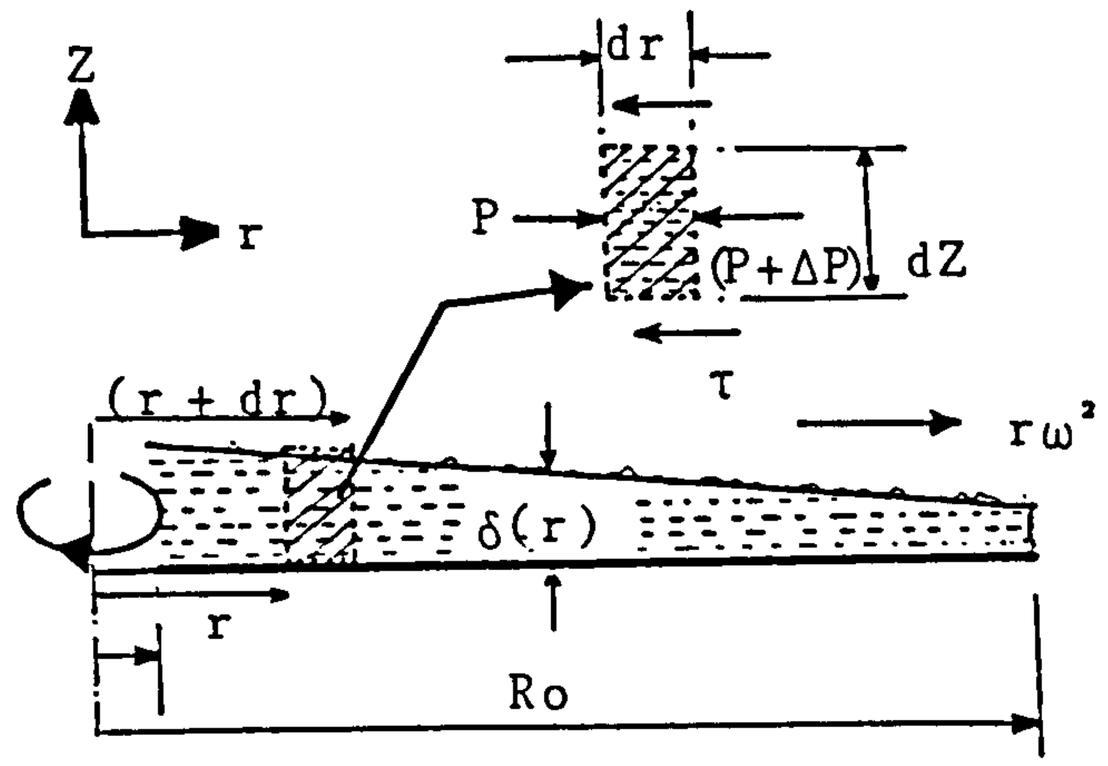

Figure 1 Fluid element at steady flow on the surface of a rotating disc.

$$2\pi\, r\, \delta(\Delta P) = 2\pi\, r dr\, \tau|_{Z=o}$$

$$\text{or} \quad \Delta P = \frac{1}{\delta} \int_{Ri}^{Ro} \tau|_{Z=o}\, dr \tag{1}$$

$$\text{where,} \quad \tau|_{Z=o} = \rho\nu \left.\frac{du_r}{dZ}\right|_{Z=o} \tag{2}$$

$$\text{and} \quad u_r = \frac{r\omega^2}{\nu} \left(\delta Z - Z^2/_2\right) \tag{3}$$

Differentiating equation (3) with respect to Z and substituting into equation (2), produced the following relationship for the shear stress;

$$\tau|_{Z=o} = \cdot : (\rho\, r\, \delta\omega^2) \tag{4}$$

Combining the equation (4) and (1), and integration led to;

$$(\Delta P) = \frac{\rho\omega^2}{2} \left(r_o^2 - r_i^2\right) \tag{5}$$

The power dissipated by the fluid due to friction, can be defined as;

$$P_f = Q_f \Delta P$$

or

$$P_f = \frac{Q_f \rho \omega^2}{2} (R_o^2 - R_i^2) \quad (6)$$

The equation (6) can be reduced into a dimensionless form by introducing the modified Reynolds, Taylor and power numbers,

$$P = \frac{1}{2} ReTa^2 \quad (7)$$

where $P = \frac{P_f \, r\rho^2}{\mu^3}$, $Re = \frac{Q}{r\nu}$ and $Ta = \frac{r^2\omega}{\nu}$

Alternate Approach

The equation (7) can also be obtained from the dimensional analysis of the variables involved, such as disc radius, density, viscosity, rotary speed and liquid rate;

$$P_f = \phi [r, \rho, \mu, \omega, Q_f] \quad (8)$$

$$\text{'or'} \quad [\frac{ML^2}{T^3}] = K [(L)^a, (\frac{M}{L^3})^b, (M/LT)^c, (\frac{1}{T})^d, (\frac{L^3}{T})^e] \quad (9)$$

Summing the respective exponents;

$$\Sigma M: \quad 1 = b + c$$

$$\Sigma L: \quad 2 = a - 3b - c + 3e$$

$$\Sigma T: \quad -3 = -c - d - e$$

Three equations with five unknowns were solved in terms of any two unknowns say d and e. Finally, the exponents were replaced by their values in equation (8) and rearrangement led to the following expression;

$$[\frac{P_f r \rho^2}{\mu^3}] = (\frac{r^2\omega}{\nu})^d (Q_f/r\nu)^e$$

or

$$p = K (Ta)^d (Re)^e \quad (10)$$

APPENDIX H

The Appendix includes;

(i) calibration curve for rotameters to measure feed rate.

(ii) calibration curve for rotameter to measure rate of cooling water.

(iii) calibration curve for tachogenerator to estimate speed of rotation.

(iv) International thermocouple reference table.

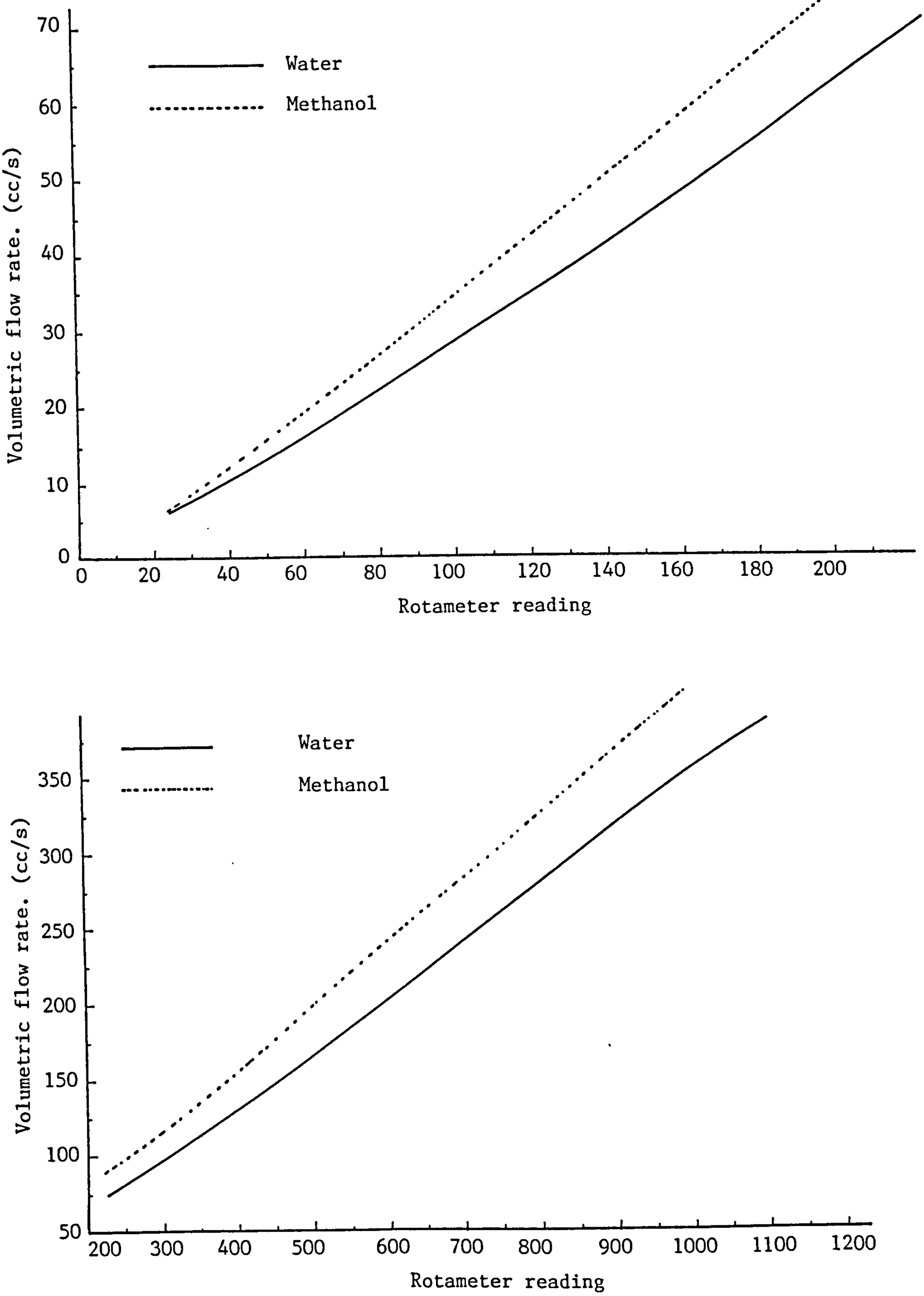

FIGURE H.1 CALIBRATION CURVE FOR ROTAMETERS

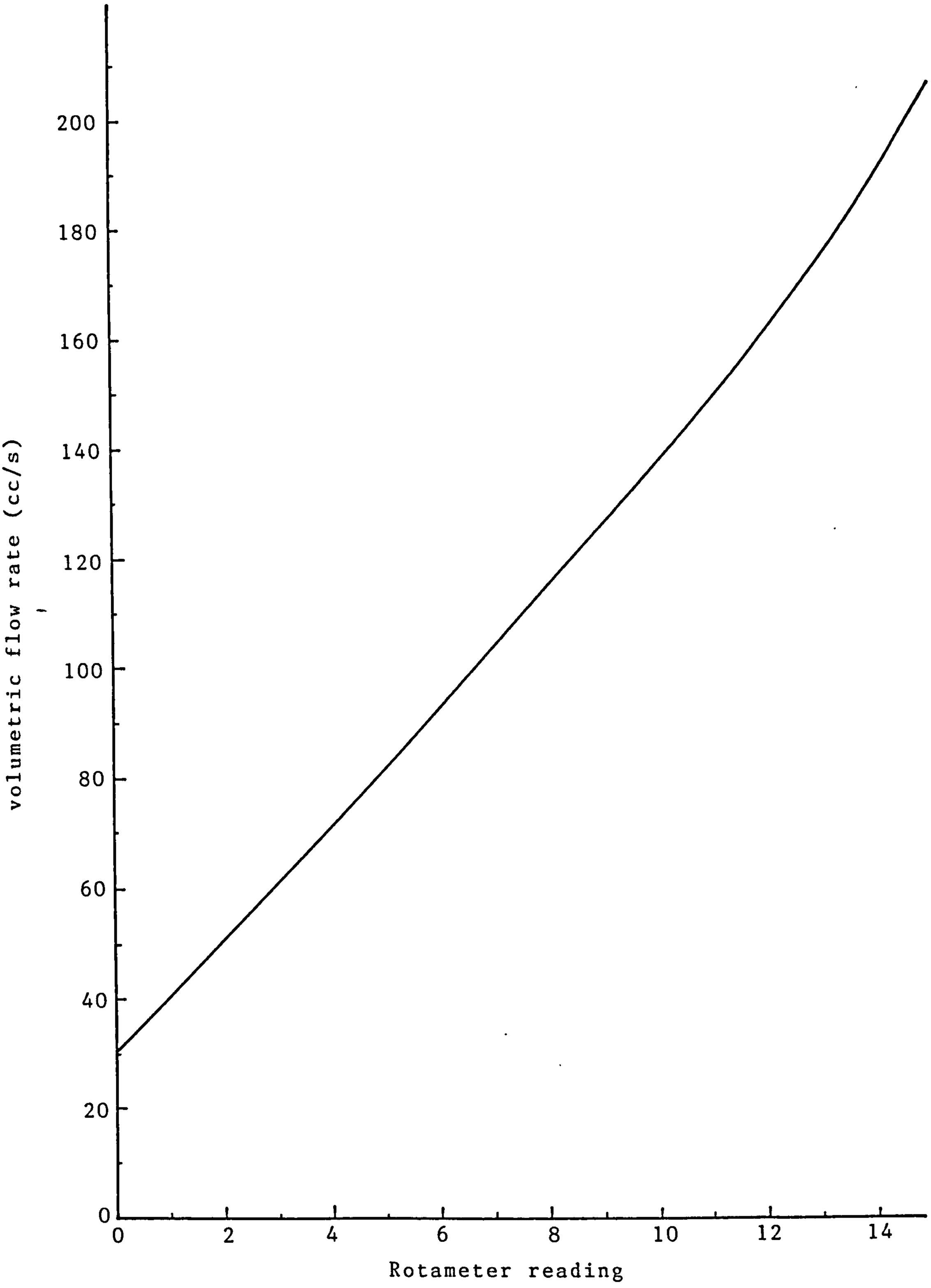

FIGURE H.2. CALIBRATION CURVE FOR ROTAMETER TO MEASURE RATE OF COOLING WATER

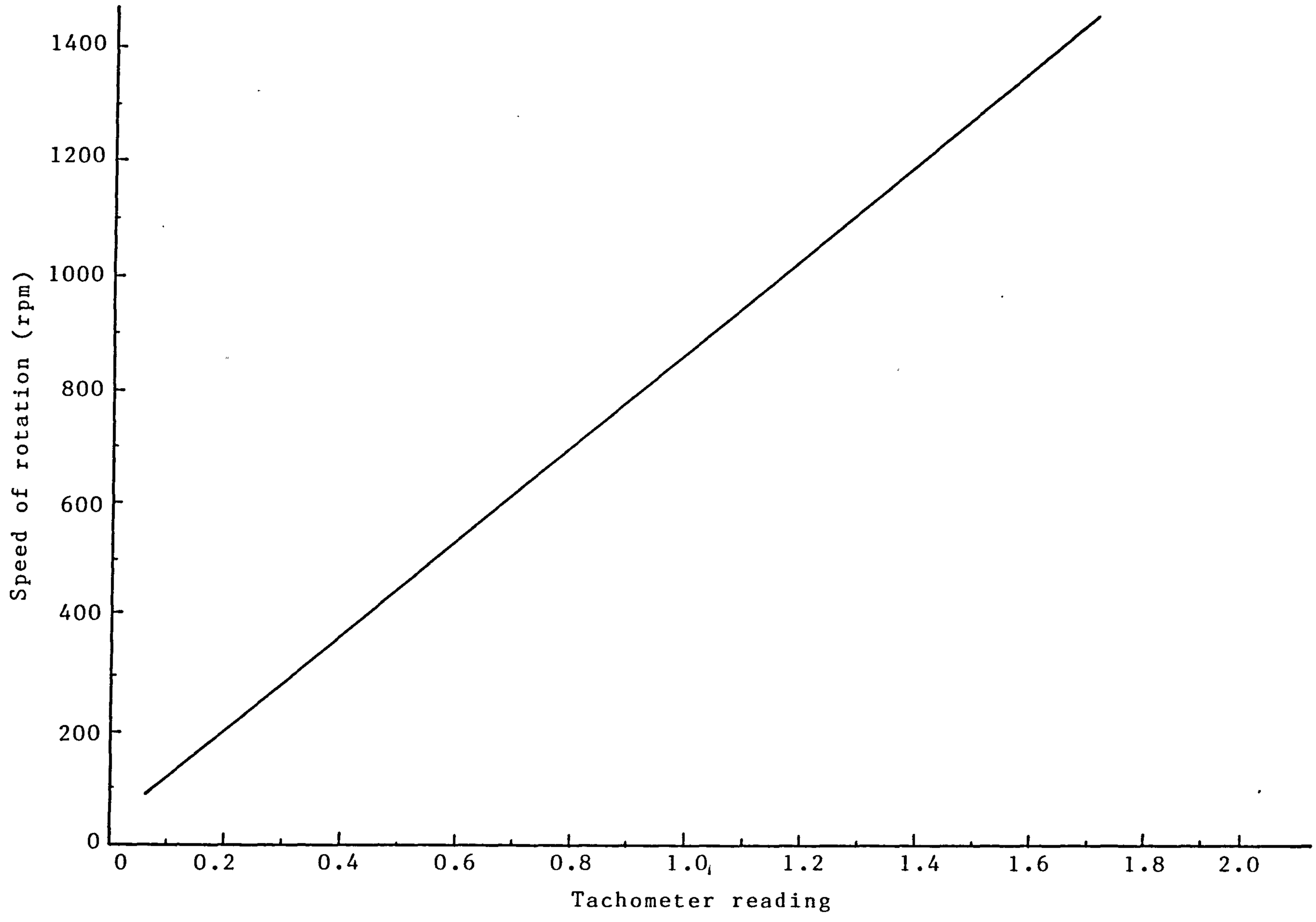

FIGURE H.3. CALIBRATION CURVE FOR TACHOGENERATOR

INTERNATIONAL THERMOCOUPLE REFERENCE TABLES FOR COPPER/CONSTANTAN

REFERENCE JUNCTION AT 0°C

°C	0	1	2	3	4	5	6	7	8	9
-270	-6258									
-260	-6232	-6236	-6239	-6242	-6245	-6248	-6251	-6253	-6255	-6256
-250	-6181	-6187	-6193	-6198	-6204	-6209	-6214	-6219	-6224	-6228
-240	-6105	-6114	-6122	-6130	-6138	-6146	-6153	-6160	-6167	-6174
-230	-6007	-6018	-6028	-6039	-6049	-6059	-6068	-6078	-6087	-6096
-220	-5889	-5901	-5914	-5926	-5938	-5950	-5962	-5973	-5985	-5996
-210	-5753	-5767	-5782	-5795	-5809	-5823	-5836	-5850	-5863	-5876
-200	-5603	-5619	-5634	-5650	-5665	-5680	-5695	-5710	-5724	-5739
-190	-5439	-5456	-5473	-5489	-5506	-5522	-5539	-5555	-5571	-5587
-180	-5261	-5279	-5297	-5315	-5333	-5351	-5369	-5387	-5404	-5421
-170	-5069	-5089	-5109	-5128	-5147	-5167	-5186	-5205	-5223	-5242
-160	-4865	-4886	-4907	-4928	-4948	-4969	-4989	-5010	-5030	-5050
-150	-4648	-4670	-4693	-4715	-4737	-4758	-4780	-4801	-4823	-4844
-140	-4419	-4442	-4466	-4489	-4512	-4535	-4558	-4581	-4603	-4626
-130	-4177	-4202	-4226	-4251	-4275	-4299	-4323	-4347	-4371	-4395
-120	-3923	-3949	-3974	-4000	-4026	-4051	-4077	-4102	-4127	-4152
-110	-3656	-3684	-3711	-3737	-3764	-3791	-3818	-3844	-3870	-3897
-100	-3378	-3407	-3435	-3463	-3491	-3519	-3547	-3574	-3602	-3629
-90	-3089	-3118	-3147	-3177	-3206	-3235	-3264	-3293	-3321	-3350
-80	-2788	-2818	-2849	-2879	-2909	-2939	-2970	-2999	-3029	-3059
-70	-2475	-2507	-2539	-2570	-2602	-2633	-2664	-2695	-2726	-2757
-60	-2152	-2185	-2218	-2250	-2283	-2315	-2348	-2380	-2412	-2444
-50	-1819	-1853	-1886	-1920	-1953	-1987	-2020	-2053	-2087	-2120
-40	-1475	-1510	-1544	-1579	-1614	-1648	-1682	-1717	-1751	-1785
-30	-1121	-1157	-1192	-1228	-1263	-1299	-1334	-1370	-1405	-1440
-20	-757	-794	-830	-867	-903	-940	-976	-1013	-1049	-1085
-10	-383	-421	-458	-496	-534	-571	-608	-646	-683	-720
0	0	-39	-77	-116	-154	-193	-231	-269	-307	-345
0	0	39	78	117	156	195	234	273	312	351
10	391	430	470	510	549	589	629	669	709	749
20	789	830	870	911	951	992	1032	1073	1114	1155
30	1196	1237	1279	1320	1361	1403	1444	1486	1528	1569
40	1611	1653	1695	1738	1780	1822	1865	1907	1950	1992

Absolute thermocouple e.m.f. in microvolts

°C	0	1	2	3	4	5	6	7	8	9
50	2035	2078	2121	2164	2207	2250	2294	2337	2380	2424
60	2467	2511	2555	2599	2643	2687	2731	2775	2819	2864
70	2908	2953	2997	3042	3087	3131	3176	3221	3266	3312
80	3357	3402	3447	3493	3538	3584	3630	3676	3721	3767
90	3813	3859	3906	3952	3998	4044	4091	4137	4184	4231
100	4277	4324	4371	4418	4465	4512	4559	4607	4654	4701
110	4749	4796	4844	4891	4939	4987	5035	5083	5131	5179
120	5227	5275	5324	5372	5420	5469	5517	5566	5615	5663
130	5712	5761	5810	5859	5908	5957	6007	6056	6105	6155
140	6204	6254	6303	6353	6403	6452	6502	6552	6602	6652
150	6702	6753	6803	6853	6903	6954	7004	7055	7106	7156
160	7207	7258	7309	7360	7411	7462	7513	7564	7615	7666
170	7718	7769	7821	7872	7924	7975	8027	8079	8131	8183
180	8235	8287	8339	8391	8443	8495	8548	8600	8652	8705
190	8757	8810	8863	8915	8968	9021	9074	9127	9180	9233
200	9286	9339	9392	9446	9499	9553	9606	9659	9713	9767
210	9820	9874	9928	9982	10036	10090	10144	10198	10252	10306
220	10360	10414	10469	10523	10578	10632	10687	10741	10796	10851
230	10905	10960	11015	11070	11125	11180	11235	11290	11345	11401
240	11456	11511	11566	11622	11677	11733	11788	11844	11900	11956
250	12011	12067	12123	12179	12235	12291	12347	12403	12459	12515
260	12572	12628	12684	12741	12797	12854	12910	12967	13024	13080
270	13137	13194	13251	13307	13364	13421	13478	13535	13592	13650
280	13707	13764	13821	13879	13936	13993	14051	14108	14166	14223
290	14281	14339	14396	14454	14512	14570	14628	14686	14744	14802
300	14860	14918	14976	15034	15092	15151	15209	15267	15326	15384
310	15443	15501	15560	15619	15677	15736	15795	15853	15912	15971
320	16030	16089	16148	16207	16266	16325	16384	16444	16503	16562
330	16621	16681	16740	16800	16859	16919	16978	17038	17097	17157
340	17217	17277	17336	17396	17456	17516	17576	17636	17696	17756
350	17816	17877	17937	17997	18057	18118	18178	18238	18299	18359
360	18420	18480	18541	18602	18662	18723	18784	18845	18905	18966
370	19027	19088	19149	19210	19271	19332	19393	19455	19516	19577
380	19638	19699	19761	19822	19883	19945	20006	20068	20129	20191
390	20252	20314	20376	20437	20499	20560	20622	20684	20746	20807
400	20869									

Absolute thermocouple e.m.f. in microvolts

TABLES

TABLE 1 SENSIBLE HEAT TRANSFER DATA

(DIST.WATER:WITH-OUT PURGING)

SPEED OF ROTATION = 600 rpm

QF	TFi	TFo	Ts	Tc	QC	qf	qc
10.00	24.80	63.10	102.20	98.80	0.53	1.59	1.36
20.00	24.80	69.30	103.00	98.60	1.46	3.70	3.75
30.00	24.80	72.50	103.20	99.20	2.94	5.95	7.57
40.00	24.80	74.40	103.40	99.30	3.26	8.25	8.37
50.00	24.80	75.60	103.20	99.50	3.61	10.56	9.28
60.00	24.80	75.10	103.20	99.50	4.38	12.55	11.26
70.00	24.80	74.20	104.00	99.70	4.88	14.38	12.55

SPEED OF ROTATION = 800.00 rpm

QF	TFi	TFo	Ts	Tc	QC	qf	qc
10.00	32.20	66.50	102.80	98.70	0.53	1.43	1.36
20.00	32.20	70.80	103.10	99.60	1.71	3.21	4.39
30.00	32.20	75.30	103.20	99.60	1.96	5.38	5.03
40.00	32.20	78.20	103.40	98.70	3.11	7.65	8.00
50.00	32.20	79.90	103.70	99.80	3.48	9.92	8.96
60.00	33.00	77.60	103.20	98.60	4.05	11.13	10.41
70.00	33.00	76.10	103.50	99.40	4.34	12.55	11.16

SPEED OF ROTATION = 1000 rpm

QF	TFi	TFo	Ts	Tc	QC	qf	qc
10.00	41.30	68.20	104.00	98.50	0.45	1.12	1.15
20.00	41.70	80.20	103.40	99.50	1.32	3.20	3.40
30.00	41.70	81.60	103.60	98.70	1.60	4.98	4.12
40.00	41.80	82.60	103.50	99.80	4.04	6.79	10.38
50.00	41.80	83.60	103.70	99.60	4.17	8.69	10.73
60.00	42.00	82.10	103.50	99.70	4.17	10.01	10.73
70.00	42.00	81.50	103.50	99.70	4.27	11.50	11.00
80.00	42.00	80.10	103.40	98.90	4.35	12.68	11.18
90.00	42.00	79.10	103.20	98.80	4.60	13.89	11.82

SPEED OF ROTATION = 1200 rpm

QF	TFi	TFo	Ts	Tc	QC	qf	qc
10.00	48.00	74.30	103.10	99.30	0.41	1.09	1.04
30.00	48.00	83.50	103.10	99.40	1.60	4.43	4.12
50.00	48.00	88.30	103.20	99.50	2.94	8.38	7.57
70.00	48.00	86.70	103.20	99.30	4.23	11.27	10.89
90.00	48.00	84.80	103.30	99.70	4.69	13.77	12.07
110.00	48.00	82.50	103.00	98.30	5.15	15.78	13.24
130.00	48.00	77.60	102.80	98.90	5.39	16.00	13.86

TABLE 2 SENSIBLE HEAT TRANSFER DATA

(DIST.WATER:WITH PURGING)

SPEED OF ROTATION = 600 rpm

QF	TFi	TFo	Ts	Tc	QC	qf	qc
10.00	20.00	77.50	102.80	97.80	0.87	2.39	2.25
20.00	20.00	81.50	103.50	99.20	1.83	5.12	4.71
30.00	20.00	84.80	103.60	99.50	2.88	8.09	7.41
40.00	20.00	86.70	103.10	98.70	4.17	11.10	10.73
50.00	20.00	88.40	102.80	97.80	5.31	14.22	13.67
60.00	20.00	87.10	103.10	98.90	6.91	16.74	17.76
70.00	20.00	86.30	102.50	99.10	7.39	19.30	19.02

SPEED OF ROTATION = 800.00 rpm

QF	TFi	TFo	Ts	Tc	QC	qf	qc
10.00	25.80	83.70	103.90	99.70	0.97	2.41	2.38
20.00	25.80	86.10	103.50	99.20	2.07	5.02	5.32
30.00	25.80	88.20	103.20	97.90	3.00	7.79	7.70
40.00	25.80	88.70	103.20	99.60	3.60	10.46	9.26
50.00	25.80	89.30	103.20	99.30	5.09	13.21	13.08
60.00	26.00	88.10	103.30	99.20	6.10	15.50	15.70
70.00	26.00	87.20	103.10	99.70	6.85	17.82	17.63

SPEED OF ROTATION = 1000 rpm

QF	TFi	TFo	Ts	Tc	QC	qf	qc
10.00	32.70	83.10	103.00	96.40	0.93	2.10	2.38
20.00	32.70	89.70	103.20	99.10	2.00	4.74	5.14
30.00	32.70	91.30	103.20	99.90	2.80	7.31	7.20
40.00	32.70	91.40	103.20	99.10	3.34	9.77	8.59
50.00	33.00	90.60	103.20	97.80	4.82	11.98	12.39
60.00	33.00	88.90	103.60	99.30	5.18	13.95	13.32
70.00	33.00	88.50	102.90	98.70	6.12	16.16	15.73
80.00	33.00	87.20	102.80	99.30	7.09	18.03	18.24
90.00	33.00	86.20	102.80	98.70	7.81	19.91	20.09

SPEED OF ROTATION = 1200 rpm

QF	TFi	TFo	Ts	Tc	QC	qf	qc
10.00	39.50	86.10	103.70	99.20	0.73	1.94	1.87
30.00	39.70	93.80	103.20	98.60	2.65	6.75	6.82
50.00	40.00	94.80	103.60	98.60	4.34	11.40	11.16
70.00	40.00	93.50	103.00	99.10	6.74	15.58	17.34
90.00	40.00	93.10	102.90	99.20	6.87	19.88	17.68
110.00	40.00	91.70	103.00	99.20	8.28	23.65	21.29
130.00	40.00	88.70	103.60	97.90	9.00	26.33	23.14

TABLE 3 SENSIBLE HEAT TRANSFER DATA

(DIST.WATER+SURFACTANT;WITH-OUT PURGING)

SPEED OF ROTATION = 600 rpm

QF	TFi	TFo	Ts	Tc	QC	qf	qc
10.00	19.50	75.80	102.80	98.80	0.90	2.34	2.33
20.00	19.50	77.70	102.90	98.60	1.91	4.84	4.92
30.00	19.50	80.40	103.10	98.90	2.63	7.60	6.77
40.00	19.50	80.30	103.10	99.10	3.91	10.11	10.06
50.00	19.50	80.10	103.20	99.10	4.72	12.60	12.15
60.00	19.50	79.10	102.90	99.20	5.31	14.87	13.67
70.00	19.50	78.30	102.70	98.80	6.26	17.12	16.10

SPEED OF ROTATION = 800 rpm

QF	TFi	TFo	Ts	Tc	QC	qf	qc
10.00	28.00	77.60	103.20	98.70	0.84	2.06	2.17
20.00	28.00	81.30	103.00	98.80	1.88	4.43	4.84
30.00	28.00	83.20	103.10	99.60	2.61	6.89	6.71
40.00	28.00	83.80	103.10	99.30	3.61	9.28	9.28
50.00	28.00	84.70	102.90	98.80	4.36	11.79	11.21
60.00	28.00	82.40	103.10	99.20	5.06	13.58	13.03
70.00	28.00	81.20	103.00	98.40	5.44	15.49	13.99

SPEED OF ROTATION = 1000 rpm

QF	TFi	TFo	Ts	Tc	QC	qf	qc
10.00	34.40	78.50	102.60	98.80	0.81	1.83	2.09
20.00	34.40	81.20	103.10	99.30	1.90	3.89	4.90
30.00	34.40	84.50	103.20	99.40	2.36	6.25	6.07
40.00	34.40	85.10	103.10	98.70	2.84	8.43	7.30
50.00	34.40	85.80	103.00	98.70	3.88	10.69	9.98
60.00	34.40	84.90	103.20	98.80	4.59	12.60	11.80
70.00	34.40	84.10	103.20	99.70	5.31	14.47	13.67
80.00	34.50	82.90	103.20	98.80	6.01	16.10	15.46
90.00	34.50	81.90	102.90	98.60	6.39	17.74	16.43

SPEED OF ROTATION = 1200 rpm

QF	TFi	TFo	Ts	Tc	QC	qf	qc
10.00	46.70	79.30	103.10	98.80	0.45	1.36	1.15
30.00	46.70	85.70	103.20	98.80	1.71	4.87	4.39
50.00	46.70	87.40	103.20	99.40	3.05	8.46	7.84
70.00	47.00	85.70	103.70	99.60	4.11	11.27	10.57
90.00	47.00	82.30	103.50	99.50	5.04	13.21	12.97
110.00	47.00	80.10	103.20	97.30	5.81	15.14	14.95
130.00	47.00	78.50	102.80	98.90	6.32	17.03	16.27

TABLE 4 SENSIBLE HEAT TRANSFER DATA

(DIST.WATER+SURFACTANT:WITH PURGING)

SPEED OF ROTATION = 600 rpm

QF	TFi	TFo	Ts	Tc	QC	qf	qc
10.00	20.00	88.50	102.80	97.80	1.03	2.85	2.65
20.00	20.00	91.40	102.90	98.70	2.17	5.94	5.59
30.00	20.00	93.50	103.50	99.30	3.53	9.17	9.07
40.00	20.00	93.80	103.10	99.30	4.92	12.28	12.65
50.00	20.00	94.70	103.20	99.70	5.96	15.53	15.33
60.00	20.00	92.90	102.90	99.00	6.80	18.19	17.50
70.00	20.00	91.30	103.20	99.80	7.99	20.76	20.55

SPEED OF ROTATION = 800.00 rpm

QF	TFi	TFo	Ts	Tc	QC	qf	qc
10.00	29.60	91.50	103.20	98.70	0.97	2.57	2.49
20.00	29.60	93.80	103.10	99.30	1.94	5.34	5.00
30.00	29.60	95.30	103.20	99.60	3.08	8.20	7.92
40.00	30.00	95.80	103.20	99.60	3.56	10.95	9.15
50.00	30.00	96.40	103.10	99.70	5.19	13.81	13.35
60.00	30.00	94.60	103.50	99.70	5.76	16.12	14.82
70.00	30.00	93.50	102.90	99.80	6.95	18.49	17.87

SPEED OF ROTATION = 1000 rpm

QF	TFi	TFo	Ts	Tc	QC	qf	qc
10.00	38.40	93.60	103.00	99.60	0.86	2.30	2.22
20.00	38.40	94.50	103.50	99.50	1.83	4.67	4.71
30.00	38.40	96.40	103.20	99.70	2.78	7.24	7.14
40.00	38.50	96.10	102.90	99.50	3.34	9.58	8.59
50.00	38.50	95.50	102.80	99.70	4.45	11.85	11.45
60.00	39.00	94.30	102.90	99.30	5.06	13.80	13.03
70.00	39.00	93.50	103.00	98.70	6.02	15.87	15.49
80.00	39.00	92.50	102.80	98.80	6.69	17.80	17.20
90.00	39.00	91.10	103.00	98.90	7.54	19.50	19.40

SPEED OF ROTATION = 1200 rpm

QF	TFi	TFo	Ts	Tc	QC	qf	qc
10.00	46.20	95.60	103.60	99.70	0.77	2.05	1.98
30.00	46.20	97.30	103.70	100.10	2.30	6.38	5.91
50.00	46.20	96.10	103.30	99.90	3.99	10.38	10.27
70.00	46.50	92.50	103.10	99.70	5.15	13.39	13.24
90.00	46.50	89.90	103.30	98.90	6.16	16.25	15.84
110.00	46.50	87.20	102.90	98.90	7.04	18.62	18.11
130.00	46.50	84.30	102.80	99.70	7.66	20.44	19.72

TABLE 5 SENSIBLE HEAT TRANSFER DATA

(DIST.WATER+SURFACTANT:WITH PURGING)

FEED RATE = 10 cc/s

N	TFi	TFo	Ts	Tc	QC	qf	qc
600.00	20.00	83.70	103.30	99.70	0.98	2.65	2.51
800.00	20.00	87.20	103.50	99.90	1.14	2.79	2.94
1000.00	20.00	88.50	103.10	99.30	1.15	2.85	2.97
1200.00	20.00	88.80	103.20	99.60	1.25	2.86	3.21

FEED RATE = 30.00 cc/s

N	TFi	TFo	Ts	Tc	QC	qf	qc
600.00	30.00	88.20	103.00	98.80	2.29	7.26	5.89
800.00	30.00	91.00	103.20	98.70	3.00	7.61	7.70
1000.00	30.00	89.90	103.00	99.60	2.86	7.47	7.36
1200.00	30.00	88.40	102.90	98.80	3.01	7.29	7.73

FEED RATE = 50.00 cc/s

N	TFi	TFo	Ts	Tc	QC	qf	qc
600.00	37.50	89.40	103.00	98.70	4.27	10.79	11.00
800.00	37.50	90.40	103.40	98.90	4.34	11.00	11.16
1000.00	37.50	91.20	102.80	98.60	4.38	11.17	11.26
1200.00	37.50	91.80	103.00	98.90	4.42	11.29	11.37

FEED RATE = 70.00 cc/s

N	TFi	TFo	Ts	Tc	QC	qf	qc
600.00	43.70	91.50	103.60	99.70	5.52	13.92	14.21
800.00	43.70	92.70	103.00	99.70	5.64	14.27	14.50
1000.00	43.70	93.80	103.60	100.10	5.71	14.59	14.69
1200.00	43.70	95.10	102.80	99.80	5.74	14.96	14.77

TABLE 6 SENSIBLE HEAT TRANSFER DATA

(DIST.WATER:WITH PURGING)

FEED RATE = 10 cc/s

N	TFi	TFo	Ts	Tc	QC	qf	qc
600.00	20.00	78.20	103.20	99.80	0.93	2.42	2.38
800.00	20.00	81.30	103.10	99.30	0.95	2.55	2.43
1000.00	20.00	84.10	102.90	98.00	1.02	2.67	2.62
1200.00	20.00	85.60	102.80	98.60	1.25	2.73	3.21

FEED RATE = 30.00 cc/s

N	TFi	TFo	Ts	Tc	QC	qf	qc
600.00	38.20	88.10	103.50	99.30	2.19	6.23	5.64
800.00	38.20	92.50	103.50	99.20	2.59	6.78	6.66
1000.00	38.20	93.40	103.20	98.90	2.97	6.89	7.65
1200.00	38.20	94.50	103.20	98.90	3.03	7.02	7.78

FEED RATE = 50.00 cc/s

N	TFi	TFo	Ts	Tc	QC	qf	qc
600.00	43.80	90.20	103.30	99.80	3.73	9.65	9.60
800.00	43.80	93.40	103.20	98.70	3.99	10.31	10.27
1000.00	43.80	95.20	103.50	98.70	4.07	10.69	10.46
1200.00	43.80	96.00	103.30	99.80	4.13	10.86	10.62

FEED RATE = 70.00 cc/s

N	TFi	TFo	Ts	Tc	QC	qf	qc
600.00	27.80	88.90	103.00	98.70	6.56	17.79	16.88
800.00	27.80	95.40	103.20	99.90	7.37	19.68	18.97
1000.00	27.80	96.40	103.50	100.00	7.47	19.97	19.21
1200.00	27.80	96.70	103.20	99.50	7.73	20.06	19.88

TABLE 7 HEAT TRANSFER,WITH PHASE CHANGE

(METHANOL:WITH PURGING)

SPEED OF ROTATION = 600 rpm

QF	TFi	TFo	Ts	Tc	Tv	Tvc	Twi	Two	Qw	Qv	Qc	qf	qc
10.0	21.0	63.0	103.5	100.2	52.0	48.0	18.0	24.3	127.0	3.8	2.0	4.2	5.2
20.0	21.0	63.0	103.5	99.9	53.5	49.0	18.0	27.5	127.8	5.8	2.1	6.7	5.3
30.0	21.0	62.5	103.5	99.9	58.2	52.0	18.0	29.5	147.8	8.1	3.6	9.5	9.1
40.0	21.0	61.0	103.0	100.1	58.7	53.5	17.0	30.2	148.0	9.3	4.2	11.3	10.9
50.0	21.0	60.8	103.5	100.1	59.0	56.8	17.0	31.6	148.0	10.3	5.5	12.9	14.2
60.0	21.0	60.8	103.3	99.8	58.8	57.2	16.0	30.7	148.0	10.3	7.0	13.7	18.0
70.0	21.0	60.7	103.5	100.2	58.5	56.6	16.0	30.1	150.0	10.1	6.6	14.2	17.0

SPEED OF ROTATION = 800.0 rpm

QF	TFi	TFo	Ts	Tc	Tv	Tvc	Twi	Two	Qw	Qv	Qc	qf	qc
10.0	26.2	64.0	103.8	101.0	61.2	60.2	14.5	26.8	130.0	7.6	2.9	7.4	7.4
20.0	27.0	63.8	103.1	100.1	62.7	60.8	14.5	40.2	125.0	15.3	5.4	14.9	13.9
30.0	27.0	64.0	102.8	99.8	63.5	61.6	14.0	43.1	150.0	20.8	8.0	20.4	20.7
40.0	27.0	64.3	103.0	99.6	64.0	63.2	14.0	43.8	150.0	21.3	7.6	21.6	19.6
50.0	27.3	64.1	102.8	99.5	63.8	58.9	14.0	38.9	160.0	18.9	7.1	20.2	18.4
60.0	28.0	63.8	103.1	99.7	63.5	59.9	14.0	33.2	168.0	15.3	7.3	17.7	18.7
70.0	28.0	62.8	102.6	98.8	63.5	60.8	14.0	35.2	170.0	17.1	7.0	19.8	18.1

SPEED OF ROTATION = 1000 rpm

QF	TFi	TFo	Ts	Tc	Tv	Tvc	Twi	Two	Qw	Qv	Qc	qf	qc
10.0	40.0	64.0	103.2	99.6	64.1	63.0	14.0	28.8	135.0	9.5	4.0	8.8	10.4
20.0	40.0	64.2	102.9	99.7	63.8	62.7	13.0	38.2	140.0	16.8	6.5	15.7	16.8
30.0	40.0	64.4	103.8	100.2	63.9	63.0	13.0	39.8	150.0	19.1	9.0	18.2	23.0
40.0	40.5	64.2	103.3	100.1	64.0	64.0	12.0	39.4	160.0	20.8	9.3	20.2	24.0
50.0	40.5	64.4	103.6	100.0	64.4	64.1	12.0	37.6	170.0	20.7	9.6	20.5	24.6
60.0	40.5	63.8	102.9	99.7	64.7	64.2	12.0	35.7	176.0	19.8	7.6	20.2	19.6
70.0	41.0	62.8	102.2	97.6	64.6	64.0	11.0	33.6	173.0	18.6	8.0	19.3	20.5
80.0	41.0	61.9	102.8	98.7	64.5	63.9	33.6	55.2	170.0	17.5	6.5	18.6	16.6
90.0	41.0	61.2	103.0	99.7	63.9	63.8	11.0	35.2	170.0	19.6	8.1	20.7	20.9

SPEED OF ROTATION = 1200 rpm

QF	TFi	TFo	Ts	Tc	Tv	Tvc	Twi	Two	Qw	Qv	Qc	qf	qc
10.0	45.0	64.0	103.5	99.5	64.5	60.8	11.0	29.2	150.0	9.2	4.4	11.8	11.3
30.0	45.0	64.5	103.2	100.2	64.3	62.1	11.0	37.8	175.0	21.1	8.9	20.8	22.9
50.0	45.2	64.2	103.2	100.0	64.4	60.3	11.0	35.9	175.0	20.7	8.7	20.1	22.3
70.0	45.7	62.2	102.5	99.3	64.1	61.5	11.0	36.7	170.0	20.8	7.3	20.5	18.8
90.0	47.0	62.7	102.8	98.7	63.9	62.6	11.0	39.2	170.0	22.8	8.3	22.8	21.4
110.0	47.0	62.4	102.6	98.7	63.8	62.2	11.0	38.6	170.0	22.3	8.4	22.9	21.7
130.0	47.0	61.9	102.5	98.6	63.8	63.0	11.0	38.3	170.0	22.1	9.3	23.2	23.9

TABLE 7 HEAT TRANSFER WITH PHASE CHANGE

(METHANOL; WITH PURGING)

SPEED OF ROTATION = 600 rpm

QF	TFi	TFo	Ts	Tc	Tv	Tvc	Twi	Two	Qw	Qv	Qc	qf	qc
10.0	55.7	64.0	103.0	100.3	64.5	61.1	11.0	28.6	135.0	8.6	5.4	10.1	13.9
30.0	56.0	64.5	103.2	100.2	64.4	63.2	11.0	39.2	140.0	18.8	7.5	17.0	19.3
50.0	56.0	64.1	103.1	100.1	64.5	63.2	11.0	39.9	145.0	19.9	8.2	18.3	21.1
70.0	56.2	64.2	103.2	99.7	64.2	62.5	11.0	41.0	145.0	20.7	8.5	19.3	22.0

SPEED OF ROTATION = 800 rpm

QF	TFi	TFo	Ts	Tc	Tv	Tvc	Twi	Two	Qw	Qv	Qc	qf	qc
10.0	57.0	64.0	102.3	99.7	64.2	61.4	11.0	28.7	140.0	9.8	5.1	10.5	13.0
30.0	57.0	64.3	102.8	99.7	64.3	62.8	11.0	40.3	150.0	20.9	8.3	18.8	21.3
50.0	58.0	64.5	103.8	100.4	64.7	61.4	11.0	41.5	160.0	23.2	8.6	21.0	22.2
70.0	58.0	64.5	103.2	99.7	64.2	63.2	11.0	42.8	170.0	25.7	9.3	23.5	24.0

SPEED OF ROTATION = 1000 rpm

QF	TFi	TFo	Ts	Tc	Tv	Tvc	Twi	Two	Qw	Qv	Qc	qf	qc
10.0	60.2	64.5	103.0	100.2	64.5	62.1	11.0	27.2	135.0	9.8	4.9	9.2	12.7
30.0	60.2	64.4	103.2	100.2	64.5	62.5	11.0	40.1	168.0	23.2	9.8	20.7	25.1
50.0	60.6	64.5	103.2	100.0	64.5	62.3	11.0	41.3	175.0	24.2	10.4	21.7	26.7
70.0	60.5	64.5	103.5	100.3	64.5	63.0	11.0	42.2	180.0	26.7	10.8	24.0	27.8
90.0	60.4	64.5	103.3	100.0	64.2	60.2	11.0	44.5	180.0	28.7	11.3	25.9	29.2

TABLE 8 SENSIBLE HEAT TRANSFER — PREDICTED VALUES

INNER RADIUS = 40 mm
OUTER RADIUS = 50 mm
SPEED OF ROTATION = 1200 rpm

QF	Qc	q	TFi	TFo	(To)ass.	(To)cal.	hf	hc	$(\delta)F$	$(\delta)c$
10.00	0.75	2.00	39.50	89.20	86.79	87.10	14.97	44.54	49.98	15.23
30.00	0.57	1.52	39.70	60.09	91.53	91.97	10.39	48.80	72.06	13.90
50.00	0.50	1.33	40.00	50.72	93.86	93.74	8.76	50.98	85.42	13.30
70.00	0.46	1.22	40.00	47.01	95.15	94.77	7.83	52.51	95.55	12.92
90.00	0.43	1.14	40.00	45.09	96.01	95.49	7.20	53.71	103.89	12.63
110.00	0.40	1.08	40.00	43.94	96.64	96.02	6.74	54.71	111.07	12.40
130.00	0.38	1.03	40.00	43.18	97.14	96.45	6.37	55.58	117.42	12.20

INNER RADIUS = 50.00 mm
OUTER RADIUS = 60.00 mm
SPEED OF ROTATION = 1200.00 rpm

QF	Qc	q	TFi	TFo	(To)ass.	(To)cal.	hf	hc	$(\delta)F$	$(\delta)c$
10.00	0.99	2.63	89.20	100.10	99.91	99.06	17.10	46.44	43.73	14.61
30.00	1.09	2.92	60.09	78.78	94.13	94.01	11.86	44.90	63.04	15.11
50.00	1.06	2.82	50.72	62.66	93.69	93.53	10.01	45.41	74.73	14.94
70.00	1.00	2.68	47.01	55.38	94.16	93.86	8.95	46.16	83.59	14.70
90.00	0.96	2.55	45.09	51.39	94.71	94.30	8.23	46.91	90.89	14.46
110.00	0.91	2.44	43.94	48.92	95.23	94.73	7.70	47.71	97.17	14.22
130.00	0.87	2.35	43.18	47.26	95.67	95.10	7.28	48.36	102.73	14.03

INNER RADIUS = 60.00 mm
OUTER RADIUS = 70.00 mm
SPEED OF ROTATION = 1200.00 rpm

QF	Qc	q	TFi	TFo	(To)ass.	(To)cal.	hf	hc	$(\delta)F$	$(\delta)c$
10.00	1.04	2.79	100.10	101.25	101.83	102.35	19.11	50.99	39.12	13.30
30.00	1.48	3.97	78.78	92.79	98.10	97.35	13.25	45.34	56.41	14.96
50.00	1.61	4.30	62.66	74.57	95.12	94.76	11.18	44.06	66.87	15.40
70.00	1.60	4.28	55.38	64.54	94.48	94.16	10.00	44.22	74.79	15.34
90.00	1.56	4.17	51.39	58.61	94.47	94.10	9.19	44.52	81.32	15.24
110.00	1.51	4.05	48.92	54.79	94.69	94.26	8.60	45.04	86.94	15.06
130.00	1.46	3.93	47.26	52.16	94.96	94.48	8.13	45.53	91.92	14.90

INNER RADIUS = 70 mm
OUTER RADIUS = 80 mm
SPEED OF ROTATION = 1200 rpm

QF	Qc	q	TFi	TFo	(To)ass.	(To)cal.	hf	hc	$(\delta)F$	$(\delta)c$
10.00	1.07	2.87	101.20	102.28	101.96	102.71	21.10	55.59	35.43	12.20
30.00	1.69	4.52	92.79	100.16	100.77	100.56	14.63	47.77	51.08	14.20
50.00	2.10	5.62	74.57	85.21	97.33	96.67	12.34	44.36	60.56	15.29
70.00	2.20	5.90	64.54	73.82	95.61	95.15	11.04	43.69	67.74	15.53
90.00	2.21	5.91	58.61	66.37	94.95	94.55	10.15	43.65	73.65	15.54
110.00	2.18	5.84	54.79	61.32	94.76	94.35	9.49	43.86	78.74	15.47
130.00	2.13	5.73	52.16	57.74	94.77	94.34	8.98	44.16	83.24	15.36

Cont'd....

INNER RADIUS = 80.00 mm
OUTER RADIUS = 90.00 mm
SPEED OF ROTATION = 1200.00 rpm

QF	Qc	q	TFi	TFo	(To)ass.	(To)cal.	hf	hc	(δ)F	(δ)c
10.00	1.07	2.88	101.90	102.26	101.97	102.97	22.93	60.32	32.60	11.24
30.00	1.74	4.67	100.16	102.11	101.87	102.47	15.90	51.33	47.00	13.21
50.00	2.49	6.66	85.21	93.57	99.73	98.73	13.41	45.60	55.71	14.87
70.00	2.76	7.40	73.82	82.45	97.28	96.61	11.99	44.05	62.32	15.40
90.00	2.86	7.66	66.37	74.17	96.01	95.49	11.03	43.53	67.76	15.58
110.00	2.88	7.72	61.32	68.18	95.38	94.91	10.32	43.43	72.44	15.62
130.00	2.86	7.68	57.74	63.76	95.08	94.63	9.76	43.55	76.58	15.57

INNER RADIUS = 90.00 mm
OUTER RADIUS = 100.00 mm
SPEED OF ROTATION = 1200.00 rpm

QF	Qc	q	TFi	TFo	(To)ass.	(To)cal.	hf	hc	(δ)F	(δ)c
10.00	1.09	2.94	102.26	102.28	101.84	102.84	24.69	64.56	30.27	10.50
30.00	1.75	4.69	102.11	102.11	101.95	102.95	17.12	55.25	43.64	12.27
50.00	2.73	7.29	93.57	98.64	100.89	100.78	14.44	47.64	51.74	14.24
70.00	3.24	8.69	82.45	89.83	99.13	98.21	12.91	44.98	57.87	15.08
90.00	3.48	9.31	74.17	81.53	97.42	96.72	11.88	43.94	62.92	15.44
110.00	3.58	9.59	68.18	75.01	96.38	95.80	11.11	43.51	67.27	15.59
130.00	3.61	9.69	63.76	69.97	95.77	95.25	10.51	43.39	71.12	15.63

INNER RADIUS = 100.00 mm
OUTER RADIUS = 110.00 mm
SPEED OF ROTATION = 1200.00 rpm

QF	Qc	q	TFi	TFo	(To)ass.	(To)cal.	hf	hc	(δ)F	(δ)c
10.00	1.12	3.02	102.28	102.30	101.82	102.82	26.38	68.46	28.32	9.90
30.00	1.76	4.71	102.11	102.11	101.95	102.95	18.30	58.93	40.83	11.51
50.00	2.84	7.60	98.64	101.10	101.64	102.08	15.44	50.21	48.40	13.51
70.00	3.60	9.65	89.83	95.34	100.37	99.87	13.80	46.43	54.14	14.61
90.00	4.03	10.77	81.53	88.05	98.95	98.05	12.69	44.73	58.86	15.17
110.00	4.24	11.36	75.01	81.48	97.62	96.89	11.87	43.95	62.93	15.43
130.00	4.35	11.67	69.97	76.10	96.73	96.10	11.23	43.58	66.53	15.56

INNER RADIUS = 110.00 mm
OUTER RADIUS = 120.00 mm
SPEED OF ROTATION = 1200.00 rpm

QF	Qc	q	TFi	TFo	(To)ass.	(To)cal.	hf	hc	(δ)F	(δ)c
10.00	1.16	3.12	102.30	102.33	101.81	102.81	28.03	71.94	26.65	9.42
30.00	1.77	4.73	102.11	102.11	101.95	102.95	19.44	62.47	38.43	10.85
50.00	2.88	7.70	101.10	101.94	101.98	102.73	16.40	53.12	45.55	12.77
70.00	3.83	10.27	95.34	98.88	101.15	101.24	14.66	48.31	50.95	14.04
90.00	4.47	11.95	88.05	93.31	100.13	99.45	13.49	45.89	55.40	14.78
110.00	4.84	12.95	81.48	87.31	98.97	98.07	12.61	44.71	59.23	15.17
130.00	5.05	13.55	76.10	81.90	97.87	97.10	11.93	44.06	62.62	15.40

Cont'd....

INNER RADIUS = 120.00 mm
OUTER RADIUS = 130.00 mm
SPEED OF ROTATION = 1200.00 rpm

QF	Qc	q	TFi	TFo	(To)ass.	(To)cal.	hf	hc	(δ)F	(δ)c
10.00	1.21	3.25	102.33	102.36	101.78	102.78	29.63	74.97	25.21	9.04
30.00	1.78	4.76	102.12	102.12	101.95	102.95	20.55	65.89	36.35	10.29
50.00	2.88	7.70	101.98	102.00	102.00	103.00	17.34	56.14	43.09	12.08
70.00	3.96	10.61	98.88	100.84	101.68	102.14	15.50	50.51	48.20	13.43
90.00	4.79	12.79	93.31	97.08	100.86	100.73	14.25	47.42	52.41	14.30
110.00	5.34	14.28	87.31	92.18	100.03	99.29	13.33	45.73	56.03	14.83
130.00	5.69	15.25	81.90	87.16	99.08	98.16	12.61	44.78	59.24	15.15

INNER RADIUS = 130 mm
OUTER RADIUS = 140 mm
SPEED OF ROTATION = 1200 rpm

QF	Qc	q	TFi	TFo	(To)ass.	(To)cal.	hf	hc	(δ)F	(δ)c
10.00	1.32	3.55	102.36	102.44	101.68	102.53	52.34	76.52	20.83	8.86
30.00	1.81	4.84	102.12	102.13	101.87	102.87	36.30	68.95	30.04	9.83
50.00	2.88	7.70	102.00	102.00	102.00	103.00	30.63	59.07	35.61	11.48
70.00	4.06	10.87	100.84	102.37	101.96	102.42	27.38	52.71	39.83	12.87
90.00	5.10	13.63	97.08	100.92	101.00	100.98	25.18	48.84	43.31	13.89
110.00	5.91	15.80	92.18	97.89	99.80	99.14	23.55	46.51	46.30	14.58
130.00	6.48	17.36	87.16	93.85	98.33	97.49	22.28	45.11	48.95	15.04

INNER RADIUS = 140.00 mm
OUTER RADIUS = 150.00 mm
SPEED OF ROTATION = 1200.00 rpm

QF	Qc	q	TFi	TFo	(To)ass.	(To)cal.	hf	hc	(δ)F	(δ)c
10.00	1.45	3.91	102.44	102.55	101.72	102.49	54.89	77.75	19.87	8.72
30.00	1.85	4.94	102.13	102.14	101.85	102.85	38.07	71.83	28.64	9.44
50.00	2.88	7.70	102.00	102.00	102.00	103.00	32.12	61.95	33.95	10.95
70.00	4.13	11.05	102.37	102.38	101.69	102.64	28.71	54.96	37.98	12.34
90.00	5.20	13.88	100.92	102.09	101.98	102.45	26.41	50.91	41.29	13.32
110.00	6.19	16.55	97.89	100.69	101.21	101.29	24.70	48.03	44.15	14.12
130.00	6.99	18.71	93.85	98.14	100.21	99.78	23.36	46.13	46.67	14.70

Cont'd....

INNER RADIUS = 150.00 mm
OUTER RADIUS = 160.00 mm
SPEED OF ROTATION = 1200.00 rpm

QF	Qc	q	TFi	TFo	(To)ass.	(To)cal.	hf	hc	$(\delta)F$	$(\delta)c$
10.00	1.61	4.34	102.55	102.68	101.78	102.43	57.38	78.55	19.00	8.63
30.00	1.89	5.06	102.14	102.15	101.84	102.84	39.80	74.45	27.40	9.11
50.00	2.88	7.71	102.01	102.01	101.99	102.99	33.58	64.74	32.48	10.47
70.00	4.21	11.25	102.38	102.39	101.69	102.64	30.02	57.10	36.33	11.88
90.00	5.22	13.93	102.09	102.09	101.90	102.90	27.61	53.14	39.50	12.76
110.00	6.31	16.86	100.69	101.85	101.92	102.36	25.82	49.90	42.23	13.59
130.00	7.27	19.45	98.14	100.50	101.27	101.39	24.42	47.59	44.64	14.25

INNER RADIUS = 160.00 mm
OUTER RADIUS = 165.00 mm
SPEED OF ROTATION = 1200.00 rpm

QF	Qc	q	TFi	TFo	(To)ass.	(To)cal.	hf	hc	$(\delta)F$	$(\delta)c$
10.00	1.70	4.59	102.68	102.76	101.84	102.37	59.21	79.56	18.41	8.52
30.00	1.92	5.13	102.15	102.16	101.83	102.83	41.07	76.54	26.55	8.86
50.00	2.89	7.75	102.10	102.10	101.89	102.89	34.64	66.72	31.47	10.16
70.00	4.25	11.36	102.39	102.39	101.69	102.63	30.97	58.71	35.20	11.55
90.00	5.23	13.96	102.09	102.09	101.90	102.90	28.48	54.80	38.27	12.38
110.00	6.32	16.88	101.85	101.91	101.96	102.94	26.64	51.46	40.92	13.18
130.00	7.34	19.63	100.50	101.06	101.87	102.29	25.20	48.96	43.26	13.85

TABLE 9 PERFORMANCE OF THE FEED DISTRIBUTOR

(PERCENTAGE OF* LIQUID PASSING THROUGH THE DISCS)

QF(cc/s)	N=500rpm	N=600rpm	N=700rpm	N=800rpm	N=900rpm	N=1000rpm	N=1100rpm	N=1200rpm
10.00	100.00	100.00	100.00	100.00	100.00	100.00	100.00	100.00
20.00	100.00	100.00	100.00	100.00	100.00	100.00	100.00	100.00
30.00	100.00	100.00	100.00	100.00	100.00	100.00	100.00	100.00
40.00	100.00	100.00	100.00	100.00	100.00	100.00	100.00	100.00
50.00	100.00	100.00	100.00	100.00	100.00	100.00	100.00	100.00
60.00	94.50	98.30	100.00	100.00	100.00	100.00	100.00	100.00
70.00	89.60	96.10	98.70	100.00	100.00	100.00	100.00	100.00
80.00	80.80	91.50	94.60	96.20	98.20	100.00	100.00	100.00
90.00	73.50	83.50	90.50	91.50	96.50	98.70	100.00	100.00
100.00	65.60	75.80	81.80	86.50	92.60	95.90	100.00	100.00
110.00	60.80	70.20	73.60	81.70	88.50	90.80	100.00	100.00
120.00	58.10	66.60	69.70	75.40	82.70	87.90	98.50	100.00
130.00	49.80	60.20	63.80	69.90	81.60	94.90	96.80	98.50

$$* \frac{\text{(Feed rate - Rate of dripping)}}{\text{(Feed rate)}} * 100$$

TABLE 10 HEAT TRANSFER(With phase change)— PREDICTED VALUES

INNER RADIUS = 40 mm
OUTER RADIUS = 50 mm
SPEED OF ROTATION = 1200 rpm

QF	Qc	Qv	q	TFi	TFo	(To)ass.	(To)cal.	hf	hs	$(\delta)F$
10.00	0.45	0.00	1.20	45.00	72.79	95.27	94.93	8.47	52.74	50.49
30.00	0.33	0.00	0.89	45.00	60.21	98.45	97.62	5.87	58.36	72.79
50.00	0.28	0.00	0.76	45.20	53.03	99.54	98.62	4.96	61.42	86.29
70.00	0.26	0.00	0.68	45.70	50.71	100.18	99.21	4.43	63.70	96.52
90.00	0.23	0.00	0.62	47.00	50.53	100.67	99.68	4.07	65.82	104.95
110.00	0.22	0.00	0.58	47.00	49.71	100.78	99.95	3.81	67.26	112.20
130.00	0.21	0.00	0.55	47.00	49.17	100.87	100.16	3.61	68.48	118.62

INNER RADIUS = 50.00 mm
OUTER RADIUS = 60.00 mm
SPEED OF ROTATION = 1200.00 rpm

QF	Qc	Qv	q	TFi	TFo	(To)ass.	(To)cal.	hf	hs	$(\delta)F$
10.00	0.85	1.23	2.28	65.00	65.00	97.26	96.59	9.67	48.72	44.17
30.00	0.67	0.95	1.79	60.21	61.35	98.99	98.08	6.71	52.90	63.69
50.00	0.62	0.00	1.66	53.03	62.30	99.12	98.19	5.66	54.27	75.49
70.00	0.58	0.00	1.53	50.71	56.98	99.50	98.55	5.06	55.43	84.45
90.00	0.53	0.00	1.41	50.53	55.07	99.96	98.98	4.65	57.18	91.82
110.00	0.50	0.00	1.34	49.71	53.26	100.21	99.21	4.35	58.04	98.16
130.00	0.48	0.00	1.28	49.17	52.05	100.37	99.42	4.12	58.90	103.78

INNER RADIUS = 60.00 mm
OUTER RADIUS = 70.00 mm
SPEED OF ROTATION = 1200.00 rpm

QF	Qc	Qv	q	TFi	TFo	(To)ass.	(To)cal.	hf	hs	$(\delta)F$
10.00	1.38	2.61	3.70	65.00	65.00	96.00	95.52	11.19	46.40	38.16
30.00	1.10	2.13	2.93	61.35	62.48	98.26	97.42	7.57	50.08	56.41
50.00	0.94	1.05	2.62	62.30	62.71	99.49	98.54	6.32	52.74	67.55
70.00	0.96	0.00	2.55	55.07	62.55	99.17	98.24	5.65	52.34	75.55
90.00	0.88	0.00	2.36	55.07	60.48	99.66	98.69	5.20	53.81	82.15
110.00	0.85	0.00	2.27	53.26	57.58	99.83	98.85	4.86	54.60	87.83
130.00	0.82	0.00	2.18	52.05	55.61	100.00	99.01	4.60	55.24	92.85

Cont'd....

INNER RADIUS = 70 mm
OUTER RADIUS = 80 mm
SPEED OF ROTATION = 1200 rpm

QF	Qc	Qv	q	TFi	TFo	(To)ass.	(To)cal.	hf	hs	$(\delta)F$
10.00	2.04	3.72	5.00	65.00	65.00	94.85	94.57	12.65	44.77	33.77
30.00	1.62	3.63	4.35	62.48	63.48	97.63	96.86	8.44	48.35	50.56
50.00	1.39	2.25	3.82	62.71	63.15	98.94	98.02	7.00	50.95	61.02
70.00	1.36	1.18	3.63	62.55	62.85	99.48	98.52	6.22	51.22	68.69
90.00	1.27	1.12	3.42	60.48	60.90	99.70	98.72	5.72	52.39	74.68
110.00	1.25	0.00	3.33	57.58	62.54	99.71	98.73	5.35	52.78	79.84
130.00	1.21	0.00	3.23	55.61	59.77	99.79	98.80	5.06	53.26	84.41

INNER RADIUS = 80.00 mm
OUTER RADIUS = 90.00 mm
SPEED OF ROTATION = 1200.00 rpm

QF	Qc	Qv	q	TFi	TFo	(To)ass.	(To)cal.	hf	hs	$(\delta)F$
10.00	2.84	4.55	6.80	65.00	65.00	93.84	93.76	13.97	43.60	30.56
30.00	2.24	5.05	6.02	63.48	64.23	97.08	96.38	9.30	47.18	45.90
50.00	1.93	3.95	5.27	63.15	63.59	98.41	97.55	7.67	49.60	55.63
70.00	1.85	2.62	4.94	62.85	63.17	99.04	98.11	6.79	50.30	62.84
90.00	1.75	2.48	4.68	60.90	61.37	99.28	98.33	6.24	51.27	68.42
110.00	1.73	0.00	4.62	57.58	63.62	99.24	98.29	5.81	51.41	73.46
130.00	1.65	0.00	4.40	59.77	64.42	99.77	98.79	5.50	52.27	77.66

INNER RADIUS = 90.00 mm
OUTER RADIUS = 100.00 mm
SPEED OF ROTATION = 1200.00 rpm

QF	Qc	Qv	q	TFi	TFo	(To)ass.	(To)cal.	hf	hs	$(\delta)F$
10.00	3.82	6.27	9.40	65.00	65.00	92.52	92.73	15.89	42.58	26.86
30.00	2.98	7.24	7.99	64.32	64.74	96.49	95.87	10.25	46.25	41.64
50.00	2.57	5.75	6.98	63.59	64.00	97.91	97.09	8.36	48.56	51.08
70.00	2.43	4.34	6.50	63.17	63.50	98.61	97.72	7.37	49.46	57.94
90.00	2.32	4.10	6.19	61.37	61.87	98.88	97.96	6.75	50.28	63.21
110.00	2.23	1.49	6.11	63.62	63.75	99.55	98.58	6.26	50.90	68.21
130.00	2.12	1.41	5.65	64.42	64.46	99.93	98.94	5.92	51.78	72.11

INNER RADIUS = 100.00 mm
OUTER RADIUS = 110.00 mm
SPEED OF ROTATION = 1200.00 rpm

QF	Qc	Qv	q	TFi	TFo	(To)ass.	(To)cal.	hf	hs	$(\delta)F$
10.00	4.93	6.27	11.40	65.00	65.00	91.94	92.26	16.66	41.80	25.62
30.00	3.84	9.72	10.30	64.74	64.95	95.79	95.29	11.28	45.40	37.84
50.00	3.32	7.99	8.98	64.00	64.36	97.41	96.65	9.06	47.69	47.12
70.00	3.11	6.36	8.32	63.50	63.83	98.19	97.34	7.94	48.72	53.74
90.00	2.98	6.00	7.95	61.87	62.38	98.50	97.62	7.26	49.43	58.77
110.00	2.82	3.24	7.68	63.75	63.89	99.21	98.27	6.72	50.34	63.52
130.00	2.67	3.07	7.12	64.46	64.51	99.62	98.64	6.35	51.25	67.22

INNER RADIUS = 110.00 mm
OUTER RADIUS = 120.00 mm
SPEED OF ROTATION = 1200.00 rpm

QF	Qc	Qv	q	TFi	TFo	(To)ass.	(To)cal.	hf	hs	$(\delta)F$
10.00	6.19	6.78	13.40	65.00	65.00	91.22	91.70	17.75	41.17	24.05
30.00	4.85	12.79	13.00	65.00	65.00	94.98	94.62	12.48	44.64	34.20
50.00	4.18	10.58	11.28	64.36	64.64	96.90	96.21	9.79	46.90	43.59
70.00	3.89	8.70	10.41	63.83	64.13	97.78	96.97	8.53	48.03	50.06
90.00	3.73	8.19	9.96	62.38	62.88	98.14	97.29	7.77	48.71	54.90
110.00	3.50	5.27	9.75	63.89	64.04	98.87	97.96	7.18	49.77	59.47
130.00	3.31	4.99	8.82	64.51	64.56	99.30	98.35	6.78	50.71	62.99

INNER RADIUS = 120.00 mm
OUTER RADIUS = 130.00 mm
SPEED OF ROTATION = 1200.00 rpm

QF	Qc	Qv	q	TFi	TFo	(To)ass.	(To)cal.	hf	hs	$(\delta)F$
10.00	7.60	7.28	15.51	65.00	65.00	90.57	91.18	18.79	40.64	22.72
30.00	6.00	13.79	16.07	65.00	65.00	94.35	94.11	13.32	43.97	32.04
50.00	5.16	13.48	13.91	64.64	64.83	96.36	95.75	10.56	46.22	40.40
70.00	4.78	11.37	13.17	64.13	64.40	97.36	96.60	9.13	47.42	46.77
90.00	4.58	10.69	12.51	62.88	63.35	97.80	96.98	8.29	48.10	51.48
110.00	4.27	7.59	11.82	64.04	64.19	98.54	97.65	7.64	49.22	55.90
130.00	4.04	7.19	10.77	64.51	64.57	98.98	98.05	7.20	50.15	59.29

INNER RADIUS = 130.00 mm
OUTER RADIUS = 140.00 mm
SPEED OF ROTATION = 1200.00 rpm

QF	Qc	Qv	q	TFi	TFo	(To)ass.	(To)cal.	hf	hs	$(\delta)F$
10.00	9.15	7.43	17.90	65.00	65.00	90.11	90.81	19.51	40.21	21.87
30.00	7.33	17.24	19.63	65.00	65.00	93.36	93.32	14.78	43.29	28.87
50.00	6.28	16.88	16.91	64.83	64.94	95.77	95.25	11.41	45.58	37.39
70.00	5.61	13.75	15.93	63.35	63.96	96.82	96.13	9.71	47.32	43.94
90.00	5.53	13.43	15.06	63.35	63.77	97.45	96.68	8.81	47.54	48.43
110.00	5.14	10.21	14.16	64.19	64.34	98.20	97.35	8.10	48.71	52.71
130.00	4.86	9.68	12.97	64.57	64.63	98.66	97.76	7.62	49.62	56.00

Cont'd....

INNER RADIUS = 140.00 mm
OUTER RADIUS = 150.00 mm
SPEED OF ROTATION = 1200.00 rpm

QF	Qc	Qv	q	TFi	TFo	(To)ass.	(To)cal.	hf	hs	$(\delta)_F$
10.00	10.86	7.91	21.30	65.00	65.00	89.58	90.38	20.46	39.83	20.86
30.00	8.85	20.33	22.72	65.00	65.00	92.33	92.52	16.36	42.64	26.09
50.00	7.55	20.33	20.30	64.94	64.99	95.14	94.73	12.32	44.96	34.65
70.00	6.76	17.13	18.99	63.96	64.41	96.42	95.79	10.36	46.65	41.18
90.00	6.56	16.57	17.90	63.77	64.13	97.11	96.38	9.35	47.10	45.63
110.00	6.12	13.15	16.78	64.34	64.48	97.87	97.05	8.56	48.22	49.83
130.00	5.78	12.48	15.44	64.63	64.69	98.35	97.48	8.05	49.12	53.03

INNER RADIUS = 150.00 mm
OUTER RADIUS = 160.00 mm
SPEED OF ROTATION = 1200.00 rpm

QF	Qc	Qv	q	TFi	TFo	(To)ass.	(To)cal.	hf	hs	$(\delta)_F$
10.00	12.47	8.30	24.51	65.00	65.00	89.18	90.05	21.29	39.77	20.04
30.00	10.58	23.05	26.83	65.00	65.00	91.30	91.72	18.03	42.01	23.67
50.00	8.98	24.46	24.13	65.00	65.00	94.41	94.13	13.37	44.36	31.91
70.00	8.03	20.96	22.39	64.41	64.71	95.98	95.42	11.06	46.04	38.58
90.00	7.74	20.10	21.05	64.13	64.43	96.74	96.06	9.92	46.61	43.03
110.00	7.21	16.43	19.69	64.48	64.60	97.52	96.74	9.04	47.73	47.19
130.00	6.81	15.60	18.19	64.69	64.75	98.03	97.19	8.48	48.64	50.33

INNER RADIUS = 160.00 mm
OUTER RADIUS = 165.00 mm
SPEED OF ROTATION = 1200.00 rpm

QF	Qc	Qv	q	TFi	TFo	(To)ass.	(To)cal.	hf	hs	$(\delta)_F$
10.00	13.50	8.55	27.46	65.00	65.00	87.61	88.55	25.54	39.97	16.70
30.00	11.51	24.77	29.50	65.00	65.00	89.82	90.47	21.29	42.15	20.04
50.00	9.78	26.90	26.28	65.00	65.00	93.73	93.55	14.64	44.49	29.14
70.00	8.73	23.07	24.25	64.71	64.80	95.65	95.11	11.78	46.22	36.22
90.00	8.38	22.03	22.76	64.43	64.54	96.50	95.83	10.47	46.84	40.75
110.00	7.80	18.22	21.28	64.60	64.65	97.29	96.52	9.50	47.97	44.91
130.00	7.37	17.30	19.69	64.75	64.78	97.82	96.99	8.89	48.89	48.02

TABLE 11 POWER CONSUMPTION(With-out pick-up nozzle & cover plate)

QF	N=500rpm			N=600rpm			N=700rpm			N=800rpm			N=900rpm			N=1000rpm		
(cc/s)	20°c	50°c	80°c	20°c	50°c	80°c	20°c	50°c	80°c	20°c	50°c	80°c	20°c	50°c	80°c	20°c	50°c	80°c
0.0	393.8	390.6	390.5	440.6	442.3	444.7	532.4	535.3	531.9	600.8	602.7	600.5	644.5	642.8	643.8	702.3	705.5	703.2
10.0	395.1	391.4	391.1	442.3	443.9	445.5	534.6	637.3	533.4	603.1	605.2	602.4	647.2	645.6	645.9	704.9	707.2	705.6
20.0	396.2	391.9	391.7	443.8	444.8	446.8	536.8	538.6	535.2	605.8	607.3	604.3	649.8	647.3	648.1	707.1	709.7	708.2
30.0	396.9	392.5	392.6	445.4	446.2	448.1	538.9	541.1	537.1	608.4	609.5	606.1	653.1	651.2	652.6	710.5	712.8	710.6
40.0	397.2	393.4	393.2	446.3	446.8	449.2	541.3	543.2	538.8	610.7	611.3	608.1	655.7	653.8	654.3	714.2	717.1	712.2
50.0	397.9	393.9	393.6	447.5	448.3	450.4	543.0	544.9	540.9	612.4	613.3	610.0	658.4	656.2	657.8	718.8	721.1	715.1
60.0	398.7	394.6	394.0	448.7	449.6	451.1	543.8	545.8	541.5	614.2	615.3	612.3	661.9	659.3	660.3	721.1	723.8	718.8
70.0	399.4	395.3	394.8	449.8	450.8	451.6	544.7	546.7	542.5	615.8	616.8	614.6	663.2	661.5	662.8	723.8	726.2	721.6

TABLE 12 POWER CONSUMPTION(With pick-up nozzle & cover plate)

QF	N=500rpm			N=600rpm			N=700rpm			N=800rpm			N=900rpm			N=1000rpm		
(cc/s)	20°c	50°c	80°c	20°c	50°c	80°c	20°c	50°c	80°c	20°c	50°c	80°c	20°c	50°c	80°c	20°c	50°c	80°c
0.0	434.6	444.8	427.8	447.2	449.4	446.6	538.3	535.4	537.8	608.7	602.5	603.2	646.7	650.7	649.5	709.8	715.7	715.2
10.0	437.8	447.4	430.6	449.9	452.1	448.7	540.8	537.9	539.5	612.3	605.4	606.5	650.7	654.2	653.1	710.5	717.8	718.7
20.0	440.2	449.2	433.1	452.3	454.2	451.4	542.4	539.7	541.3	615.8	608.9	607.8	655.2	659.8	658.7	711.2	721.1	722.4
30.0	441.2	452.1	434.8	454.2	484.3	454.4	546.7	542.8	544.2	620.1	613.5	612.6	659.8	663.9	667.7	720.9	725.4	724.6
40.0	445.8	454.9	439.2	459.7	460.3	457.8	548.7	544.2	548.6	624.5	617.2	616.8	663.9	667.7	666.6	724.3	727.8	727.1
50.0	444.6	457.3	441.2	461.5	462.3	461.7	552.6	549.3	548.9	625.8	620.3	619.5	668.9	672.3	671.4	728.3	730.2	729.8
60.0	447.1	460.5	444.1	466.5	467.1	464.5	555.4	551.7	554.3	629.7	623.5	622.7	672.3	676.4	675.3	731.6	735.5	734.4
70.0	449.8	463.3	447.3	467.4	468.7	469.1	558.4	557.1	557.7	632.1	627.5	626.8	676.3	674.4	679.3	731.9	737.3	738.1

POWER IN 'WATTS'

TABLE 13 COMARISON OF MEASURED & PREDICTED VALUES

(%age deviation)

OF	N=1200rpm				N=1000rpm				N=800rpm				N=600rpm			
(cc/s)	1	2	3	4	1	2	3	4	1	2	3	4	1	2	3	4
10.00	-27.29	-22.74	-16.60	-6.75	-34.09	-23.04	-19.39	-8.23	-35.13	-24.60	-18.18	-11.05	-37.80	-25.46	-23.46	-12.75
30.00	-18.29	-15.98	-8.68	-4.88	-24.08	-17.42	-11.05	-5.41	-26.85	-18.53	-13.78	-6.57	-28.50	-20.73	-16.39	-7.82
50.00	-13.60	-14.15	-7.93	-5.57	-18.48	-15.28	-11.16	-5.59	-21.93	-11.76	-12.71	-4.35	-25.80	-19.83	-12.85	-7.23
70.00	-15.17	-14.86	-7.96	-7.22	-18.78	-15.93	-12.57	-6.92	-23.70	-15.68	-12.43	-3.59	-23.43	-18.54	-10.74	-5.79
90.00	-15.30	-14.50	-4.96	-5.18	-17.59	-15.10	-10.68	-5.08								
110.00	-15.20	-13.93	-2.49	-3.13												
130.00	-17.00	-16.50	-3.20	-2.98												

1_ WATER,WITHOUT PURGING.

2_ WATER+SURFACTANTS,WITHOUT PURGING.

3_ WATER,WITH PURGING.

4_ WATER+SURFACTANTS,WITH PURGING.

$$\%age\ deviation = \frac{(Ttheo. \_ Texp.)}{(Ttheo.)} * 100$$